CHALMERS TEKNISKA HÖGSKOLA

CHALMERS UNIVERSITY OF TECHNOLOGY
GÖTEBORG
SWEDEN

Importance of Water Composition for Prevention of Internal Copper and Iron Corrosion

by

Eva Lind Johansson

Chalmers University of Technology
Department of Sanitary Engineering
Dissertation no 8
Göteborg 1989

ABSTRACT

Long term studies of copper and iron corrosion in drinking water pipes under varied pH, carbonic species, calcium, chloride, sulphate and organic concentration conditions were carried out in the laboratory and field. The conditions were controlled to represent reality as closely as possible with flow conditions simulating mains and household connections.

Soft, unbuffered water, which is common for Swedish natural waters, was found to be detrimental to both copper and iron pipe systems. Chloride, sulphate and organic material under certain conditions increased metal corrosion rate.

Copper corrosion rate decreased at neutral and high pH, while iron corrosion rate was reduced at neutral pH and in the presence of carbonic species, due to the formation of protective layers. Calcium also aided protective layer formation in iron pipes.

In relality it is necessary to compromise and protect combined copper/iron systems. The compromise is achieved through the addition of carbonic species as a pH control. This recommendation has been implemented at local municipal waterworks and a reduction in water quality problems related to pipe corrosion has been found.

PREFACE

In an investigation during the late 1970's, of the deterioration of water quality during passage of the distribution system, problems with corrosion products in the water were detected. This investigation initiated a research project called "Water distribution problems and counteractions" supported by the Swedish Council for Building Research and National Swedish Environmental Protection Board. The studies have been carried out at the Department of Sanitary Enginering, Chalmers University of Technology, Göteborg, Sweden. The laboratory experiments have been located at the Department's research facility at the Lackarebäck Water Treatment Plant. The field tests have been carried out at different water works mostly in the vicinity of Göteborg.

Corrosion problems are not specific for Swedish conditions and investigations have been carried out in many countries with various water compositions. The whole puzzle has not been identified and it is the intention that this study will contribute to ongoing research efforts.

To the research project a discussion group was connected and I thank the members: Professor Einar Mattsson, Swedish Corrosion Institute, Stockholm, Jan Hjort, Stockholm Water and Sewage Works and Rolf Bergström, VIAK AB, Stockholm.

The experimental investigation was partly carried out by Rolf Hammarberg and Kristina von Schenck. I will give Rolf Hammarberg my special thanks for our time together. I thank Östen Andersson for his enthusiasm and advice and Dr. Bela Kaffehr for discussions and criticism during the investigation. The analyses have been carried out by the staff at Lackarebäck Waterworks and at the laboratory at the department. I wish to thank Birgitta Lagerholm and Eva Ekstedt for help with water analyses. I thank Lars Eklund at The Swedish Institute for Silicate Research who helped me with analyses at the scanning electron microscope.

I thank those who helped me from a linguistic point of view. Lars Lind, my husband, helped me with the translation and the logical argumentation, Lisbeth Teiffel interpreted and typed out the scrawl. Dr. Greg Morrison and Lora Sharp-McQueen corrected the language.

I wish to thank my supervisor Dr. Torsten Hedberg deeply for backing me up and supporting the research and myself all the time. He has been a stimulating adviser and project leader.

Göteborg in September 1989

Eva Johansson

CONTENTS

1. INTRODUCTION

The task of the local water authority is to supply enough water of good quality at the right pressure to the consumer. Unfortunately, water quality often deteriorates in the distribution system due to internal pipe corrosion.

The corrosion process affects not only the water quality but also results in water loss due to leaks in the network, increase in pumping head due to the build up of deposits and a tendency to pipe breakage.

1.1 The municipal water distribution system

The drinking water distribution system consists of water mains and service pipes which supply the plumbing system within the houses. Both circulation and branch systems are used for water distribution in the mains. Those pipes calculated to supply fire fighting water are usually large with a long detention time (VAV 1979).

Water mains are constructed of concrete, cast iron, steel and plastic (Figure 1.1) at present PVC is the most commonly used material. Sometimes the iron surface is coated with a lining, e.g. asphalt, bitumen, cement mortar or polymer.

Most service pipes are copper, but the most commonly installed material nowadays is plastic. In the plumbing system copper still dominates although previously galvanized steel was used (Figure 1.2).

Water flow in the distribution system can vary greatly. At the end of the branch system the water can stagnate during periods of low usage.

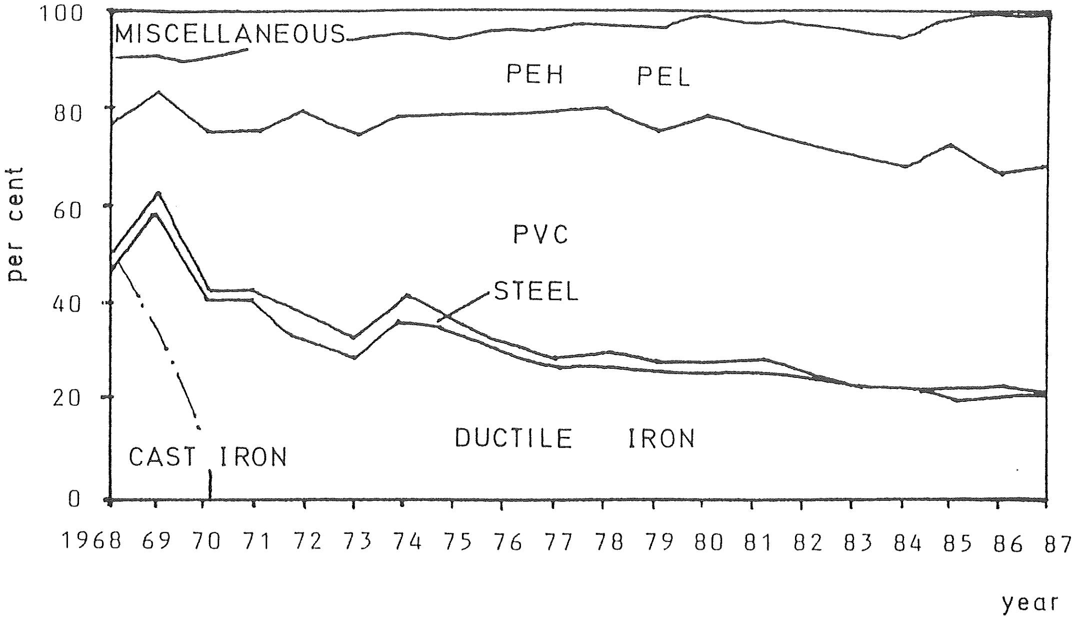

Figure 1.1 Percentages of different pipe materials used in water mains 1968-87, the statistics are from Ljunggren (1989).

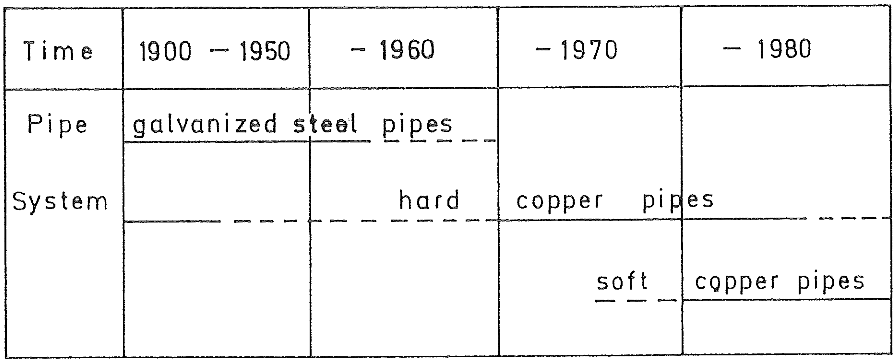

Time	1900 – 1950	– 1960	– 1970	– 1980
Pipe	galvanized s	teel pipes		
System		hard	copper pi	pes
			soft	copper pipes

Figure 1.2 Material used in plumbing systems since 1900, from BFR (1981).

1.2 Problems and damage caused by corrosion

Both internal and external corrosion can damage a pipe. During internal corrosion, metal from the pipe material is dissolved into the water, and this changes the properties of both the pipe and the water. In addition, various deposits can be formed on the surface of the pipe. Corrosion can take place either locally or along the full length of the pipe.

Water quality may be consistent when leaving a waterworks, however during transit through the distribution network the water quality may deteriorate. One example shows variation in different parameters. The turbidity in water leaving the water works (normally less than 0.5 FTU) has increased to 1-2 FTU in the network (Figure 1.3).

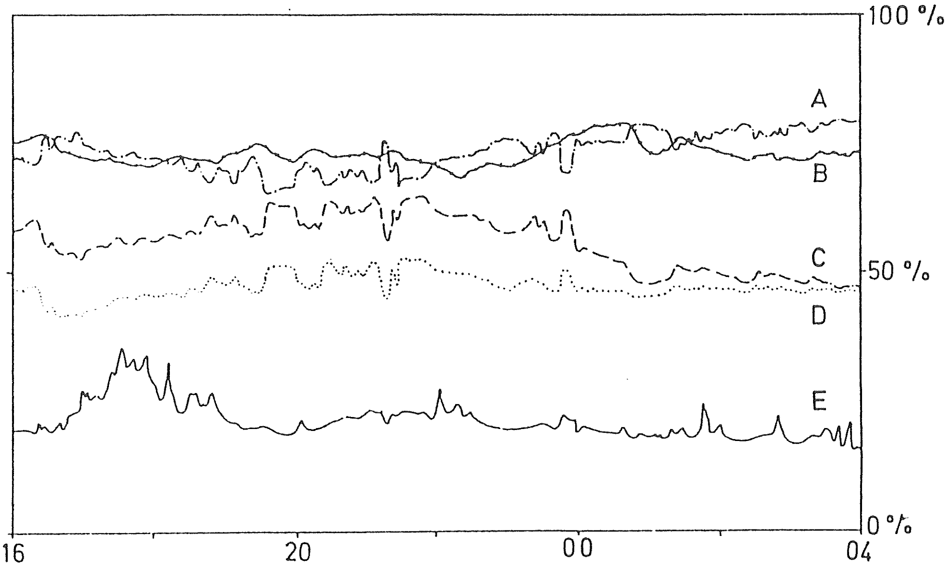

Figure 1.3 Variation in water quality in a distribution network in a larger town with a consistent water quality from the waterworks, Sjölander et al. (1982).

From top -•A•-• conductivity 0-70 ms/m
—B— temperature 0-20^{0}C
--C--- redox 150-250 mV
..D... pH 7-8
—E— turbidity 0-5.0 FTU

Corrosion can cause a deterioration of water quality and thus result in increased concentrations of copper and iron. For copper low pH values lead to the corrosion of copper pipes and therefore at acid or near neutral pH the concentration of copper in drinking water, fed through copper pipes, rises (Figure 1.4). High copper concentration therefore directly indicates copper pipe corrosion and it is clear that at pH values below 8.5 the Swedish drinking water standard of 0.05 mg l^{-1} is exceeded. The prevention of this corrosion will be discussed in detail in Chapters 3 through 6.

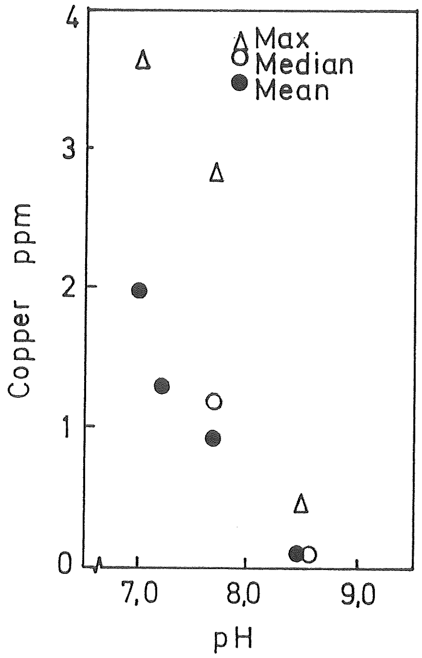

Figure 1.4 Copper concentration in tap water from waters with different pH, Hedberg (1982).

In a similar way, high iron concentrations in drinking water indicate iron pipe corrosion (Figure 1.5). In this case the highest iron concentrations are found at low water hardness in extreme cases. It is these extreme cases that require a solution to their corrosion problems. pH also plays an important role in iron corrosion. Corrosion of iron pipes is discussed in detail in Chapters 7 through 10.

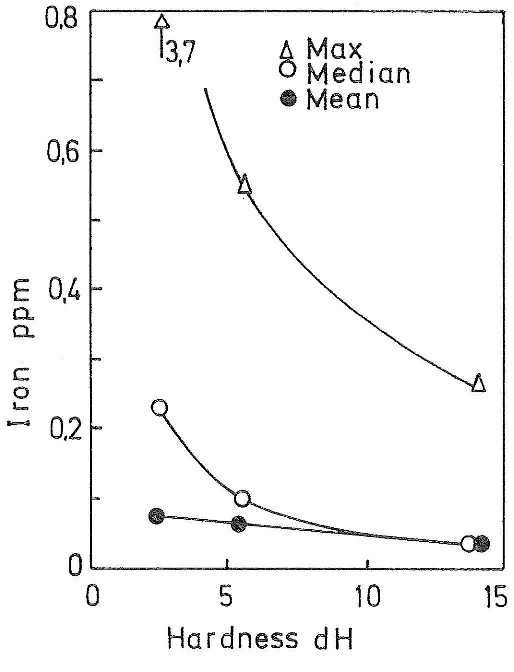

Figure 1.5 Iron concentration in tap water from waters with different hardness, Hedberg (1982).

Internal uniform corrosion has its greatest effect on water quality and does not usually affect pipe strength. A localised attack, on the other hand, can cause leakage. Deposits, e.g. corrosion products or precipitations from the water, decrease the pipe diameter and therefore lead to distribution problems due to a lower capacity and the requirement for a higher pumping head. Deposits and deteriorated water quality are most common in small pipes (Svensson 1984).

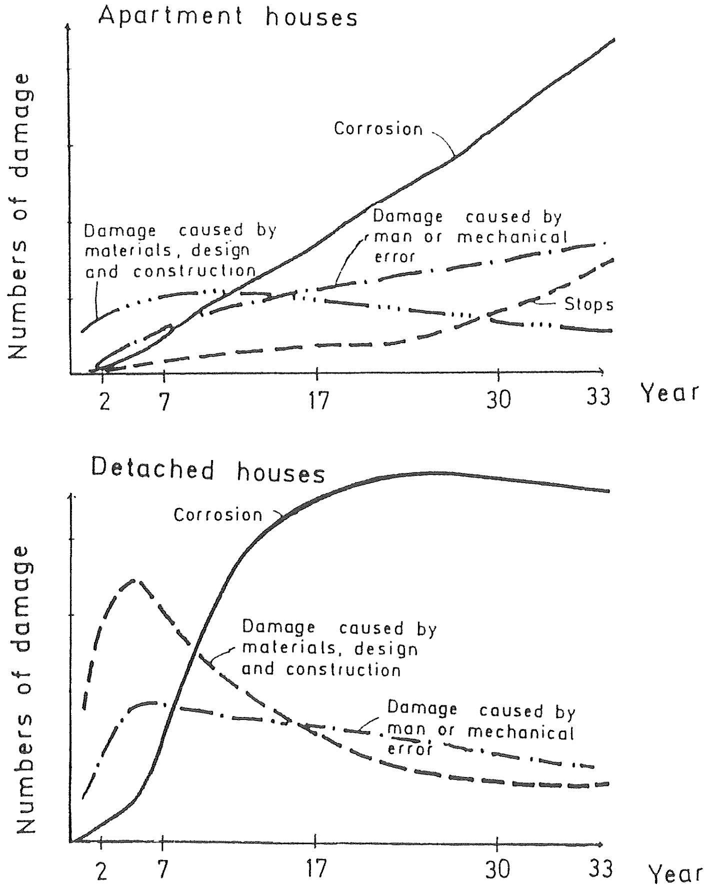

Figure 1.6 Operation time before damage in apartment and detached houses, from BFR (1981).

Corrosion attacks are most frequent in older pipe networks (Figure 1.6). Corrosion damage in the water mains is limited to the external corrosion of cast iron and steel which leads to pipe rupture. Corrosion damage in cast iron pipes accounts for 11% of the total corrosion damage (Bendixen and Hydén 1981).

Corrosion problems are increasing in Sweden since the replacement rate for old pipes is slow. A pipe has an estimated life expectancy of 50 to 100 years, but the present rate of replacement is one pipe per several hundred years.

Before 1983 drinking water quality had to be satisfactory at source (i.e. the waterworks). However, since July 1983 the Swedish government, through the National Food Administration, has required tap water to be of drinking quality at the tap. This effectively forces the municipalities to solve their corrosion problems.

1.3 Corrosion costs

Insurance company statistics show that 30-35% of all water damage to real estate is caused by corrosion and this amounts to a cost of 250 million SEK in Sweden during 1983 (Westlund 1984).

No study has been done for the nationwide cost of corrosion in water mains. However, maintenance and operation costs have increased substantially during the past decade (Figure 1.7).

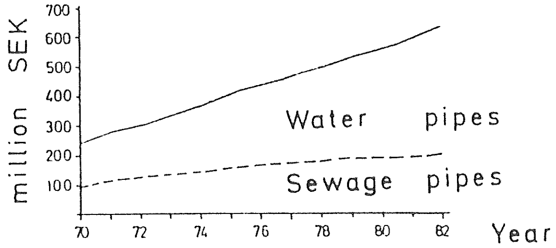

Figure 1.7 Maintenance and operation costs during 1970-82, from Säfwenberg (1984).

Municipal operation expenses include a higher pumping demand due to in-pipe blockage, flushing and cleaning, replacement and renovation of corroded pipes and valves and cost for water losses. In Sweden the loss through leakage is estimated at 10-20% of the total water fed into the mains system.

In areas with obvious corrosion problems, such as discoloured water, consumers are not always required to pay the full water rates.

1.4 Factors affecting corrosion

Water composition is an important factor in either increasing or hindering corrosion. In water treatment, chemicals are added to improve water quality, but the same chemicals may also affect corrosion. Water treatment also alters the amount of organic matter, which in turn affects corrosion reactions and scale forming properties. Environmental factors, such as acidification, affect the surface and ground water quality.

Table 1.1A and B show a summary of the literature recommendations for water quality to prevent pipe corrosion.

From the tables one can see that a high pH value is recommended for copper pipes while a moderate pH value is recommended for iron pipes. A question is of course how to minimise corrosion in a network consisting of both iron and copper pipes? This study will investigate whether corrosion can be avoided in such mixed iron and copper systems.

Table 1.1 Recommendations on ways to decrease internal corrosion (A) iron and (B) copper.

A

	1	2	3	4	5	6	7	8
pH	not a low value	> 7,0	high value	no dependency	6,8 − 7,3	> 7,0	—	no dependency
HCO_3^-	not a low conc.	2-3 mmol/l	high conc.	—	>0,4 mmol/l	—	high conc.	not a low conc.
Ca^{2+}	not a low conc.	—	—	—	0,04 - 0,10 mmol over-saturated	—	—	see ref. 5
CO_2	—	—	—	not a high conc.	—	—	—	low conc
Cl^-	depend on the HCO_3^-	low conc.	$\frac{Cl^-}{HCO_3} < 0{,}5$ mol/l	—	$\frac{Cl^- + SO_4^{2-}}{HCO} < 0{,}2$ mg/l	low conc.	low conc.	$\frac{Cl^- + SO_4^{2-}}{HCO} < 0{,}5$ mg/l
SO_4^{2-}	—	low conc.	—	—		low conc.	low conc.	
O_2	>4 mg/l	must be present	must not be present	zero or high conc.	—	—	—	not on saturation
Org. mat.	low conc.	low conc.	—	—	low conc.	—	high conc.	must be present
Temp.	—	—	low value	—	—	low value	—	low value

---

1. Ainsworth et al. (1981).

2. van der Kooij, D. and Zoeteman, B.C.J. (1979).

3. Andersson, R. and Berry, D. (1981).

4. Kristiansen, H. (1981).

5. Merill, D.T. and Sanks, R.L. (1977a, 1977b and 1978).

6. Nielsen, K. (1980).

7. Sontheimer, H., Kölle, W. and Snoeyink, V.L. (1981).

8. Ryder, R.A. (1978).

B

	1	2	3	4	5	6	7	8	9
pH	8.0	9.0	—	high value	at $CaCo_3$ equilibrium	> 7.0	> 7.4	high dependency	6.0 - 8.0
HCO_3^-	0,2 - 0.5 mmol/l	>1.0 mmol/l	high conc.	high conc.	—	must be present	>1,5 mmol/l	high conc.	high conc.
Ca^{2+}	—	not dependent on	—	—	—	—	—	—	—
CO_2	—	—	—	low conc.	—	—	—	low conc.	—
Cl^-	$\frac{Cl^-}{HCO_3^-} < \frac{1}{3}$ mol/l	—	$\frac{Cl^-}{HCO_3^-} < \frac{1}{2}$ mol/l	low conc.	—	low conc.	low conc.	$\frac{Cl^- + SO_4^{2-}}{HCO_3^-} < 0,5$ mol/l	—
SO_4^{2-}	—	low conc.	—	$SO_4^{2-} < HCO_3^-$	—	$0,01 < \frac{SO_4^{2-}}{HCO_3^-} < 0,14$ mg/l	$\frac{SO_4^{2-}}{HCO_3^-} < 1$ mg/l		—
O_2	not low conc. not high conc	low conc	—	low conc.	must be present	must be present	—	under saturation value	—
Org. mat.	—	low conc.	—	low conc.	must be present	—	—	must be present	—
Temp.	low value	—	low value	low value	—	—	—	—	—

---

1. Ainsworth et al. (1981).

2. Elzenga, C.H.J and Boorsma, H.J. (1974).

3. Andersson, R. and Berry, D. (1981).

4. Kristiansen, H. (1981).

5. Campbell, M.S. and Turner, M.E.D. (1980).

6. Ailor, W.H. (1971).

7. Mattsson, E. and Fredriksson, A.-M. (1968).

8. Ryder, R.A. (1979).

9. Lihl, F. and Klamet, H. (1969).

2. OBJECTIVES OF THE INVESTIGATION

This study attempts to shed light on the different factors affecting internal uniform corrosion of copper and iron pipes in drinking water distribution networks. The investigation concentrates on these materials because of their common utilisation in water distribution systems in Sweden.

Many corrosion studies have been carried out all over the world but as different parts of the world have different waters it is not possible to transfer the results to Swedish corrosion problems. In Sweden the waters are often very soft, have low alkalinity and are often acidified.

Several researchers have formulated recommendations with the objective of decreasing internal corrosion, but many of the recommendations are contradictory. This may be explained by the fact that many studies have been carried out within a limited water quality range.

Thus, in this study the objective is to investigate how different waters affect copper and iron corrosion and to study the development of protective layers and the properties of these layers.

Based on literature studies and experiments the objective is also to formulate an approach for corrosion prevention for copper and for iron.

Different techniques to measure corrosion are also to be examined. Corrosion is assessed in single pipe and continuous flow test rigs, constructed from copper and iron, using drinking water with a variety of chemical compositions.

This investigation will also emphasise the importance of the simultaneous study of iron and copper as these materials are often studied separately, even though combined iron and copper pipe networks are relatively common.

3. COPPER CORROSION - LITERATURE REVIEW

The literature review on internal copper corrosion is divided into three sections:

- types of corrosion attack
- parameters affecting uniform copper corrosion
- conclusions with conceivable reactions for corrosion and protective layer formation

3.1 Uniform corrosion

Loss of material affecting the whole metal surface is defined as uniform corrosion. During uniform corrosion the oxygen concentration in the water decreases and the copper concentration in the water increases (cuprosolvency increases). As corrosion is uniform the change in pipe wall thickness is negligible and it takes a long time before the strength of the pipe is affected. Uniform corrosion is therefore more of a hygiene problem than a technical problem and for this reason uniform corrosion has not been as widely studied as pitting corrosion. A number of observations have been reported, but few explanations of these observations exist. This investigation will concentrate on uniform corrosion.

3.2 Pitting corrosion

Localised corrosion (pitting corrosion), is common in copper installations. In the literature three different types of pitting corrosion, which are called type I, II and III, are discussed.

3.2.1 Type I

Type I pitting corrosion is characterised by deep and narrow pits with a malachite ($CuCO_3 \cdot Cu(OH)_2$) scale containing cuprite

(Cu_2O) in the inner part of the pit. Corrosion of type I has been thoroughly studied, mainly in the UK and West Germany, since this type has caused substantial and expensive damage for decades. Type I corrosion is found in combination with a residual carbon film on the inside of the pipes from the annealing process. The carbon film has a higher electrochemical potential than the pipe itself, which increases the corrosion rate under the carbon film. This corrosion type appears only in cold water conduits carrying groundwater. (Lucey 1967, 1972, 1974 and 1975, Gilbert 1966, Campbell 1954 and 1971, Campbell and Turner 1980, von Franquê 1968, Lihl and Klamet 1969 and Cornwell et al. 1973). According to Lucey (1972), an increase in sulphate, sodium or oxygen content increases corrosion, while increases in chloride or nitrate content decrease corrosion. Additionally, the absence of an inhibitive organic compound is a major factor for corrosion rate increase (Campbell 1954). Type I corrosion has been solved by changing the production method so that the formation of a carbon film is avoided. A residual carbon limit of 0.2 mg C dm^{-2} has been introduced.

3.2.2 Type II

Type II pitting corrosion is characterised by deep pits, which contain crystalline cuprous oxide (CuO), greenish-black cuprous oxide and basic copper sulphate. A scale of cupric (Cu_2O) and cuprous oxide (CuO) cover the pit. Corrosion type II is found only in hot water installations when the water contains oxygen. A temperature above 60^0C favours this type of corrosion. Localised attacks appear a few years after installation and have been found primarily in Scandinavia, Germany and the UK. The attack increases at low pH and high sulphate concentration relative to hydrogen carbonate concentration. There is a pronounced risk for type II corrosion if the mass ratio of HCO_3^-/SO_4^{2-} is greater than one (Mattsson and Fredriksson 1968, von Franquê et al. 1972 and 1975 and Mattsson 1980).

3.2.3 Type III

Type III pitting corrosion is characterised by a shallower, broader pit than type I. Sulphates are present in the corrosion products. Pitting corrosion of type III has only been noted in a few places in Germany and Sweden. Some researchers consider this to be a modified type I corrosion (Cruse et al. 1985). The appearance of the pits indicates spotty corrosion (von Franqué et al. 1975). This corrosion type appears in waters with high pH, low hardness and low salt content, (von Franqué et al. 1975, Linder 1979 and Linder and Lindman 1982). The exact cause of type III corrosion is not known.

3.3 Erosion corrosion

A pure copper surface is readily eroded by water with high flow velocity and erosion increases when pH is low and oxygen content is high. Erosion pits appear in the flow direction, primarily in bends, valves and connections at elevated velocities. If gas bubbles or particles are present in the water the corrosion attack increases. Particles appear when turbulent flow removes deposits from the surface. Besides the water velocity, the duration of the flow and the water temperature affect this corrosion.

Erosion can be virtually eliminated if excessive water velocities are avoided. Guidelines for water velocities in copper pipes have been set up by e.g. Swedish Building Code (SBN 80). This guideline states various maximum velocities for different temperatures and different types of conduits (Table 3.1).

Table 3.1 Swedish Building Code (SBN 80) installation guidelines for minimising erosion corrosion in copper pipes.

	Maximum water velocity m s^{-1} at different temperatures			
	10°C	50°C	70°C	90°C
Distribution pipe				
replaceable	4.0	3.0	2.5	2.0
non replaceable	2.0	1.5	1.3	1.0
Connection pipe				
replaceable	16.0	12.0	10.0	8.0
non replaceable	4.0	3.0	2.5	2.0
Circulation pipe	2.0	1.5	1.3	1.5

This is a technical installation problem and will not be discussed further.

3.4 Origin of uniform copper corrosion

Parameters affecting uniform corrosion in stagnant water include oxygen, pH, species of carbonic acid, calcium, chloride, sulphate and organic matter. These parameters will now be further treated and their importance for the corrosion mechanism discussed.

3.4.1 Importance of oxygen on copper corrosion

When copper is in contact with water containing oxygen, copper ions are dissolved from the metal surface and the oxygen is consumed in accordance with the following electrochemical reactions (equations 3.1-3.3).

Anode: $Cu^0 \rightarrow Cu^+ + e^-$ (3.1)

$Cu^+ \rightarrow Cu^{2+} + e^-$ (3.2)

Cathode: $\frac{1}{2}O_2 + H_2O + 2e^- \rightarrow 2OH^-$ (3.3)

The concentration of oxygen at the metal surface determines the rate of copper corrosion (Pisigan and Singley 1987). If the metal surface is free from deposits then corrosion rate is driven either by the reaction kinetics at the anode and the cathode, or by the transport of oxygen or reaction products. The slowest of these processes determines the corrosion rate (Hilburn 1983). When there are deposits on the metal surface the same factors contribute to the reaction rate, but the slow transportation of oxygen and reaction products through the deposit is critical (Hilburn 1983 and Cruse et al. 1985).

As diffusion through the water is high the kinetics of the anode determine the corrosion rate in a pipe with a new copper surface. When deposits on the surface have appeared (these appear immediately when the corrosion starts if the pH is not too low) the relationship will be more complicated. The transport rate for oxygen, through the deposits, slows down. When the surface is covered by deposits the cathodic, as well as the anodic, reaction are rate determined (Hilburn 1983 and Cruse et al. 1985).

Three phases can be identified:

1. Initial corrosion; new copper surface with high concentration of oxygen, the anodic reaction is rate determined.
2. Copper surface covered with deposits; high concentration of oxygen in water bulk, the transport of oxygen by diffusion is rate determined.
3. Copper surface covered with deposits; low concentration of oxygen in water bulk, oxygen transport is limited, no driving force which results in reduced corrosion rate.

Phase 1. Initial corrosion

Copper is oxidised from Cu^0 to either Cu(I) or Cu(II). The ratio between the two copper ions depend on the total copper concentration and the surrounding environment. There is an equilibrium between Cu(I), Cu(II) and Cu^0 according to Tronstad and Veimo (1940) as shown in equation (3.4)

$$Cu^{2+} + Cu^0 \rightarrow 2Cu^+ \qquad (3.4)$$

From the Nernst equation and standard electrode potentials, (where Cu^+=0,522 V and Cu^{2+}=0.345 V), the following equation (3.5) can be derived:

$$\lg\left(\frac{[Cu^+]}{[Cu^{2+}]^{\frac{1}{2}}}\right) = -3.05 \qquad (3.5)$$

Table 3.2 shows the relative concentrations of Cu(I) and Cu(II) at different total concentrations of copper according to equation (3.5). It can be seen that Cu(II) dominates in the water at higher total copper concentrations, while at lower total copper concentrations, Cu(I) dominates.

Table 3.2 Corresponding values for Cu^{2+} and Cu^+ in mol l^{-1} (Tronstad and Veimo 1940).

Concentration mol l^{-1} Cu^{2+}	Cu^+	Cu_{tot}
1	10^{-3}	1
10^{-2}	10^{-4}	10^{-2}
10^{-4}	10^{-5}	$1.1 \cdot 10^{-4}$
10^{-6}	10^{-6}	$2 \cdot 10^{-6}$
10^{-8}	10^{-7}	$1.1 \cdot 10^{-7}$

Copper ions precipitate as different corrosion products after reaction with oxygen and/or water depending on the water composition. The first formed compound is always Cu_2O (Ives and Rawson 1962) as shown in equation (3.6).

$$2Cu^{+} + H_2O \rightleftarrows Cu_2O + 2H^{+} \qquad (3.6)$$

Cruse et al. (1985), on the other hand, have the opinion that a Cu_2O film is formed directly by the anodic reaction shown in equation (3.7).

$$4Cu^{0} + \tfrac{1}{2}O_2 + H_2O \rightarrow 2Cu_2O + 2H^{+} + 2e^{-} \qquad (3.7)$$

However, both equations (3.6) and (3.7) result in the same end product.

Figure 3.1 shows two models proposed by Hilburn (1983) called the direct-dissolution model and the dissolution-and-film-growth model. As soon as a film of corrosion products forms reactions can begin.

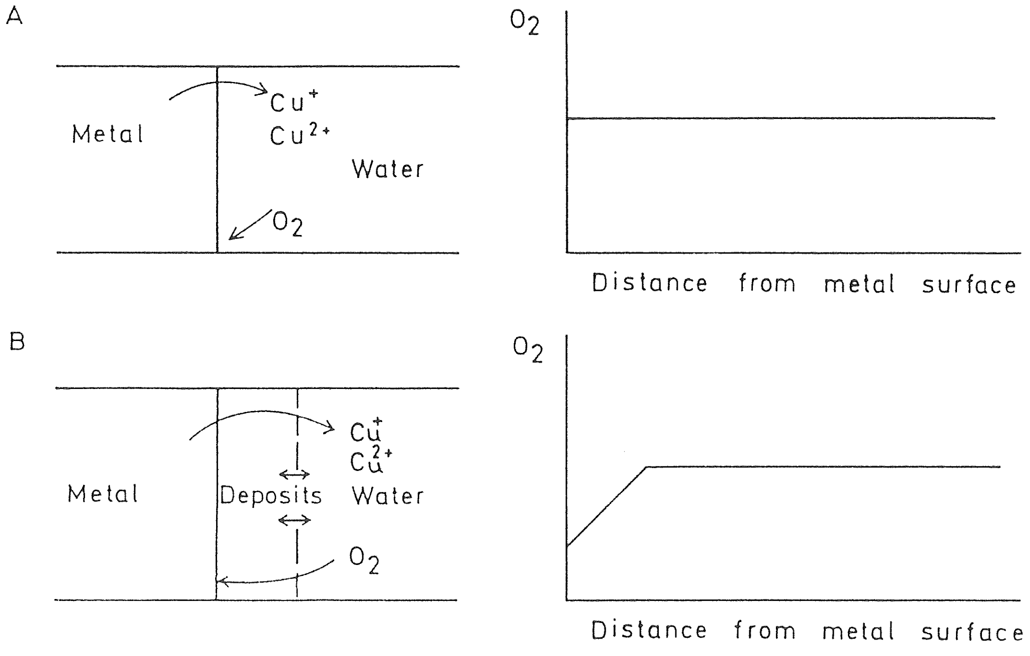

Figure 3.1 (A) Initial corrosion and (B) Corrosion when the surface is covered by deposits (Hilburn 1983)

Phase 2. After Cu_2O film formation

As soon as a Cu_2O film covers the copper surface the film itself also affects the corrosion rate. There will be a steady-state between precipitation and dissolution (Figure 3.1B). If oxygen concentration decreases then the rate of copper dissolution will also decrease. Cuprosolvency is then controlled by oxygen diffusion through the Cu_2O film (Hilburn 1983).

If the pH of the water increases, the Cu_2O layer dissolves and other corrosion products precipitate as CuO, $Cu(OH)_2$ and $CuCO_3 \cdot Cu(OH)_2$, (Ives and Rawson 1962 and Obrecht and Pourbaix 1967), as shown in equations (3.8-3.14).

Dissolution of Cu_2O to Cu^+:

$$Cu_2O + 2H^+ \rightleftarrows 2Cu^+ + H_2O \qquad (3.8)$$

Dissolution of Cu_2O to Cu^{2+}:

$$Cu_2O + 2H^+ \rightleftarrows 2Cu^{2+} + H_2O + 2e^- \qquad (3.9)$$

$$\tfrac{1}{2}O_2 + H_2O + 2e^- \rightarrow 2OH^- \qquad (3.3)$$

Dissolution of Cu_2O and formation of $CuCO_3 \cdot Cu(OH)_2$:

$$\tfrac{1}{2}Cu_2O + H_2O + 2CO_2 + \tfrac{1}{4}O_2 \rightleftarrows Cu(HCO_3)_2 \qquad (3.10)$$

$$Cu(HCO_3)_2 \rightleftarrows \tfrac{1}{2}(CuCO_3 \cdot Cu(OH)_2) + \tfrac{1}{2}H_2O + 1\tfrac{1}{2}CO_2 \qquad (3.11)$$

Cu_2O is primarily formed in cold water while CuO is formed in hot water (Elzenga and von Franqué 1986).

$$Cu(HCO_3)_2 \rightleftarrows CuO + H_2O + 2CO_2 \qquad (3.12)$$

Dissolution of CuO to Cu^{2+}:

$$CuO + 2H^+ \rightleftarrows Cu^{2+} + H_2O \qquad (3.13)$$

Formation of $Cu(OH)_2$ from Cu^{2+}:

$$Cu^{2+} + \tfrac{1}{2}O_2 + H_2O + 2e^- \rightarrow Cu(OH)_2 \qquad (3.14)$$

$$Cu^0 \rightarrow Cu^+ + e^- \qquad (3.1)$$

In stagnant water the oxygen concentration at the metal surface decreases as a result of corrosion (Tronstad and Veimo 1940 and Obrecht and Pourbaix 1967). If the concentration of dissolved copper or oxygen is plotted versus time, it can be seen that the corrosion rate slows when the oxygen concentration decreases (Figure 3.2).

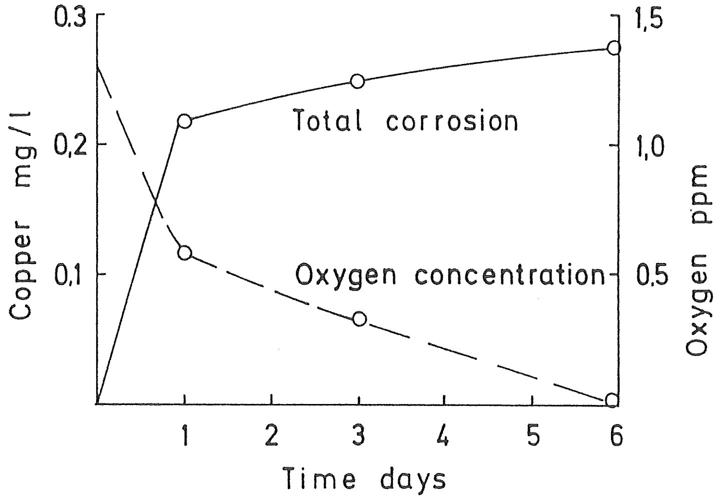

Figure 3.2 Dissolved copper versus time as a function of oxygen concentration (Obrecht and Pourbaix 1967).

Phase 3. When oxygen concentration is limited

After prolonged corrosion the oxygen concentration at the metal surface and through the precipitated deposits may approach or reach zero. The oxygen concentration in the water bulk is also low at this time (Figure 3.3).

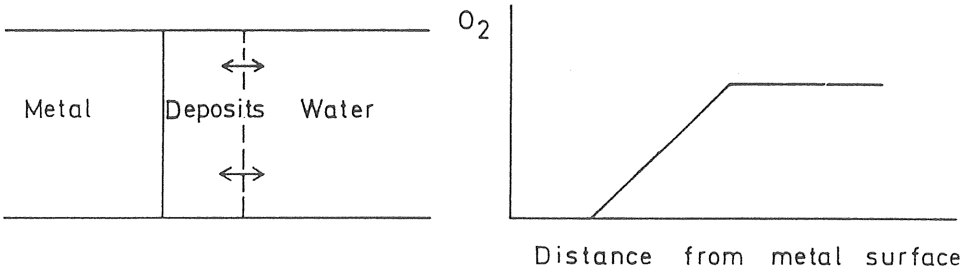

Figure 3.3 The oxygen concentration near the metal surface with precipitated deposits (Hilburn 1983).

Continued corrosion is dependent on the diffusion of oxygen from the bulk solution to the deposits and then through the deposits to the metal surface.

If the oxygen concentration at the metal surface is near zero the corrosion products may be redissolved, which results in an increase in copper concentration. The metal surface is no longer covered and, when the water is exchanged with water having a higher oxygen content, corrosion continues according to Phase 1 (initial corrosion).

The rate of redissolution of corrosion products and formation of other products is dependent on the pH and carbon dioxide concentration in the water.

3.4.2 Importance of pH on copper corrosion

Many studies show that pH is an important parameter for copper corrosion, one example is shown in Figure 3.4 (Cox and Dillon 1980). When the pH is below 6, a substantial increase in corrosion rate occurs. The corrosion rate also increases above pH 10 (Tronstad and Veimo 1940, Gilbert 1966, Meyer 1981, Hilburn 1983, Vik and Bjerkelund 1985 and Cruse et al. 1985).

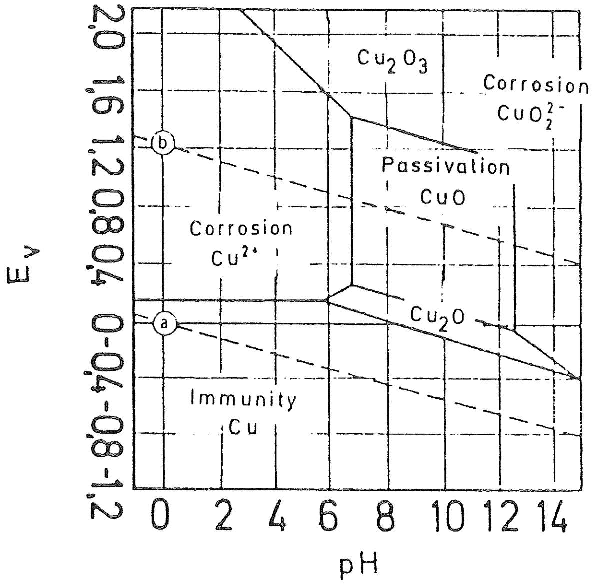

Figure 3.4 Dissolved copper in mg l^{-1} versus pH (Cox and Dillon 1980).

In corroded copper pipes the copper species, Cu^{2+}, Cu_2O, CuO and $Cu(OH)_2$ are found, depending on pH and redox potential, according to the Pourbaix' diagram (Obrecht and Pourbaix 1967) shown in Figure 3.5.

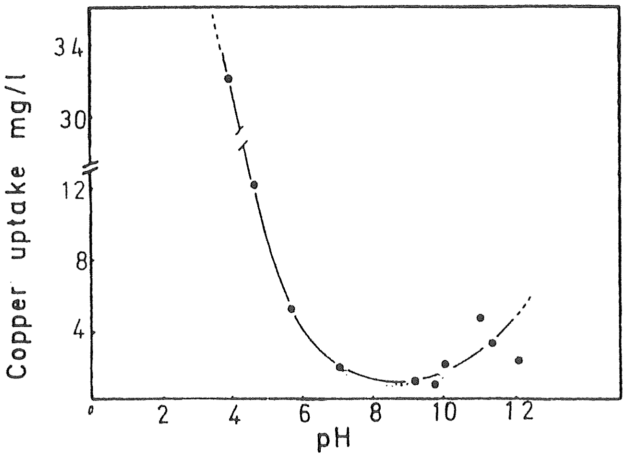

Figure 3.5 Pourbaix diagram over the system $Cu\text{-}H_2O$ (Obrecht and Pourbaix 1967).

$Cu(OH)_2$ has the highest solubility, followed by CuO and Cu_2O, the latter being the most stable (Tronstad and Veimo 1940 and Obrecht and Pourbaix 1967). Both Tronstad and Veimo (1940) and

Hilburn (1983) found that CuO exists at a lower pH than Cu_2O. But the Pourbaix diagram shows that Cu_2O exists in a weakly oxidising environment at pH values between 6 and 12. Sunda and Hansson (1979) have shown that the concentration of free Cu^{2+} decreases due to complex formation when pH increases.

3.4.3 Effect of carbonic acid, hydrogen carbonate, carbonate and calcium on copper corrosion

In a water containing a high concentration of total carbonic species (carbonic acid, hydrogen carbonate and carbonate) at pH 7-9, hydrogen carbonate (HCO_3^-) dominates. Under these conditions the compound $CuCO_3 \cdot Cu(OH)_2$ may be formed. This compound is more stable than CuO, especially at acid pH (Stumm and Morgan 1981), as shown in Figure 3.6. The amount of free Cu^{2+} in relation to total copper concentration changes, depending on hydrogen carbonate concentration and pH (Table 3.3).

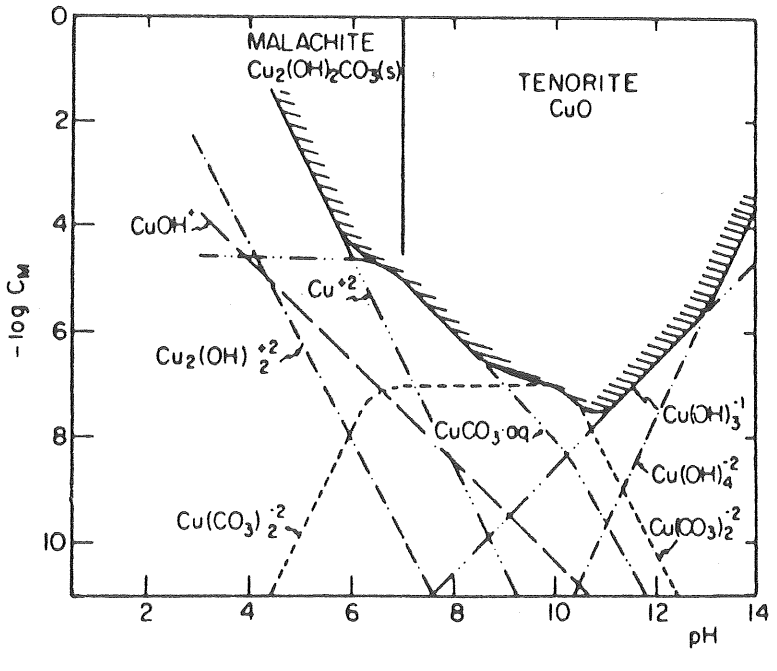

Figure 3.6 The solubility of $CuCO_3 \cdot Cu(OH)_2$ and CuO versus pH (Stumm and Morgan 1981). $C_T = 10^{-2}M$.

Table 3.3 The relationship between free Cu^{2+} and total Cu in per cent at different pH values and hydrogen carbonate concentrations. (Snoeyink and Jenkins 1980).

	HCO_3^- concentration, mg l^{-1}		
pH	30	60	152
7	25	14	9
7.5	11	6	3
8	-	2	0.9

Table 3.3 shows that the amount of dissolved Cu^{2+} decreases with an increasing concentration of hydrogen carbonate and increasing pH, which implies that less $CuCO_3{\cdot}Cu(OH)_2$ can be formed in the presence of carbonate and hydroxide complexes. The Pourbaix diagram for the system copper-hydrogen carbonate versus pH demonstrates the latter point (Figure 3.7).

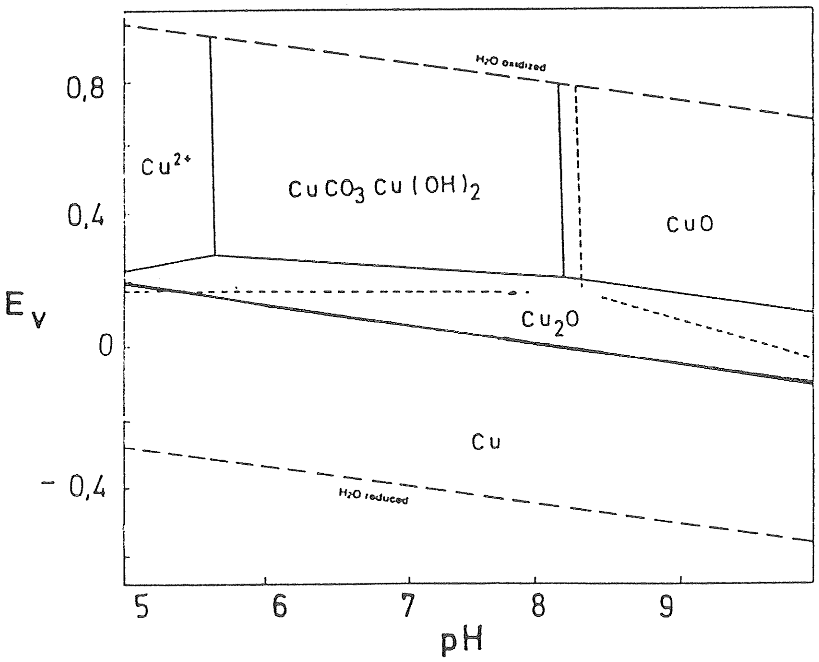

Figure 3.7 Pourbaix diagram for the system $Cu\text{-}H_2O$ - HCO_3, 1.0 mg l^{-1} dissolved copper and 61 mg l^{-1} total carbonic species as HCO_3^- (Pisigan and Singley 1987).

An investigation by Pisigan and Singley (1987) did not show any difference in copper corrosion rate at different alkalinities.

There is disagreement in the literature regarding the importance of the impact of carbonic acid/carbon dioxide on corrosion rate. An increase of CO_2 at constant pH increases the possibility of precipitation of $CuCO_3 \cdot Cu(OH)_2$ on the metal surface (Kristiansen 1977). Due to the lower protection provided by $CuCO_3 \cdot Cu(OH)_2$ compared to Cu_2O, the corrosion rate also increases with increasing CO_2 (Figure 3.8). At increased CO_2 concentration the dissolved copper concentration increases, while the partitioning of copper in the deposits is constant (Kristiansen 1982). Obrecht and Pourbaix (1967) state that cuprosolvency increases by a factor of 10 in the presence of CO_2. Cruse et al. (1985), however, stated that CO_2 does not have any influence on the corrosion rate. These inconsistent findings can be accounted for

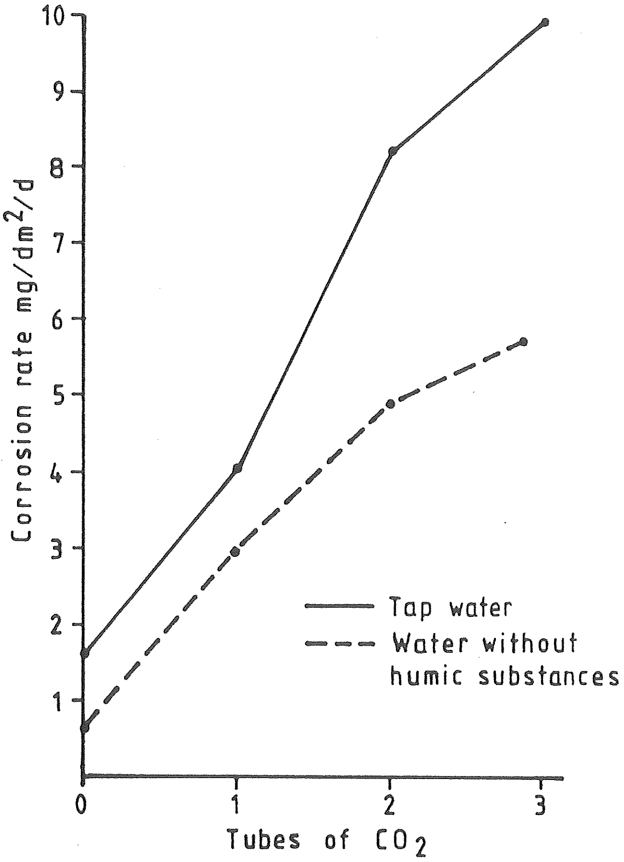

Figure 3.8 Corrosion rate as a function of relative carbon dioxide additions with and without any organic matter, from Kristiansen (1977).

by poor experimental control of pH. It is difficult to control CO_2 concentration and hold other parameters stable. For example additions of carbonic acid also decrease the pH, which in turn affects corrosion.

When the concentration of calcium and total carbonic species are high, in combination with a high pH, the solubility product of calcium carbonate is exceeded and it may precipitate. In the cathodic reaction OH^- forms and the resulting pH increase results in the precipitation of $CaCO_3$ according to equations (3.15) and (3.16):

$$HCO_3^- + OH^- \rightarrow CO_3^{2-} + H_2O \qquad (3.15)$$

$$Ca^{2+} + CO_3^{2-} \rightarrow CaCO_3(s) \qquad (3.16)$$

von Franqué et al. (1975) and Gilbert (1976) found that the precipitation of $CaCO_3$ increases the risk of pitting corrosion. Pisigan and Singley (1987) found $CuCO_3 \cdot Cu(OH)_2$ instead of $CaCO_3$ when the Langlier index (LI) was +0.33 (definition of LI in Section 7.8). $CaCO_3$ could be in an amorphous phase or not precipitated under the test conditions.

The morphology and structure of the precipitation determines the amount of protection. If the surface is not covered by highly crystalline $CaCO_3$ or other corrosion products it will be susceptible to corrosion. A steady state condition between precipitation and dissolution of $CaCO_3$ will be established (Stumm and Morgan 1981). Tronstad and Veimo (1940) as well as Elzenga (1986) also found that a higher concentration of calcium and hydrogen carbonate leads to increased corrosion.

3.4.4 Influence of chloride and sulphate on copper corrosion

The influence of chloride (Cl^-) and sulphate (SO_4^{2-}) on copper corrosion has been investigated by several workers (Lucey 1967, Mattsson and Fredriksson 1968, Obrecht and Pourbaix 1967, Lihl and Klamet 1969, Cornwell 1973, von Franqué 1972, 1975, 1978, Cox and Dillon 1980 and Linder 1982). Chloride is especially important for corrosion. The chloride ion has a small ionic radius and can easily penetrate deposits and can also easily form copper complexes which give the result that even a low concentration of chloride may lead to an increased corrosion under deposits.

The reaction (eq. 3.17-3.18) between copper and chloride leads to the formation of CuCl which reacts with water to form Cu_2O. Release of chloride results in decreased pH. Continued corrosion takes place underneath the deposit according to the cathodic reaction, shown in equation (3.19), CuCl will precipitate if pH < 3-4 (Cornwell et al. 1973) as shown in Figure 3.9.

$$Cu^+ + Cl^- \rightarrow CuCl \qquad (3.17)$$

$$2CuCl + H_2O \rightarrow Cu_2O + 2H^+ + 2Cl^- \qquad (3.18)$$

$$2H^+ + 2e^- \rightarrow H_2 \qquad (3.19)$$

Mattsson and Fredriksson (1968) and Mattsson (1980) showed that the ratio of sulphate to hydrogen carbonate content of the water affects pitting corrosion (type II). They stated that a high pH and a high HCO_3^-/SO_4^{2-} ratio would lead to a reduction in pitting corrosion. The presence of sulphates in the precipitation products indicates a low pH at the metal surface, since copper sulphate can only exist at low pH (see diagram in Figure 3.9).

Linder (1982) explains this as a localised attack of type III corrosion. Obrecht and Pourbaix (1967) have made an Pourbaix diagram for the system $Cu-CO_2-SO_4^{2-}-Cl^--H_2O$ which shows possible precipitation reactions at various pH values (Figure 3.9).

Obrecht and Pourbaix (1967) state that a small increase of chloride or sulphate concentration increases both uniform and pitting corrosion. von Franqué (1972), von Franqué et al. (1975) and von Franqué (1978) stated that high concentrations of calcium and hydrogen carbonate and/or low pH, in combination

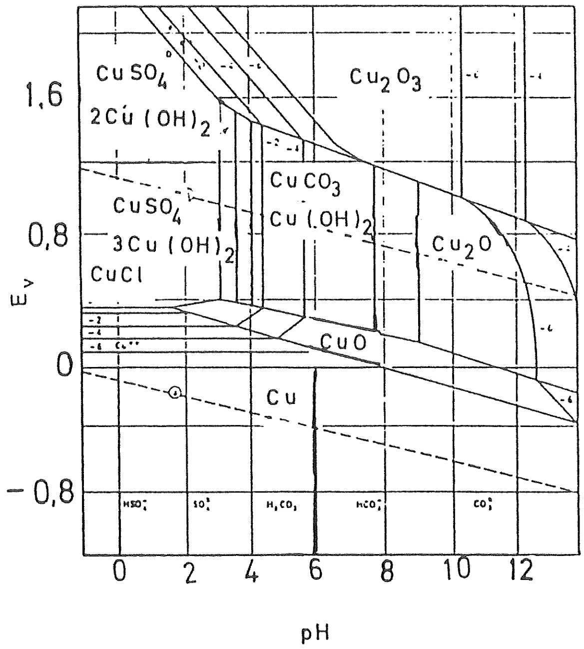

Figure 3.9 Pourbaix diagram for the system $Cu-CO_2-SO_4^{2-}-Cl^--H_2O$ (Obrecht and Pourbaix 1967).

with chloride and sulphate lead to deep pits. In an investigation by Stone et al. (1987) it was found that an increased concentration of either chloride or sulphate increased the corrosion rate. But an addition of hydrogen carbonate at increased chloride or sulphate concentration reduces the corrosion rate increase.

However, an investigation by Cox and Dillon (1980) demonstrated that an increased concentration of chloride does not affect cuprosolvency.

3.4.5 Influence of organic matter on corrosion and formation of protective layers

Organic matter may form complexes with copper ions in water and change the morphology of precipitates.

The Cu^{2+} ion forms complexes with organic substances, which retain the copper in solution and therefore no corrosion products precipitate (Sunda and Hansson 1979). However, the corrosion rate increases with an increase in organic matter (Kristiansen 1977 and 1982), as shown in Figures 3.8 and 3.10.

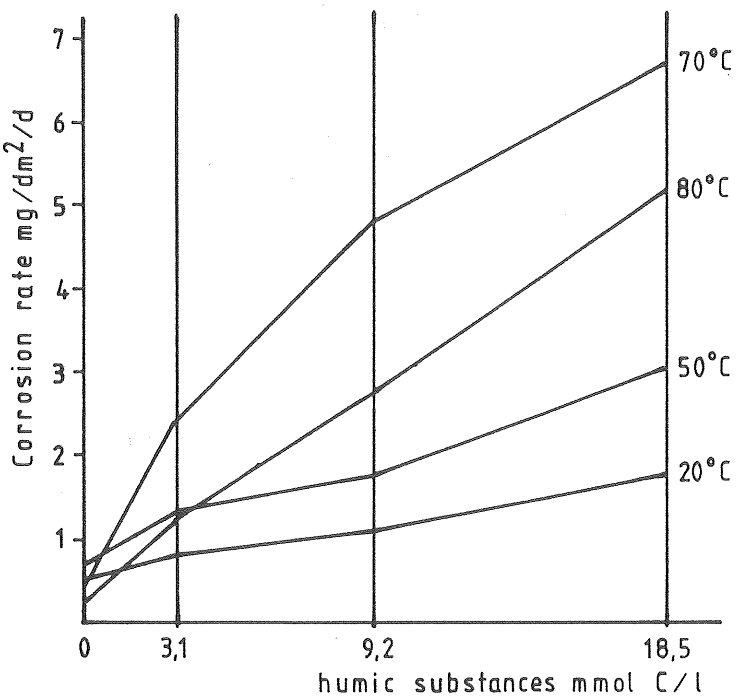

Figure 3.10 Corrosion rate as a function of organic carbon, from Kristiansen (1982).

Organic matter also affects the precipitation of $CaCO_3$ (Rudek 1979) by adsorption on the calcium carbonate crystal. Campbell and Turner (1980) found $CaCO_3$ to precipitate either as "nodules" or as "eggshells" on the metal surface, depending on the temperature and the content of organic matter in the water. Nodular precipitation does not provide a working protective layer. The "eggshell" $CaCO_3$ precipitation presumably incorporates organic colloidal matter (Campbell and Turner 1980).

Pliefke (1979) mentioned that when organic compounds were added to the water the corrosion rate decreased. This was shown by using organic compounds as inhibitors.

3.4.6 Influence of added inhibitors on copper corrosion

Inhibitors, such as phosphate and silicate are often added to water in order to reduce corrosion.

Meyer (1981) found that the corrosion rate declined after 6-12 months when no phosphate was used but with phosphate addition the corrosion rate declined immediately to a low but constant level (Figure 3.11). Ryder and Wagner (1985) showed that orthophosphate decreased the corrosion rate while polyphosphate increased the corrosion rate. Silicates have no effect on the corrosion rate of copper (Ryder and Wagner 1985).

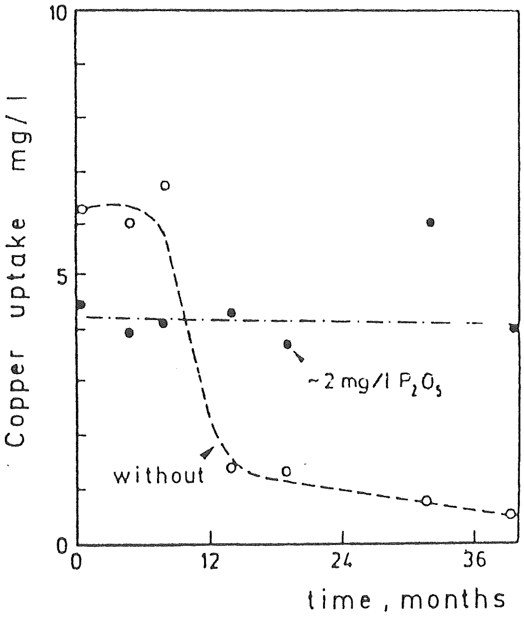

Figure 3.11 Corrosion rate with and without phosphates added, from Meyer (1981).

3.5 Conclusion of copper corrosion

Internal uniform corrosion and formation of corrosion products depend on the surrounding environment. Formation of an effective protective layer minimises corrosion by decreasing the diffusion of oxygen to the metal surface.

The effective layer may consist either of corrosion products or of species from the the water or of combinations of corrosion products and precipitated species from the water.

In the literature Cu_2O, CuO, $Cu(OH)_2$ and $CuCO_3 \cdot Cu(OH)_2$ have been mentioned as corrosion products that can precipitate and form protective layers (Figures 3.5 and 3.7). Cu_2O is the most stable product. This product will theoretically be formed when the water is oxidised at a pH value between six and twelve and when the content of calcium, total carbonic species and organic matter are low. Under highly oxidising conditions CuO will form instead of Cu_2O. CuO is less protective than Cu_2O but is almost as stable. When the pH is either under six or above twelve, neither of these compounds exist and therefore no protective layer can be formed.

If the content of total carbonic species is increased, $CuCO_3 \cdot Cu(OH)_2$ will form within a pH interval of six to eight. This corrosion product does *not* have the same protective properties as Cu_2O and CuO.

When calcium is found in water with a high content of total carbonic species and at a high pH, $CaCO_3$ will precipitate. $CaCO_3$ must be highly crystalline and completely cover the copper surface if it is to act as a protective layer. If $CaCO_3$ does not cover the surface then the $CaCO_3$ precipitation will contribute to an increased corrosion rate.

In water with natural organic matter or salts, complex formation may result in a low concentration of free copper ion and hence no precipitation of copper corrosion products takes place. This results in a high corrosion rate.

3.6 Conceivable corrosion reactions and protective layer formation

From the literature one can see that the most important parameters involved in the avoidance of corrosion and the formation of protective layers are pH, oxygen and total carbonic species.

In order to explain what happens in different water compositions, six different cases are studied theoretically (Table 3.4).

It has been assumed that the corrosion processes start from a water saturated with oxygen. The oxygen is consumed as the corrosion process proceeds.

Table 3.4 Six water compositions as a base to explain the model for conceivable corrosion reactions and protective layer formation.

Case 1	Low content of total carbonic acid	low pH (pH<6.5)
2	- " -	medium pH (6.5<pH<9)
3	- " -	high pH (pH>9)
4	High content of total carbonic acid	low pH (pH<6.5)
5	- " -	medium pH (6.5<pH<9)
6	- " -	high pH (pH>9)

<u>Case 1</u>: (Typical for acid ground water in west Sweden)

In this case the following occurs with one anodic and one cathodic reaction as primary reactions and a secondary reaction where Cu^+ reacts with the water.

Primary reactions

Anode $Cu^0 \rightarrow Cu^+ + e^-$ (3.1)

Cathode $\frac{1}{2}O_2 + 2H^+ + 2e^- \rightarrow H_2O$ (3.20)

Secondary reaction

$$2Cu^+ + H_2O \rightleftarrows Cu_2O + 2H^+ \quad (3.6)$$

The cathodic reaction is a sum of equations (3.21) and (3.22), (Hilburn 1983).

$$O_2 + 2H^+ + 2e^- \rightarrow H_2O_2 \qquad (3.21)$$

$$H_2O_2 + 2H^+ + 2e^- \rightarrow 2H_2O \qquad (3.22)$$

In the initial reactions, equations (3.1), (3.20) and (3.6), Cu^+ is free but it is also possible for Cu^0 to convert to Cu_2O immediately and this results in a passive protective layer. However, if Cu^+ is free in the water it may oxidise to Cu^{2+} and avoid Cu_2O formation (equations 3.7 and 3.20).

Anode $4Cu^0 + \frac{1}{2}O_2 + H_2O \rightarrow 2Cu_2O + 2H^+ + 2e^-$ (3.7)

Cathode $\frac{1}{2}O_2 + 2H^+ + 2e^- \rightarrow H_2O$ (3.20)

If Cu_2O forms it will be dissolved at the anode (equation 3.9) when oxygen is present.

$$Cu_2O + 2H^+ \rightleftarrows 2Cu^{2+} + H_2O + 2e^- \qquad (3.9)$$

$$\frac{1}{2}O_2 + 2H^+ + 2e^- \rightarrow H_2O \qquad (3.20)$$

Cu_2O could also be dissolved in a low pH environment where equation (3.6) is driven to the left.

Oxygen is the driving force for corrosion and when the oxygen concentration at the metal surface decreases, corrosion also decreases. In waters containing a low concentration of oxygen the copper ions exist as Cu^+ (Tronstad and Veimo 1940) according to equation (3.4).

$$Cu^{2+} + Cu^0 \rightarrow 2Cu^+ \qquad (3.4)$$

Dissolution of Cu_2O (equation 3.9) may provide a local increase in pH leading to a CuO precipitation that is stable above pH 7 (equation 3.13). During the latter reaction pH is locally decreased and CuO redissolved. According to Obrecht and Pourbaix (1967) Cu^{2+} is the most common corrosion product at pH below six.

$$Cu^{2+} + H_2O \rightleftarrows CuO + 2H^+ \qquad (3.13)$$

The corrosion reactions, at low pH and low content of total carbonic species, result in no increase in pH and Cu^{2+} dissolved in the water.

Case 2: (Typical for treated drinking water in west Sweden)

In Case 2 the reactions corresponding to those in Case 1 take place. The only exception is that OH^- instead of H_2O is formed at the cathode.

Anode $$Cu^0 \rightarrow Cu^+ + e^- \qquad (3.1)$$

Cathode $$\tfrac{1}{2}O_2 + H_2O + 2e^- \rightarrow 2OH^- \qquad (3.3)$$

Formation of Cu_2O takes place according to the following reaction

$$2Cu^+ + H_2O \rightleftarrows Cu_2O + 2H^+ \qquad (3.6)$$

According to Cruse et al. (1985) the following reaction, equation (3.7), takes place at pH > 6, resulting in the formation of Cu_2O.

Anode $$4Cu^0 + \tfrac{1}{2}O_2 + H_2O \rightarrow 2Cu_2O + 2H^+ + 2e^- \qquad (3.7)$$

Cathode $$\tfrac{1}{2}O_2 + H_2O + 2e^- \rightarrow 2OH^- \qquad (3.3)$$

All the reactions give constant pH, and the H^+ formed reacts with OH^- formed. Higher pH retards the copper dissolution, as previously mentioned. The Cu_2O formed is not as readily dissolved as in Case 1, since the H^+-concentration is lower than in Case 1. When the oxygen concentration at the metal- or oxide-surface decreases, the reactions stop and Cu_2O remains as a protective layer.

At medium pH and low content of total carbonic species there will be no change in pH and protective layer of Cu_2O on the metal surface.

Case 3: (Typical for ground water treated by dolomitic filters)

In Case 3 the reactions correspond to those in Case 1 and 2

Anode $Cu^0 \rightarrow Cu^+ + e^-$ (3.1)

Cathod $\frac{1}{2}O_2 + H_2O + 2e^- \rightarrow 2OH^-$ (3.3)

Cu_2O is formed according to equation (3.6) or also according to equation (3.7) or (3.23) (Cruse et al. 1985). The latter reaction takes place when the oxygen content is limited.

$$2Cu^+ + H_2O \rightleftarrows Cu_2O + 2H^+ \qquad (3.6)$$

$$4Cu^0 + \tfrac{1}{2}O_2 + H_2O \rightleftarrows 2Cu_2O + 2H^+ + 2e^- \qquad (3.7)$$

Anode $2Cu^0 + 2OH^- \rightleftarrows Cu_2O + H_2O + 2e^-$ (3.23)

Cathode $\frac{1}{2}O_2 + H_2O + 2e^- \rightarrow 2OH^-$ (3.3)

Cu(II) as soluble species is favoured at $pH > 9.5$ (Sunda and Hansson 1979), which means that reactions according to equation (3.7) and (3.23) may not take place. In the presence of Cu(II) in an oxygen rich environment $Cu(OH)_2$ can be formed instead according to equation (3.14), with equation (3.1) as anode.

$$Cu^{2+} + \tfrac{1}{2}O_2 + H_2O + 2e^- \rightarrow Cu(OH)_2 \qquad (3.14)$$

At even higher pH, although uncommon in drinking water, $Cu(OH)_2$ is dissolved and $Cu(OH)_x$-complexes are formed, where $x > 2$ (Stumm and Morgan 1981). $Cu(OH)_2$ is not a stable product and has not been identified on a copper surface (Obrecht and Pourbaix 1967). However, CuO is formed according to equation (3.13). In this case the formed H^+ is mopped up by the high OH^- concentrations in the water and CuO remains on the metal surface

$$Cu^{2+} + H_2O \rightleftarrows CuO + 2H^+ \tag{3.13}$$

Therefore case 3 results in either CuO or Cu_2O on the surface or copper as complexes in solution at very high pH.

Case 4: (Typical for ground water in medium hard water areas)

When the content of total carbonic species is high and the pH is < 6.5 the presence of carbonic acid dominates according to equation (3.24).

$$HCO_3^- + H^+ \rightleftarrows H_2CO_3 \rightleftarrows H_2O + CO_2 \tag{3.24}$$

The primary reactions are the same as in Case 1.

Anode $$Cu^0 \rightarrow Cu^+ + e^- \tag{3.1}$$

Cathode $$\tfrac{1}{2}O_2 + 2H^+ + 2e^- \rightarrow H_2O \tag{3.20}$$

The secondary reaction:

$$2Cu^+ + H_2O \rightleftarrows Cu_2O + 2H^+ \tag{3.6}$$

According to Cruse et al. (1985) Cu_2O formation takes place in the following way

Anode $$4Cu^0 + \tfrac{1}{2}O_2 + H_2O \rightarrow 2Cu_2O + 2H^+ + 2e^- \tag{3.7}$$

Cathode $$\tfrac{1}{2}O_2 + 2H^+ + 2e^- \rightarrow H_2O \tag{3.20}$$

The presence of carbon dioxide may redissolve copper (Tronstad and Veimo 1940, Ives and Rawson 1982). Copper metal can be dissolved by carbonic acid according to a reaction suggested by Ives and Rawson (1982), equation (3.25).

$$Cu^0 + H_2O + 2CO_2 + \tfrac{1}{2}O_2 \rightleftarrows Cu(HCO_3)_2 \qquad (3.25)$$

The formed $Cu(HCO_3)_2$ is immediately transformed to $CuCO_3 \cdot Cu(OH)_2$

$$Cu(HCO_3)_2 \rightleftarrows \tfrac{1}{2}(CuCO_3 \cdot Cu(OH)_2) + \tfrac{1}{2}H_2O + 1\tfrac{1}{2}CO_2 \qquad (3.11)$$

Initial corrosion is faster than in Case 1 due to the influence of carbonic acid (equation 3.24). Corrosion ceases when the supply of oxygen is limited. At $pH < 8.6$, $CuCO_3 \cdot Cu(OH)_2$ is the stable precipitation product (Obrecht and Pourbaix 1967). During formation of this product, carbon dioxide is again formed. Carbon dioxide in the bulk solution may dissolve Cu_2O according to equation (3.10).

$$\tfrac{1}{2}Cu_2O + H_2O + 2CO_2 + \tfrac{1}{4}O_2 \rightleftarrows Cu(HCO_3)_2 \qquad (3.10)$$

The result will be the same as in reactions (3.25) and (3.11). The formed $Cu(HCO_3)_2$ could also be converted to CuO (Ives and Rawson 1982), equation (3.26).

$$Cu(HCO_3)_2 \rightleftarrows CuO + H_2O + 2CO_2 \qquad (3.26)$$

Low pH also causes formed Cu_2O to redissolve to either Cu(I) or Cu(II) according to equation (3.6), (Hilburn 1983) and equation (3.9), (Cruse et al. 1985) when oxygen is present.

$$Cu_2O + 2H^+ \rightleftarrows 2Cu^+ + H_2O \qquad (3.6)$$

$$Cu_2O + 2H^+ \rightleftarrows Cu^{2+} + H_2O + 2e^- \qquad (3.9)$$

$$\tfrac{1}{2}O_2 + 2H^+ + 2e^- \rightarrow H_2O \qquad (3.20)$$

The low pH also dissolves CuO and $CuCO_3 \cdot Cu(OH)_2$ precipitations to Cu^{2+}, according to equations (3.13) and (3.27), when the oxygen concentration is limited.

$$CuO + 2H^+ \rightleftarrows Cu^{2+} + H_2O \qquad (3.13)$$

$$CuCO_3 \cdot Cu(OH)_2 + 4H^+ \rightleftarrows 2Cu^{2+} + 3H_2O + CO_2 \qquad (3.27)$$

The result of Case 4 is a low pH with a high copper concentration in the water. At pH < 6, Cu(II) is most commonly found, (Stumm and Morgan 1981). Analysis of the water before the oxygen is consumed will result in a higher copper content than in Case 1 but after all oxygen is consumed the copper content should be the same.

Case 5: (Typical for south Sweden)

In the pH interval 6,5-9 most of the carbonic species exist as hydrogen carbonate (HCO_3^-). The reactions taking place are:

Primary reactions:

Anode $Cu^0 \rightarrow Cu^+ + e^-$ (3.1)

Cathode $\frac{1}{2}O_2 + H_2O + 2e^- \rightarrow 2OH^-$ (3.3)

Secondary reaction:

$$2Cu^+ + H_2O \rightleftarrows Cu_2O + 2H^+ \qquad (3.6)$$

or if Cu_2O is formed immediately (Cruse et al. 1985)

Anode $2Cu^0 + OH^- \rightarrow Cu_2O + H_2O + 2e^-$ (3.7)

Cathode $\frac{1}{2}O_2 + H_2O + 2e^- \rightarrow 2OH^-$ (3.3)

Cu_2O may, as in Case 4, be redissolved depending on the carbonic species concentration, (Ives and Rawson 1982).

$$\tfrac{1}{2}Cu_2O + H_2O + 2CO_2 + 1/4O_2 \rightleftarrows Cu(HCO_3)_2 \qquad (3.10)$$

At high oxygen concentrations $CuCO_3 \cdot Cu(OH)_2$ may be formed immediately according to equation (3.11), (Ives and Rawson 1982).

$$Cu(HCO_3)_2 \rightleftarrows \tfrac{1}{2}(CuCO_3 \cdot Cu(OH)_2) + \tfrac{1}{2}H_2O + 1\tfrac{1}{2}O_2 \qquad (3.11)$$

When the oxygen decreases in concentration the anodic and cathodic reactions stop and Cu_2O and $CuCO_3 \cdot Cu(OH)_2$ remain as a protective layer. At higher total carbonic species concentration and unchanged pH, the Cu(II)-concentration decreases in relation to the total copper ion concentration, while Cu(I) exists in solution and forms Cu_2O.

Consequently, in this case protective layers form which consist of, depending on the oxygen content, Cu_2O or $CuCO_3 \cdot Cu(OH)_2$ with some Cu(I) and Cu(II) dissolved. However, the share of Cu(II) is lower than at corresponding pH with lower total carbonic species content. An increase in total carbonic species content results in less $CuCO_3 \cdot Cu(OH)_2$ formation to Cu_2O. Since $CuCO_3 \cdot Cu(OH)_2$ is not as dense as Cu_2O, corrosion might continue when $CuCO_3 \cdot Cu(OH)_2$ is formed.

Case 6: (Typical for water treated with a dolomitic filter)

In this case there is no significant difference from Case 3, except that at high pH most of the total carbonic species exist as carbonate (CO_3^{2-})

$$HCO_3^- + OH^- \rightleftarrows CO_3^{2-} + H_2O \qquad (3.28)$$

The anodic and cathodic reaction will then be similar to the other cases:

Primary reactions

Anode $Cu^0 \rightarrow Cu^+ + e^-$ (3.1)

Cathode $\frac{1}{2}O_2 + H_2O + 2e^- \rightarrow 2OH^-$ (3.3)

Secondary reaction

$$2Cu^+ + H_2O \rightarrow Cu_2O + 2H^+ \quad (3.6)$$

From the presentation in Case 3, Cu(II) is favoured at pH > 9.5 which makes it difficult for Cu_2O formation. The Cu(II) reacts with CO_3^{2-} and forms complexes according to equation (3.29) and (3.30), (Sunda and Hanson 1979).

$$Cu^{2+} + CO_3^{2-} \rightleftarrows CuCO_3\ (aq) \quad (3.29)$$

$$Cu^{2+} + 2CO_3^{2-} \rightleftarrows Cu(CO_3)_2^{2-} \quad (3.30)$$

While oxygen still remains, Cu(II) and oxygen react to form $Cu(OH)_2$. At even higher pH, $Cu(OH)_2$ is dissolved by formation of complexes with OH^-, equations (3.14) and (3.31).

$$Cu^{2+} + \frac{1}{2}O_2 + H_2O + 2e^- \rightarrow Cu(OH)_2 \quad (3.14)$$

$$Cu(OH)_2 + nOH^- \rightarrow Cu(OH)_{2+n}^{n-} \quad (3.31)$$

Cu_2O or CuO is the main protective coating. Corrosion continues at very high pH which implies that Cu(II) is found in solution as complexes.

A schematic summary of the corrosion situation and possibilities for protective layer formation from the cases is listed for the different water compositions in Table 3.5.

Table 3.5 Corrosion and protective layer formation situation at different water compositions.

	pH		
	< 6.5	6.5 - 9	> 9
low total carbonic acid content	corrosion Cu^{2+} in water	protection Cu_2O	protection CuO or Cu(II) in water
high total carbonic acid content	corrosion Cu^{2+} in water	protection $CuCO_3 \cdot Cu(OH)_2$ and Cu(I)/Cu(II) in water or Cu_2O	protection CuO or Cu(II) in water

4. SCOPE OF COPPER INVESTIGATION

In order to verify the conceivable corrosion reactions and protective layer formation, investigations concerning the effect of pH, different concentrations of total carbonic species, calcium, chloride and sulphate on uniform internal copper corrosion were made. The concentrations of the species were varied independently.

The values for the parameters and the concentrations of species were chosen as representative for concentrations common in Sweden.

- The pH was varied between 5 and 9.5.
- The content of total carbonic acid was held at either 10, 60 or 100 mg HCO_3^- l^{-1}.
- The calcium content was varied between 1.0 and 35 mg Ca^{2+} l^{-1}.
- Chloride content was varied between 3 and 120 mg Cl^- l^{-1}.
- Sulphate content was varied between 5 and 85 mg SO_4^{2-} l^{-1}.
- The organic content varied between nondetectable (< 1) and 6.0 mg l^{-1}.
- The temperature was regulated in laboratory tests to 15^oC. In the field tests the temperatures varied between 0 and 20^oC.

The investigation was carried out both in the laboratory under controlled conditions and at several water works. In the laboratory a water with a low content of inorganic species as well as organic matter was produced by ion-exchange. To this water chemicals were added to predetermined concentrations. In order to compare the artificial waters with natural waters, several field tests were carried out.

Copper pipes are normally only used in the plumbing system which often has stagnant water and the test system was constructed to simulate the plumbing system.

Two different test systems have been used. One consisted of two copper pipes in series. This was called the "rig test" and was supplied with water automatically for four hours per day. The rest of the day the water was stagnant. The other system, called the "pipe test", consisted of a small copper pipe which was manually emptied and refilled with water once a day. The test water used in the laboratory is presented in Table 4.1.

Table 4.1 Water composition for the two tested systems.

	Rig test	Pipe test
pH	7.5, 8.5, 9.5	5, 6, 7, 8
HCO_3^- mgl^{-1}	10, 100	10, 60, 100
Ca^{2+} mgl^{-1}	2.5, 35	2.5, 15, 30
SO_4^{2-} mgl^{-1}	8, 42.5, 85	20, 100
Cl^- mgl^{-1}	8, 32.5, 65	25

As corrosion processes and the formation of protective layers are very slow processes each water was studied in long term tests for between 70 and 175 days.

A detailed description of the test system and analytical and sampling procedures can be found in Appendix A.

5. RESULTS OF COPPER CORROSION INVESTIGATION

The results presented in this chapter originate from two types of laboratory tests; rig tests and pipe tests. In this study 59 different waters under controlled conditions were used. In addition rig tests were carried out at 15 waterworks. Experimental details are presented in Appendix A.

Some results have been published previously (Hedberg and Johansson 1986a, Hedberg and Johansson 1986b, Johansson and Hedberg 1988).

Corrosion studies normally require several months to reach a steady state. During this time it is important to maintain the water composition constant. This required the preparation of large quantities of standard water (3000 l) once a week.

In the pipe test, two 0.5 m copper pipes were tested for each water. The copper pipes were emptied and refilled once a day and the mean of copper concentration in the water from the two pipes determined by either flame or electrothermal atomic absorption spectrometry. In the rig test, 2.5 m copper pipes were used. The type of corrosion (uniform or pitting) was observed by installing 0.5 m of the copper pipe in a plexiglas pipe. This allowed direct inspection. In the rig the water was allowed to stand for 20 hours with streaming for four hours every day. The copper concentration was measured in the water during the standing period.

Copper concentration was found to increase over the first 30 days, and after reaching a maximum concentration decreased to a background value at about 75 days (Figure 5.1).

The maximum value of copper was, in most cases, reached after 20 to 30 days and therefore the value of copper uptake used in the following discussion is taken from the last week of the test period.

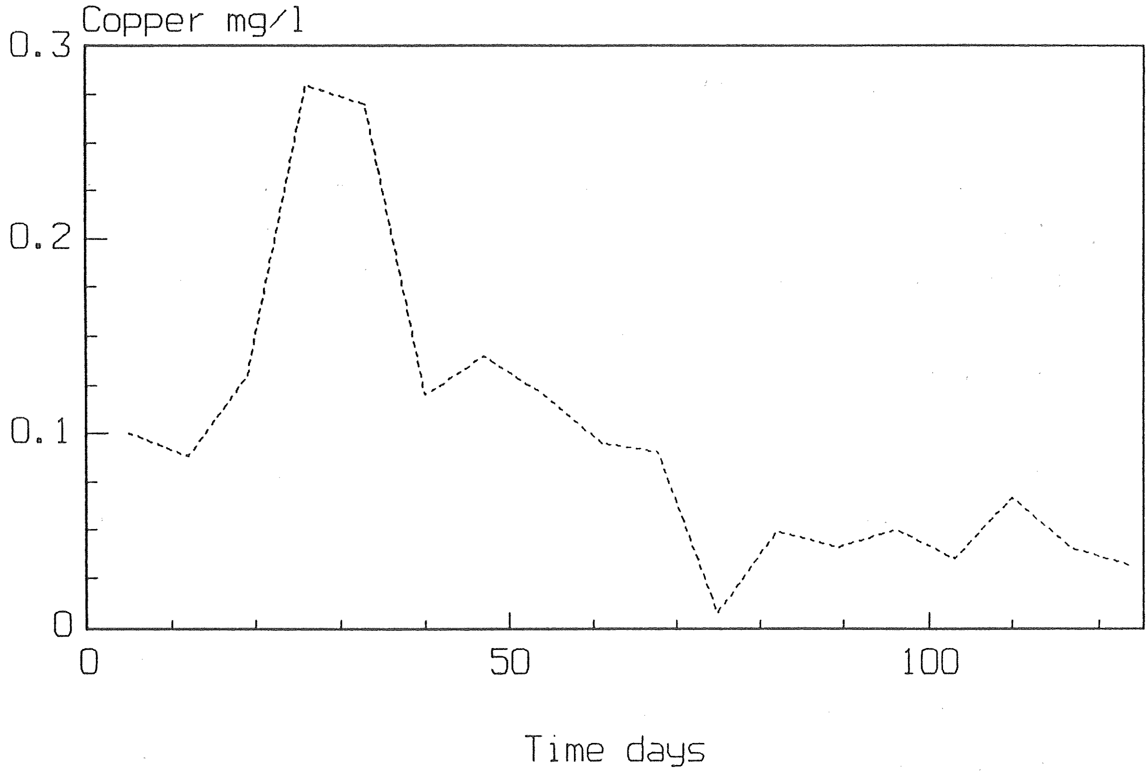

Figure 5.1 Copper concentration versus time typical for rig test.

Oxygen concentration may affect the corrosion rate. Studied waters were saturated with oxygen and the oxygen concentration was measured after the exposure time. In the pipe tests the oxygen concentration varied between 1 and 10 mg O_2 l^{-1}. It is important that the water is not oxygen free as corrosion does not occur in the absence of oxygen. In such a case where oxygen is totally consumed the experimental results would not be meaningful as this rarely occurs in the drinking water network. To stop corrosion, formation of corrosion products must be possible.

As the corrosion reaction consumes oxygen the oxygen concentration can be used as an indirect measure of copper corrosion. This is shown by the anodic (equation 5.1) and cathodic reactions (equation 5.2).

$$Cu \rightarrow Cu^+ + e^- \qquad (5.1)$$

$$\tfrac{1}{2}\, O_2 + H_2O + 2e^- \rightarrow 2OH^- \qquad (5.2)$$

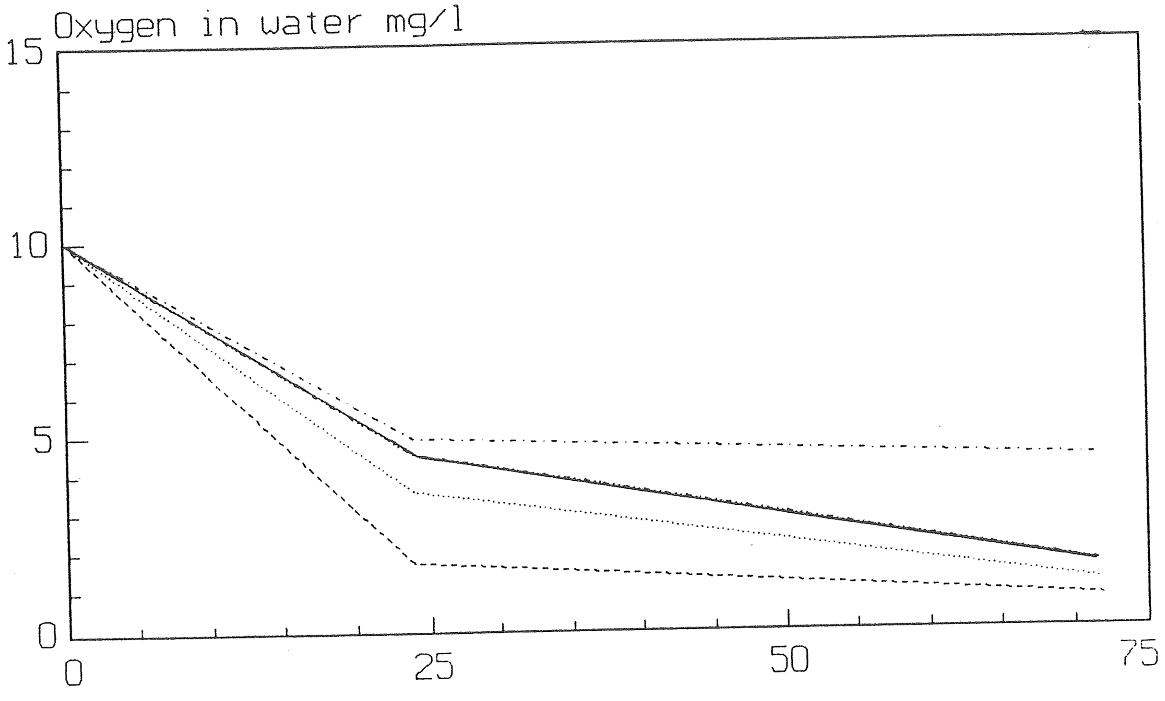

Figure 5.2 Oxygen concentration in pipe tests versus time.
---- pH 5, •••• pH 6, —— pH 7, •-•-• pH 8.

Figure 5.2 shows that the consumption of oxygen by the test rig increases with a decrease in pH, so that at pH 5 the residual oxygen concentration at the end of the experiment is less than 1 mg O_2 l^{-1}. As corrosion rate also increases with a decrease in pH, the theoretical relationship between oxygen consumption and copper corrosion (equations 5.1 and 5.2) is proved experimentally.

Water in direct contact with air and with a temperature of 15°C has a dissolved oxygen concentration of 10.1 mg O_2 l^{-1}. Theoretically this oxygen content can allow the release of 20 mg Cu^{2+} l^{-1} at the anode. A correlation between oxygen in water during the standing period and copper uptake is shown in Figure 5.3. Oxygen was consumed during corrosion, but also during formation of corrosion products such as Cu_2O, CuO and $CuCO_3 \cdot Cu(OH)_2$. The oxygen concentration in water decreased faster at the beginning for 60 mg HCO_3^- l^{-1} than for 10 mg HCO_3^- l^{-1}.

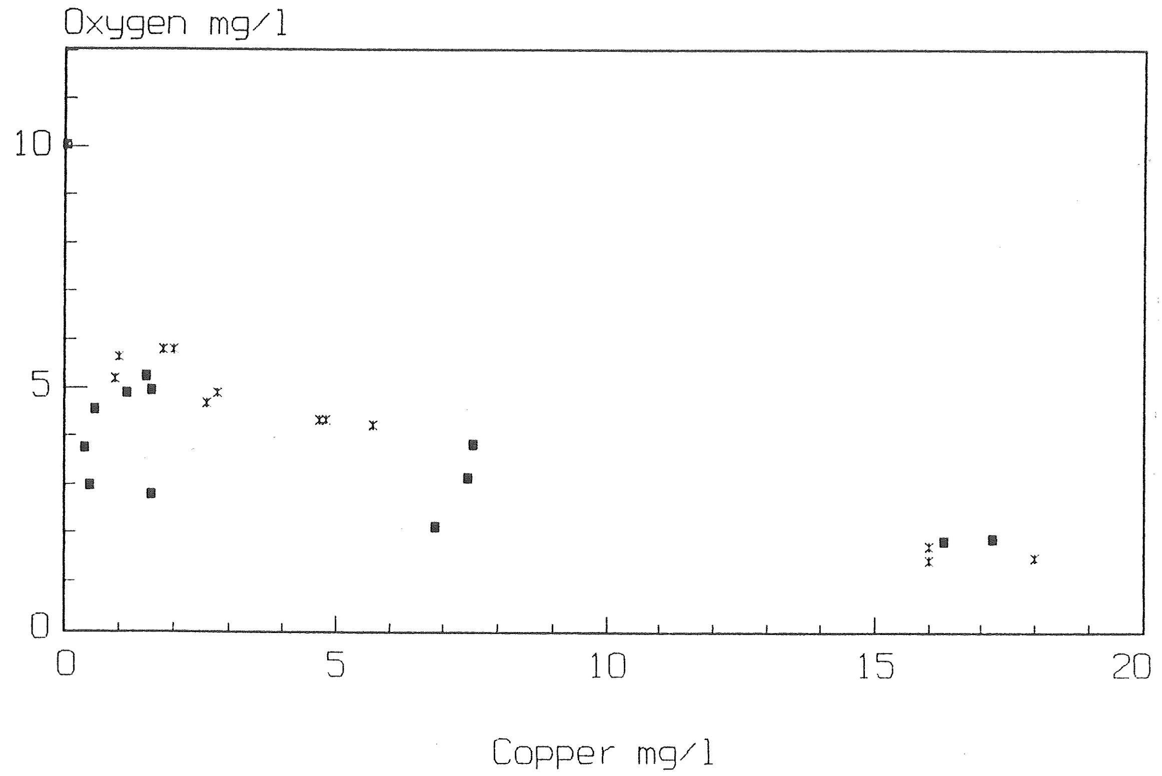

Figure 5.3 Oxygen in water versus copper concentration at (*) 10 mg HCO_3^- l^{-1}, (■) 60 mg HCO_3^- l^{-1} (pH range 5 to 8).

5.1 Importance of pH and concentration of total carbonic species on copper corrosion

In Figure 5.4 all the results obtained from rig tests carried out in the laboratory and at waterworks are plotted. This can be done because the same equipment and test procedures were used for all rig tests. Corresponding results from the pipe tests are shown in Figure 5.5.

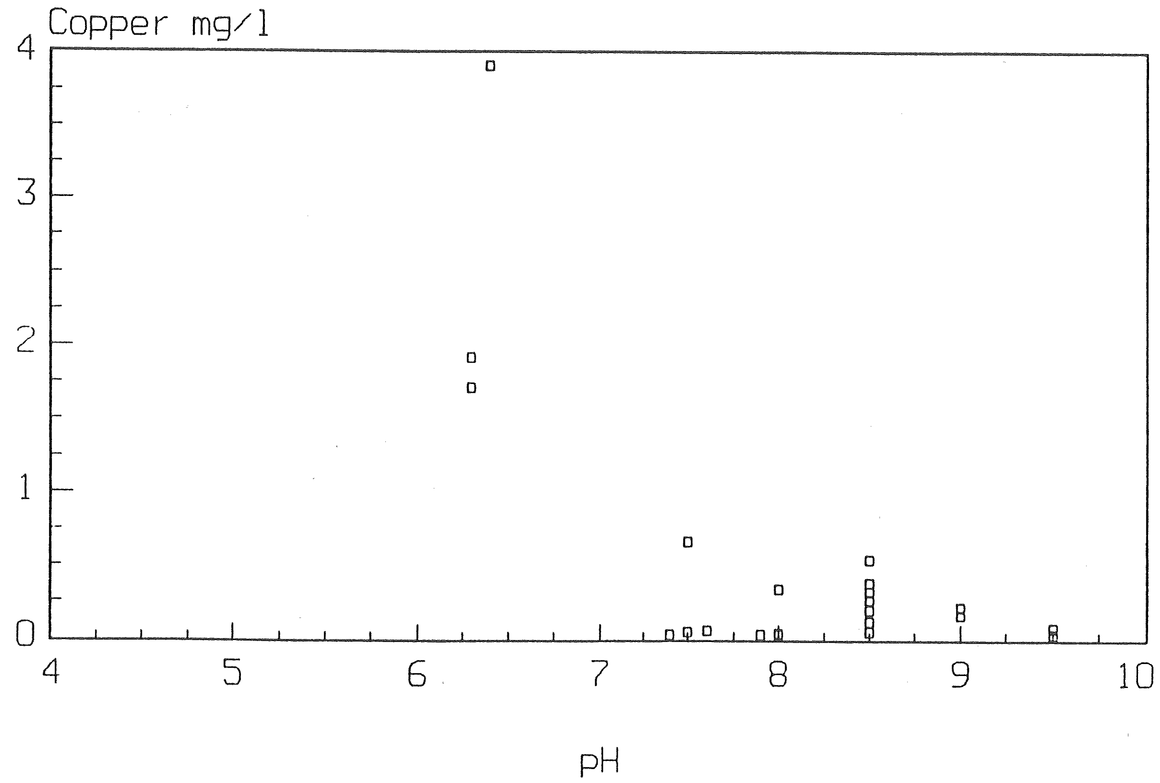

Figure 5.4 Copper concentration from all rig test studies.

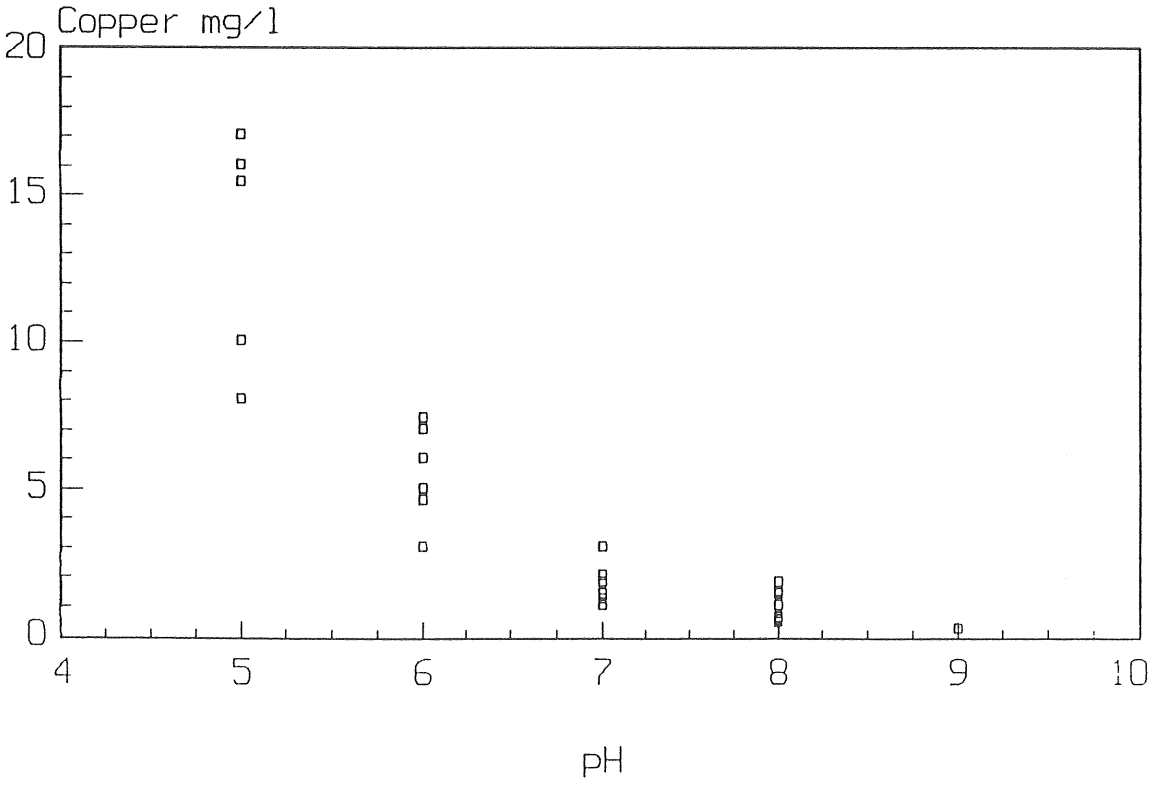

Figure 5.5 Copper concentration from all pipe test studies.

Figures 5.4 and 5.5 clearly demonstrate the effect of pH. This is in agreement with many similar studies which have shown that an increase in pH results in a decrease in cuprosolvency (Tronstad and Veimo 1940, Gilbert 1966, Cox and Dillon 1980, Meyer 1981, Hilburn 1983, Cruse et al 1985 and Vik and Bjerkelund 1985).

However, a significant deviation is observed which is due to other parameters that may affect copper corrosion. In order to study the effect of different parameters it is necessary to isolate the influence of each individual parameter.

In Figure 5.6 the results from a variation in pH and total carbonic species concentration (pH 7.5-9.5 at 10 and 100 mg HCO_3^- l^{-1}) is shown. Clearly an increase in carbonic species concentration increases copper corrosion around pH 7-8. Therefore although pH effects are dominant for copper corrosion below pH 7.0, at more neutral pH values, which are more usual for drinking water in Sweden, carbonic species concentration is more critical for copper corrosion.

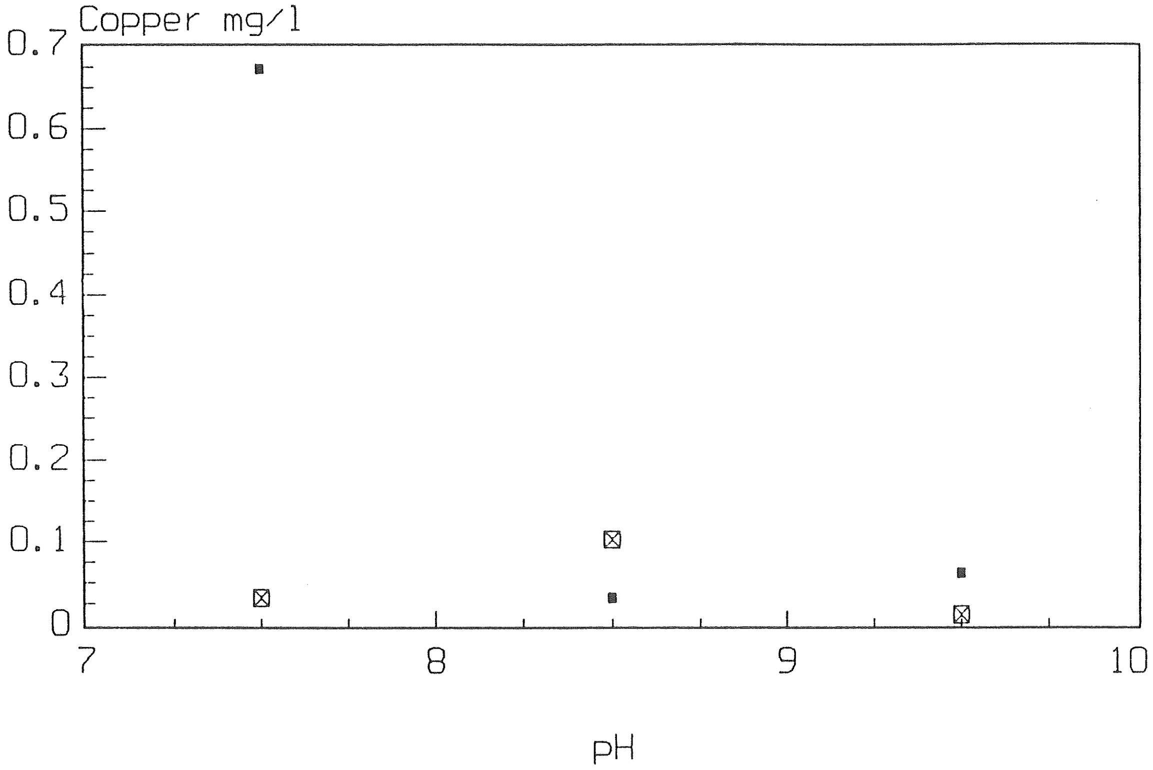

Figure 5.6 Copper concentration versus pH from laboratory rig tests at ⊠ 10 mg HCO_3^- l^{-1}, ■ 100 mg HCO_3^- l^{-1}

Under the test conditions in this study, where contact with the air was unavoidable, it was not possible to satisfactorily separate the individual effects of pH and carbonic species. However, it is suggested that future studies might investigate pH and carbonic species in controlled laboratory tests by the use of pH buffers (other than carbonate) under a nitrogen atmosphere.

In order to explain the copper corrosion results at different total carbonic species concentrations and pH the following solubility diagram derived by Lindman and Mattsson (1982) and Mattsson (1988) may be used (Figure 5.7). The figure is valid for a copper concentration of 1 mg l^{-1}. In the diagram our own experiments are marked 1-14.

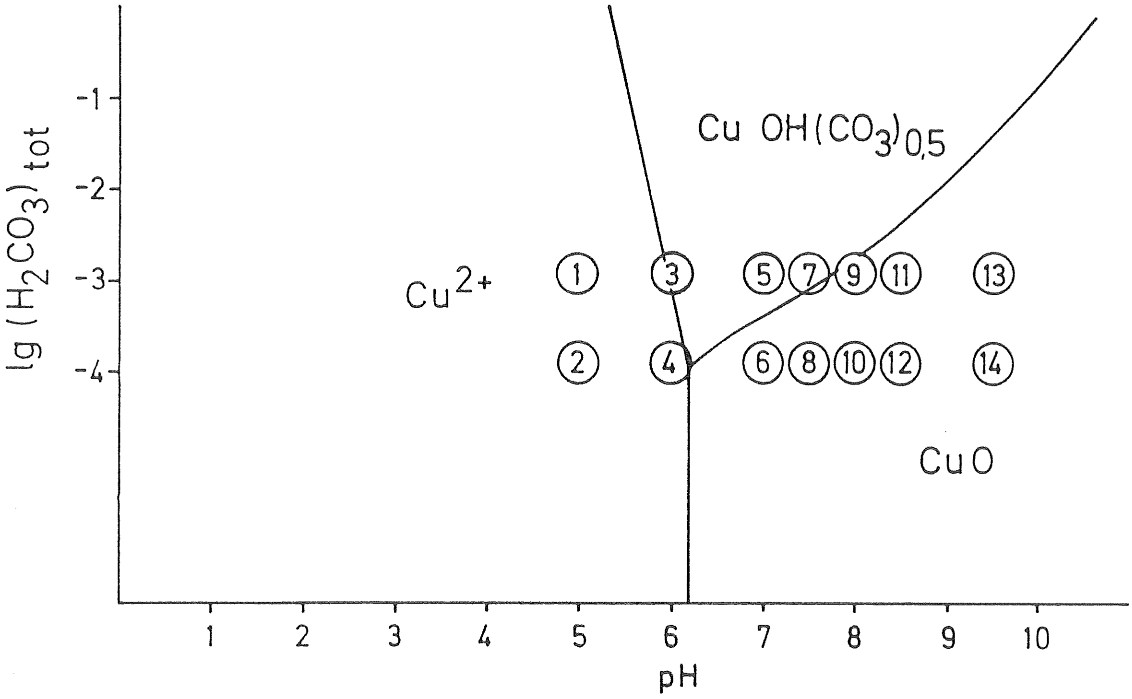

Figure 5.7 Solubility diagram for $CuOH(CO_3)_{0.5}$ and CuO at different concentration of total carbonic species and pH with the experiments marked 1-14.

For pipe tests 1-4 in the diagram the cuprosolvency was high with 1 and 2 having the highest cuprosolvency. For rig tests marked 8 and 11-14 the cuprosolvency was very low. To avoid corrosion at low pH around 6 it is necessary to have a high concentration of total carbonic species, as $CuOH(CO_3)_{0.5}$ is the protective compound (Stumm and Morgan 1981 and Figure 3.6). At pH > 7 (common in Swedish drinking water) it is not necessary for carbonic species to be present in the water as Cu_2O or CuO is the protective compound. This observation can also be seen in Figure 5.3 where a high oxygen consumption for 60 mg $HCO_3^- l^{-1}$ results in a higher copper concentration.

It is important to avoid conditions under which the solid phase of $CuOH(CO_3)_{0.5}$ and CuO is just stable due to the pH and carbonic species content. Experiments marked 3, 6 and 9 in Figure 5.7 is example of this.

Concerning the importance of CO_2 it was suggested in the literature survey that initial corrosion may be high when the CO_2 concentration is high (Figures 5.8 and 5.9).

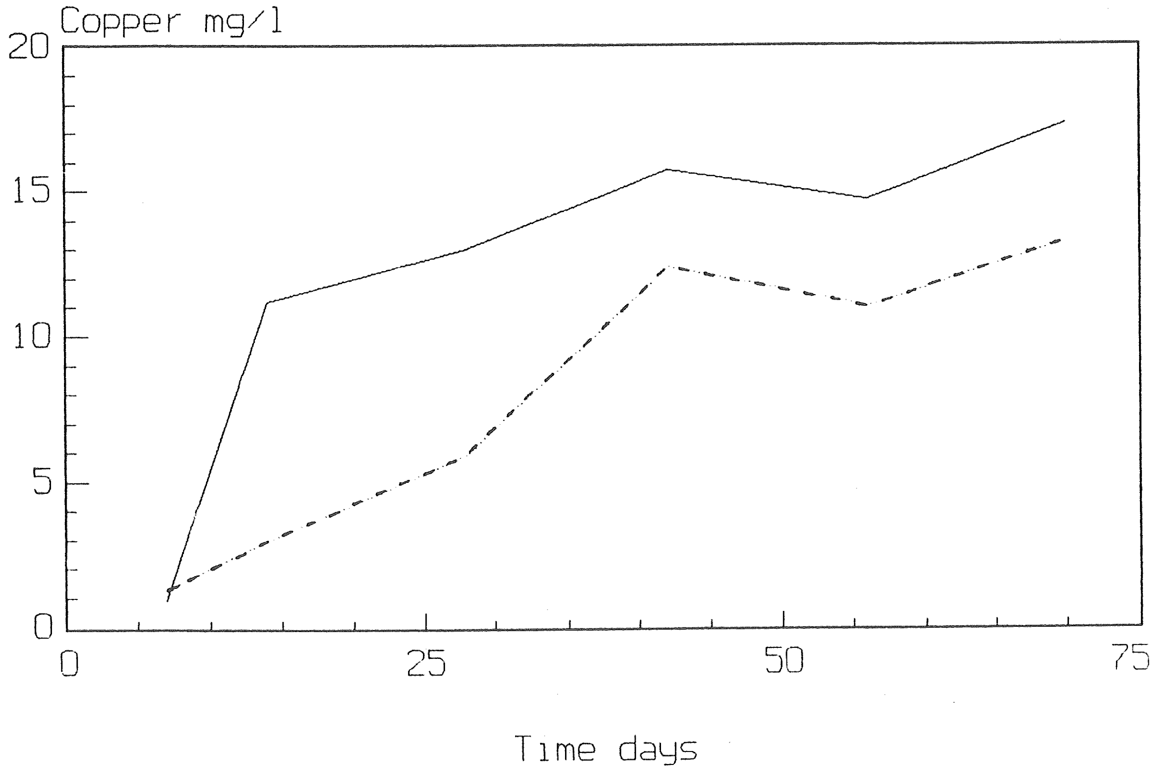

Figure 5.8 Copper concentration versus time for 10 (——) and 100 mg (-···-) $HCO_3^- l^{-1}$ at pH 5 from pipe test.

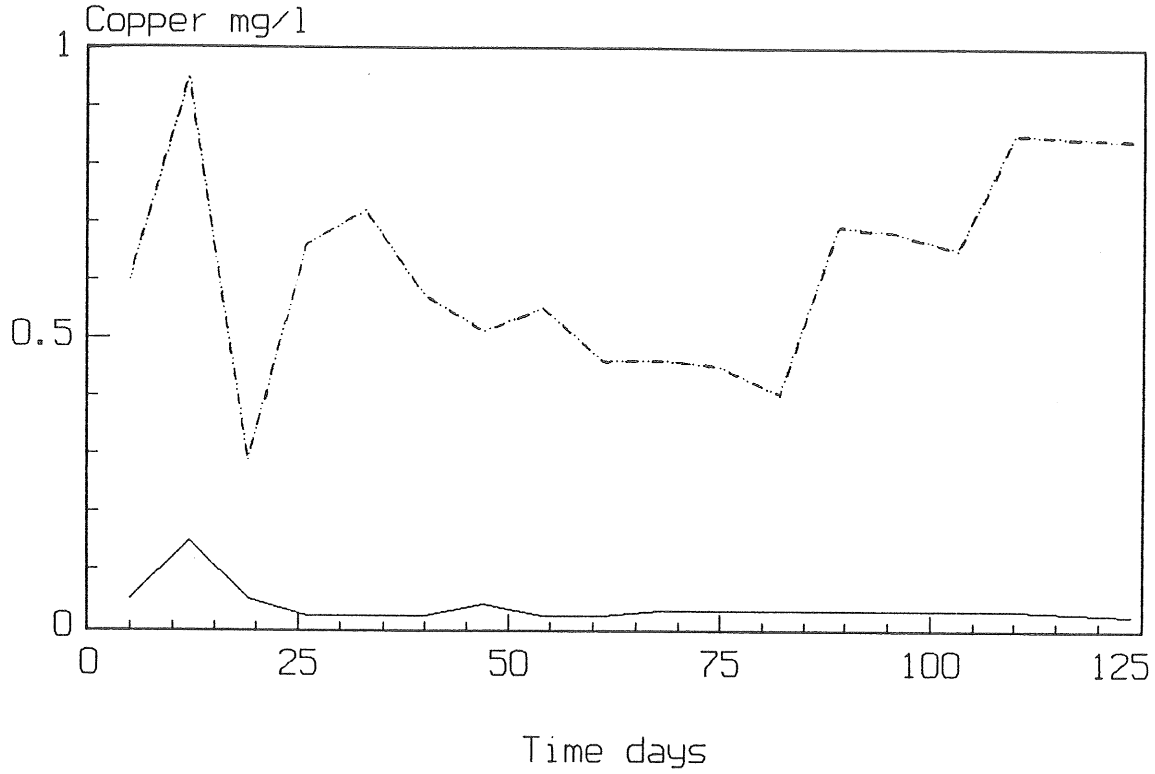

Figure 5.9 Copper concentration versus time for 10 (——) and 100 (-•••-) mg HCO_3^- l^{-1} at pH 7.5 from rig test.

In a comparison of results, from the pipe test carried out at pH 5, and from the rig test at pH 7.5 (both with 10 and 100 mg HCO_3^- l^{-1}) no difference in initial corrosion rate at different CO_2 is formed.

The difference in cuprosolvency is more dependent on the pH than the concentration of total carbonic species, Figure 5.10. At low pH when the CO_2 concentration is high no difference in copper uptake could be noticed. Cruse et al (1985) stated that CO_2 does not have any influence on the corrosion rate.

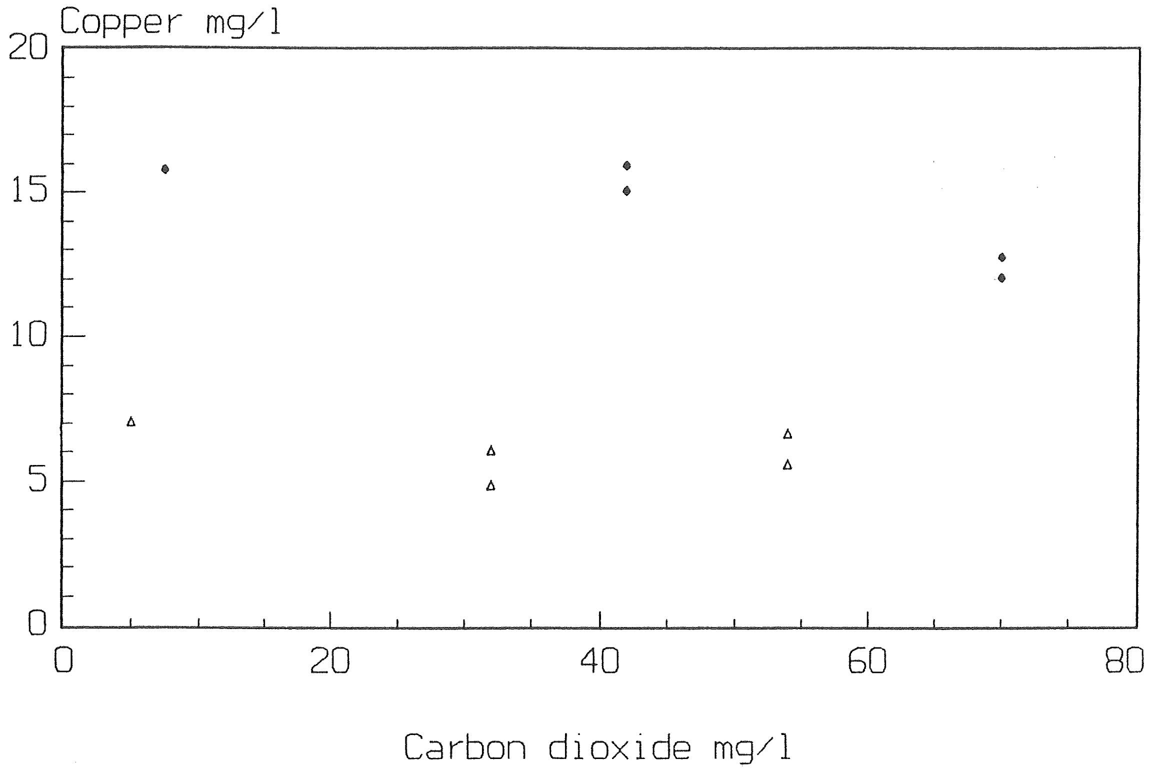

Figure 5.10 Copper concentration versus carbon dioxide at different pH from pipe tests.
◆ pH 5, Δ pH 6

This investigation indicates that the most important parameter for uniform corrosion is the pH. To solve the corrosion problem in a water with low pH the best way is to raise the pH and at the same time allowing the formation of protective Cu_2O. This corresponds to Case 1 and 2 in the model for conceivable corrosion reactions and protective layer formation in Section 3.5. In a water with low pH and high CO_2 concentration, as in model Case 4, the best way to decrease corrosion is to aerate the water. This results in a pH increase and $CuOH(CO_3)_{0.5}$ formation as protective layer (Case 4 and 5).

5.2 Influence of calcium on copper corrosion

The effect of calcium on copper corrosion is illustrated in Figures 5.11, 5.12 and 5.13. From Figure 5.11 it is important not to draw any real conclusions because of many parameters such as pH, carbonic species, salts and organic matter which is more uncontrolled.

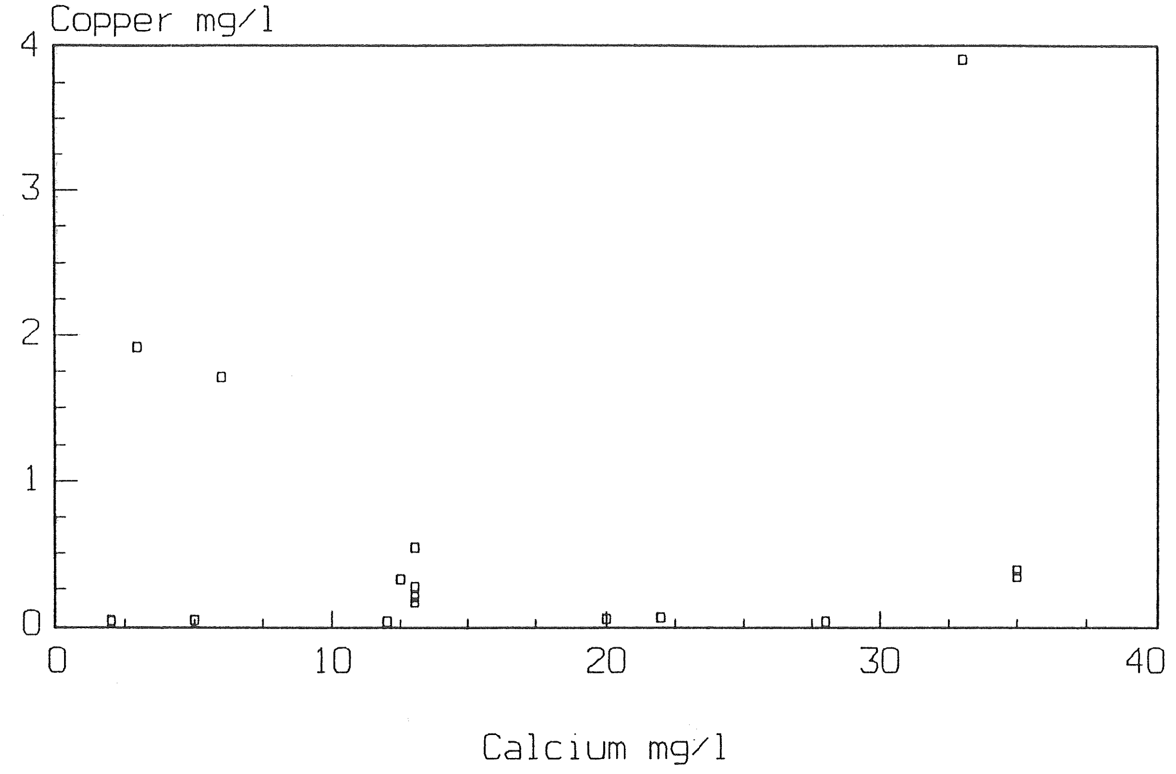

Figure 5.11 Copper concentration versus calcium concentration of the water from rig tests.

It is necessary to maintain a constant pH. For rig tests pH 8.5 was chosen and for pipe tests pH 8.

In Figures 5.12 and 5.13 it is seen that an increase in the calcium concentration results in a slightly increased cuprosolvency. Stagnant water prevent $CaCO_3$ to precipitate. It requires a high degree of supersaturation before $CaCO_3$ precipitates under such conditions. At a higher pH values $CaCO_3$ may precipitate as a coated protective layer on the copper surface. At the point where $CaCO_3$ just precipitates, the precipitation of $CaCO_3$ increases the risk of pitting corrosion (von Franquē et al. 1975, Gilbert 1976). From Figure 5.13 it is seen that an increase in Ca^{2+} at pH 8 and various HCO_3^- concentrations increase the cuprosolvency. However the increase is greater at 60 mg HCO_3^- l^{-1} than for 100 mg HCO_3^- l^{-1}. The observation may be due to a precipitation of $CuCO_3 \cdot Cu(OH)_2$ instead or beside $CaCO_3$. At 100 mg HCO_3^- l^{-1} a more protective layer of $CaCO_3$ may be formed.

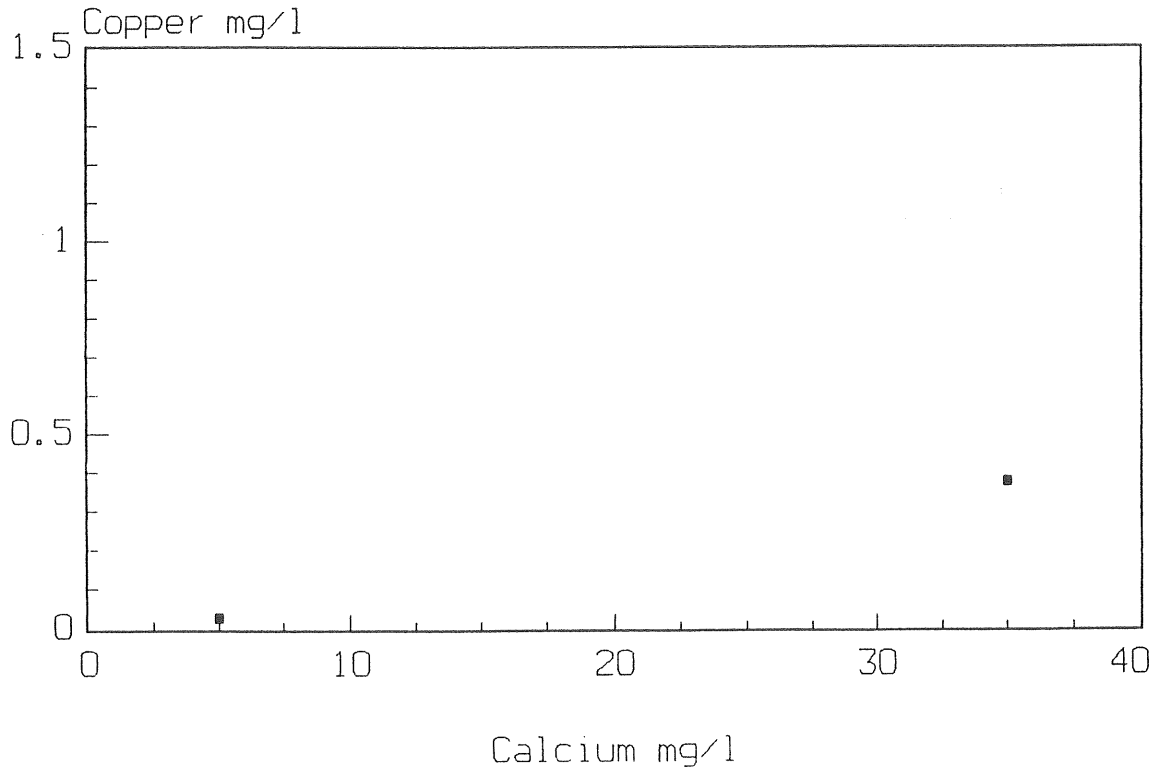

Figure 5.12 Copper concentration versus calcium concentration of the water at pH 8.5 and 100 mg HCO_3^- l^{-1} from rig tests.

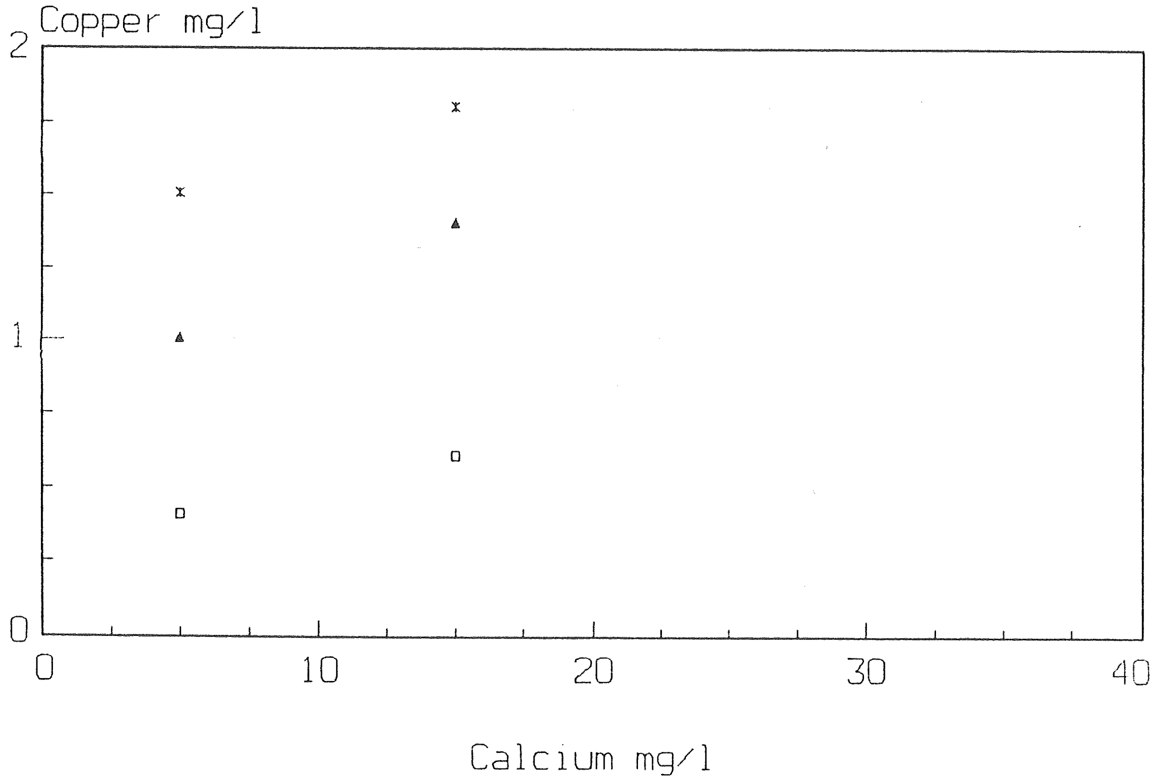

Figure 5.13 Copper concentration versus calcium concentration of the water from pipe tests at pH 8 and (□) 10 mg HCO_3^- l^{-1}, (*) 60 mg HCO_3^- l^{-1} and (▲) 100 mg HCO_3^- l^{-1}.

5.3 Influence of chloride and sulphate on copper corrosion

The influence of chloride on copper corrosion was studied using rig tests in the laboratory. The influence of sulphate was studied using both rig and pipe tests in laboratory. To reduce pitting corrosion of type II a high ratio of HCO_3^- to SO_4^{2-} (in mg l^{-1}) should be maintained (Mattsson and Fredriksson 1968, Mattsson 1980, Mattsson 1988). The influence of this ratio, for sulphate and also for chloride instead of sulphate, on uniform corrosion is shown in Figures 5.14 and 5.15, respectively.

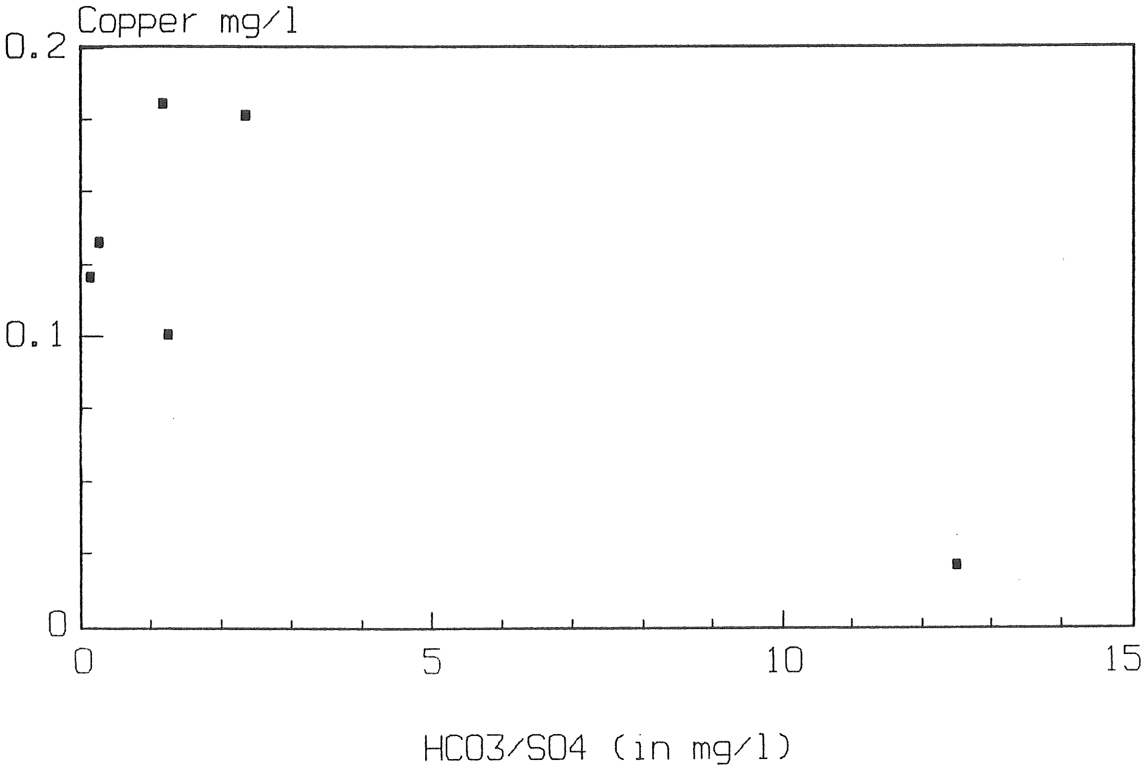

Figure 5.14 Copper concentration versus hydrogen carbonate to sulphate at pH 8.5 from rig tests in laboratory.

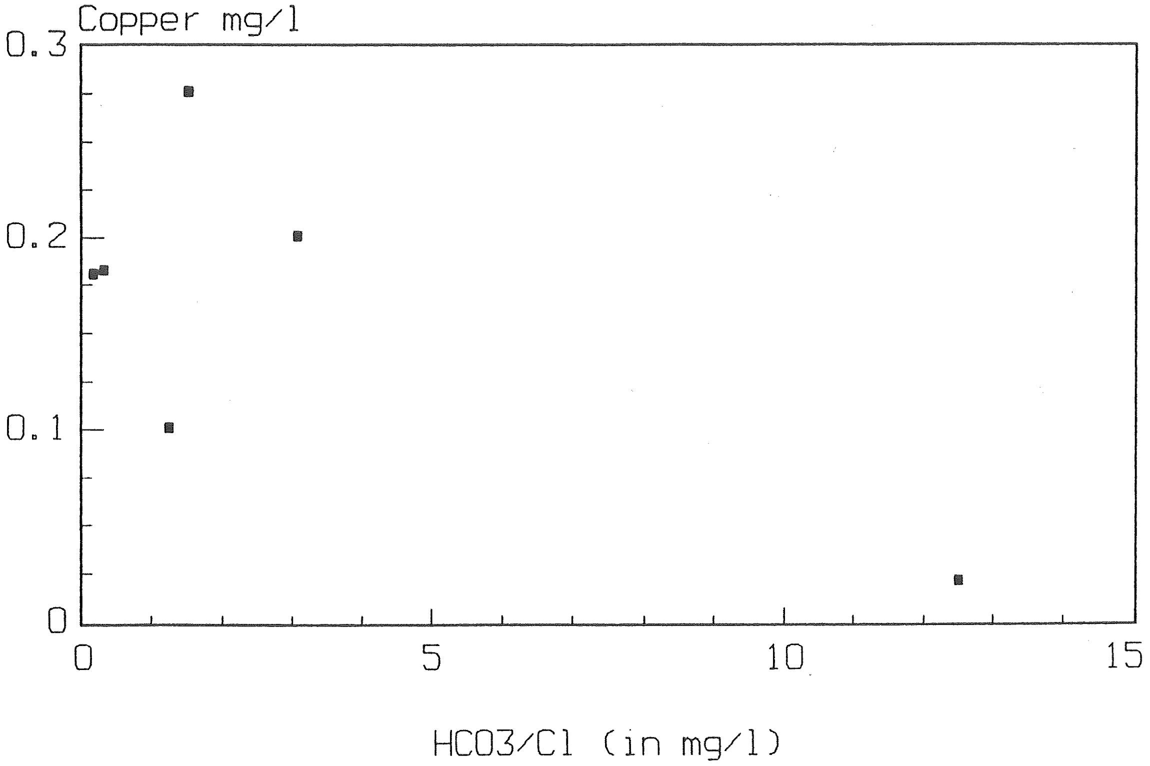

Figure 5.15 Copper concentration versus hydrogen carbonate to chloride at pH 8.5 from rig tests in laboratory.

Only a high ratio of hydrogen carbonate to either sulphate or chloride results in low cuprosolvency. At a low ratio (0.10-3.0) no correlation between copper uptake and HCO_3^-/SO_3^{2-} or HCO_3^-/Cl^- ratio was found. Figures 5.16 and 5.17 show that a low concentration of either sulphate or chloride, in the presence of 100 mg HCO_3^- l^{-1}, provides low cuprosolvency. However, an increase in carbonic species concentration and either sulphate or chloride concentration results in increased cuprosolvency. This has also been observed by Stone et al. (1987). The higher cuprosolvency may be due to the higher ionic strength which prevents protective layer formation.

When the water contains calcium, and the concentration of carbonic species at pH 8.5 is high, $CaCO_3$ is precipitated on the copper surface. Copper uptake was high and independent of either sulphate or chloride concentration.

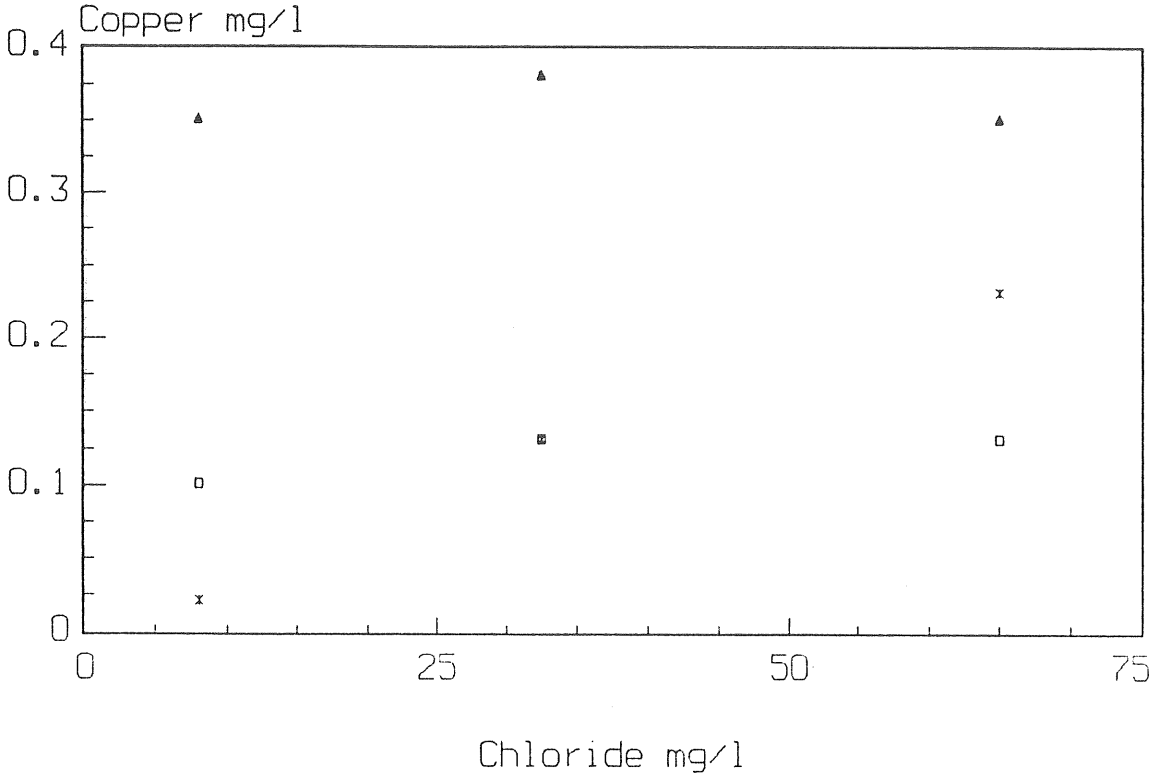

Figure 5.16 Copper concentration versus chloride concentration from laboratory rig tests.

- * 10 mg HCO_3^- l^{-1}, 25 mg $Ca^{2+}l^{-1}$
- □ 100 mg HCO_3^- l^{-1}, 25 mg $Ca^{2+}l^{-1}$
- ▲ 100 mg HCO_3^- l^{-1}, 35 mg $Ca^{2+}l^{-1}$

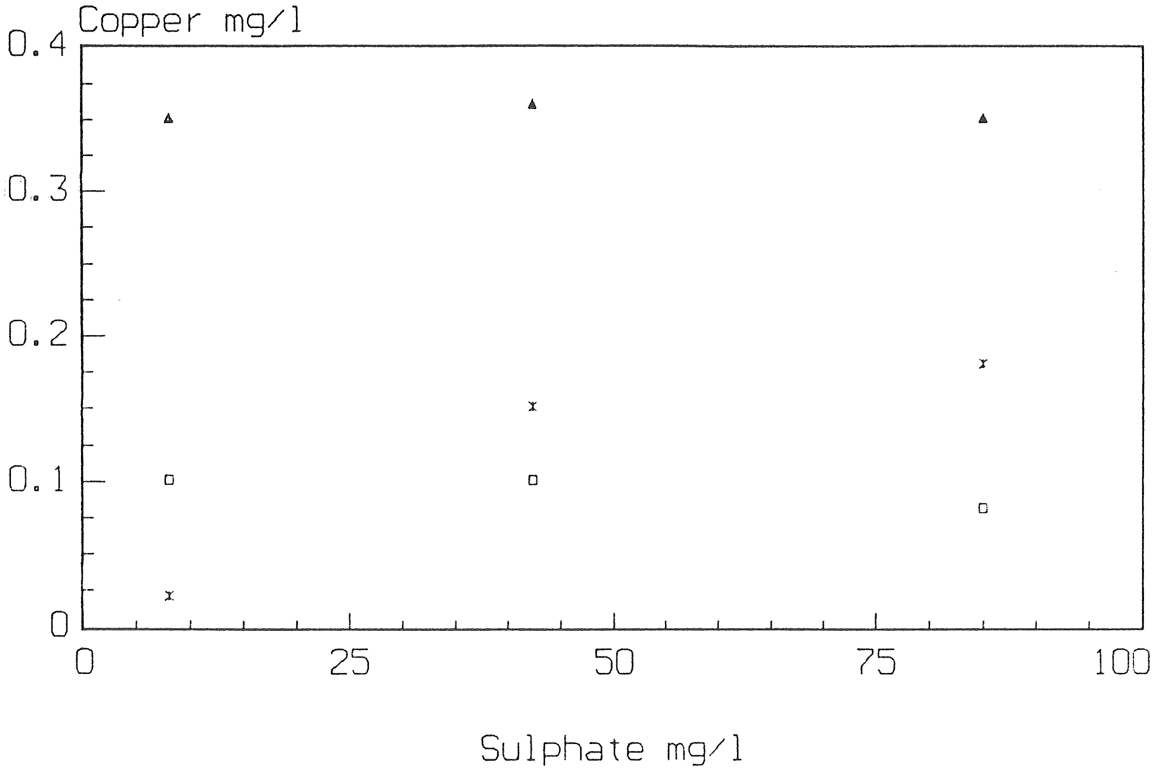

Figure 5.17 Copper concentration versus sulphate concentration from laboratory rig tests.

- * 10 mg HCO_3^- l^{-1}, 25 mg $Ca^{2+}l^{-1}$
- □ 100 mg HCO_3^- l^{-1}, 25 mg $Ca^{2+}l^{-1}$
- ▲ 100 mg HCO_3^- l^{-1}, 35 mg $Ca^{2+}l^{-1}$

The influence of two sulphate concentrations in the pipe tests at pH 5 to 8 (and 10, 60 and 100 mg HCO_3^- l^{-1}) was also tested (Figure 5.18). An increased sulphate concentration from 20 to 100 mg l^{-1} did not induce any noticeable change in cuprosolvency.

A low concentration of chloride and sulphate in the presence of a low concentration of total carbonic species results in pitting corrosion (Linder 1979 and Linder and Lindman 1982), but an increase in chloride reduces the pitting tendency and may increase uniform corrosion slightly.

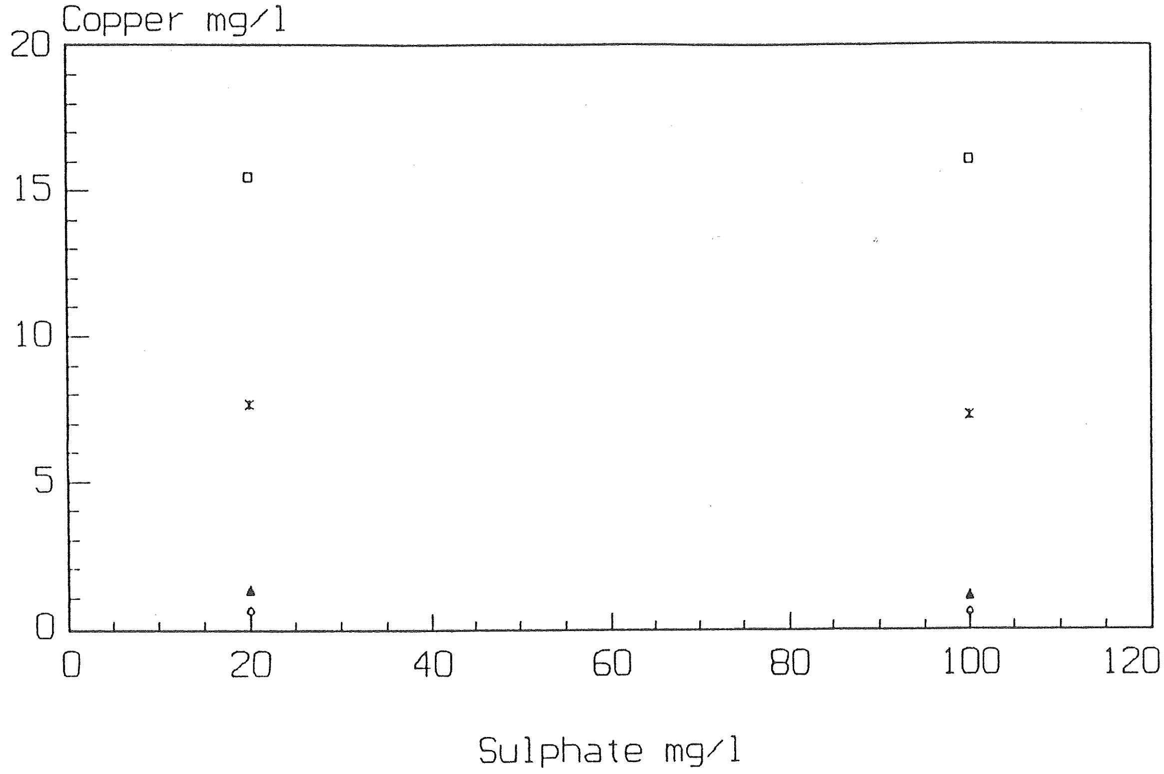

Figure 5.18A Copper concentration versus sulphate concentration at ◻ pH 5, * pH 6, ▲ pH 7, ◊ pH 8 at 10 mg HCO_3^- l^{-1}.

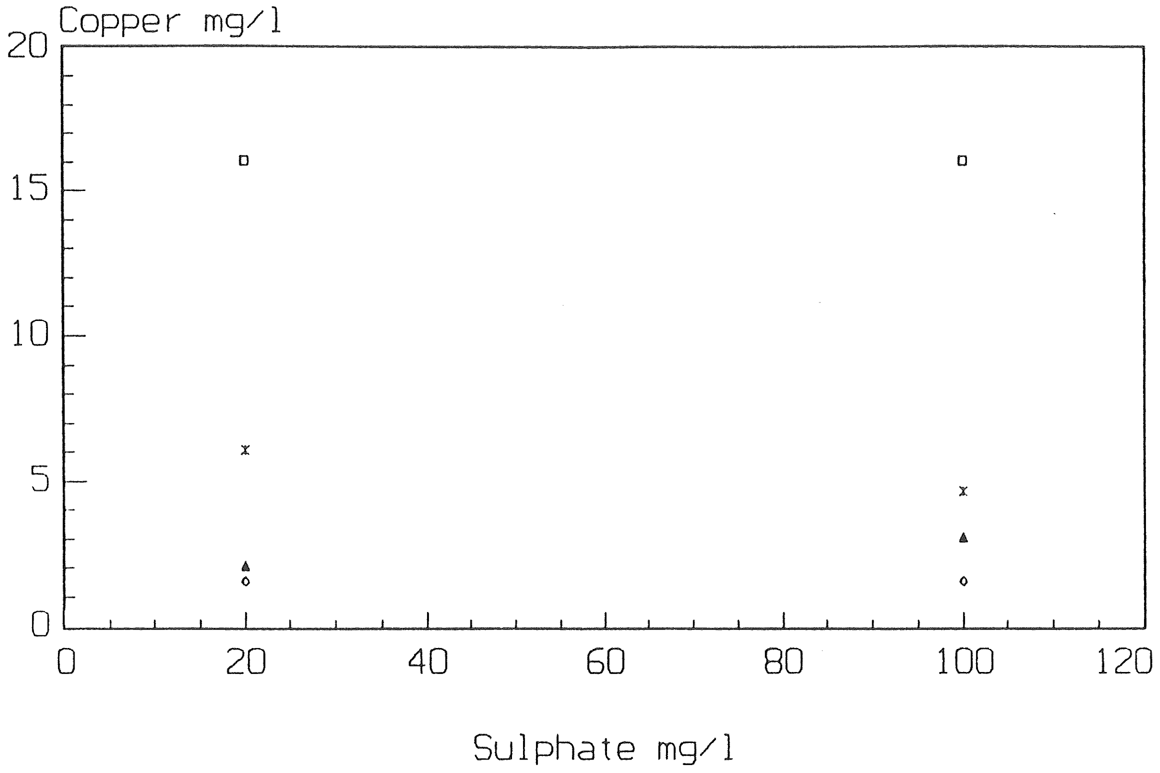

Figure 5.18B Copper concentration versus sulphate concentration at □ pH 5, * pH 6, ▲ pH 7, ◊ pH 8 at 60 mg HCO_3^- l^{-1}.

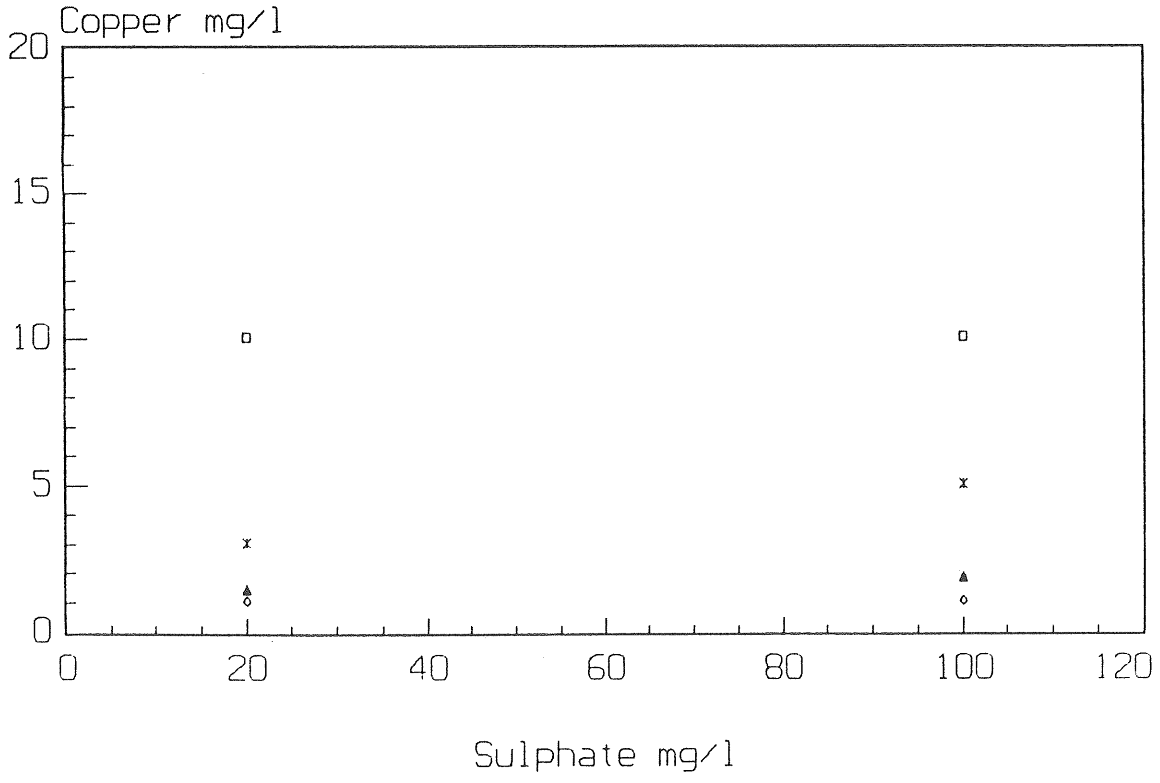

Figure 5.18C Copper concentration versus sulphate concentration at □ pH 5, * pH 6, ▲ pH 7, ◊ pH 8 at 100 mg HCO_3^- l^{-1}.

5.4 Influence of organic matter on copper corrosion

At the waterworks a variety of different treatment methods are used. During treatment some organic matter can be transformed to a smaller molecular weight or some may be removed. Because of the treatment the molecular weight distribution will be changed. In this study the water was treated either by rapid sand filtration or by rapid sand and activated carbon filtration. The organic matter was characterised by gel filtration (Appendix A). Molecular weight ranges of 1000-5000 (Sephadex G-25) and 1000-30 000 (Sephadex G-50) were investigated. The first eluted fractions represent the highest molecular weights. Figures 5.19-5.21 show the molecular weight distribution of organic matter in raw water, sand filtered raw water and sand and activated carbon filtered raw water.

A rapid sand filtered water undergoes no change in molecular weight distribution. However, an activated carbon filtration absorbs organic matter with a low molecular weight, which increases the proportion of organics with a high molecular weight.

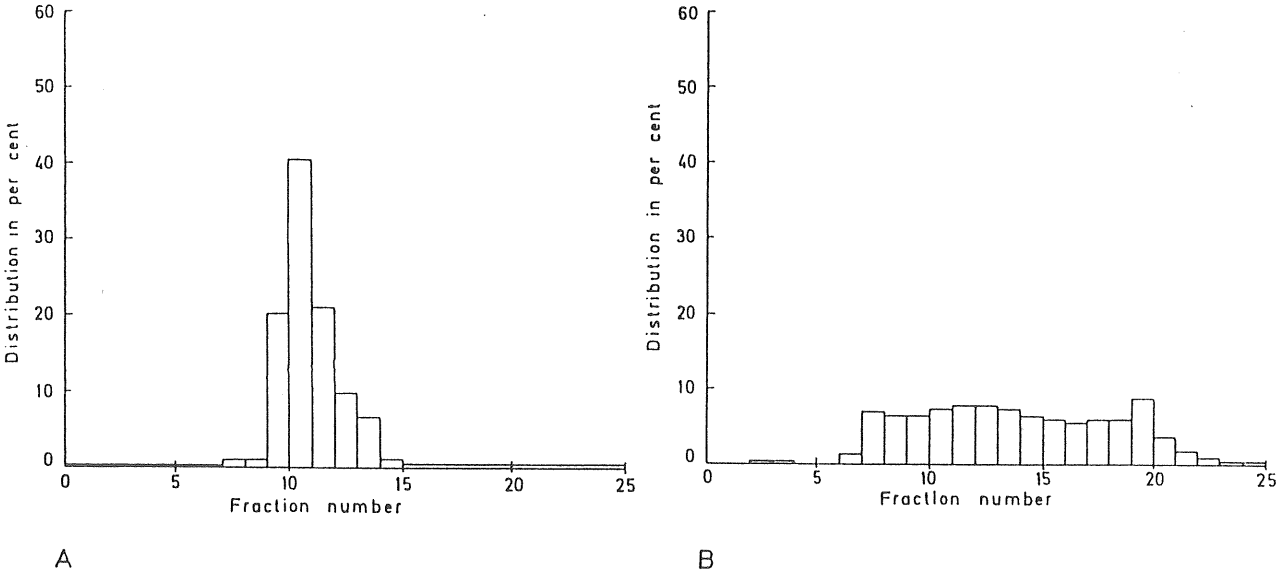

Figure 5.19 Fractions with different molecular weight for raw water. (A) 5000-1000 molecular weight range, (B) 30 000-1000 molecular weight range.

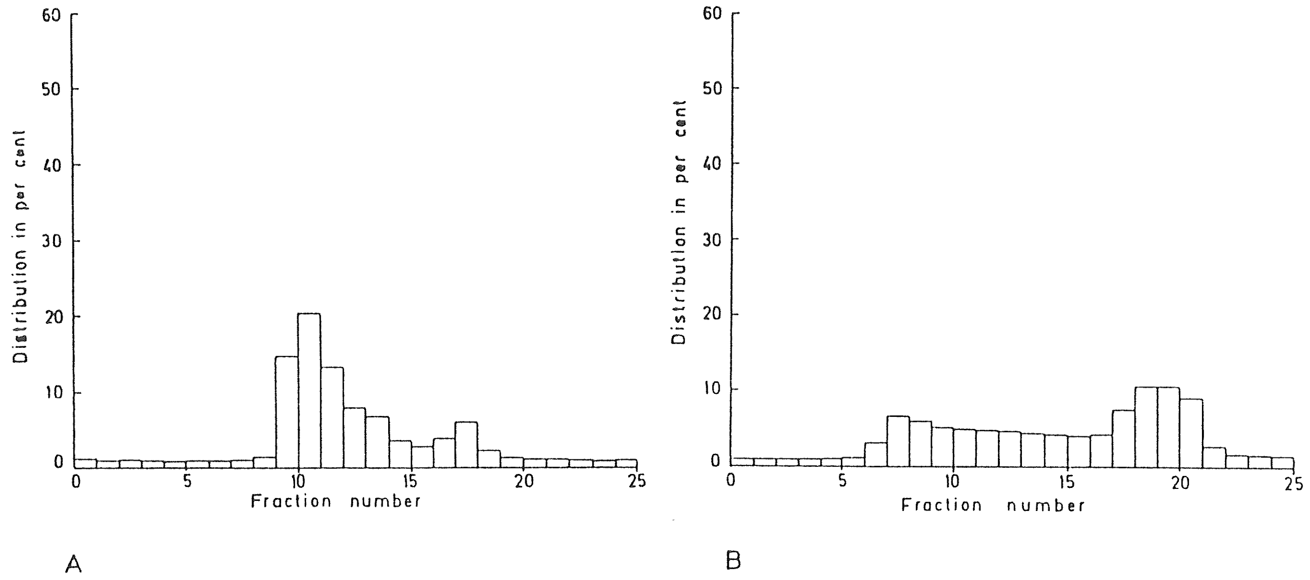

Figure 5.20 Fractions with different molecular weight for rapid sand filtered water. (A) 5000-1000 molecular weight range, (B) 30 000-1000 molecular weight range.

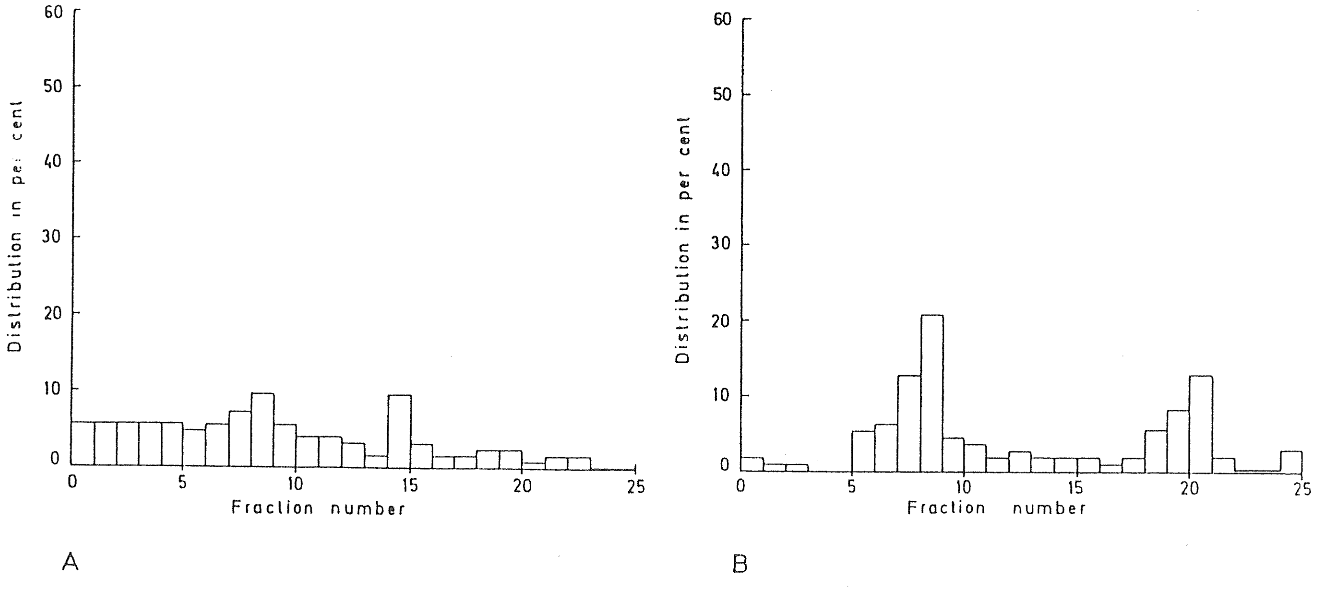

Figure 5.21 Fractions with different molecular weight for sand and activated carbon filtered water. (A) 5000-1000 molecular weight range, (B) 30 000-1000 molecular weight range.

If the molecular weights of the organic matter is related to corrosion it can be seen that the cuprosolvency was higher for the sand and activated carbon filtered water than for the water that was only sand filtered (Figure 5.22). The only difference between the water was the content of organic matter which was reduced in the activated carbon filter. The pH was adjusted to 8.5.

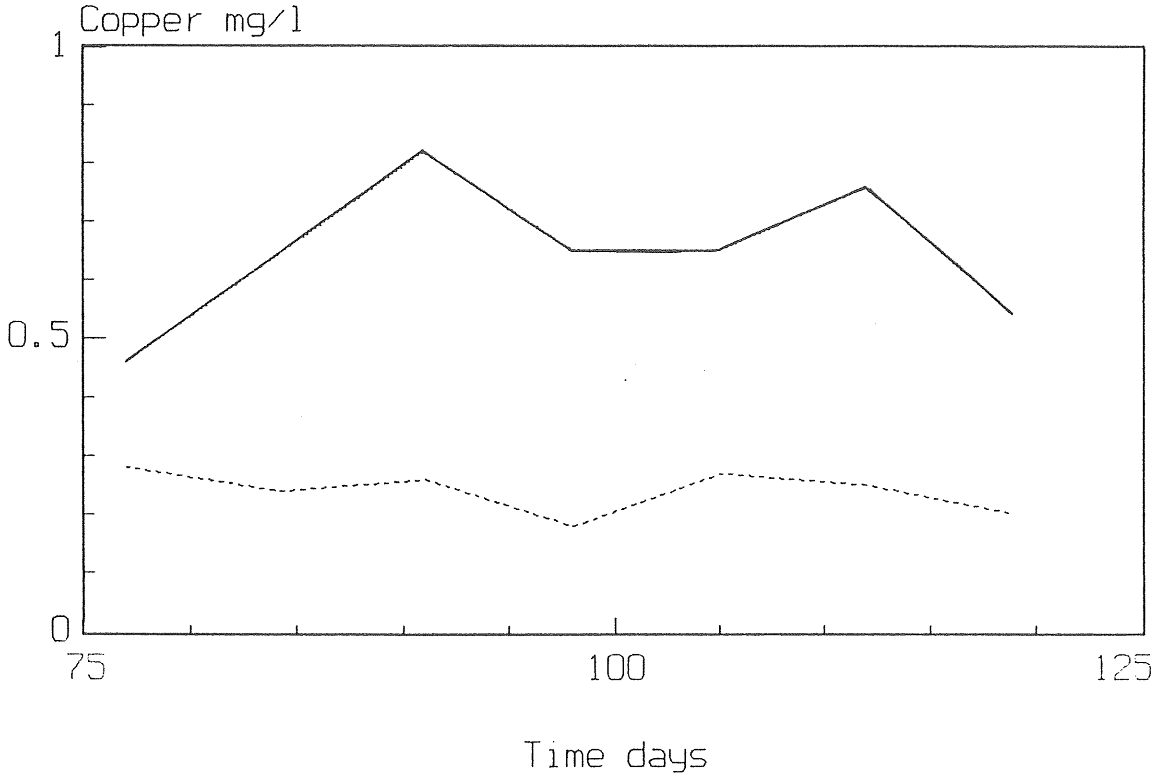

Figure 5.22 Copper concentrations versus time for (---) sand filtered water, (——) sand and activated carbon filtered water.

Figures 5.23 and 5.24 show the distribution of copper bound to the organic matter. The copper was not necessarily found in the fractions with the highest amount of organic matter.

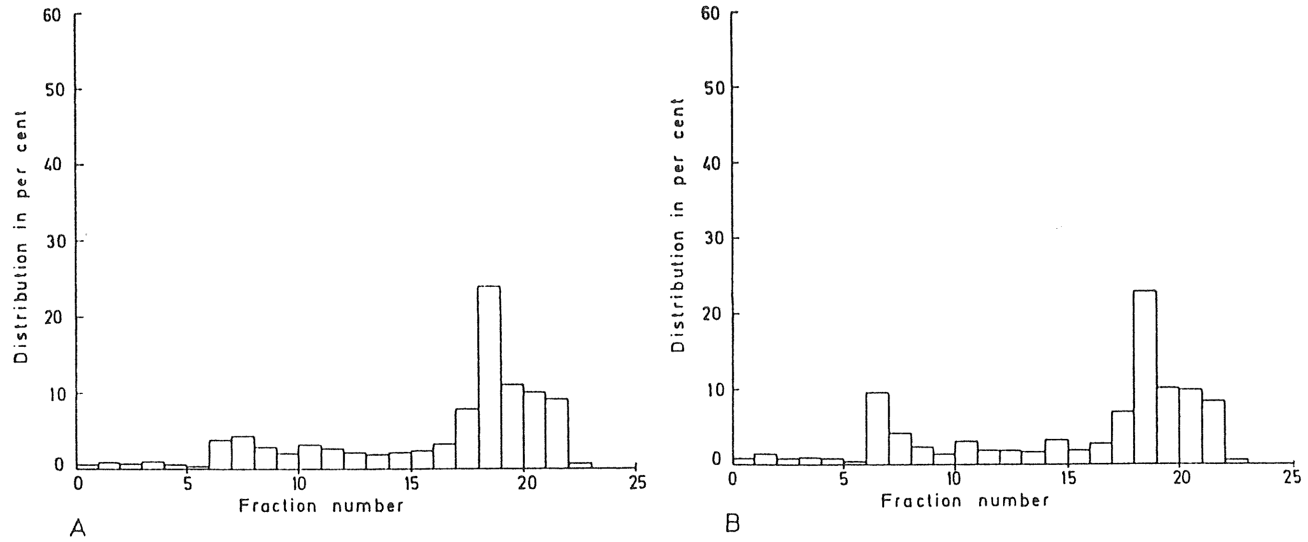

Figure 5.23 Determination of copper in various molecular weight fractions of rapid sand filtered water. (A) 5000-1000 molecular weight range, (B) 30 000-1000 molecular weight range.

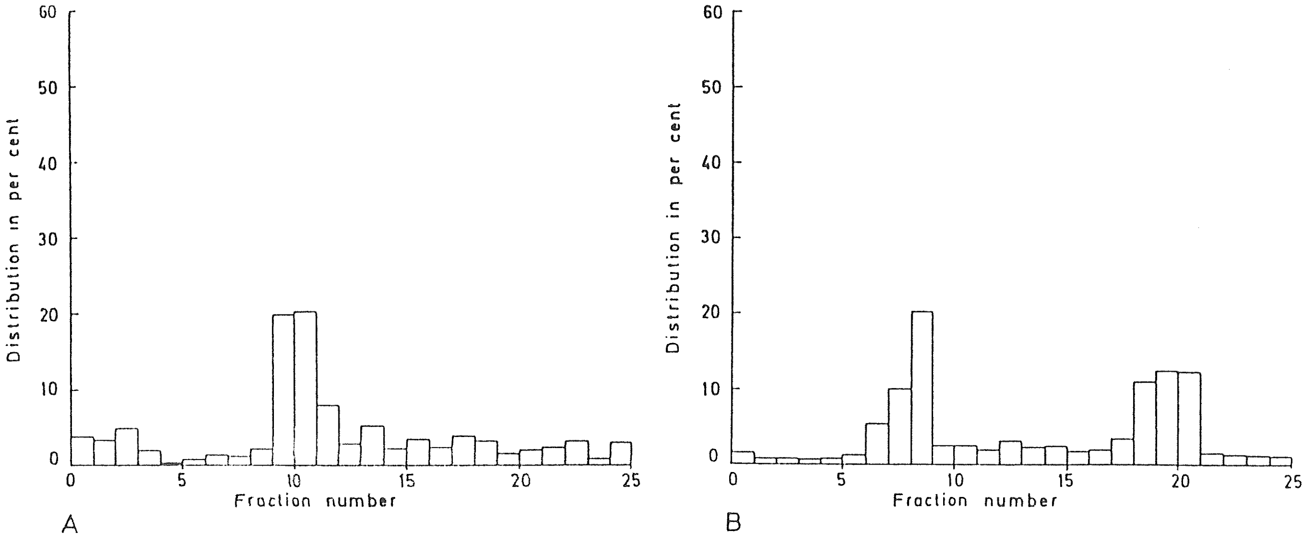

Figure 5.24 Determination of copper in various molecular weight fractions of sand and activated carbon filtered water. (A) 5000-1000 molecular weight range, (B) 30 000-1000 molecular weight range.

Corresponding tests were carried out using raw water that was chemically precipitated and precipitated water with an additional ozonation where the organic matter was degraded into the smaller size fractions. The cuprosolvency was slightly higher for the precipitated and ozonated water than for the precipitated water and both were higher than for the sand filtered water.

The absence of organic matter results in a higher copper concentration in the water and therefore organic matter provides a protective effect against corrosion. Gel filtration showed that copper ions were not always detected in the fractions with the highest amount of organic matter. The copper ions were common in fractions with medium sized molecules. When water with a high concentration of organic matter is treated with ozone, the molecular distribution changes from large sized to smaller sized molecules and cuprosolvency increases.

6. MINIMISATION OF UNIFORM COPPER CORROSION

The results presented in Chapter 5 allow an interpretation of the extent of copper corrosion expected for the different pH and total carbonic species concentrations presented in Section 3.5.

In Case 1 (pH < 6.5, total carbonic species concentration is low), an increase in pH allows the formation of protective Cu_2O or CuO, while an increase in total carbonic species concentration produces a protective layer of $CuOH(CO_3)_{0.5}$. Either NaOH addition or dolomite filters (which are easier to handle) provide an increase in pH, in the latter case as a result of $Mg(OH)_2$ dissolution. Where calcium concentration is high only an increase in pH is possible, otherwise $CaCO_3$ is precipitated, which provides no protection against corrosion in copper pipes. Instead the corrosion rate increases. In this case only pH should be increased.

In Case 2 (6.5 < pH < 9, total carbonic species concentration is low), an increase in pH, by small additions of sodium hydroxide, allows the formation of Cu_2O or CuO protective layers. Dolomite filters are not very effective at relatively neutral pH values due to the low CO_2 concentration. Addition of Na_2CO_3 leads to the formation of a layer of $CuOH(CO_3)_{0.5}$ which is not as effective in corrosion control as Cu_2O and CuO.

In Case 3 (pH > 9, total carbonic species concentration is low) the pH is already high enough for the formation of CuO or Cu_2O protective layers and therefore no remedial action is required. A pH above 9.5 is not recommended in any case because of the possibility for complex formation without any protection against corrosion.

In Case 4 (pH < 6.5, total carbonic species concentration is high) an increase in pH leads to the formation of $CuOH(CO_3)_{0.5}$ as a protective layer. High total carbonic species concentration rules out the possibility of the formation of the preferred Cu_2O

or CuO layers. Increase in pH can be achieved either by aearation, or by combined aeration and the addition of NaOH, or by the use of dolomite filters without aeration. In a calcium rich water it is very important to avoid the formation of a $CuOH(CO_3)_{0.5}$ layer instead of $CaCO_3$.

In Case 5 (6.5 < pH < 9, total carbonic species concentration is high) the lower pH allows a suitable increase in pH due to the removal of CO_2 by aeration. Under these conditions either Cu_2O and CuO, or $CuOH(CO_3)_{0.5}$, layers may form depending on the HCO_3^- concentration. A high pH also results in $CaCO_3$ formation when calcium is present.

In Case 6 (pH > 9, total carbonic acid concentration is high), the pH is sufficiently high to prevent copper corrosion. It could be too high to prevent corrosion (over 9.5). However, in the presence of calcium (see Section 5.2) corrosion may occur when the water is medium hard. It is not fully understood why corrosion occurs under these conditions, although the formation of an incomplete $CaCO_3$ precipitation may be important as in hard water (where a complete $CaCO_3$ precipitation should form) corrosion is not found. Preventive action includes water softening by ion exchange, followed by either aeration or the addition of sodium hydroxide. Under such treatment either $CuOH(CO_3)_{0.5}$ or Cu_2O and CuO can form as protective layers.

7. IRON CORROSION - LITERATURE REVIEW

The literature review on internal iron corrosion is divided into five sections:

- type of corrosion attack
- chemical reactions involved in corrosion
- influence of water composition on corrosion rate
- oxidation of iron(II) to iron(III) and discussion of parameters that influence oxidation
- formation of protective layers in iron pipes both in laboratory tests and in distribution networks

7.1 Types of iron corrosion

7.1.1 Uniform corrosion

Uniform corrosion can be defined as iron corrosion at anodic and cathodic sites over the whole metal surface. Uniform corrosion is not a problem for pipe strength since the wall thickness of metal pipes is usually over-dimensioned by up to 3 mm. Under certain circumstances corrosion products and precipitations from the water allow the formation of protective layers which may decrease the corrosion rate. However, water quality problems may occur if voluminous corrosion products form, as the deposits may break off and become suspended at high water velocity which results in metal embrittlement.

7.1.2 Localised corrosion

Two types of localised attack may develop on an iron surface. Before use an iron pipe is in contact with atmospheric oxygen and is covered by a protective layer of iron oxide (Fe_2O_3). In the natural state this structure is irregular and imperfect.

If the passivating layer is damaged when the pipe is installed then water, and its dissolved species, can reach the unprotected iron surface and cause localised corrosion. Another type of localised corrosion occurs when heterogeneous deposits are present, due to variations in oxygen concentration over the pipe surface. As the oxygen concentration is lower under the deposit than in the water bulk, a difference in potential is created and this accelerates iron dissolution under the deposit. Deposits may consist of particles attached to the metal surface, corrosion products, microbiological organisms and combinations thereof.

7.1.3 Graphitisation - grey cast iron corrosion

Graphitisation (a corrosion attack characteristic of cast iron) can occur in two different ways, galvanic corrosion and selective corrosion.

Cast iron consists of 3-4% carbon as graphite. A difference in potential between carbon and iron occurs on contact with water. Since iron has the lower potential, it will be dissolved first. The corrosion products which precipitate on the surface are of the same type as those formed when iron materials, which have a lower carbon content than cast iron, corrode. After corrosion, the remaining pipe will be a combination of a graphite network, corrosion products and other iron compounds, such as Fe_3C and Fe_3P (Larson et al. 1956).

During graphitisation the shape of the pipe remains intact, but the strength deteriorates due to lower density and higher porosity in the material residue (Kirby 1978, Sotkovski 1980).

When cast iron corrodes, two separate layers are formed; an outer one containing corrosion products and an inner layer in which the cast iron residue is found (Kölle and Rösch 1978, Vuorinen et al. 1985). The specific surface area of the cast iron residue is increased by a factor of 4-5 (Vuorinen et al. 1985). However, density decreases from 7.1 to about 2 g cm^{-3} with a void space of 53% in the outer layer (Kölle and Rösch 1978).

7.2 Origin of iron corrosion

Iron corrosion is an electrochemical reaction between the metal surface and the surrounding water and species soluble in it. The reaction is determined by the electrode potential of the metal and the thermodynamic potential of equilibrium for the reaction. Oxidation of the metal takes place only when the electrode potential exceeds the equilibrium potential. The equilibrium potential indicates whether the environment in the boundary layer between water and metal is oxidised or reduced.

A difference in potential between two points results in a transfer of electrons and anodic and cathodic reactions take place simultaneously, equations (7.1) and (7.2).

Anode $Fe \rightarrow Fe^{2+} + 2e^-$ (7.1)

Cathode $\frac{1}{2}O_2 + H_2O + 2e^- \rightarrow 2OH^-$ (7.2)

To prevent corrosion, oxygen on the metal surface must be removed and oxygen transport towards the metal surface must be reduced.

In Figure 7.1 the different compounds of iron are shown as a function of potential and pH, in the iron/water system. Below the lower dotted line the environment is fully reducing and at higher potential the environment is increasingly more oxidising. An increased potential corresponds to an increased oxygen concentration. This diagram is based on thermodynamic data and therefore does not consider the kinetics of the formation of the compounds (Obrecht and Pourbaix 1967, Pourbaix 1969 and Pourbaix 1972). In drinking water equilibrium conditions are unlikely to exist as the system is continually changing due to water flow. The situation is further complicated by the presence of organic compounds which can complex and remove available Fe. However, the Pourbaix diagram does provide a guide as to the likely species present, as long as the limitations are recognised.

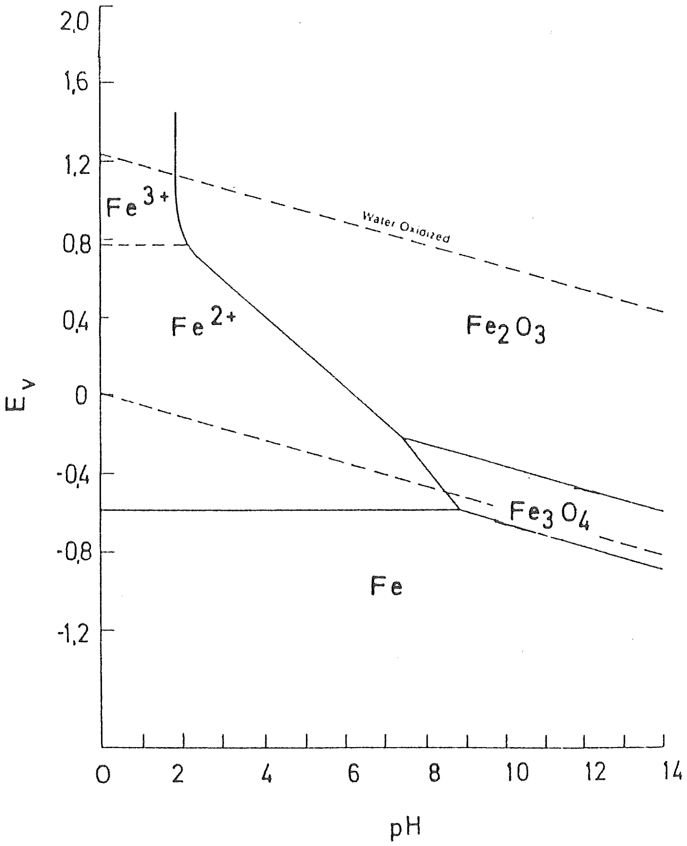

Figure 7.1 Equilibrium potential-pH diagram for the system Fe-H_2O (from Obrecht and Pourbaix 1967).

When corrosion products are precipitated on a metal surface a difference in potential is created between the inside and the outside of the deposit. Because of the difference in oxygen concentration a current and an electron migration in the opposite direction occurs and an oxygen concentration cell appears. Anodic sites develop under the deposits and lead to the dissolution of iron (Figure 7.2). In addition, oxygen concentration is low and the pH decreases as the dissolved iron(II) reacts with water (equation 7.3).

$$Fe^{2+} + H_2O \rightleftarrows FeOH^+ + H^+ \qquad (7.3)$$

When H^+ concentration exceeds 10^{-4} mol l^{-1} (pH 4.0) a further cathodic reaction, shown in equation (7.4), takes place under the deposits. Iron dissolves and pits are formed.

$$\text{Anode:} \quad Fe \rightarrow Fe^{2+} + 2e^- \qquad (7.1)$$

$$\text{Cathode:} \quad 2H^+ + 2e^- \rightarrow H_2 \qquad (7.4)$$

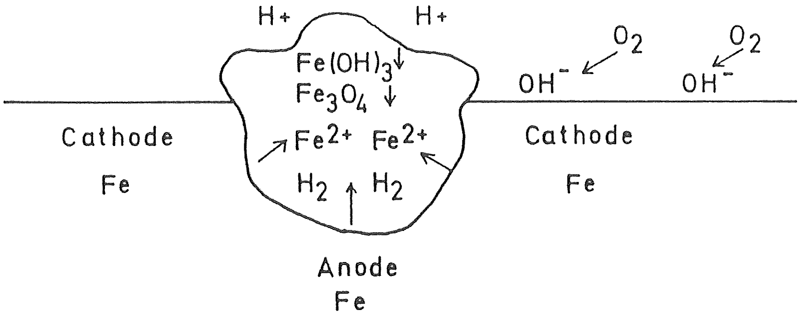

Figure 7.2 Pitting attack under deposits pH < 4.0 (from Obrecht and Pourbaix 1967).

In a water containing chloride or sulphate the potential at the anode decreases further. This is a result of the low pH value under the deposits. Following reaction (7.4), reaction (7.5) takes place and the pH decreases further.

$$4FeOH^+ + 4H_2O + 8Cl^- \rightarrow 4FeOOH + 8H^+ + 8Cl^- + 4e^- \qquad (7.5)$$

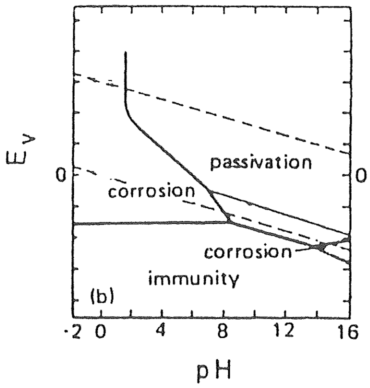

Figure 7.3 Theoretical conditions for no corrosion, corrosion and passivation caused by a protective layer (Pourbaix 1969).

Figure 7.3 gives ideas as to how measures to reduce corrosion can be made by increasing the potential, the oxygen concentration or the pH at the metal surface.

In Figure 7.4 various iron compounds are shown as a function of potential and pH (Stumm and Morgan 1981). The presence of carbonate results in the formation of $FeCO_3$ which can prevent corrosion.

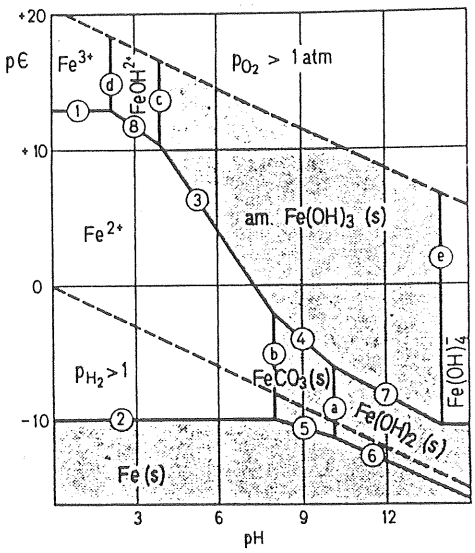

Figure 7.4 Equilibrium potential versus pH for the system $Fe\text{-}CO_2\text{-}H_2O$ valid for a total content of carbonic species of 10^{-3} M (from Stumm and Morgan 1981). 1-8 and a-e refer to the equations.

	pε Functions	
$Fe^{3+} + e = Fe^{2+}$	$p\varepsilon = 13 + \log\{Fe^{3+}\}/\{Fe^{2+}\}$	(1)
$Fe^{2+} + 2e = Fe(s)$	$p\varepsilon = -6.9 + \frac{1}{2}\log\{Fe^{2+}\}$	(2)
$Fe(OH)_3$ (amorph, s) $+ 3H^+ + e = Fe^{2+} + 3H_2O$	$p\varepsilon = 16 - \log\{Fe^{2+}\} - 3pH$	(3)
$Fe(OH)_3$ (amorph, s) $+ 2H^+ + HCO_3^- + e = FeCO_3(s) + 3H_2O$	$p\varepsilon = 16 - 2pH + \log\{HCO_3^-\}$	(4)
	where $\{HCO_3^-\} = C_T\alpha_1$	
$FeCO_3(s) + H^+ + 2e = Fe(s) + HCO_3^-$	$p\varepsilon = -7.0 - \frac{1}{2}pH - \frac{1}{2}\log\{HCO_3^-\}$	(5)
$Fe(OH)_2(s) + 2H^+ + 2e = Fe(s) + 2H_2O$	$p\varepsilon = -1.1 - pH$	(6)
$Fe(OH)_3(s) + H^+ + e = Fe(OH)_2(s) + H_2O$	$p\varepsilon = 4.3 - pH$	(7)
$FeOH^{2+} + H^+ + e = Fe^{2+} + H_2O$	$p\varepsilon = 15.2 - pH - \log(\{Fe^{2+}\}/\{FeOH^{2+}\})$	(8)
	pH Functions	
$FeCO_3(s) + 2H_2O = Fe(OH)_2(s) + H^+ + HCO_3^-$	$pH = 11.9 + \log\{HCO_3^-\}$	(a)
$FeCO_3(s) + H^+ = Fe^{2+} + HCO_3^-$	$pH = 0.2 - \log\{Fe^{2+}\} - \log\{HCO_3^-\}$	(b)
$FeOH^{2+} + 2H_2O = Fe(OH)_3(s) + 2H^+$	$pH = 0.4 - \frac{1}{2}\log\{FeOH^{2+}\}$	(c)
$Fe^{3+} + H_2O = FeOH^{2+} + H^+$	$pH = 2.2 - \log(\{Fe^{3+}\}/\{FeOH^{2+}\})$	(d)
$Fe(OH)_3(s) + H_2O = Fe(OH)_4^- + H^+$	$pH = 19.2 + \log\{Fe(OH)_4^-\}$	(e)

7.3 Chemical reactions involved in the corrosion mechanism

The corrosion rate primarily depends on the pH value, although at pH > 4 oxygen concentration at the metal surface is also important. Formation of a protective layer which retards corrosion depends on the precipitation of various compounds from the water. The solubility and physical properties of the precipitation determines the effectiveness of the protective layer.

Corrosion of iron commences with the dissolution of iron at the anode as well as reaction with oxygen to form hydroxide at the cathode, as indicated in equations (7.1) and (7.2).

$$Fe \rightarrow Fe^{2+} + 2e^- \qquad (7.1)$$

$$\tfrac{1}{2}O_2 + H_2O + 2e^- \rightarrow 2OH^- \qquad (7.2)$$

In a study by Whitman et al. (1924) it was assumed that $Fe(OH)_2$ was formed during corrosion. This study showed that there was a high pH value at the metal surface independent of bulk solution pH, and that at this high pH $Fe(OH)_2$ is formed. However, at increased water velocities they found low pH values close to the metal surface.

In a study by Baylis (1926) regarding the solubility of $Fe(OH)_2$ and $FeCO_3$ he found that Fe(II) is converted to Fe(III) at high pH values. Baylis assumes that $Fe(OH)_2$ is formed close to the metal surface with $FeCO_3$ on top of the $Fe(OH)_2$. He states that the pH close to a metal surface is about the same as in the water bulk, since the presence of hydrogen carbonate in the studied water suppressed the increase of hydroxide.

Kooijmans (1938) found that in water containing high carbonate concentrations, high iron(II) content was found in the precipitations. In water without carbonates the content of iron(III) was high in the iron precipitations. This phenomenon is the same as in Figure 7.5.

At a pH value higher than 9, the absence of $FeCO_3$ precipitation allows an increase of corrosion (Larson and King 1954, Larson and Skold 1958). Iron(II) is rapidly oxidised to iron(III) at high pH which prevents the precipitation of $Fe(OH)_3$.

According to Olson and Twardowski (1975), two possible forms of reaction exist, where dissolved iron, in the form of iron(II), may react to form a number of iron compounds (Figure 7.5).

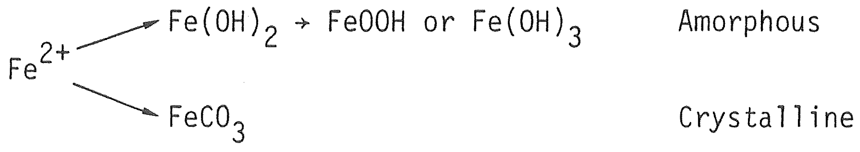

Figure 7.5 Two different compounds for iron(II), from Olson and Twardowski (1975).

Singer and Stumm (1970) studied the precipitation of various iron (II) compounds and formulated the conditions for formation of $FeCO_3$ and $Fe(OH)_2$ from solubility data. The study was based on well waters containing carbonic species. The solubility of iron(II) was dependent on the presence of precipitated $FeCO_3$.

Iron solubility products from CRC Handbook (1988) at 25^0 are:

$$Fe^{2+} + CO_3^{2-} \rightarrow FeCO_3(s) \qquad K_s = 3.07 \cdot 10^{-11}\ M^2 \qquad (7.6)$$

$$Fe^{2+} + 2OH^- \rightarrow Fe(OH)_2(s) \qquad K_s = 4.87 \cdot 10^{-17}\ M^3 \qquad (7.7)$$

Figure 7.6 shows the iron compounds formed as a function of iron concentration and pH value. $FeCO_3$ can occur up to pH 10.5 but above that pH, $Fe(OH)_2$ dominates.

Larson (1966) stated that iron(II) is oxidised to iron(III) and precipitates as FeOOH (Figure 7.5).

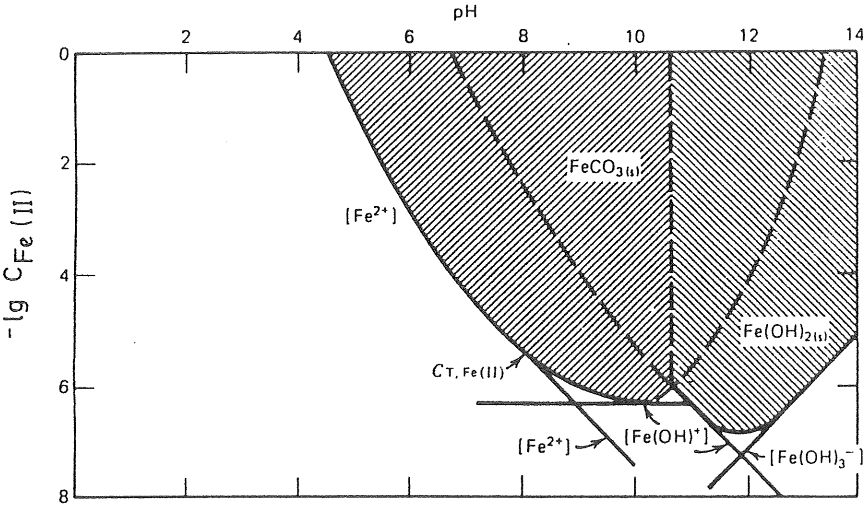

Figure 7.6 The solubility of iron(II) as a function of pH (from Snoeyink and Jenkins 1980).

von Schikorr (1930) found that various iron oxyhydroxides are formed during the oxidation of iron(II) to iron(III), depending on the environment and the rate of oxidation (Figure 7.7).

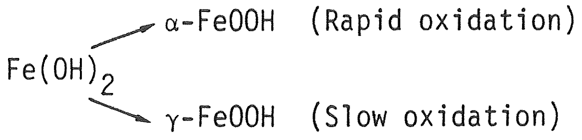

$$Fe(OH)_2 \begin{cases} \nearrow \alpha\text{-FeOOH} & \text{(Rapid oxidation)} \\ \searrow \gamma\text{-FeOOH} & \text{(Slow oxidation)} \end{cases}$$

Figure 7.7 Oxidation products for iron(II) (from von Schikorr 1930).

More recent investigations have shown α-FeOOH to be more stable than γ-FeOOH, but in most cases γ-FeOOH is formed (Sung and Morgan 1980).

In contrast, Sontheimer et al. (1981) stated that iron(II) is transformed into iron(III) via $FeCO_3$-precipitation, whilst maintaining the $FeCO_3$ crystalline structure (Figure 7.8).

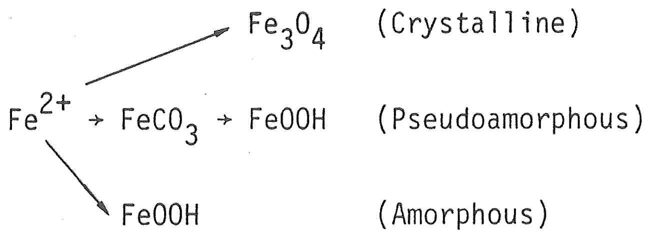

Figure 7.8 Oxidation products for iron(II) (from Sontheimer et al. 1981).

Kuch and Sontheimer (1986) made a comparison of water pipe corrosion with atmospheric corrosion. Under the latter conditions γ-FeOOH is reduced to Fe_3O_4. Kuch (1988) stated that metallic iron dissolved during non steady-state conditions when γ-FeOOH is reduced (equations 7.8 and 7.1). In a water pipe this reaction usually takes place under stationary conditions, either in stagnant water or in a closed system without oxygen addition.

$$3\gamma\text{-FeOOH} + H^+ + e^- \rightarrow Fe_3O_4 + 2H_2O \qquad (7.8)$$

$$Fe \rightarrow Fe^{2+} + 2e^- \qquad (7.1)$$

When the flow is resumed and oxygen is supplied, oxidation can occur.

When iron corrodes, several corrosion products can precipitate depending on the environment. $FeCO_3$ and Fe_3O_4 are considered to provide good protective properties.

7.3.1 Importance of oxygen on iron corrosion

Oxygen concentration in the water, and at the metal surface, is an important factor for iron corrosion. Transfer of oxygen takes place by water movement or in stagnant water by diffussion. The structure and the porosity of the precipitations formed determine the potential for oxygen diffusion to the metal surface. Diffusion of oxygen to the metal surface determines the rate of oxidation of Fe(II) to Fe(III) (Whitman et al. 1924, Larson and King 1954).

In stagnant water an oxygen gradient develops between the water bulk and the pipe surface and the oxygen concentration can only be equalised by diffusion. In flowing water there is only an oxygen gradient through the laminar layer (Kuch and Sontheimer 1986).

To minimise corrosion the oxygen concentration should be either 0 mg l^{-1} or over 4 mg l^{-1}. von Schikorr (1930), Haupt (1939/40), Stumm (1956) and Hall and Smith (1974) have studied the effects of various oxygen concentrations on corrosion product formation. Iron corrosion was most severe at low oxygen concentration and in order to reduce corrosion a threshold value of 40% O_2 saturation was suggested.

7.3.2 Importance of pH on iron corrosion

Iron corrosion is influenced by pH. The cathodic reaction provides a local increase in pH value close to the metal surface according to equation (7.2).

$$\tfrac{1}{2}O_2 + H_2O + 2e^- \rightarrow 2OH^- \qquad (7.2)$$

This pH increase affects the precipitation of corrosion products. At pH values up to 9, both $FeCO_3$ and $Fe(OH)_2$ precipitate. High pH (above 10.5) favours $Fe(OH)_2$ formation (Larson and King 1954, Larson and Skold 1958, Snoeyink and Jenkins 1980 and Stumm and Morgan 1981). At low pH values where no precipitation of iron compounds takes place (Figure 7.4) the oxidation rate for iron(II) to iron(III) is low (Olson and Twardowski 1975).

However, in the absence of carbonate the corrosion rate increases. In a long-term investigation done by Larson and Skold (1958) the corrosion rate was lowest at pH 7 in a water containing 125 mg l^{-1} HCO_3 and a ratio of chloride to alkalinity of 0.2 (water hardness was zero).

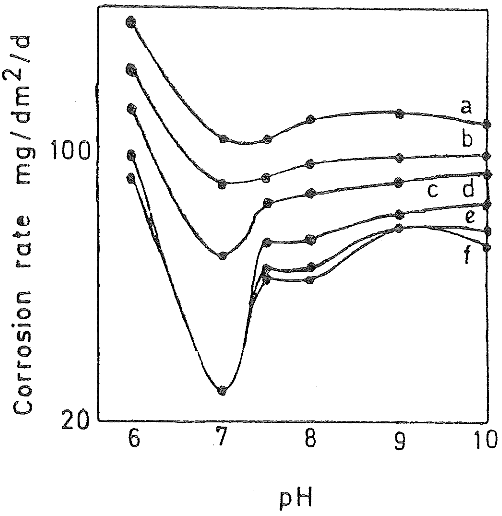

Figure 7.9 Corrosion rate versus pH, from Larson and Skold (1958). (Curves a, b, c, d, e and f correspond to 1, 10, 20, 50, 100 and 150 days.)

The extent of the change in pH as iron corrosion progresses depends on the buffer capacity (β). The buffer capacity is dependent on the content of total carbonic species and pH. Figure 7.10 is an illustration of buffer capacity at different pH and content of total carbonic species (C_T 0-150 mmol l^{-1}).

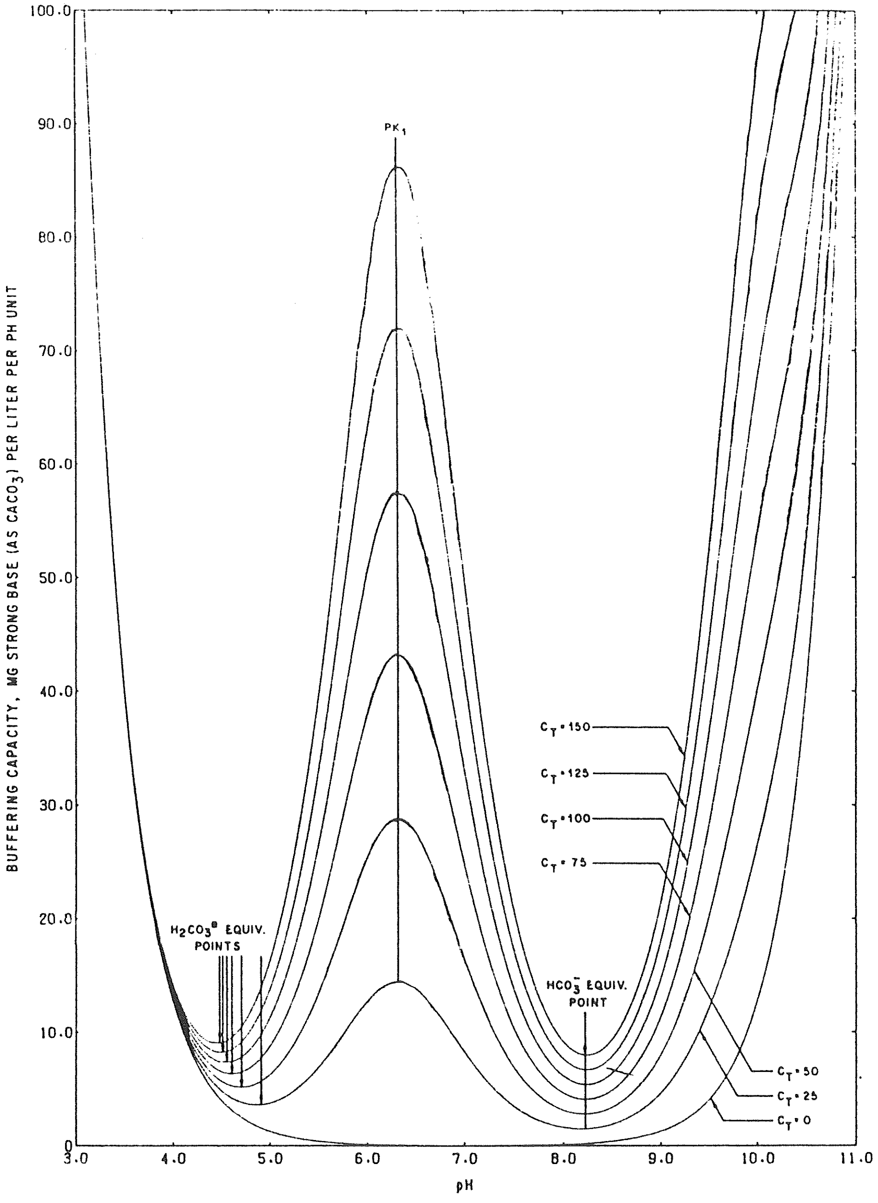

TEMP. = 25.0 DEG CENTIGRADE, IONIC STRENGTH = .01000

Figure 7.10 Buffer capacity versus pH at different total carbonic species values (C_T 0-150 mmol l^{-1}), (Sanks 1980).

Figures 7.11 and 7.12 show the corrosion rate as a function of pH and buffer capacity at different concentrations of total carbonic species (Pisigan and Singley 1987). When the buffer capacity is low at pH 8.4 the corrosion rate is high.

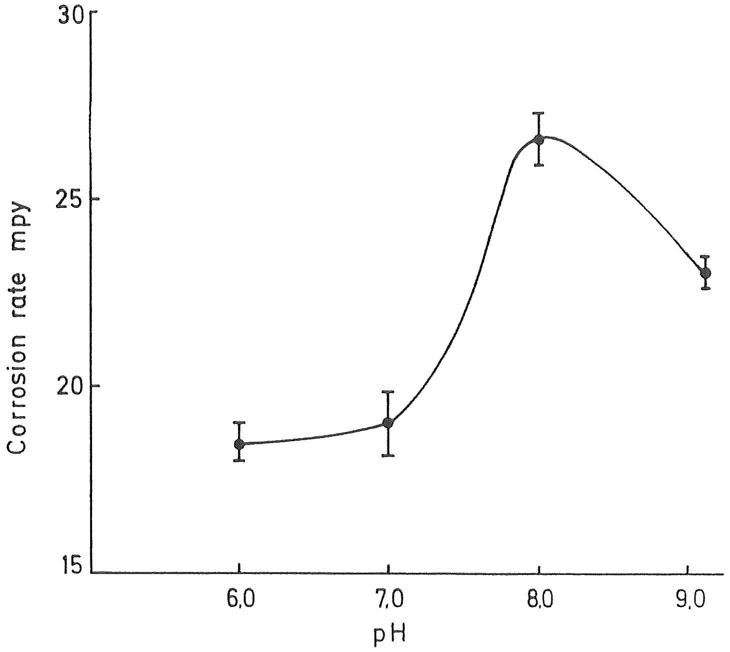

Figure 7.11 Corrosion rate versus pH, after Pisigan and Singley (1987). (1 mpy = 24.5 µm y^{-1})

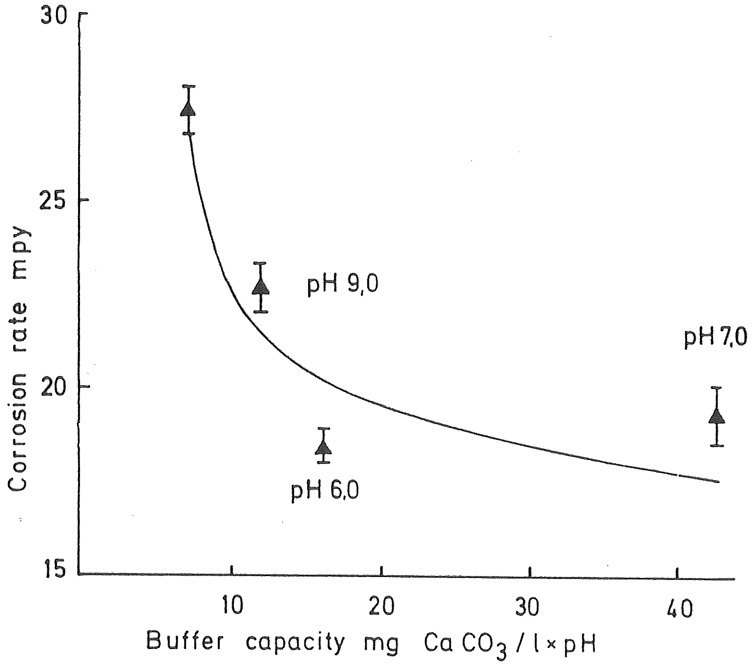

Figure 7.12 Corrosion rate versus buffer capacity with different pH values, from Pisigan and Singley (1987). (1 mpy = 24.5 µm y^{-1})

7.3.3 Importance of chloride and sulphate on iron corrosion

Baylis (1926) stated that negatively charged ions are attracted to the metal surface due to the difference in electrical potential. In the oxygen free zone the ions encounter iron(II) and adsorbed soluble complexes of iron(II) with chloride or sulphate are then formed. Thus the concentration of chloride or sulphate increases at the metal surface. Corrosion rate dependence on chloride concentration varies with pH (Larson and King 1954) and this also applies to a lesser extent to sulphate. Figure 7.13 shows the corrosion rate at pH 7 and 9 for high concentrations of chloride and sulphate and different alkalinities. A high pH results in a higher corrosion rate when chlorides are present and a high salt content at low alkalinity also results in a high corrosion rate.

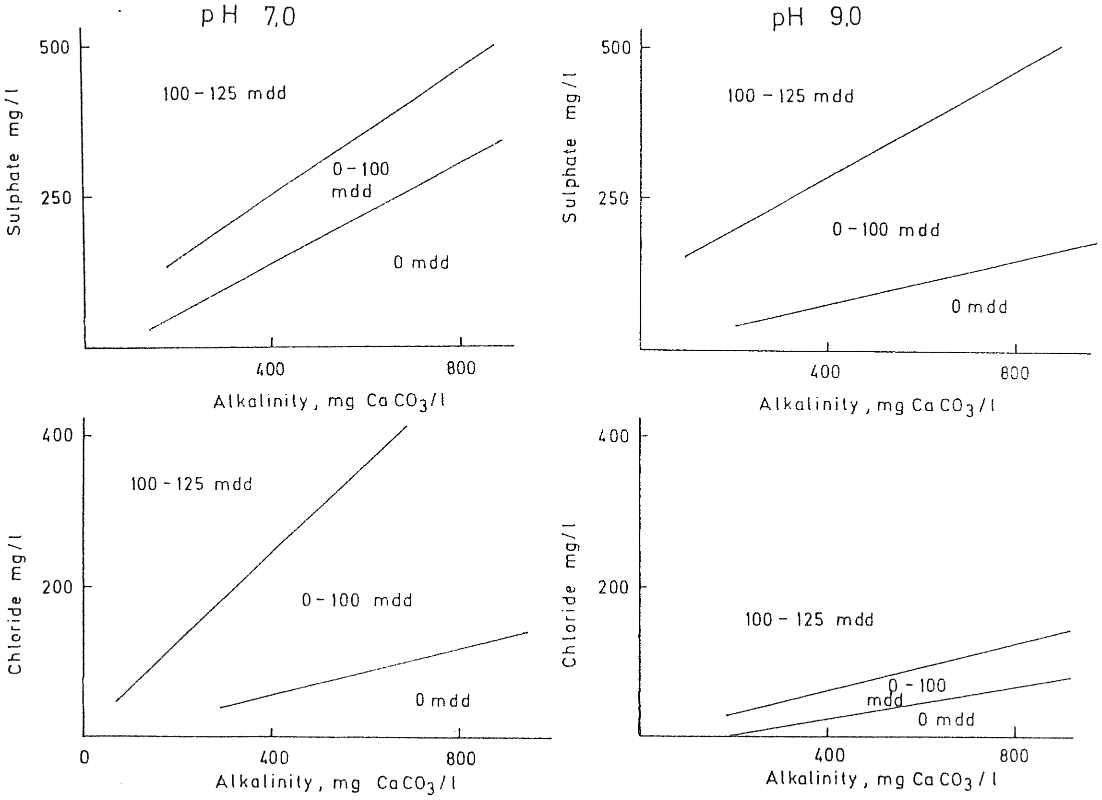

Figure 7.13 Corrosion rates at various chloride and sulphate concentrations, with different alkalinity and when pH is 7 and 9 (Larson and King 1954). (mdd = mg dm^{-2} d^{-1}). The solid lines represent boundaries of sectors in which the corrosion rates were as shown.

Pisigan and Singley (1987) found that corrosion rate versus the ratio of buffer capacity (β) to conductivity (I) is independent of the pH (Figure 7.14). An increase in conductivity leads to an increase in corrosion at constant buffer capacity, but when the buffer capacity increases at a constant conductivity the corrosion rate decreases.

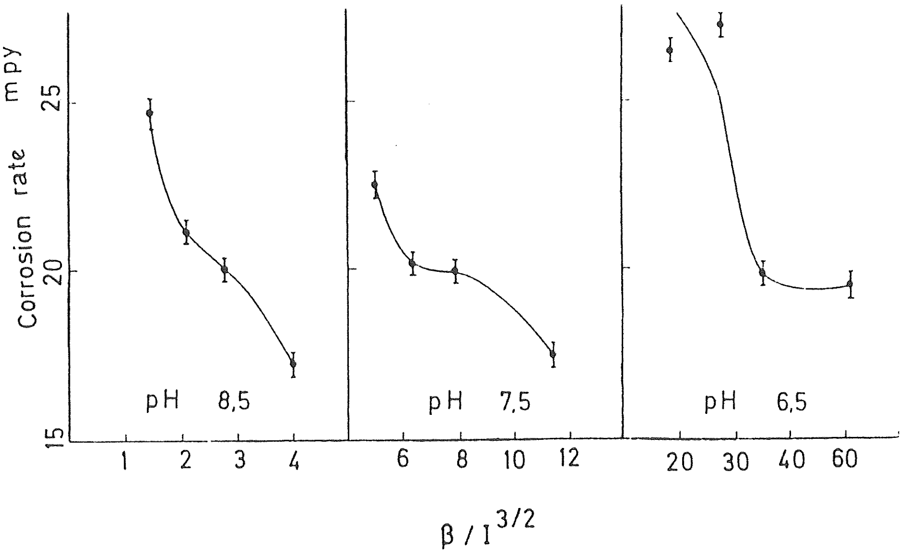

Figure 7.14 Corrosion rate versus buffer capacity to conductivity with different pH (Pisigan and Singley 1987). (1 mpy = 24.5 μm y^{-1})

The presence of chloride and sulphate in the corrosion products prevent $FeCO_3$ from precipitating on the metal surface (Baylis 1953).

Rudek et al. (1979) carried out corrosion studies with waters containing high salt content at two pH values and with organic matter added (Figure 7.15). The figure shows that the corrosion rate increased with pH, however, this increase is reduced in the presence of organic matter. The chloride content in the experiments was very high and could not be compared to the content in drinking water.

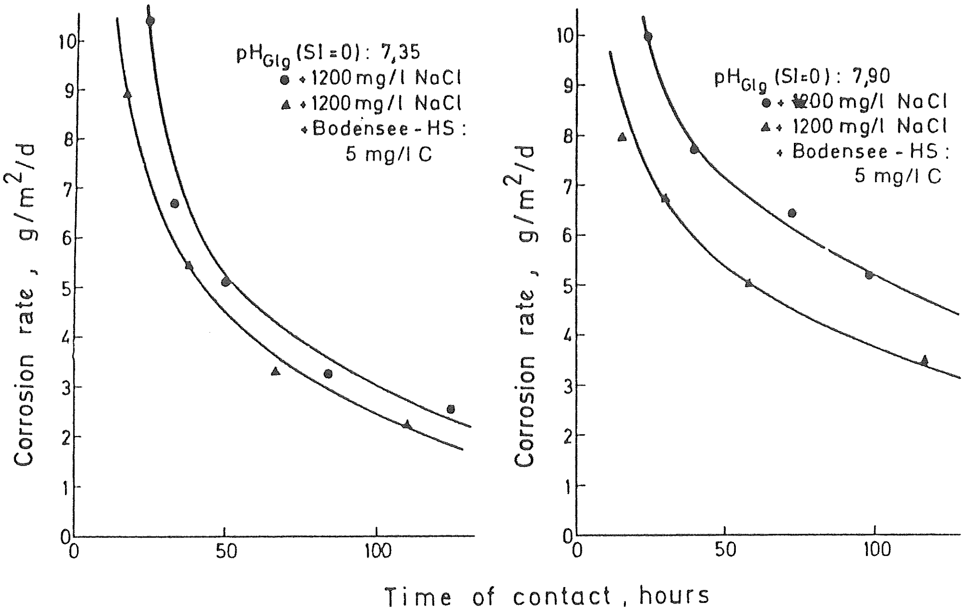

Figure 7.15 Corrosion rate as a function of time when pH is 7.35 and 7.9 at 1200 mg NaCl l^{-1} with and without organic matter (from Rudek et al. 1979).

When chloride is present, hydrochloric acid (HCl) which of course has a low pH is present on the metal surface at the point of corrosion (the anode). On the cathodic site, however, the pH is high as a consequence of the oxygen transition to hydroxide. Singley and Ahmadi (1985) developed the theory of Wranglén (1974) as follows; in the formed pit, the cathodic reaction no longer takes place by oxygen reduction, but rather by hydrogen ion reduction to hydrogen at low pH. The corrosion continues under the precipitation in the absence of oxygen. Chloride transport is possible through the porous precipitates because chloride has a small ionic radius. Figure 7.16 illustrates the mechanism.

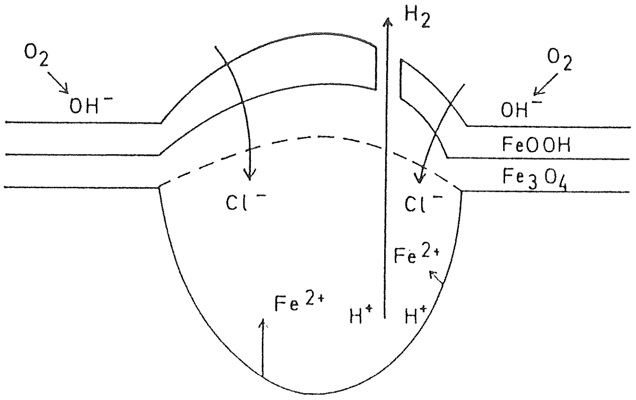

Figure 7.16 The effect of chloride on corrosion, from Wranglén (1974).

In pits below deposits, where sulphate is present in a reducing environment, sulphate reducing bacteria can survive (Costello 1969 and Lee et al. 1980). These bacteria utilise the sulphate and catalyse reaction (7.9) which acts as a cathodic reaction where iron is dissolved at the anode (Eistrat and Thorén 1980) during the formation of FeS, reaction (7.10).

$$Fe \rightarrow Fe^{2+} + 2e^- \tag{7.1}$$

$$SO_4^{2-} + 8H^+ + 8e^- \rightarrow S^{2-} + 4H_2O \tag{7.9}$$

$$Fe^{2+} + S^{2-} \rightarrow FeS \tag{7.10}$$

Reaction with H^+ to form H_2 may also take place at low pH. The risk of attack from sulphate reducing bacteria increases with increasing concentration of organic matter in the water (Ainsworth et al. 1981 and Tuovinen et al. 1980).

Chlorides and sulphates are also important for the oxidation of iron(II) to iron(III) (Stumm and Lee 1961, Sung and Morgan 1980, Hoffman 1981, Legrand and Leroy 1984 and Millero 1985). (Compare with Section 7.4, Kinetics for Fe(II) to Fe(III) oxidation.) Chloride and sulphate prevent the oxidation of iron(II) through complex formation. The effect of chloride on iron(II) oxidation is shown in Figure 7.17. The positive effect of complex formation of iron(II) could not outweigh the disadvantages of the increased pitting attacks.

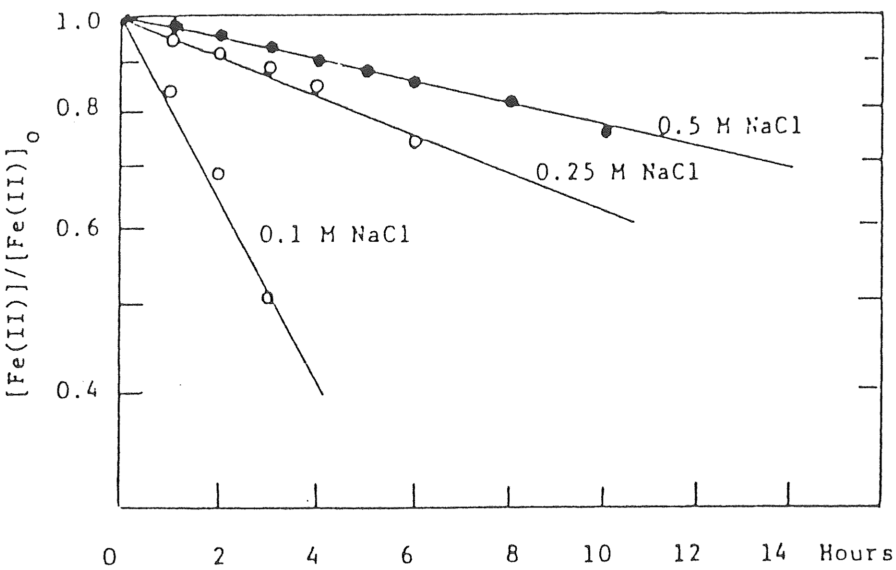

Figure 7.17 The ratio of remaining iron(II) to original iron(II) at different chloride concentrations, from Sung and Morgan (1980).

Larson and Skold (1958) studied the effect of chloride and sulphate for pitting corrosion. A ratio is then developed $(Cl^-+2SO_4^{2-})/HCO_3^-$. Nowadays this is a DIN standard in Germany. A ratio higher than 1 (using molar concentrations) increases pitting. A high buffer capacity counteracts the increase in corrosion.

7.3.4 Importance of water velocity on iron corrosion

Figure 7.18 illustrates the oxygen concentration gradient at the metal surface under laminar and turbulent flow conditions. Under laminar flow conditions, the water velocity close to the metal surface is very low or nearly zero. Under turbulent flow conditions, however, a thin layer close to the metal surface moves with a slower water velocity than the bulk water.

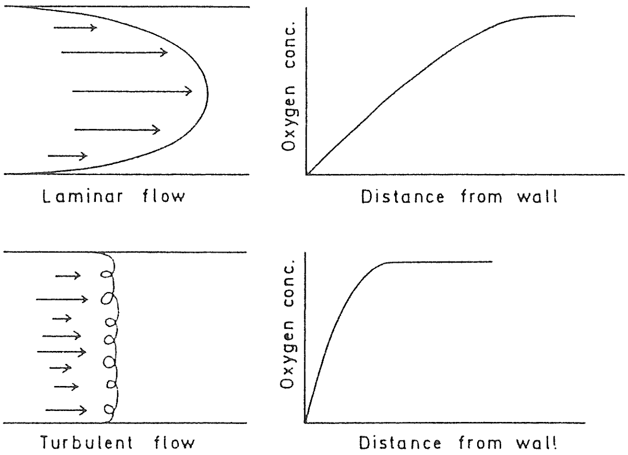

Figure 7.18 Concentration gradient for oxygen when the flow is turbulent or laminar, according to Larson (1966).

At low water velocity, an equilisation of oxygen concentration takes place by diffusion, while at high water velocities the oxygen concentration is equalised by the turbulence of the water (Eliassen et al. 1956, Larson 1960 and Larson 1966). The thickness of the laminar layer depends on the water velocity and the friction factor. The Reynold's Number is a function of the pipe diameter, the water velocity and the viscosity, equation (7.11). The friction factor is a function of the pipe's surface roughness and Reynold's number is related to laminar layer thickness, equation (7.12). The roughness increases with additional deposit caused by increased corrosion (Larson 1960).

$$Re = \frac{vd}{\nu} \tag{7.11}$$

$$\delta = \frac{32.8\nu}{v\sqrt{f}} \tag{7.12}$$

d = hydraulic diameter
δ = thickness of laminar layer
v = water velocity
ν = viscosity
Re = Reynold's Number
f = friction factor

The thickness of the laminar layer decreases with increasing deposition of corrosion products because of the increased water velocity when the diameter of the pipe decreases. Thus, oxygen transport to the metal surface increases, which in turn increases the corrosion rate. It is not only the concentration of species in the water close to the metal surface that varies with the water velocity, but also the appearance of the deposits (Baylis 1953). Dissolution and precipitation of deposits at the outer limit of the deposit structure are in equilibrium. Outer deposits may be torn loose during increased or irregular water velocity (Figure 7.19).

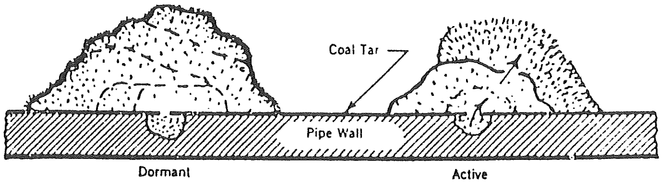

(a) Ordinary Tubercles

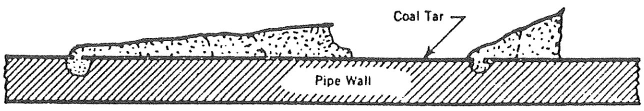

(b) Cone-shaped Tubercles

Figure 7.19 Appearance of deposits at various water flow velocities, according to Baylis (1953).
(a) low velocity, (b) very high velocity.

At high water velocity, water transports corrosion products which precipitate and sediment in areas where the water velocity decreases. This implies that where uniform corrosion attack takes place and the oxygen supply is high, no precipitation of corrosion products takes place. Deposits are found when the water is stagnant. In these places the oxygen concentration is low.

Water velocity affects the various species effect on corrosion rate. One example, found by Larson et al. (1956), is that high water velocity is (in a chloride containing water) less damaging if the total content of carbonic species is raised (Figure 7.20).

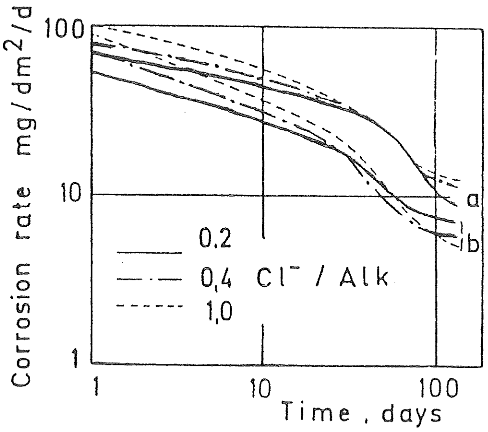

Figure 7.20 Corrosion rate as a function of time with different chloride concentrations to alkalinity ratios with (a) 0.6 m s^{-1} water velocity at pH 8.2 and with (b) 1.7 m s^{-1} at pH 7.8, from Larson and Skold (1957).

Stumm and Morgan (1981), on the other hand, stated that high water velocity in a water containing salts accelerates the corrosion rate. Salt ions easily come in contact with crystal nuclei of corrosion products and adsorb on them, which results in porous precipitations through which species in the water, i.e. oxygen, salts or iron, diffuse through easily. They also stated that at a low water velocity the corrosion rate is independent of the salt content of the water.

Water velocity influences the formation of corrosion prevention products, especially crystalline products. The rate limits for crystallisation are the thickness of the laminar layer, the diffusion rate and the molecular size. An increased water velocity accelerates the corrosion rate and the probability of crystal growth by collisions, although the necessary chemical conditions must be present. At low water velocity the diffusion rate is corrosion rate determined and crystallisation is controlled by diffusion. Crystallisation requires energy in order to form an organised structure with a well defined surface. When the water velocity is high, energy is available for crystallisation. Crystallisation requires also some degree of supersaturation (Snoeyink and Jenkins 1980). The supersaturation must be greater at low water velocity or when there are other species present in the water. As an example, in a water containing calcium and hydrogen carbonate or phosphate, an increased water velocity decreases the corrosion rate. At high water velocities the compounds precipitate more easily (Larson 1966).

Kölle and Sontheimer (1977) found that the corrosion rate increased when the water velocity was increased from 0.004 to 0.1 m s^{-1}. Eliassen et al. (1956) and Singley and Lee (1984a) reported an increase in the corrosion rate if the water velocity increases from 0.1 to 0.3 m s^{-1} in the pH range 5-10. A further increase from 0.3 and 0.7 m s^{-1}, will, however, decrease the corrosion (Eliassen et al. 1956) as shown in Figure 7.21. The explanation is that the transition from laminar to turbulent flow no longer increases the corrosion rate with increasing water velocity.

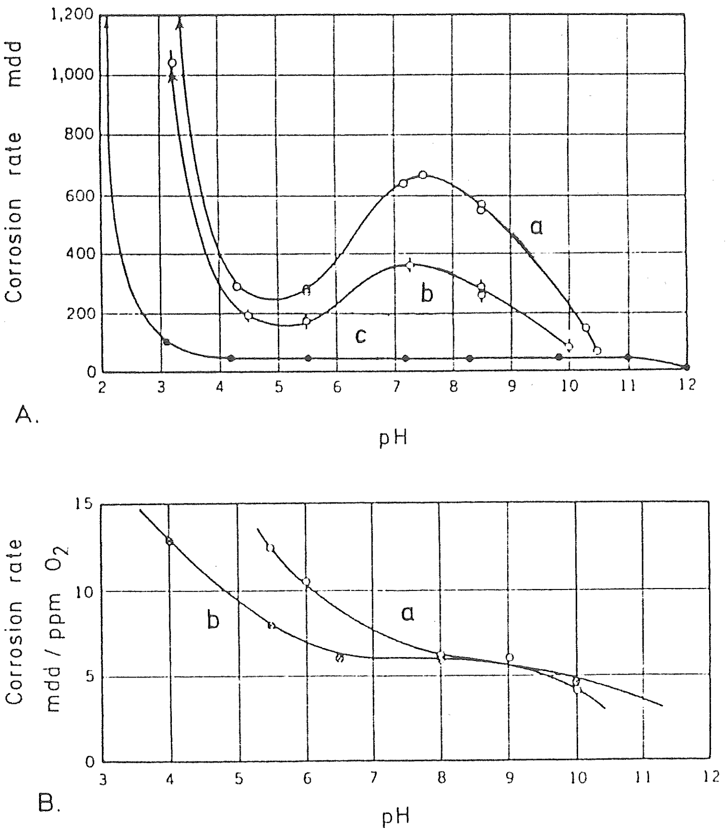

Figure 7.21 (A) Corrosion rate versus pH at a water velocity of (a) 0.3 m s^{-1}, (b) 0.1 m s^{-1} and (c) 0 m s^{-1}.
(B) Corrosion rate versus pH at a water velocity of (a) 0.3 and (b) 0.7 m s^{-1}, from Eliassen et al. (1956). (mdd = mg dm^{-2} d^{-1})

Williams et al. (1984) showed, by weight loss of coupons, the influence of high and low water velocities, which is illustrated in Figure 7.22. An inhibitor was added to the water. At low water velocity the weight loss was independent of the treatment but at a high velocity the corrosion rate decreased due to the influence of water velocity on precipitation of the inhibitor.

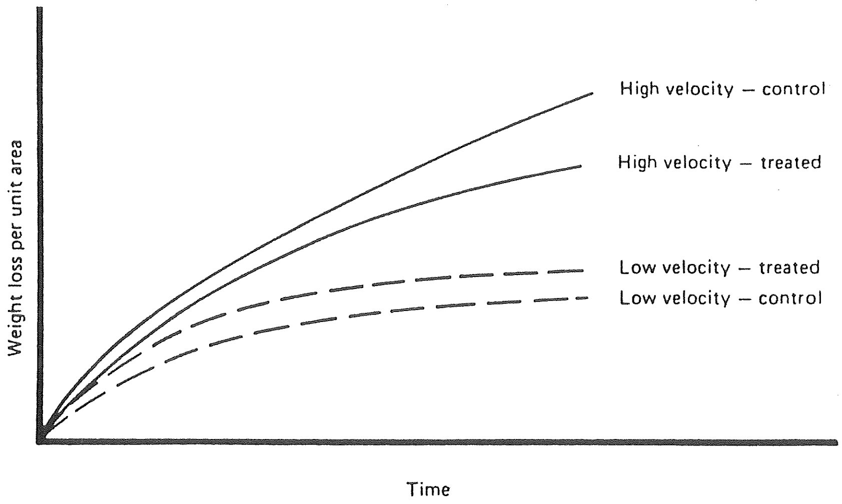

Figure 7.22 Weight loss as a function of time at two different water velocities with and without any treatment against corrosion, according to Williams et al. (1984).

The conclusion is that a low water velocity and even a high water velocity increase the corrosion rate. At low water velocity corrosion products that prevent corrosion do not precipitate. At high water velocity the deposits are carried away and oxygen easily reaches the metal surface.

7.4 Kinetics of oxidation of iron(II) to iron(III)

To prevent corrosion it is important that iron remains as iron(II) and does not oxidise to iron(III) as a precipitate of FeOOH. In the following section the influence of pH, oxygen, chloride and sulphate are considered.

7.4.1 The dependence of pH and oxygen on the oxidation rate of iron(II)

The corrosion reaction requires oxygen when the $pH > 4$ and iron(II) is dissolved. Iron(II) oxidises to iron(III) depending on the oxygen content and pH according to equation (7.13).

$$\mathrm{Fe(II)} + \tfrac{1}{4}\mathrm{O_2} + 2\mathrm{OH^-} + \tfrac{1}{2}\mathrm{H_2O} \rightleftarrows \mathrm{Fe(OH)_3(s)} \qquad (7.13)$$

Stumm and Lee (1961) showed that iron oxidation is first order with regard to oxygen and second order with regard to pH (equation 7.14).

$$\frac{d[\mathrm{Fe(II)}]}{dt} = -K[\mathrm{Fe(II)}]\,[\mathrm{OH^-}]^2\, p_{\mathrm{O_2}} \qquad (7.14)$$

where

$$K = 8(\pm 2.5) \cdot 10^{13}\ \mathrm{l^2 atm^{-1} min^{-1} mol^{-2}} \qquad \text{at } 20^{\circ}\mathrm{C}$$

This implies a hundred fold increase in oxidation rate for a unit increase of pH. Pankow and Morgan (1981) found that iron(II) is fully oxidised to iron(III) in 10 seconds at pH 8.5, 60 seconds at pH 8 and in over an hour at pH 7. At pH 6 the oxidation reaction took one week. The reaction rate constant is a function of temperature. Stumm and Lee (1961) found that a temperature increase of 15°C increased the rate of reaction by a factor of 10.

More recent research has shown that other components besides pH and oxygen concentration affect the rate of oxidation of iron(II) to iron(III), including buffer capacity, organic matter and ionic strength (Jobin and Gosh 1972, Theis and Singer 1974, Olson and Twardowski 1975, Sung and Morgan 1981 and Stumm and Morgan 1981).

7.4.2 The dependence of buffer capacity on the oxidation rate of iron(II)

As discussed previously the buffer capacity is dependent on pH and the total concentration of carbonic species.

Hydroxide ion is formed in the cathodic reaction (equation 7.2). The pH increases but if carbonic acid or hydrogen carbonate is present in the water, hydrogen carbonate or carbonate formation is favoured (equations 7.15 and 7.16).

$$\tfrac{1}{2}O_2 + H_2O + 2e^- \rightarrow 2OH^- \qquad (7.2)$$

$$H_2CO_3 + OH^- \rightarrow HCO_3^- + H_2O \qquad (7.15)$$

$$HCO_3^- + OH^- \rightarrow CO_3^{2-} + H_2O \qquad (7.16)$$

When ionic iron(II) is present in the water, it may be precipitated rather than becoming bound as an iron(III) compound (equations 7.6 and 7.7).

$$Fe^{2+} + CO_3^{2-} \rightleftarrows FeCO_3 \qquad K_s = 3.07 \cdot 10^{-11} M^2 \qquad (7.6)$$

$$Fe^{2+} + 2OH^- \rightleftarrows Fe(OH)_2 \qquad K_s = 4.87 \cdot 10^{-17} M^3 \qquad (7.7)$$

Equation (7.17) for the oxidation rate of iron(II) in waters with a high buffer capacity (β) was developed by Jobin and Gosh (1972). This equation is a further development of equation (7.15).

$$\frac{d[Fe(II)]}{dt} = -K[Fe(II)][OH^-]^2 \, p_{O_2} \, \beta^{\frac{1}{2}} \qquad (7.17)$$

where

$$K = \beta \cdot 10^{14} \; l^2 atm^{-1} mol^{-2} min^{-1}$$

7.4.3 Effect of organic matter on the oxidation rate of iron(II)

Organic matter present in the water affects the oxidation of iron(II) in various ways. It affects oxidation partly by changing the environment at the metal surface. Humic and fulvic acids both lower the pH which prevents the iron(II) oxidation and allows the complexation of iron(II). Dissolved organic matter retains iron(II) in solution. According to Theis and Singer (1974) the following reactions take place between iron and organic matter (equations 7.19 and 7.20):

$$Fe(II) + \tfrac{1}{2}O_2 + \text{organics} \xrightarrow[\text{slow}]{} Fe(III) - \text{organic complex} \qquad (7.19)$$

$$Fe(III)\text{-organic complex} \xrightarrow[\text{fast}]{} Fe(II) + \text{ox. organic compound} \qquad (7.20)$$

During the formation of the organic complex, iron(II) acts only as a catalyst for the oxidation of the organic matter. Reaction (7.19) is slow which tends to allow the retention of Fe(II) (Stumm and Morgan 1981). Jobin and Gosh (1972), however, found that a reaction between iron(II) and organic matter results in an iron(II)-complex rather than an iron(III)-complex (equation 7.20). At high oxygen concentrations, iron(II) is oxidised to iron(III) which is precipitated as FeOOH (equations 7.21 and 7.22).

$$\text{Organics} + Fe(II) \rightarrow Fe(II) - \text{organic complex} \qquad (7.20)$$

$$Fe(II) \xrightarrow{O_2} Fe(III) \qquad (7.21)$$

$$Fe(III) + 3OH^- \rightarrow FeOOH + H_2O \qquad (7.22)$$

Reaction (7.20) is primarily valid for tannins but not for humic and fulvic acids (Jobin and Gosh 1972, Theis and Singer 1974). In a comparison between humic acids and tannins, the tannins were found to cause a stronger retardation of iron oxidation than the humic acids (Jobin and Gosh 1972) as illustrated in Figure 7.23.

Rudek et al. (1979) studied the influence of organic matter on iron oxidation and found that a high concentration of organic matter in the water retards the oxidation of iron(II). The effects are, however, dependent on the origin of the organic matter. The molecular weight and the acid number of organic matter are also important in oxidation. A high molecular weight and a high acid number reduces the corrosion rate most effectively. However, in natural waters, the molecular weight is nor-

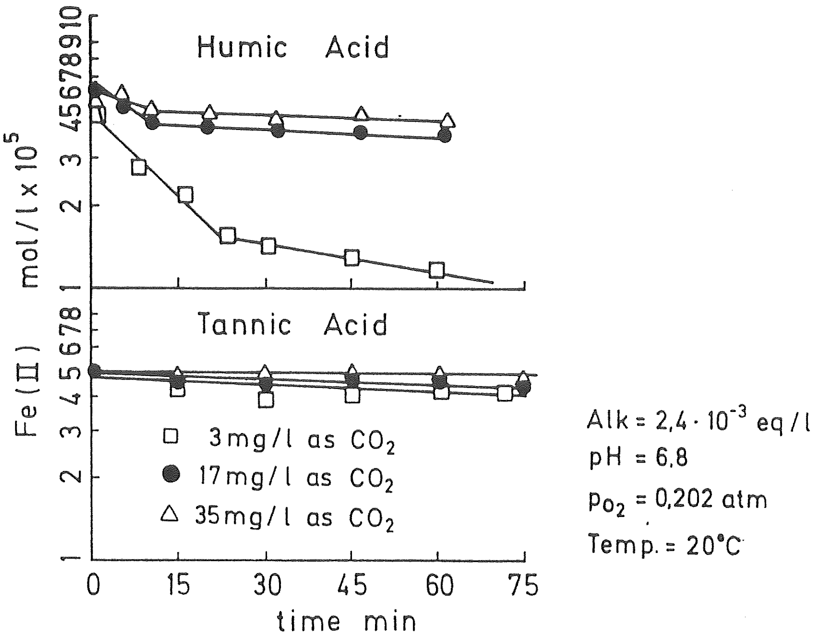

Figure 7.23 Oxidation of iron(II) in water with tannins and humic acids, from Jobin and Gosh (1972).

mally both high and low and the acid number is low. The molecular weight is decreased and the acid number is increased by treatment with a strong oxidising agent such as ozone. Figure 7.24 shows how iron(II) in water decreased with time in relation to the amount of organic carbon.

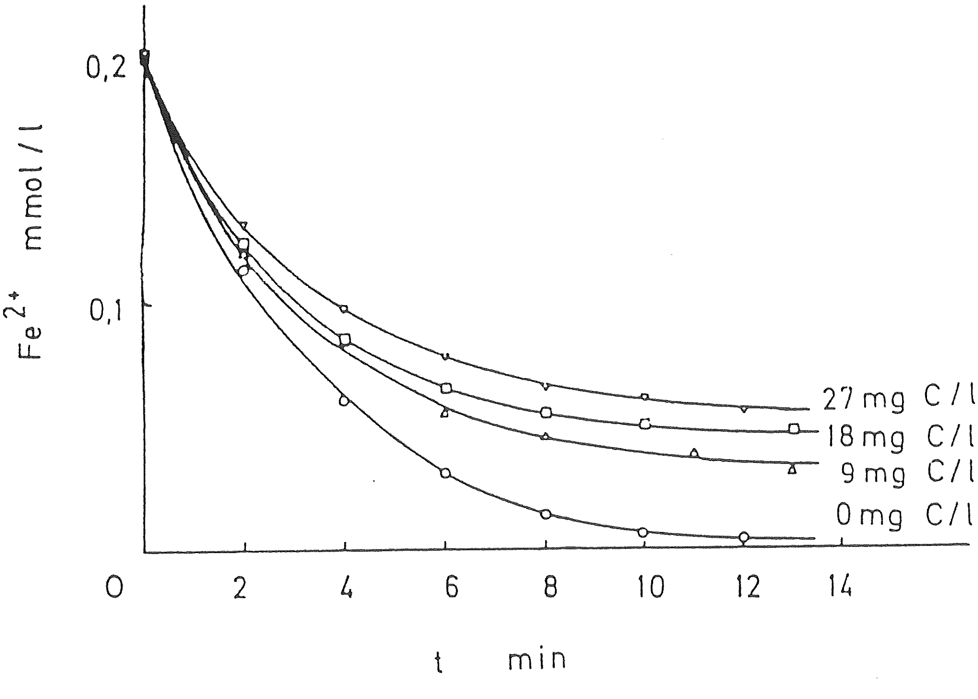

Figure 7.24 Concentration of iron(II) as a function of time at different organic carbon concentrations, from Rudek (1979).

Complex formation is believed to depend on the presence of carboxylic groups in the organic matter. Tannins have a higher number of carboxylic groups per mole available than humic acids. An iron complex requires two carboxylic groups, according to reaction (7.23) and (7.24).

$$2(R\text{-}COOH) + 2OH^- \rightarrow 2(R\text{-}COO^-) + 2H_2O \qquad (7.23)$$

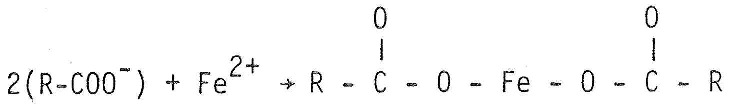

$$2(R\text{-}COO^-) + Fe^{2+} \rightarrow R - \overset{\overset{O}{|}}{C} - O - Fe - O - \overset{\overset{O}{|}}{C} - R$$

(7.24)

The stability of the complexes decrease at high pH. Theis and Singer (1974) found that complexed iron(II) is ionised at pH 10.8 and the iron(II) is transformed to iron(III) and precipitates as FeOOH.

7.4.4 Effect of ionic strength on the oxidation rate of iron(II)

Sung and Morgan (1980) compared various reaction rate constants for oxidation. The tests were done under varying ionic strength (I) and they found a relation between the rate and $\sqrt{I}$ (equation 7.25). Equation (7.25) represents a refinement of equation (7.15).

$$\frac{d[Fe(II)]}{dt} = - K [Fe(II)] [OH^-]^2 \, p_{O_2} \sqrt{I} \qquad (7.25)$$

where

$$pK = -13.76 + 2.06\sqrt{I}$$

The ionic strength was varied both by addition of various salts and by different concentrations of chloride. The importance of ionic strength in complex formation between Fe(II) and chloride was studied by Millero (1985). Besides the formation of soluble complexes, the oxidation depends on the formation of neutral and soluble ion-pairs, especially with chlorides (Legrand and Leroy 1984, Millero 1985). Models for the oxidation of iron(II) to iron(III) have been developed with regard to various parameters and species (Pankow and Morgan 1981, Hoffman 1981, Legrand and Leroy 1984, Millero 1985).

Legrand och Leroy (1984) developed a rate equation (7.26) for iron oxidation. A number of species besides oxygen and OH^- are included:

$$-\frac{d[\mathrm{Fe(II)}]}{dt} = \frac{k_1[\mathrm{Fe(II)}][O_2][OH^-]^2}{1 + \frac{[HCO_3^-]}{K_1} + \frac{[SO_4^{2-}]}{K_2} + \frac{[Cl^-]}{K_3} + \frac{[NO_3^-]}{K_4}} \left(1 + \frac{3}{1 + \frac{[Ca^{2+}]}{K_7} \quad \frac{[Mg^{2+}]}{K_8}}\right) \tag{7.26}$$

where

$k_1 = 0.27 \cdot 10^{12}$
$pK_1 = 1.9$
$pK_2 = 2.6$
$pK_3 = 1.8$
$pK_4 = 1.2$

$pK_7 = 3.4$
$pK_8 = 3.1$

From the equation it is seen that OH^- and O_2 are those species which are of most importance for oxidation. The oxidation rate is decreased by additions of hydrogen carbonate, sulphate, chloride or calcium.

Oxidation of iron(II) can be prevented in a water with a high calcium concentration by the formation of CaO_2^+ (equation 7.32) (Legrand and Leroy 1984, Millero 1985). During the oxidation of iron(II) to iron(III), O_2^- is formed (equations 7.27-7.30). The reactions are valid for pH values between 6 and 8 (Millero 1985).

$$Fe^{2+} + O_2 \rightarrow Fe^{3+} + O_2^- \quad (7.27)$$

$$Fe(OH)^+ + O_2 \rightarrow Fe(OH)^{2+} + O_2^- \quad (7.28)$$

$$Fe(OH)_2 + O_2 \rightarrow Fe(OH)_2^+ \quad (7.29)$$

$$Fe(OH)^+ + H_2O \rightarrow Fe^{3+} + 2OH^- + O_2^- \quad (7.30)$$

$$Fe^{2+} + O_2^- + 2H^+ \rightarrow Fe^{3+} + H_2O_2 \quad (7.31)$$

$$Ca^{2+} + O_2^- \rightarrow CaO_2^+ \quad (7.32)$$

The oxidation of iron(II) to iron(III) is dependent on several species in the water, but the most important parameters are normally pH and the concentration of oxygen. If carbonic acid or hydrogen carbonate is present in the water the effect of OH^- is repressed without an increase in oxidation. Calcium ties up the O_2^- from reaction (7.27) as a complex and reaction (7.31) stops which provides a decrease in iron(II) oxidation. Cl^- and SO_4^{2-} also decrease iron(II) oxidation by complex formation (Millero 1980). pH, calcium concentration and carbonic species concentration are parameters which are relatively easy to control. On the other hand, it is difficult to change parameters such as water flow velocity, oxygen concentration and salt concentration.

7.5 Effect of calcium carbonate precipitation on iron corrosion

A protective layer could consist of many compounds of iron. $FeCO_3$ is generally regarded as the most suitable (Sontheimer et al. 1981). Tillmans et al. (1927) found protective layers consisting of $CaCO_3$ crystals when the water was in $CaCO_3$ saturation. The layer also consists of iron oxides. When the water was supersaturated they also found non-crystalline $CaCO_3$ with a high content of iron in form of FeOOH. This layer was not found to be protective.

For many years it has been accepted that a protective layer for iron should consist of $CaCO_3$. Larson and Skold (1957) and Larson (1960) consider for example that the only way to decrease iron corrosion is to create conditions which cause calcium carbonate to precipitate on the metal surface. Calcium carbonate precipitation decreases corrosion mainly because it prevents oxygen from diffusing through the deposit to the metal surface (Larson 1966). Stumm (1956) stated that a thin protective layer with a high $CaCO_3$ content is better than a thick protective layer without $CaCO_3$.

The following section discusses parameters that influence the precipitation of $CaCO_3$ such as pH, total carbonic species content and the content of calcium and organic matter. The formation of calcium carbonate containing protective layers is also described.

Sontheimer et al. (1981) have shown the importance of calcium for iron corrosion (Figure 7.25). From the figure it can be seen that an increased calcium concentration gives a lower corrosion rate and a higher content of iron(II) in the precipitation. As iron(II) remains and is not oxidised to iron(III) there is a possibility for the precipitation of iron(II) containing compounds which can protect against corrosion, especially at high concentration of hydrogen carbonate and a rather low pH.

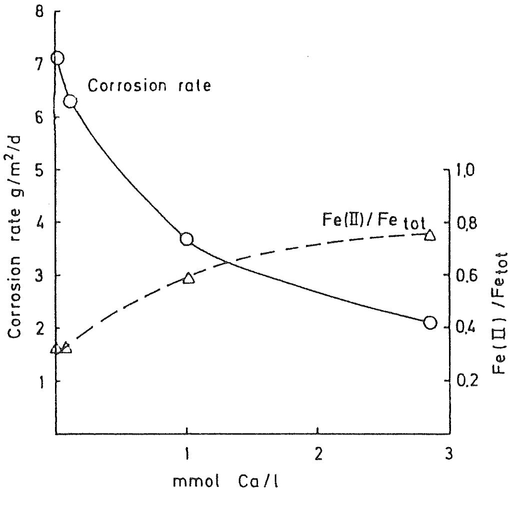

Figure 7.25 Influence of calcium on corrosion rate, from Sontheimer et al. (1981), pH 7.35, 75 mg $HCO_3 l^{-1}$.

7.5.1 Importance of pH, carbonic species and calcium on calcium carbonate precipitation

Calcium carbonate precipitation depends on the pH close to the metal surface and the pH of the water bulk. The pH at the metal surface is controlled by the cathodic reaction:

$$\tfrac{1}{2}O_2 + H_2O + 2e^- \rightarrow 2OH^- \qquad (7.2)$$

The concentration of hydrogen carbonate or carbonate depend on the original concentration of total carbonic species and the amount of hydroxide that forms during the corrosion reaction.

$$HCO_3^- + OH^- \rightleftarrows CO_3^{2-} + H_2O \qquad (7.17)$$

If carbonate and calcium are both present, $CaCO_3$ will precipitate if the solubility product is exceeded.

$$Ca^{2+} + CO_3^{2-} \rightleftarrows CaCO_3(S) \quad K_s = 4.96 \cdot 10^{-9} M^2 \qquad (7.34)$$

Below pH 8.5, calcium carbonate precipitation competes with precipitation of $FeCO_3$:

$$Fe^{2+} + CO_3^{2-} \rightleftarrows FeCO_3(s) \quad K_s = 3.07 \cdot 10^{-11} M^2 \qquad (7.6)$$

At high pH, iron(II) is oxidised to iron(III) rather than forming $FeCO_3$, and FeOOH in addition to $CaCO_3$ precipitates. In order for $CaCO_3$ or $FeCO_3$ to precipitate, the solubility products must be attained, which depends on the concentration of the involved species. At low concentrations of either calcium or hydrogen carbonate, no $CaCO_3$ precipitation takes place and this cannot be compensated for by increasing pH (Haase 1952 and Larson 1966).

Tillmans et al. (1927) studied the influence of carbonic acid on iron corrosion. They determined the equilibrium concentrations for $CaCO_3$ and for CO_2. The CO_2 content should not be higher than that in equilibrium with adsorbed CO_2 as aggressive CO_2 dissolves precipitations of iron and calcium compounds. Free carbonic acid is also present which reacts with iron and forms $FeCO_3$. At equilibrium in the calcium-carbonic acid system, neither precipitation nor dissolution of calcium carbonate is observed.

In a surface water in contact with calcium rich soil, with the assumption that CO_2 from the air dissolves in the surface water, equilibrium is reached under the following conditions at pH 8.4: Ca^{2+} = 20 mg l^{-1}, HCO_3^- = 58 mg l^{-1}, CO_3^{2-} = 0.59 mg l^{-1} (Kelley and Anderson 1935 and Haase 1952). Under these conditions $CaCO_3$ remains in solution. An increase in concentration of calcium, hydrogen carbonate or pH will lead to $CaCO_3$ precipitation. With an increase in carbonic acid concentration, Ca^{2+}, HCO_3^- and CO_3^{2+} remain in solution (equation 7.35).

$$CaCO_3 + CO_2 + H_2O \rightleftarrows Ca^{2+} + 2HCO_3^- \tag{7.35}$$

Uusitalo and Heinanen (1962) state that the following criteria need to be fulfilled in order to provide a protective layer by precipitation:

- The water may not contain aggressive carbonic acid.
- The flow velocity should exceed 0.5 m s^{-1}.
- The hydrogen carbonate content should exceed 44 mg l^{-1}. If the flow velocity statement is not fulfilled, the HCO_3^- content should be increased to 131 mg l^{-1}.
- The oxygen concentration should not be below 6 mg l^{-1}.

In a water with low buffer capacity more calcium carbonate will precipitate than in a water with higher buffer capacity, depending on the stronger tendency for pH increase during corrosion (Stumm 1956 and McClanahan and Mancy 1974).

In natural waters ionic strength (salt content) affects $CaCO_3$ precipitation, the precipitated amount decreases when $CaCO_3$ solubility increases (Tillmans et al. 1927 and Kooijmans 1938). Oxygen is another factor of major importance. A higher oxygen concentration will provide a quicker and more extensive precipitation (Stumm 1956). At higher water velocities, oxygen is more easily transported towards the metal surface due to the thinner laminar layer at the surface (Larson 1960). Thus, an increase in water velocity causes an increased $CaCO_3$ precipitation (McCauley 1960, Larson 1966). The precipitation of $CaCO_3$ is dependent on the pH and the concentration of calcium and carbonate. The precipitation rate increases with pH. McClanahan and Mancy (1974) found during tests that the permeability of precipitation products increase slightly with increased pH. At high concentrations of calcium, the permeability decreases. The morphology of the $CaCO_3$ is dependent on the precipitation rate. A slow precipitation will give a crystalline structure while a quick precipitation will usually give an amorphous structure (Tillmans et al. 1927). An amorphous structure does not provide a satisfactory protection for the metal surface, as it is a porous and permeable precipitation (Haase 1935, 1952).

7.5.2 Influence of organic matter on calcium carbonate precipitation

Organic matter changes the solubility and precipitation rate of calcium carbonate. Both the concentration and the type of organic matter have an influence on the precipitation rate (Haase 1952, Rudek and Sontheimer 1976, Rudek 1979). Organic matter retards the precipitation of calcium carbonate, but the effect is reduced when there is an increased content of calcium (Rudek and Sontheimer 1976 and Wagner 1980).

The precipitation takes place according to the following rate equation (Rudek 1979).

$$\frac{d[Ca^{2+}]}{dt} = -kO([Ca^{2+}][CO_3^{2-}] - \frac{K_s}{f_I}) \quad (7.36)$$

where

f_I = correction factor dependent on ionic strength
k = constant depending on the organics
K_s = solubility product of $CaCO_3$
O = the surface of $CaCO_3$

The precipitation rate decreases proportionally to a higher molecular weight and increased acid number of the organic matter. It is not possible to achieve these conditions at the same time. When the molecular weight distribution is changed towards smaller molecules (for instance by ozone degradation) the acid number increases. Table 7.1 shows how the rate constant for calcium carbonate precipitation decreases with increasing concentration of organic matter. Table 7.2 shows the effects of an ozone treatment of a water containing humic acids. The result will be a more crystalline calcium carbonate with protective properties.

Table 7.1 Changes in rate constant (k) for $CaCO_3$ precipitation depending on the water content of humic acids, according to Rudek (1979).

Conc. humics mg DOC l^{-1}	Rate const. for $CaCO_3$ (k) $mol^{-1}\ l^2\ s^{-1}\ g^{-1}$
0	14.8
2	8.2
5	4.8
7.5	3.0
10	2.3

Table 7.2 Changes in rate constant (k) for $CaCO_3$ precipitation after ozone treatment in a water containing humic acids, according to Rudek (1979).

Conc. humics mg DOC l^{-1}	Conc. ozone mg l^{-1}	Rate const. for $CaCO_3$ (k) mol^{-1} l^2 s^{-1} g^{-1}
2.55	-	6.2
2.32	2.5	3.8
1.91	5.3	3.7

The effect of ozone has been reported by Wagner (1980). Figure 7.26 shows how the content of iron decreased in an ozone treated water compared to an untreated one. In the ozone treated water organic matter was adsorbed on the $CaCO_3$ surface and the precipitation rate was slowed down which results in a higher degree of crystallinity and the formation of more protective layers.

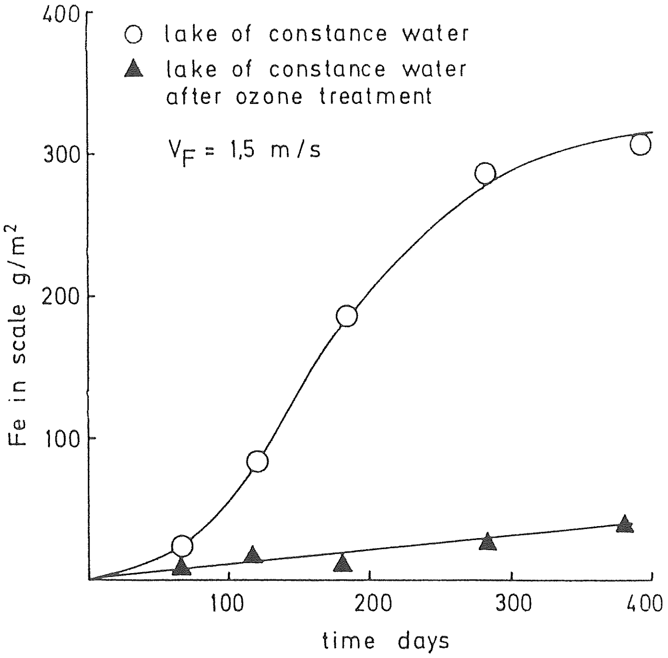

Figure 7.26 Influence of ozone treatment on iron-content in scale (Wagner 1980).

When organic matter adsorbs on the surface of the crystal nuclei of $CaCO_3$ and $FeCO_3$, the degree of crystallinity increases (Rudek 1979). An adsorption could also lead to crystallisation even if the water is slightly unsaturated with regard to the solubility product.

Liao and Randtke (1985) examined $CaCO_3$ precipitation in the presence of organic matter. The content of calcium was 240 mg l^{-1} and carbonate 360 mg l^{-1} at pH 11 with an organic carbon concentration of 3 mg l^{-1}. Amorphous $CaCO_3$ was first formed, which was quickly transformed into crystals. The organic matter adsorbed on the $CaCO_3$ and 75% of the fulvic acid in the water disappears in 30 seconds when $CaCO_3$ precipitates, and in 30 minutes all of it has disappeared. The Ca^{2+}-ion increases the adsorption of organic matter on $CaCO_3$. The adsorption of fulvic acids increases with pH. A pH change from 9 to 11 increases adsorption from 28% to 35%. Complex formation between Ca^{2+} and organic matter also increases with pH.

7.5.3 Formation of corrosion prevention layer containing calcium carbonate

Tillmans et al. (1927) found that various types of protective layers are formed in different water compositions. In a water under conditions where $CaCO_3$ may precipitate (supersaturated), the iron(II) content in precipitations on the metal surface was higher than in a water where calcium, hydrogen carbonate and carbonate were at equilibrium. Under saturated conditions, separate $CaCO_3$ crystals were formed on the iron surface. In the supersaturated condition, a porous $CaCO_3$ precipitation was formed. Species from the water and corrosion products diffuse through the porous layer and iron(II) is precipitated on the surface. The pH was around 7.5 and the total content of carbonic species was 97.5 mg l^{-1} in the saturated case and 126.5 mg l^{-1} when the water was supersaturated.

The protective layers were found to contain Ca^{2+}, Fe(II) and Fe(III) in various proportions depending on the water composition. Certain rules regarding the composition of the protective layer were established. Haase (1935) and Kooijmans (1938) assumed that two compounds are formed, $CaCO_3 \cdot Fe(OH)_3$ and $CaCO_3 \cdot Fe(OH)_2$. To provide effective protection a high proportion of iron(II) was required in the deposit. The iron(II) proportion changes with time. Kooijmans (1938) found, after a few days, 5% iron(II) in the precipitation while, after a year, the iron(II) content increased to 20% when calcium was present in the water. In a water with low pH and a high content of hydrogen carbonate, but no calcium, a protective layer was still formed, but with an iron(II) content higher than 50% Kölle and Sontheimer (1977) confirmed this result. Analysis showed that soft water gave a precipitation with a high calcium content (20%) while hard water gave a lower proportion of calcium (2%). A protective layer with less than 2% calcium was effective if the iron(II) content was above 25% (Rudek 1979). A protective layer has to contain iron(II) besides calcium. A calcium carbonate precipitation is only protective if the precipitation rate has been slow under saturated conditions.

7.6 Structure of natural protective layers

A protective layer may not be stable and its composition may vary with time. Kooijmans (1938) found that a protective layer changes with time by studying the change in ratio between Fe^{2+} and Ca^{2+} in a deposit. Wagner (1977) and Sontheimer et al. (1979) found that the calcium content in a protective layer depends on the exposure time and the calcium concentration in the water (Figure 7.27).

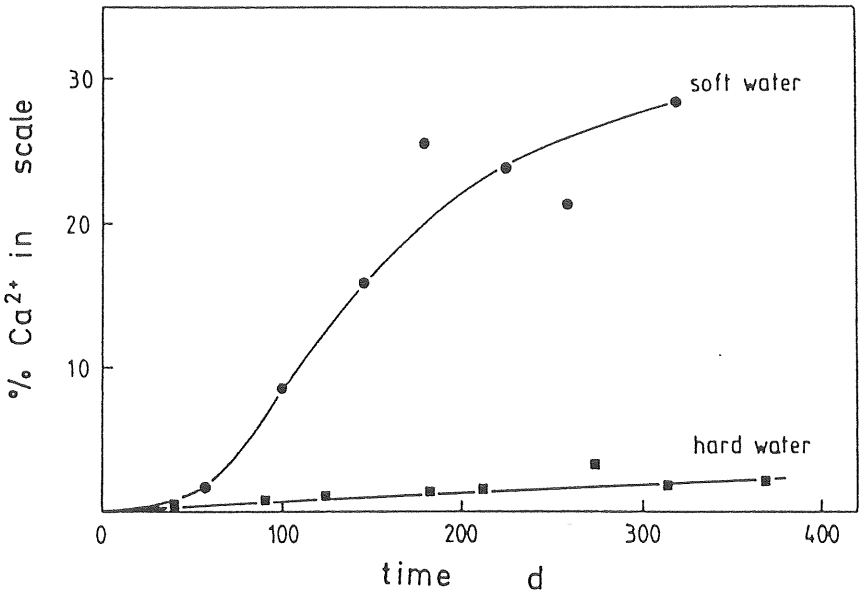

Figure 7.27 Influence of water hardness on the calcium content of corrosion deposits, from Sontheimer et al. (1979).

The hard water used in the investigation of Sontheimer et al. (1979) contained up to 140 mg Ca^{2+} l^{-1} and greater than 300 mg HCO_3^- l^{-1} with a pH value ≅7, while the soft water had a calcium concentration of 20 mg Ca^{2+} l^{-1} at a pH value ≅8. Unfortunately, no account of pH was taken although this is important for $CaCO_3$ precipitation. Stumm (1956) performed four day tests which showed that calcium in the precipitation is evenly distributed through the layer (Figure 7.28). His water contained 82 mg Ca^{2+} l^{-1} and 125 mg HCO_3^- l^{-1} at pH 8.4. The distribution of calcium in the layer changed with time and water composition.

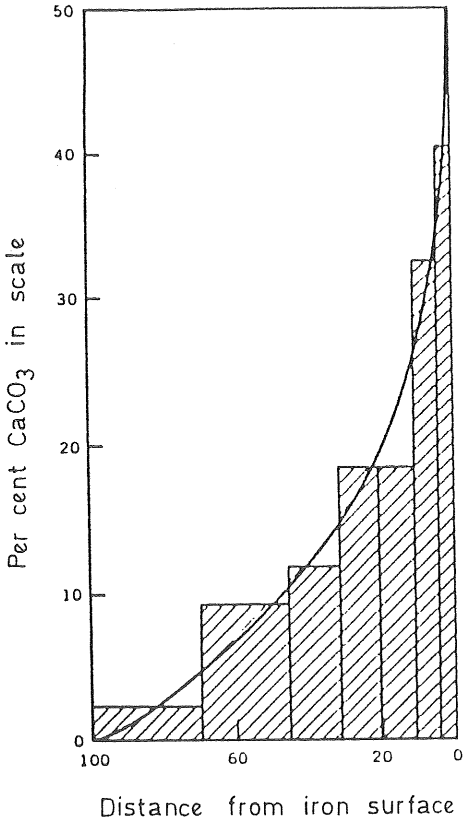

Figure 7.28 Changes in film composition in relation to relative distance from surface (Stumm 1956).

Kooijmans (1938) found protective layers both with and without calcium carbonate. The waters he studied are listed in Table 7.3. From the table it can be seen that in cases where $CaCO_3$ precipitates, the pH was much higher than the saturation pH (pH_s). In addition, the concentrations of calcium and hydrogen carbonate were high in the case which made $CaCO_3$ precipitation possible.

Table 7.3 The water composition in Kooijman's study of the content of the deposits.

	$CaCO_3$ in the deposits $mg\ l^{-1}$	$CaCO_3$ absent in the deposits $mg\ l^{-1}$
Ca	95.6	36.5
HCO_3^-	278	115
Cl^-	36	14
SO_4^{2-}	31.7	4.5
$KMnO_4$	9	3.4
pH	8.1	7.4
pH_s	7.1	7.9

When there was $CaCO_3$ in the deposits, the calcium/iron(II)+(III) was 10% and the iron(II)/iron$_{tot}$ was 22%. When the protective layer consisted only of iron, the iron(II)/iron$_{tot}$ was 33% (Kooijmans 1938). Tuovinen et al. (1980) found an iron(II)/-iron(III) ratio of 2.0 to 1.2. The calcium concentration and the alkalinity were both about 35 mg l^{-1}. The water also contained organic matter and the microbiological activity caused primarily localised corrosion attack. Organic matter reduced $CaCO_3$ precipitation.

Baylis (1926) compared $FeCO_3$ solubility with $CaCO_3$ solubility at various pH and hydrogen carbonate concentrations. $FeCO_3$ was found to precipitate in a nearly oxygen free environment near the metal surface. The $FeCO_3$ was insoluble at a pH and hydrogen carbonate concentration closely following the calcium carbonate curve.

Stumm (1956) and Feigenbaum et al. (1978a) also found that the relative distribution of calcium in a precipitation depends on pH (Figure 7.29A and B).

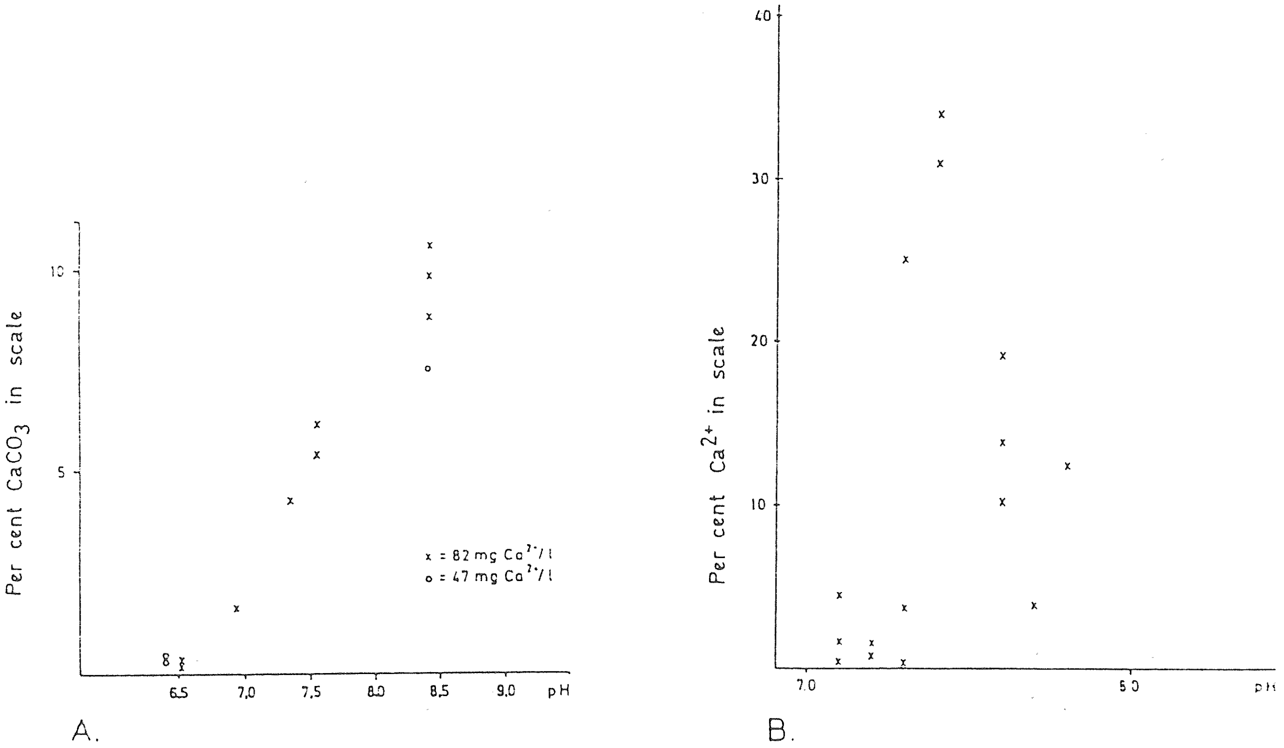

Figure 7.29 Calcium content of deposits versus pH, from (A) Stumm (1956) and (B) Feigenbaum et al. (1978a).

Baylis (1926) stated that a deposit which was formed on a metal surface did not cover the surface completely but was active. It had porosities where iron(II) was transported to the surface, oxidised and precipitated as FeOOH on top of the existing deposits. In this way a continuous growth of the precipitation takes place (Figure 7.30). In the presence of hydrogen carbonate, this additional growth did not take place, since the $FeCO_3$ gave a more protective layer.

1. Pit starting 2. Inactive

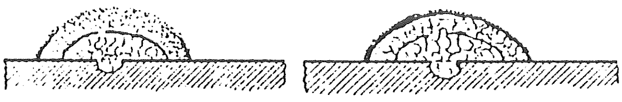

3. Active after break 4. Again inactive

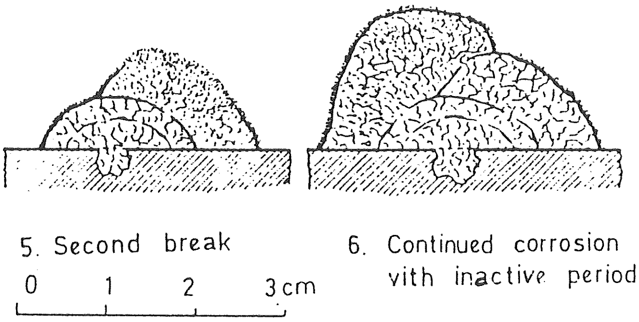

5. Second break 6. Continued corrosion vith inactive periods

Figure 7.30 Formation of corrosion products, according to Baylis (1926).

These independent investigations of natural protective layers have collectively shown that the deposits consist of differing layers deposited on top of each other with a clear separation between them. Such investigations were performed by Kölle (1977), Feigenbaum et al. (1978a) and Bigham and Tuovinen (1985). Below is a summary of the reported appearance of the precipitations with regard to the water composition.

Kölle (1977) and Kölle and Sontheimer (1977) investigated the protective layers of a 100-year-old pipe from a distribution network in Hanover, West Germany. A cross section of a deposit is shown in Figure 7.31. The water composition of Hanover is given in Table 7.4.

Table 7.4 Water composition at different Hanover water works, according to Kölle and Sontheimer (1977).

	Fuhrberg	Berkhof	Grasdorf	Harz
pH	8.0	8.0	7.0	9.0
Ca^{2+} mg l^{-1}	70	28	140	16
HCO_3^- mg l^{-1}	95	128	293	43

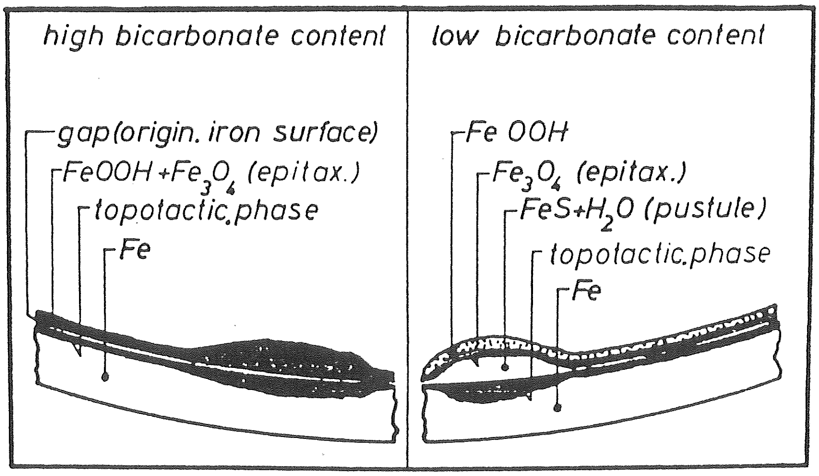

Figure 7.31 Cross-section of deposits from pipes when water contains high and low concentrations of hydrogen carbonate, from Kölle (1977).

Figure 7.31 shows the cross-section of a pipe with layers of corrosion products which Kölle (1977) characterises as topotactical (inner) and epitaxial (outer). In addition, he points out that the inner layer is independent of the hydrogen carbonate content. The topotactical layer basically consisted of an amorphous structure containing 10% $FeCO_3$ and Fe_2O_3. The epitaxial layer consisted primarily of Fe_3O_4 and $FeCO_3$ together with FeOOH. In addition, Kölle and Rösch (1978) found traces of organic matter on the surface. The pore volume was found to be 15% in the topotactical layer and 53% in the epitaxial layer (Kölle and Rösch 1978).

Contrary to the above, Feigenbaum et al. (1978a) in a number of studied cases found a porous inner layer and a compact crystalline outer layer. The outer crystalline layer consisted of four phases; $CaCO_3$, $FeCO_3$, Fe_3O_4 and FeOOH. The inner layer consisted of FeOOH and Fe_3O_4. The ratio of Fe/Ca varied between 0.002 and 1.82. Percentage iron by weight in the total deposit varied between 7% and 73%, while calcium varied between 0.4% and 34% (Figure 7.32). When the proportion of calcium in the deposit was low, the pH of the water was also low. The water composition was varied: Ca^{2+} 56-248 mg l^{-1}, HCO_3^- 113-201 mg l^{-1}, pH 7.1-7.8, Cl^- 42-539 mg l^{-1} and SO_4^{2-} 15-875 mg l^{-1}. The calcium part of the deposits was found to be highest when the calcium and hydrogen carbonate concentrations in the water were high and pH was also high (in 4 cases out of 15). Figure 7.31 shows the X-ray intensity of iron and calcium through the scale.

Bigham and Tuovinen (1985) studied deposits from 40- to 50-year-old pipes and found deposits consisting of various layers, in accordance with earlier studies (Figure 7.33). The surface crust consisted of iron(III) oxyhydroxides, the magnetic membrane consisted of Fe_3O_4 and the fluid interior was α-FeOOH.

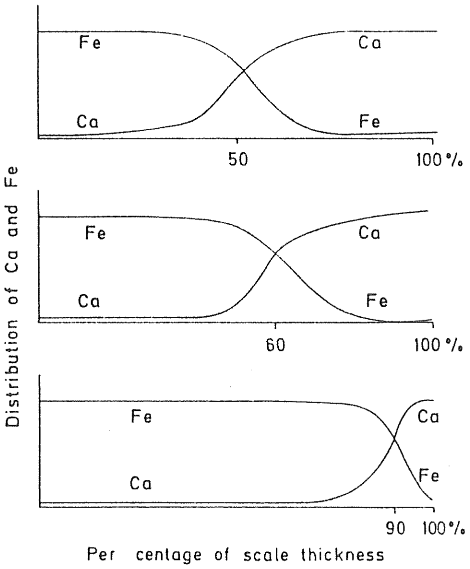

Figure 7.32 Distribution of Ca and Fe in deposits analysed by X-ray spectrometry, from Feigenbaum et al. (1978a).

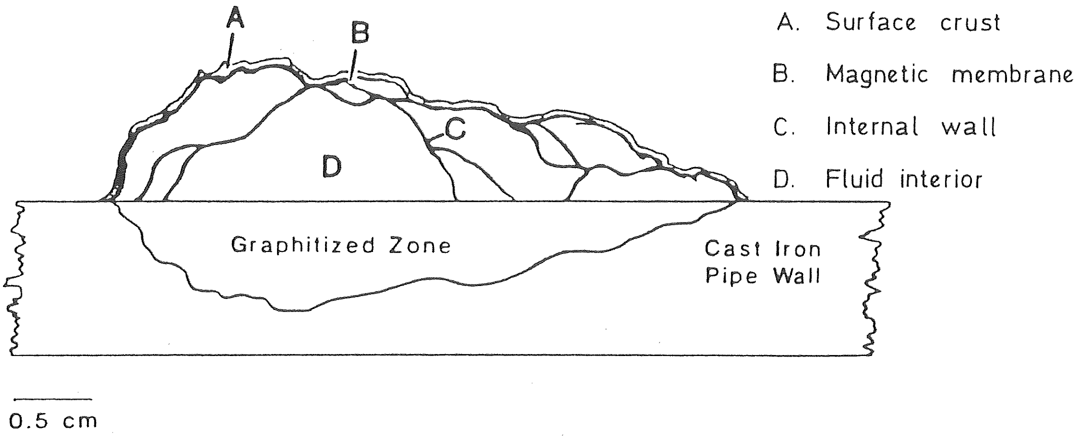

Figure 7.33 Cross-section of deposits on a 50 year old pipe, according to Bigham and Tuovinen (1985).

Other species in the water, such as silicates, phosphates or organic matter, may form deposits with protective properties. Haupt (1939/40) found that water unsaturated with respect to $CaCO_3$ does contain protective layers. The layers contained large amounts of silicates and phosphates. The pipes had a thin rust layer which did not seem to provide a complete covering. Kegel (1942) found that natural protective layers consisted not only of calcium carbonate, iron oxide and traces of manganese, but also of salts, silicates, phosphates and organic matter. Tuovinen et al. (1980) found organic matter in the deposits in their investigation. Vuorinen et al. (1985) found organic matter adsorbed on the surface of the deposits. Organic matter also affects the precipitation of iron carbonate, which is facilitated by the retardation of the oxidation of iron(II) to iron(III) by complex formation (Section 7.4.3). Chlorides and sulphates in the water also affect $CaCO_3$ precipitation and decrease the amount of calcium in the deposit.

In natural protective layers the relative amount of iron(II) compared to total iron and the content of calcium depend exclusively on the water composition. If the content of calcium and hydrogen carbonate is high the iron(II) predominates in deposits at low pH, while Ca predominates at high pH. In water with a low calcium concentration and a high content of carbonic species, at low pH, the iron(II) content is high in the deposits, but if the pH is high then iron(III) dominates.

7.7 Corrosion models and protective layer models

The corrosion theories and corrosion prevention models, that are proposed in the literature, are based on tests with natural or artificial waters of various composition performed during both shorter and longer periods of time. Some researchers have developed corrosion models from studies of old pipes in existing distribution systems.

Two theories exist. Some researchers assume a protective layer needs to be formed from calcium carbonate while others assume a protective layer can contain only iron compounds. Most individual investigations include a limited number of water compositions within a narrow concentration interval. The usual studied parameters are: calcium and hydrogen carbonate concentration at various pH values, and variations in ionic strength, organic matter, phosphates and silicates.

Haupt (1939/40) showed that iron, calcium and phosphate are bound together as a protective layer. These salts coprecipitate on the metal surface and prevent oxygen from reaching the metal. The structure is shown in Figure 7.34.

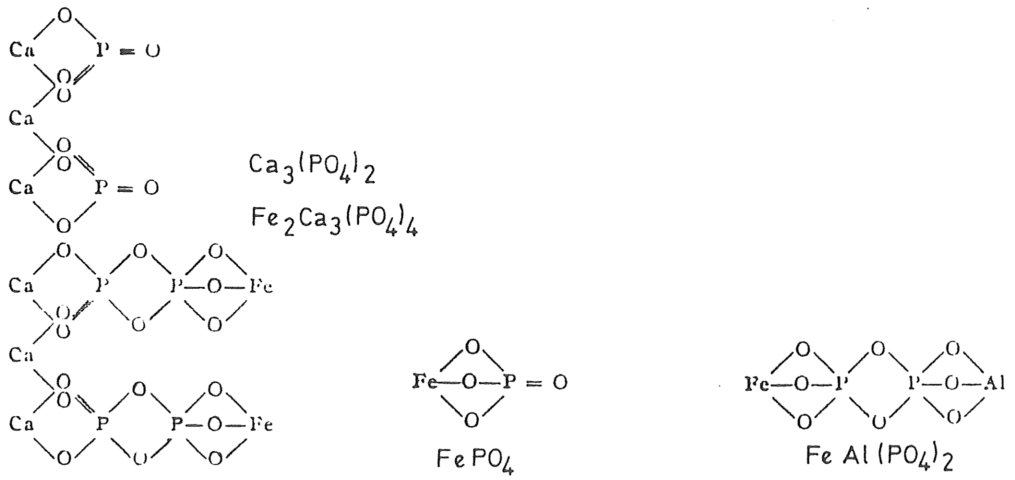

Figure 7.34 Formation of compounds with calcium and/or iron and phosphates found in protective layers, according to Haupt (1939/40).

Corrosion may sometimes continue even when a complete protective layer exists. Feigenbaum et al. (1978b) described how defects such as pores in the protective layer affect the transport of oxygen and/or salts which could penetrate the deposit and cause continuing corrosion. The model below indicates the mechanism (Figure 7.35).

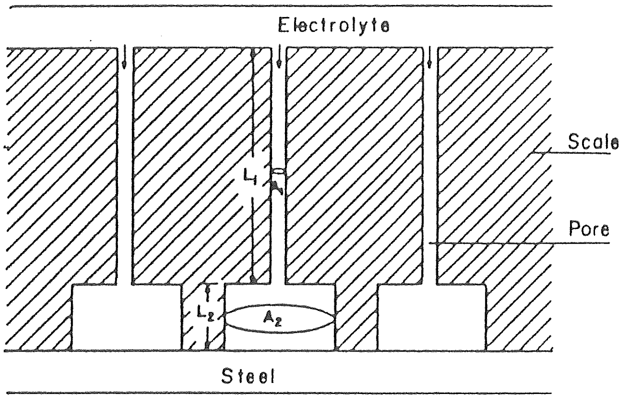

Figure 7.35 Deposit with defects where oxygen and salts can penetrate to the metal surface, according to Feigenbaum et al. (1978b).

Singley and Ahmadi (1985) summarised various models for protective layer formation depending on the chemical environment close to the metal surface. A comparison with atmospheric corrosion was made (Figure 7.36). Depending on the environment, the deposits are built up of different compounds.

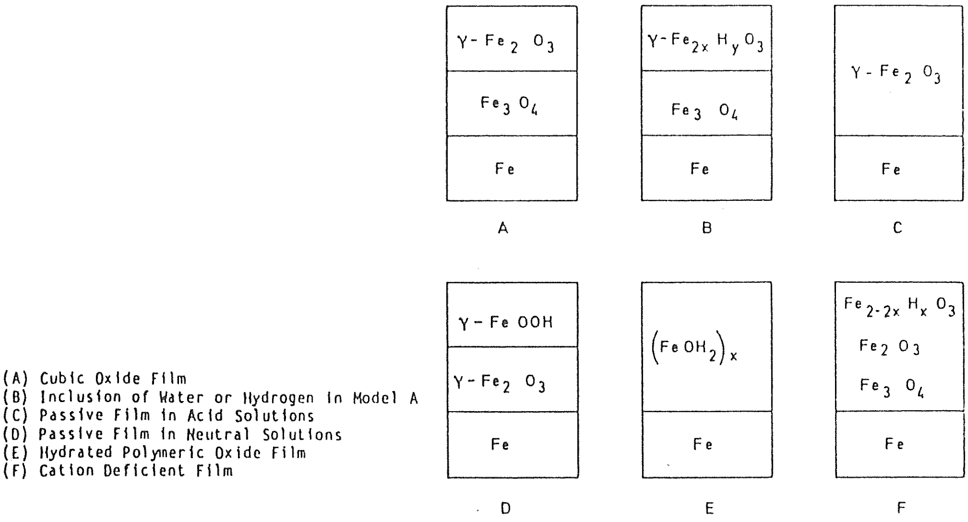

Figure 7.36 Various natural types of protective layers on iron, according to Singley and Ahmadi (1985).

A (passive) protective layer will break apart when the water contains chloride which can penetrate into the structure creating free passage to the metal surface (Figure 7.37).

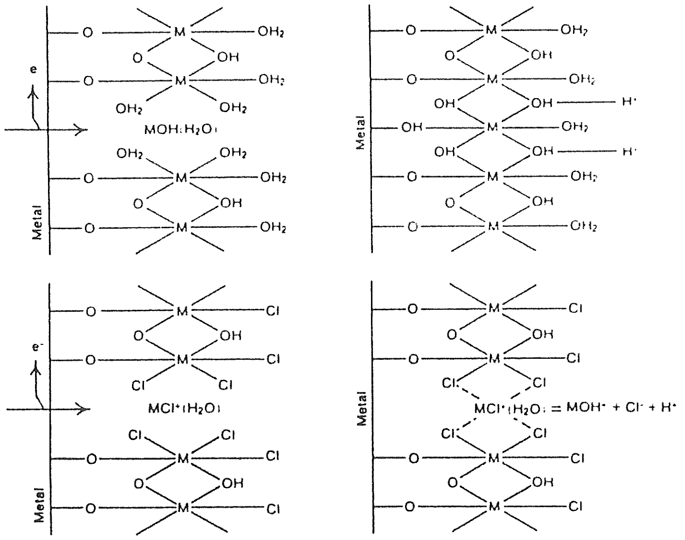

Figure 7.37 Chloride attack on an oxyhydroxide film, according to Singley and Ahmadi (1985).

Another model, mentioned by Singley and Ahmadi (1985), describes deposits as a "shell" consisting of FeOOH and Fe_3O_4. Under this shell there are corrosion products and species from the water. Corrosion takes place below the shell, in the form of either chlorides or microbiological attack (e.g. sulphate reducing bacteria), both of which cause localised attack such as pittings. The penetration capability of species in the water depends on their concentration and ionic radius. The "shell" might act as a cathode and the metal below as an anode, which increases the corrosion below the deposit (Figure 7.38).

Sontheimer et al. (1979 and 1981) also developed a model, known as the siderite model, from their investigations of old pipes as well as from new experiments. This model is based on the assumption that it is $FeCO_3$ that precipitates instead of $CaCO_3$. This is in accordance with the solubility products of $FeCO_3$ and $CaCO_3$ which are $3.0 \cdot 10^{-11}$ M^2 and $5.0 \cdot 10^{-9}$ M^2, respectively, or in other words, $FeCO_3$ is less soluble than $CaCO_3$. The protection is created by the crystalline structure of iron carbonate.

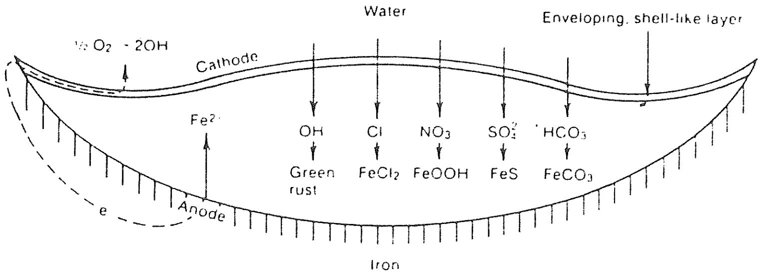

Figure 7.38 Penetration of salts through a protective layer of corrosion products, according to Singley and Ahmadi (1985).

The assumptions are based on the following reactions:

Primary reactions (corrosion)

$$Fe \rightarrow Fe^{2+} + 2e^- \qquad (7.1)$$

$$\tfrac{1}{2}O_2 + H_2O + 2e^- \rightarrow 2OH^- \qquad (7.2)$$

Secondary reactions (development of protective layers)

$$HCO_3^- + OH^- \rightarrow CO_3^{2-} + H_2O \qquad (7.17)$$

$$Fe^{2+} + CO_3^{2-} \rightarrow FeCO_3(s) \qquad (7.6)$$

$$Ca^{2+}\ CO_3^{2-} \rightarrow CaCO_3(s) \qquad (7.34)$$

$$2Fe^{2+} + \tfrac{1}{2}O_2 + 4OH^- \rightarrow 2FeOOH(s) + H_2O \qquad (7.37)$$

Tertiary reactions (rearrangement of protective layers)

$$2FeCO_3 + \tfrac{1}{2}O_2 + H_2O \rightarrow 2FeOOH(s) + 2CO_2 \quad \text{pseudoamorphous} \quad (7.38)$$

$$3FeCO_3 + \tfrac{1}{2}O_2 \rightarrow Fe_3O_4 + 3CO_2 \qquad (7.39)$$

During reaction (7.37) it is assumed that the structure and properties of the crystalline $FeCO_3$ is retained which prevents corrosion, although a transition to less favourable FeOOH has taken place and this does not normally prevent corrosion.

In spite of all the useful models and theories about corrosion and protective layers, an index to predict corrosion is usually used which is supposed to indicate if a water has a potential to form a protective layer which can stop or hinder corrosion. The index determines solely the $CaCO_3$ precipitation potential, which in reality has no importance at all for the corrosivity estimation of a water. Some indices used for the prediction of corrosion are presented below.

7.8 Indices used for prediction of corrosion

In a recent summary by Rossum and Merill (1983) it was stated that an index only reveals if a water is unsaturated, saturated or supersaturated with regard to calcium carbonate. None of the indices presented indicate anything about the corrosivity of a water.

The Langlier index (LI) (Langlier 1936), is based on the premise that the concentration of calcium and carbonate ions must exceed the solubility product of calcium carbonate. LI is the difference between actual pH of the water and the pH (pH_s) which corresponds to $CaCO_3$ precipitation at the given calcium concentration and concentration of total carbonic species in the water.

$$LI = pH - pH_s \qquad (7.40)$$

where

$$pH_s = pK_2 - pK_s + p[Ca^{2+}] + p[H_2CO_3 + HCO_3^- + CO_3^{2-}] \qquad (7.41)$$

$K_2 = 4.7 \cdot 10^{-11}$

$K_s = 5.0 \cdot 10^{-09}$

Ca in $mol\ l^{-1}$

$(H_2CO_3 + HCO_3^- + CO_3^{2-})$ in $mol\ l^{-1}$

Other researchers have in the meantime tested and refined the theories of Langlier (for instance, Strohecker 1937, Hoover 1938). The usual comment is that the LI takes no account of the oxygen content or the amount of organic matter in the water (Hoover 1938).

Hoover developed a nomogram based on a formula with the same parameters as Langliers'. From this nomogram, pH_s can easily be obtained when the other parameters are known. The nomogram is often used even today to obtain the tendency of $CaCO_3$ precipitation for different waters. DeMartini (1938) points out, however, that Strohecker assumes the hydrogen carbonate concentration and the alkalinity to be the same. He also says that the LI does not indicate the corrosion tendency. Larson and Buswell (1942) extends the LI with a correction for salt content and temperature and Schock (1984) has pointed out that this correction lowers the pH_s by 0.1-0.3 units. Axt (1961) developed a nomogram for the determination of different concentrations of CO_3^{2-}, HCO_3^-, Ca^{2+} and CO_2 at various pH values and solubility products.

Ryznar (1944) developed an index known as the Ryznar index (RI), which is also frequently used probably because of its simplicity. The RI was developed to obtain a quantitative measure of the calcium carbonate precipitation.

$$RI = 2pH_s - pH \tag{7.42}$$

$RI < 7$ Protective precipitation of calcium carbonate which results in slight corrosion and no "red water" problem

Another index, developed for asbestos cement pipes, is sometimes used, inadvertently, to determine precipitations in pipes of other materials. This index is called the Aggressiveness Index (AI) and was introduced by Milette et al. (1980).

$$AI = pH + \lg[Ca^{2+}][H_2CO_3 + HCO_3^- + CO_3^{2-}] \qquad (7.43)$$

where

Ca^{2+} in mg $CaCO_3$ l^{-1}

$(H_2CO_3 + HCO_3^- + CO_3^{2-})$ in mg $CaCO_3$ l^{-1}

The water is not aggressive to asbestos cement pipes when AI exceeds 12. There is some measure of agreement between the values for LI, RI and AI in very corrosive waters.

Two other indices based on the calcium carbonate solubility product are the Driving Force Index (DFI) (McCauley 1960) and the Momentary Excess Index (ME). (Dye 1952). If DFI > 1 the water is supersaturated and if DFI < 1 the water is unsaturated with regard to $CaCO_3$. A supersaturated water has ME > 0 and an unsaturated ME < 0.

$$DFI = \frac{[Ca^{2+}][CO_3^{2-}]}{K_s} \qquad (7.44)$$

$$K_s = ([Ca^{2+}]-ME)([CO_3^{2-}]-ME) \qquad (7.45)$$

where

$K_s = 5.0 \cdot 10^{-9}$

Merill and Sanks (1977a, 1977b and 1978) used an index which is called the "Calcium Carbonate Precipitation Potential (CCPP) which was graphically shown by Caldwell and Lawrence (1953), while Ainsworth has developed a computer program based on this index. A positive CCPP number indicates the amount of $CaCO_3$ in mg which should precipitate to obtain an equilibrium condition in 1 litre of water containing calcium and carbonate. The CCPP is directly related to reaction kinetics. The growth rate of crystal formation follows an equation described by Rossum and Merill (1983).

$$\mathrm{CCPP} = 10^5\left[(\mathrm{Ca}^{2+})-(\mathrm{Ca}^{2+})^*\right] \qquad (7.46)$$

$$\frac{dC}{dt} = -KS(C-C^*)^n \qquad (7.47)$$

where

C = Concentration in the water in mol l^{-1}
C^* = Saturation concentration in mol l^{-1}
S = Surface area
K = Rate constant
n = Constant

In order to obtain agreement between an index and the actual corrosion tendency, parameters such as oxygen concentration, organic matter, salt concentration, pipe material and tendency for complex formation with dissolved metal ions, which directly affect corrosion, should be included.

Feigenbaum et al. (1978b) developed an empirical index from their investigation which includes the influence of chloride and sulphate on the calcium carbonate solubility (equation 7.48).

$$Y = AH + B([\mathrm{Cl}^-] + [\mathrm{SO}_4^{2-}])e^{-0.25H} + C \qquad (7.48)$$

where

$A = 35 \cdot 10^{-4}$
$B = 0.34$
$C = 19.0$
$H = [\mathrm{Ca}^{2+}][\mathrm{HCO}_3^-]^2/[\mathrm{CO}_2]$
$Y > 500$ gives low corrosion attack
$Y < 200$ gives high corrosion attack

Singley (1981) assumed that it was impossible to develop only one index, since there are so many different chemical properties which affect corrosion. As an example phosphate inhibitors are not described in any index. All metal ions in a water, whether they are original or dissolved, do not necessarily precipitate, but some of them are tied up in various complexes. Therefore, according to Singley (1981), a corrosion index must be supplemented with a "Metal Ion Complex Capacity Index" (MICC), to obtain the amount of metal available for precipitation.

In recent years a number of computer programs based on the various indices have been developed. One example is "WATSPEC2" which Pisigan and Singley (1985) used. A number of assumptions concerning water chemistry at various concentrations of species are included in the program.

If the user of an index understands the effects on corrosion when a water is unsaturated, saturated or supersaturated with $CaCO_3$, it is possible to use one of the indices for prediction of corrosion. It is useful to compare pH, total content of carbonic species and calcium content in the water with the values in the index in relation to the expected composition of protective layers with regard to the water content of salts and organic matter which influence both precipitation and corrosion.

7.9 Conclusions and proposed corrosion prevention model

To decrease or prevent corrosion the metal surface should be covered and separated from the water bulk by a protective layer. This layer can be formed in different ways:

- Precipitation of species existing in the water, either spontaneously or by environmental modification, for instance, by changing the temperature or pH.
- Addition of inhibitors or substances to the water which may precipitate on the metal surface, such as, phosphates, silicates or calcium compounds.
- Precipitation of corrosion products which are formed by reaction with the water and the metal ion or with species in the water and the metal, for example, $FeCO_3$ and Fe_3O_4.

There are certain requirements for the protection layer if it is to provide effective corrosion prevention: (a) The coating must fully cover the metal surface with no gaps or damage (b) Precipitations need a certain degree of crystallinity and must have the right morphology, which is only obtained when a trace amount of contaminant is present in the coating.

7.9.1 Corrosion prevention model

A hypothesis in the form of a model can be used to summarise the literature presented in this chapter. The model is divided into different cases according to various water compositions.

Because corrosion reactions do not follow the same sequence in all water environments, water composition strongly affects corrosion, corrosion rate and the composition of protective layers. From the literature it can be seen that no one model is valid for the prevention of iron corrosion under all conditions. Working protective layers, which decrease corrosion, do not form under all conditions. In some cases corrosion will continue until there is no longer any iron metal present. In addition to the chemical environment in contact with the metal, corrosion is affected by physical factors such as water velocity, temperature and the thickness of the formed deposit.

Three cases are presented, in which pH, calcium and total carbonic species concentration are included. The significance of organic matter is only briefly mentioned. The concentrations and values for the parameters are chosen to cover typical Swedish conditions under which iron corrosion might occur.

Case I considers a very soft water with low alkalinity and low ionic strength. Three pH intervals are compared and formed precipitations are predicted.

In Case II the importance of different contents of total carbonic species is taken into account under the same pH conditions as in Case I.

In Case III corrosion prediction in waters which contain calcium and hydrogen carbonate in various concentrations at varying pH values is presented.

7.9.1.1 Case I

During iron corrosion the solid metal is oxidised to iron(II) at the same time as oxygen at the metal surface is reduced to hydroxide ion. In waters with a low content of total carbonic species, a pH increase takes place at the metal surface. Close to the metal surface pH will thus be high and independent of the pH in the water bulk. An increase in pH increases the rate of iron(II) oxidation to iron(III). Iron(III) precipitates as FeOOH on the metal surface (Figure 7.39).

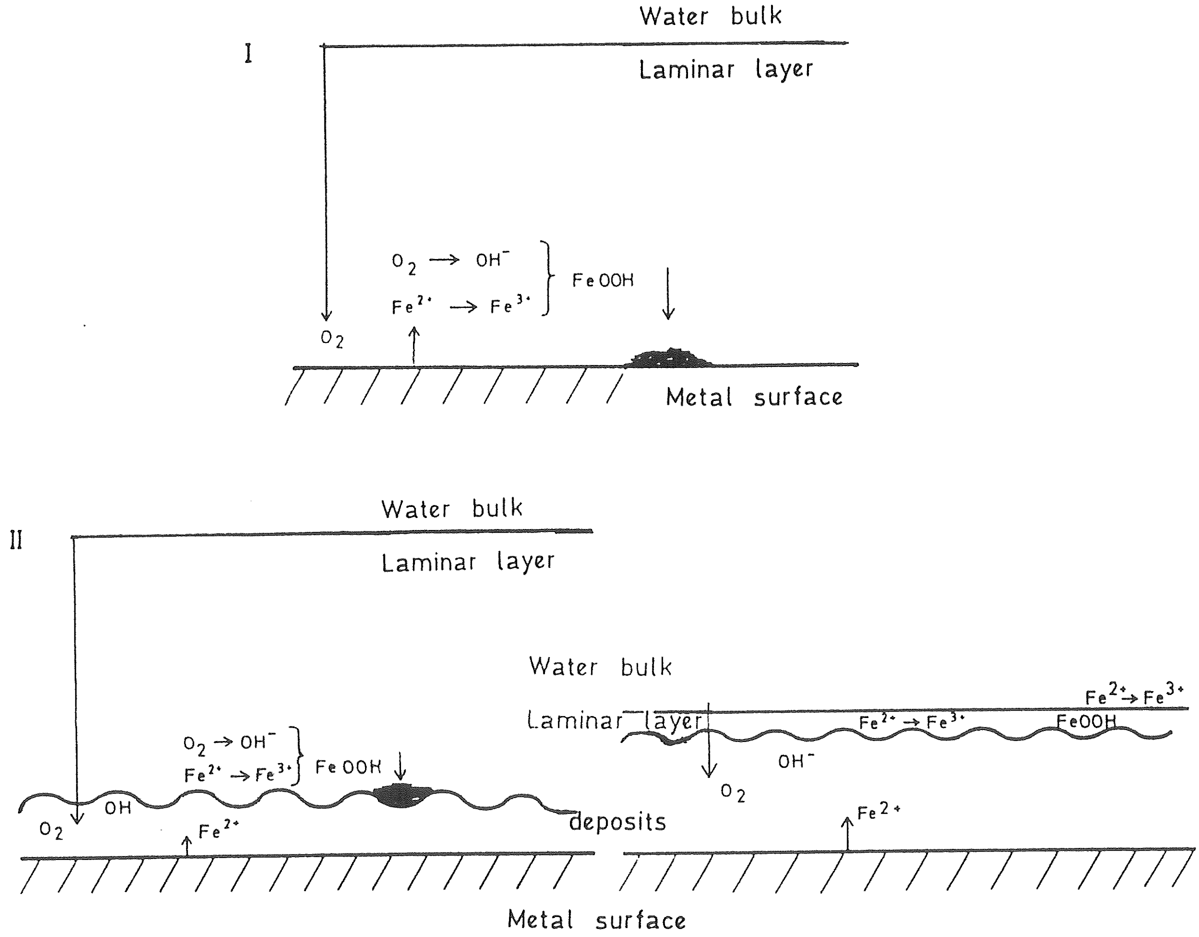

Figure 7.39 Oxygen transport through the laminar layer and formation of corrosion products, Case I. (I) new pipe with no deposits, (II) old pipe with deposits at two different water velocities.

The following reactions take place at the metal surface:

Anode $Fe \rightarrow Fe^{2+} + 2e^-$ (7.1)

Cathode $\frac{1}{2}O_2 + H_2O + 2e^- \rightarrow 2OH^-$ (7.2)

$$2Fe^{2+} + \frac{1}{2}O_2 + 4OH^- \rightarrow 2FeOOH(s) + H_2O \qquad (7.36)$$

Corrosion in Case I results in the sole formation of FeOOH deposits which have rather porous and amorphous properties and do not provide effective protection. Given enough time FeOOH will precipitate and cover the metal surface. The rate of subsequent corrosion depends on the rate of oxygen transport through the deposit. The oxygen has to diffuse through the formed deposits into the metal, and dissolved iron(II) must diffuse out and then be oxidised to iron(III) in order to be precipitated through reaction with oxygen and hydroxide. This process is also affected by water velocity.

High water velocity decreases the laminar layer and reduces the diffusion distance, which in turn increases the transportation of oxygen and formation of species by the corrosion reactions. Deposits might also be flushed away from the metal. The reduced deposit thickness further facilitates the diffusion of oxygen. Increased oxygen concentration at the metal surface leads to increased corrosion and further precipitation.

In those cases where organic matter is present iron(II) may form complexes and thus remain as iron(II) regardless of increased pH. This reduces corrosion if the complex is precipitated on the metal surface as a protective layer, otherwise it will not give any protection at all and corrosion continues. Chlorides and sulphates increase corrosion rate due to increased attack under the deposit.

7.9.1.2 Case II

When the content of total carbonic species is high in the water, it has a buffering effect on the hydroxide ions formed at the cathode. Instead of a pH increase, a transformation to hydrogen carbonate or to carbonate takes place.

If the pH is < 6.5 the carbonic acid concentration is high and the hydrogen carbonate concentration is too low to allow $FeCO_3$ precipitation. Instead, Fe_3O_4 may be formed which also provides effective protection. If the pH is < 8.5 in the water, the iron(II) remains and may precipitate as $FeCO_3$. $FeCO_3$ is crystalline and is effective as a protective layer (Figure 7.40).

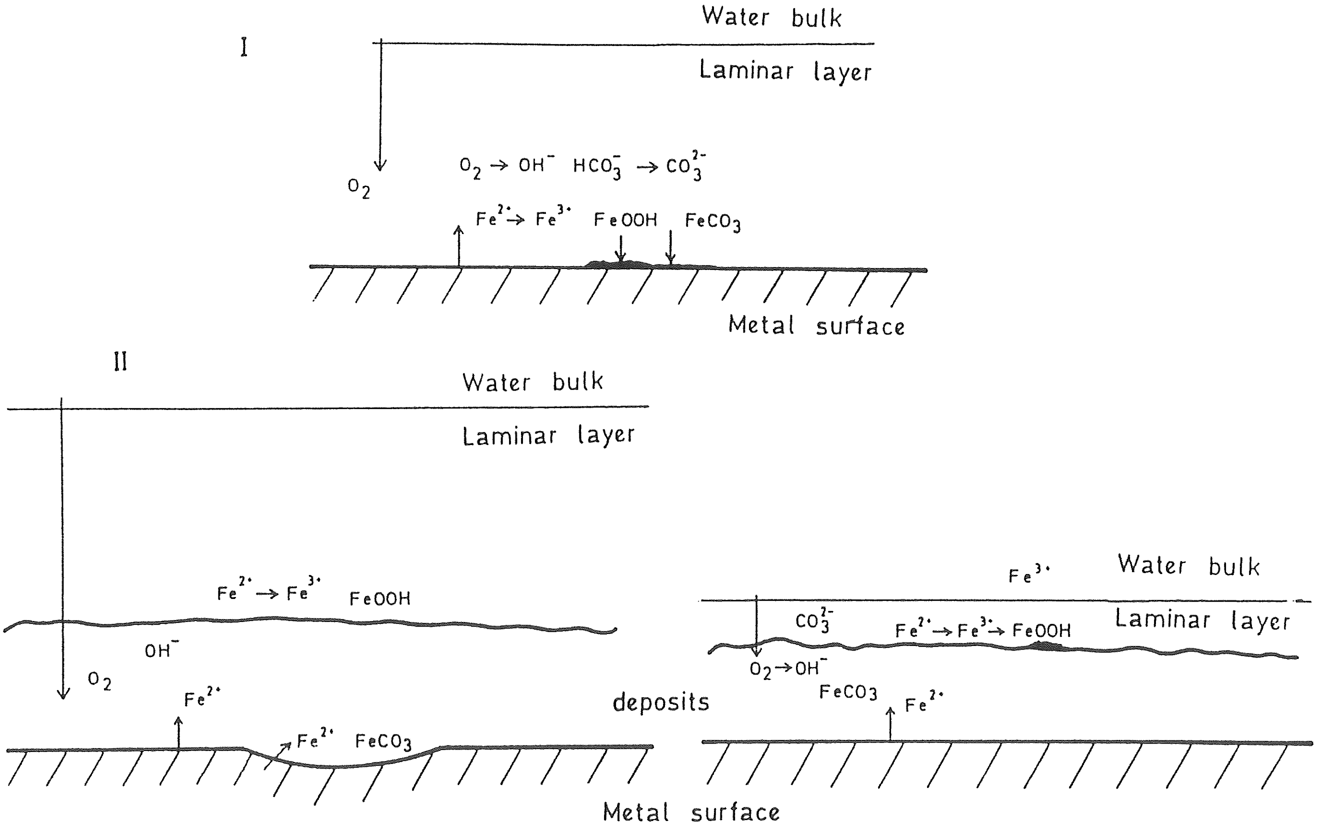

Figure 7.40 Oxygen transport through the laminar layer and formation of corrosion products, Case II. (a) new pipe with no deposits, (b) old pipe with deposits.

In waters with high pH values an increased oxidation of iron(II) to iron(III) takes place which also reduces the possibility of $FeCO_3$ precipitation. Instead, FeOOH is precipitated as shown in the equations below.

a) In waters without organic matter
b) In waters with organic matter present

$$\text{Anode} \quad Fe \rightarrow Fe^{2+} + 2e^- \qquad (7.1)$$

$$\text{Cathode} \quad \tfrac{1}{2}O_2 + H_2O + 2e^- \rightarrow 2OH^- \qquad (7.2)$$

Low pH < 6.5

$$H_2CO_3 + OH^- \rightarrow HCO_3^- + H_2O \qquad (7.15)$$

$$\text{a)} \quad 3Fe^{2+} + \tfrac{1}{2}O_2 + 6HCO_3^- \rightarrow Fe_3O_4(s) + 3H_2O + 6CO_2 \qquad (7.49)$$

$$\text{b)} \quad Fe^{2+} + \text{org mat} \rightarrow Fe(II) - \text{org mat} \qquad (7.50)$$

Medium pH 6.5 < pH < 9

$$HCO_3^- + OH^- \rightarrow CO_3^{2-} + H_2O \qquad 7.16)$$

$$\text{a)} \left\{ \begin{array}{ll} 3Fe^{2+} + \tfrac{1}{2}O_2 + 6HCO_3^- \rightarrow Fe_3O_4(s) + 3H_2O + 6CO_2 & (7.6) \\ Fe^{2+} + CO_3^{2-} \rightarrow FeCO_3(s) & (7.8) \\ 2Fe^{2+} + \tfrac{1}{2}O_2 + 4OH^- \rightarrow 2FeOOH(s) + H_2O & (7.37) \end{array} \right.$$

$$\text{b)} \quad Fe^{2+} + \text{org mat} \rightarrow Fe(II) - \text{org mat} \qquad (7.50)$$

High pH > 9

$$\text{a)} \quad 2Fe^{2+} + \tfrac{1}{2}O_2 + 4OH^- \rightarrow 2FeOOH(s) + H_2O \qquad (7.37)$$

$$\text{b)} \left\{ \begin{array}{ll} Fe^{2+} + \text{org mat} \rightarrow Fe(II) - \text{org mat} & (7.50) \\ Fe^{2+} \rightarrow Fe(III) - \text{org mat} & (7.51) \end{array} \right.$$

In waters where organic matter is present iron(II) will form complexes and thus prevent $FeCO_3$ from precipitating. Complex formation of iron with organic matter increases at lower pH in water. High acid number and low molecular weight of the organic matter give the most stable complexes. But the tendency to form complexes is more prominent when the molecular weight is high. The complexes may tie up the ionic iron and decrease the possibility of precipitation. If the Fe(II)-organic matter complex is destroyed then $FeCO_3$ and/or Fe_3O_4 precipitate at medium and low pH. At high pH the formation of $FeCO_3$ competes with the oxidation of iron(II) to iron(III) in order to form an effective protection.

Organic matter can also slow down precipitation and an increased number of small crystal nuclei form, which creates a denser layer with effective protection.

Water velocity is important when a metal surface is covered by deposits. A high water velocity increases the transport of both oxygen and carbonic species to the deposits and this availability allows $FeCO_3$ precipitation. At high pH, the increased oxygen transport favours the oxidation of iron(II) and FeOOH precipitation. It can be concluded that low pH provides increased protection at high water velocities. At high pH, FeOOH precipitates, independent of the water velocity.

7.9.1.3 Case III

In waters where calcium is present and the content of total carbonic species is high, $CaCO_3$ may precipitate. Precipitation is facilitated by a higher degree of supersaturation with regard to $CaCO_3$.

As a general rule a natural hard water has a low pH due to the carbonic species equilibrium which causes formation of deposits with a lower proportion of calcium than a soft water at medium or high pH. In waters with low pH, Fe_3O_4 will be precipitated as

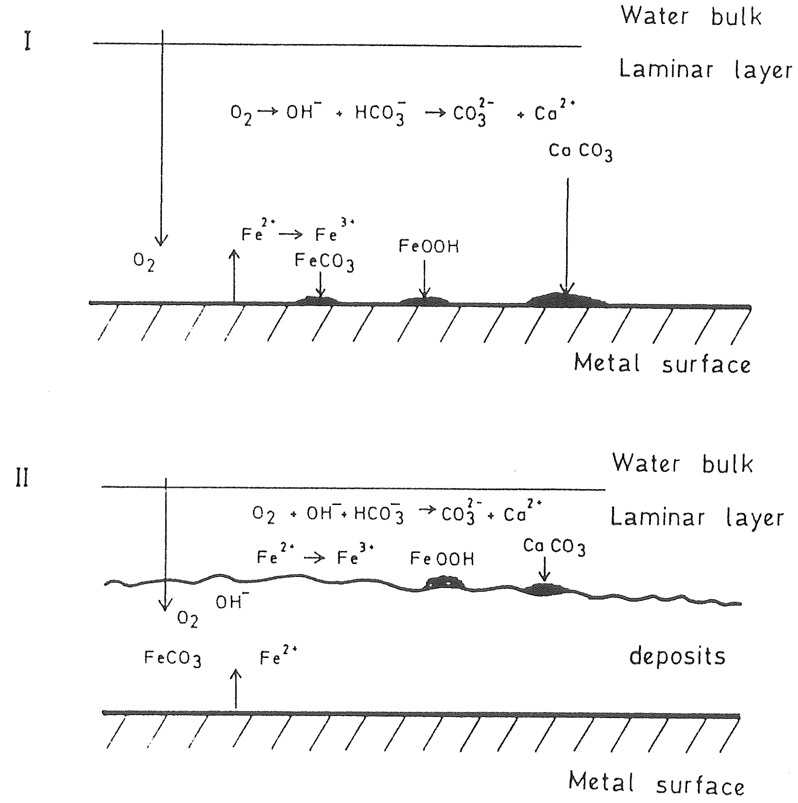

Figure 7.41 Oxygen transport through the laminar layer and formation of corrosion products, Case III. (I) new pipe with no deposits, (II) old pipe with deposits.

in Case II. At medium pH the $FeCO_3$ and $CaCO_3$ formation compete with each other. At high pH, however, oxidation of iron(II) to iron(III) takes place and FeOOH is formed. The carbonic species might then precipitate only as $CaCO_3$ (Figure 7.41). The oxidation of iron(II) can be prevented by the presence of calcium in the water.

Another factor critical for calcium carbonate precipitation is the availability of carbonate and the rapid transport of OH^-. At low water velocity, no $CaCO_3$ may precipitate because of the slow transport of O_2, HCO_3^- and Ca^{2+} towards the metal surface. At higher water velocity, however, $CaCO_3$ precipitates. An assumption is that the higher velocity implies higher kinetic energy which allows micro crystals to agglomerate more easily and facilitates $CaCO_3$ precipitation. A calcium carbonate layer with high crystallinity is effective for corrosion prevention. When calcium carbonate precipitates, pH decreases, which allows the retention of iron(II) in solution, however, the carbonate is already occupied and corrosion is prevented by the previously formed covering $CaCO_3$ layer. Diffusion of oxygen cannot take place through the deposit and therefore corrosion slows down. However, a non-covering $CaCO_3$ precipitation may lead to iron compound precipitation in the deposit. At medium pH, high calcium and hydrogen carbonate concentration, $FeCO_3$ will precipitate. At higher pH the deposit will contain $CaCO_3$ as well as $FeCO_3$ or FeOOH. A high pH causes a higher rate of precipitation and a more amorphous and porous deposit with a greater amount of FeOOH. Calcium carbonate precipitation is retarded both by low water velocity and by organic matter in the water. The organic matter retards $CaCO_3$ precipitation by adsorption on the surface which results in a more crystalline precipitation. The organic matter available for adsorption can be reduced by complex formation with iron(II). But at increased pH the organic compounds become less dissociated and might be precipitated which reduces the complex formation. Organic compounds with low molecular weight and low acid number, which do not form complexes easily will also remain dissolved in the water. The adsorption tendency is also low. The bound iron(II)-compounds may form a $FeCO_3$ precipitate at low pH depending on a reversed complex reaction.

Since organic matter retards calcium carbonate precipitation and lowers the precipitation rate, the deposit will be more crystalline and the potential for oxygen and iron diffusion through the deposit decreases.

In the following equations a) and b) refer to water without or with organic matter present, respectively.

Anode $Fe \rightarrow Fe^{2+} + 2e^-$ (7.1)

Cathode $\frac{1}{2}O_2 + H_2O + 2e^- \rightarrow 2OH^-$ (7.2)

Low pH < 6.5

$$H_2CO_3 + OH^- \rightarrow HCO_3^- + H_2O \qquad (7.15)$$

$$a)\quad 3Fe^{2+} + \tfrac{1}{2}O_2 + 6HCO_3^- \rightarrow Fe_3O_4(s) + 3H_2O + 6CO_2 \qquad (7.49)$$

$$b)\quad Fe^{2+} + \text{org mat} \rightarrow Fe(II) - \text{org mat} \qquad (7.50)$$

Medium pH $6.5 < pH < 9$

$$HCO_3^- + OH^- \rightarrow CO_3^{2-} + H_2O \qquad (7.16)$$

$$a)\ \begin{cases} Fe^{2+} + CO_3^{2-} \rightarrow FeCO_3(s) & (7.6) \\ 2Fe^{2+} + \tfrac{1}{2}O_2 + 4OH^- \rightarrow 2FeOOH(s) + H_2O & (7.37) \\ Ca^{2+} + CO_3^{2-} \rightarrow CaCO_3(s) & (7.34) \end{cases}$$

$$b)\ \begin{cases} Fe^{2+} + \text{org mat} \rightarrow Fe(II) - \text{org mat} & (7.50) \\ Ca^{2+} + CO_3^{2-} + \text{org mat} \overset{\text{slow}}{\rightarrow} CaCO_3(s) - \text{org mat} & (7.52) \end{cases}$$

The reactions in a) compete with each other. If $FeCO_3$ forms, then neither reaction (7.34) nor (7.37) can take place and if $FeCO_3$ does not form the other two take place.

High pH > 9

$$a)\ \begin{cases} 2Fe^{2+} + \tfrac{1}{2}O_2 + 4OH^- \rightarrow 2FeOOH(s) + H_2O & (7.37) \\ Ca^{2+} + CO_3^{2} \rightarrow CaCO_3(s) & (7.34) \end{cases}$$

$$b)\ \begin{cases} Fe^{2+} + \text{org mat} \rightarrow Fe(II) - \text{org mat} & (7.50) \\ Ca^{2+} + CO_3^{2-} + \text{org mat} \overset{\text{slow}}{\rightarrow} CaCO_3(s) - \text{org mat} & (7.52) \end{cases}$$

Besides pH, calcium and carbonic species, the composition of the protective layer may be affected by other compounds in the water such as sulphates and chlorides, or by microbiological growth (which increases in the presence of organic matter) or by elevated temperature. Salts increase the corrosion rate in such a way that it is important to form a working protective layer. The problem is that salts decrease the possible formation of precipitates having protective properties.

As a conclusion it can be said that the proposed model for iron corrosion and prevention of corrosion has been formulated on the assumption that an effective protective layer consists of a crystalline structure of $FeCO_3$, Fe_3O_4 or $CaCO_3$. The deposits must thus contain iron(II) or calcium but not iron(III). When the precipitate consists almost entirely of FeOOH it will not act as a protective layer. A number of assumptions are made in the model which have to be verified in the following investigation.

- Increased pH close to the metal surface gives a higher iron(III) content in the deposit in relation to the total iron content.

- A relatively high content of total carbonic species in the water gives a higher iron(II) content in the deposit in relation to the total iron content.

- Increased pH at constant content of total carbonic species and calcium concentration results in an increased calcium content in the protective layer.

- Increased content of total carbonic species and/or calcium concentrations in a water at low pH yields only insignificant amounts of calcium in the precipitate.

- When the calcium content of the deposit is high the iron(II) related to total iron is low and vice versa.

8. SCOPE OF IRON CORROSION INVESTIGATION

A number of hypotheses are presented in the proposed corrosion prevention model. In order to verify the model the following studies were made.

The investigation was directed towards studying the effect that changes in water composition can have on internal iron corrosion, corrosion rate and the formation of protective layers.

In the investigation water composition was varied with regard to pH, total carbonic acid, calcium, chloride and sulphate concentrations. The corrosion studies were carried out at sixteen water works as laboratory and field tests (Appendix A). In the laboratory tests artificial drinking water was produced from an ion-exchanged water with a low content of inorganic species and organic matter to which chemicals was added as predetermined concentrations (Appendix A).

The following parameters were regulated:

- pH was varied between 5.0 and 9.5.

- The total content of carbonic acid was varied between 10 and 100 mg HCO_3^- l^{-1}.

- Calcium content was up to 35 mg Ca^{2+} l^{-1}.

- Chloride was added up to 65 mg Cl^- l^{-1}.

- Sulphate was added up to 85 mg SO_4^{2-} l^{-1}.

- The temperature was maintained at 15^oC.

The water used in the field tests varied in the following way:

- pH was between 6 and 9.5.

- The content of total carbonic acid varied between 6 and 137 mg HCO_3 l^{-1}.
- The calcium content was up to 40 mg Ca^{2+} l^{-1}.
- The chloride content was up to 155 mg Cl^- l^{-1}.
- The sulphate content was up to 72 mg SO_4^{2-} l^{-1}.
- The organic matter content varied between 1 and 15 mg l^{-1}.
- The water temperature was up to 20°C.
- Water velocity was 0.01-0.7 m s^{-1}.

Several methods were used for the corrosion rate studies. The used test water is present in Table 8.1.

Table 8.1 Water composition for the different test methods.

	Coupon rig test	Oxygen consumption rig test	Pipe test
pH	7.5, 8.5, 9.5	7.5, 8.5	5, 6, 7, 8
HCO_3 mg l^{-1}	10, 100	10, 100	10, 60, 100
Ca^{2+} mg l^{-1}	2.5, 35	2.5	2.5, 15, 30
SO_4^{2-} mg l^{-1}	8, 42.5, 85	8, 42.5, 85	20, 100
Cl^- mg l^{-1}	8, 32.5, 65	8, 32.5, 65	25

Weight loss was measured in corrosion rigs with coupons both in laboratory and field tests (Appendix A). The weight loss was the mean value for four coupons removed after a predetermined time (2, 4-5, 8-9, 14-15, 18-19 and 23-25 weeks).

Oxygen consumption during the corrosion process was also measured in two laboratory tests (Appendix A). The oxygen content was maintained by continuously feeding fresh water saturated with oxygen.

Corrosion rate was also calculated from iron uptake by stagnant water contained in iron pipes in the laboratory (Appendix A).

The formation of protective layers was studied on the coupons from the corrosion rigs and on iron pipes with continuously flowing water at the water works by scanning electron microscopy with energy dispersive analysis. Corrosion product analyses were also made using a wet chemical technique (Appendix A).

9. RESULTS OF IRON CORROSION INVESTIGATION

9.1 Iron corrosion measurement methods

The easiest and simplest method to determine a corrosion attack is an analysis of the iron content of the water after it has passed through a distribution network. Under conditions when no deposits form, the iron concentration in the water corresponds directly to dissolved (corroded) iron from the metal surface. In this case the iron concentration can be used for a determination of the life-time of an iron pipe. It is also possible to use an indirect method to measure the colour or turbidity of the water as long as those parameters are correlated to corrosion products only.

Another method for measuring corrosion is to measure the oxygen consumption. Oxygen is consumed when iron corrodes but it is also consumed by iron oxidation. If the oxygen measurement is combined with an analysis of iron in the water, information can be obtained about iron dissolution and oxidation. However, there will be no answer concerning the amount of iron that has been dissolved, oxidised and precipitated. A more complete picture can be obtained if the oxygen consumption measurement is combined with both an analysis of iron concentration in the water and an analysis of the composition of deposits. An important advantage of this method is that oxygen can be measured on-line which allows the continuous control of corrosion. The method can be used in tests on the same pipe material with the actual dimensions that are used in a distribution system. The method can also be used directly in a distribution system.

The last method used in the investigation is based on weight loss measurements of immersed, removable coupons. This is a direct method of measuring iron weight loss. It is easy to inspect the deposits after the exposure time or, if the corrosion test rig is made of transparent material, it is possible to observe the formation of deposits under the whole test period. However, there are some disadvantages in this method. One is that the coupons often do not have the same shape as the pipe and this results in different hydraulic conditions around the coupons than in a pipe. There could also be problems obtaining coupons of exactly the same material composition as the pipe. Another problem is that in some cases it takes a long time both for the weight loss to be detectable and for the protective layers to develop. It is possible to have pipe sections as "coupons" in a distribution network but there is more flexibility in removal of the usual kinds of coupons. When the coupons are removable the corrosion process can be controlled during the test period.

The used methods presented here is also decribed by Singley and Lee (1984b). For all the methods it is important to know that the determined value of corrosion must be seen in relation to the limitations of the test techniques or test system. In this study the corrosion data has not been used for an estimation of pipe life-time.

The different methods are presented in Appendix B.

Weight loss of coupons (Appendix B.2)
Dissolved iron concentration in water (Appendix B.3)
Oxygen consumption (Appendix B.4)

Table 9.1 compares the corrosion rate measured by weight loss of coupons (I) and oxygen consumption (II) after a test period of 70 days. The results for I were approximately twice those obtained for II under two different concentrations of carbonic species. The lower value obtained for II can be attributed to loss of oxygen in corrosion products, or in other words, the oxygen consumption cannot solely be attributed to iron corrosion.

Table 9.1 Comparison of iron corrosion rate measured by weight loss of coupons (I) and oxygen consumption (II) after 70 days at pH 7.5.

	Corrosion rate, mg dm^{-2} d^{-1}	
Method	HCO_3^- 10 mg l^{-1}	HCO_3^- 100 mg l^{-1}
I	86	49
II	44	20

Measurement of dissolved iron concentration was used to provide an indirect indication of iron corrosion processes and the formation of protective coatings. Most importantly measurements of dissolved iron provide an indication of water quality deterioration or improvement as a result of in-pipe corrosion.

9.1.1 Weight loss of coupons

In Figure 9.1 the results for weight loss of coupons at pH 7.5, 8.5 and 9.5 and at carbonic species concentrations of 10 and 100 mg HCO_3 l^{-1}, are presented. An immediate observation is that iron corrosion is rapid over the first 30 days and then continues to increase at a steady rate until the end of the experiments. At 100 mg HCO_3 l^{-1} the corrosion rate appears to have ceased, probably due to the precipitation of $FeCO_3$.

The precipitation of $FeCO_3$ requires the presence of Fe(II) and CO_3^{2-} in the water. Fe(II) forms at the anode when iron corrodes. At a pH of around 8.5 the sole form of total carbonic species is HCO_3^- which is converted to CO_3^{2-} due to the formation of OH^- at the cathode. If the pH is too high then the Fe(II) is oxidised to Fe(III) which makes $FeCO_3$ precipitation impossible.

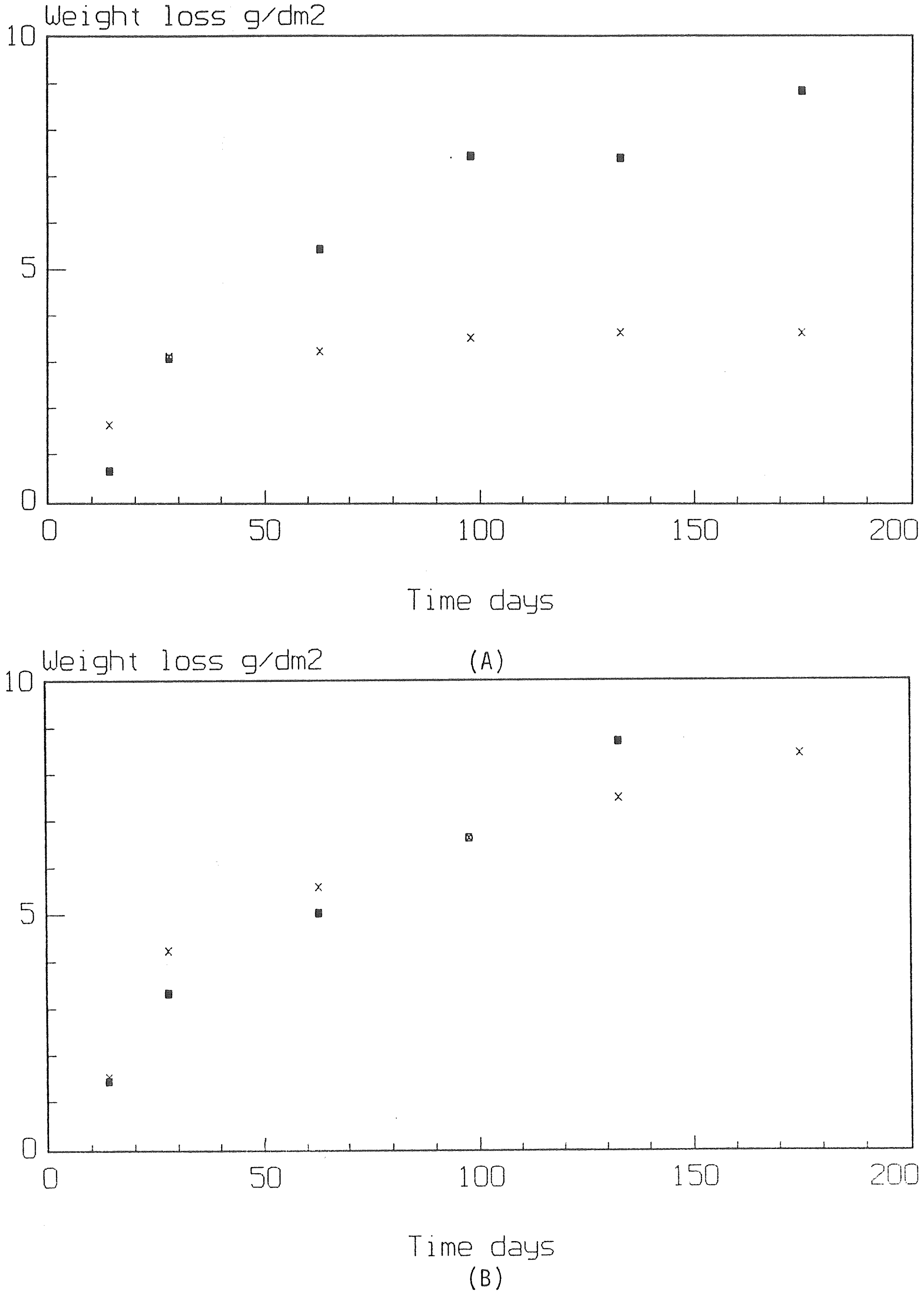

Figure 9.1 Weight loss versus time at different pH values A) 7.5, B) 8.5 and C) 9.5, when the content of total carbonic species was (■) 10 mg HCO_3^- l^{-1} and (x) 100 mg HCO_3^- l^{-1}.

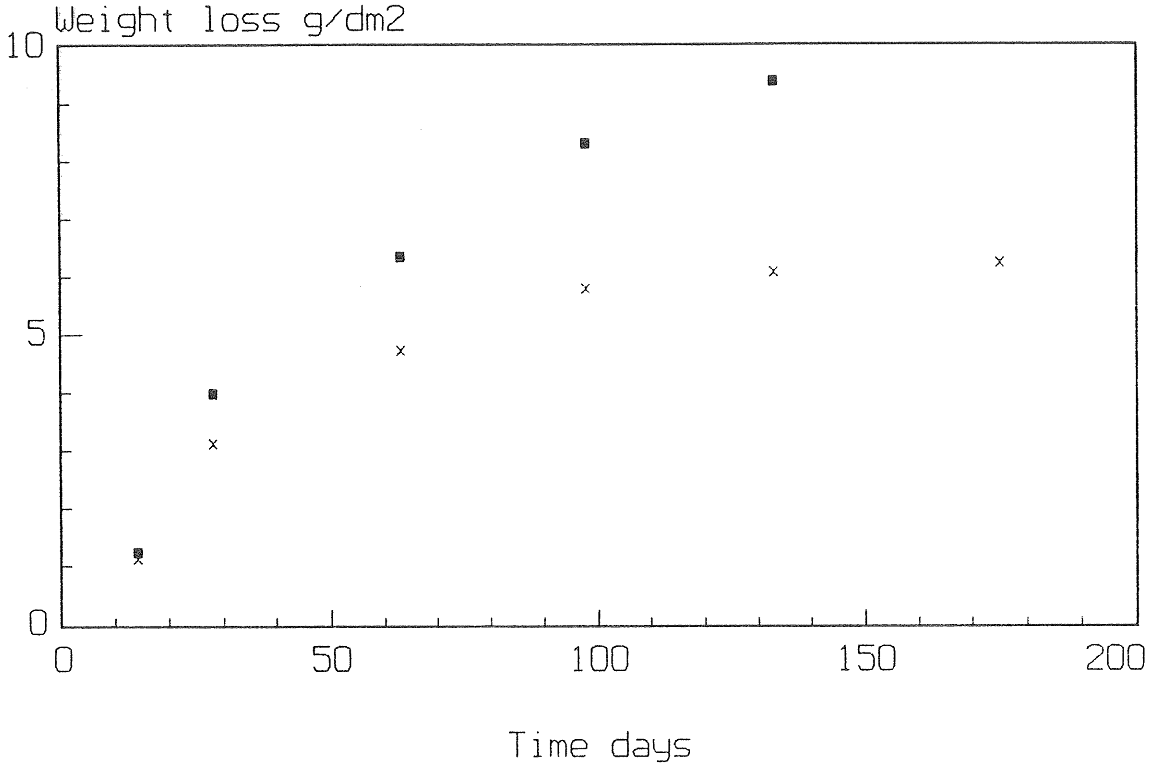

(C)

9.1.2 Oxygen consumption

Oxygen is consumed during iron corrosion (equation 9.2) and the rate of oxygen consumption therefore varies with the corrosion process, as shown in Figure 9.2. In addition oxygen consumption is reduced in the presence of carbonic species which agrees with the findings from coupon weight loss (Figure 9.1).

Anode $\quad Fe \rightarrow Fe^{2+} + 2e^-$ (9.1)

Cathode $\quad \frac{1}{2}O_2 + H_2O + 2e^- \rightarrow 2OH^-$ (9.2)

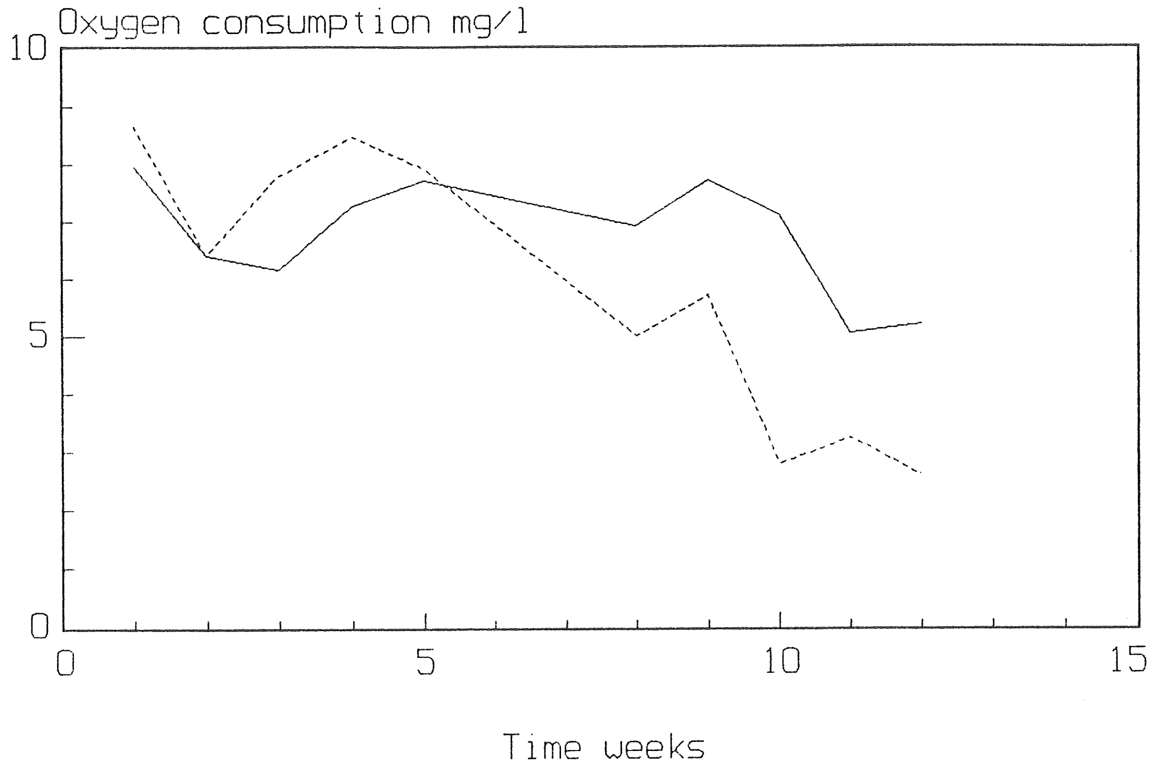

Figure 9.2 Oxygen consumption in an iron pipe, pH 8.5, Ca^{2+} 5 mg l^{-1}, Cl^{-} 32 mg l^{-1}. (——) 10 mg HCO_3^- l^{-1} and (----) 100 mg HCO_3^- l^{-1}.

9.1.3 Dissolved iron concentration

At low pH values iron is rapidly dissolved and therefore high dissolved iron concentrations are found in tap water (Figure 9.3). However, at a higher pH and carbonic species concentration a coating of $FeCO_3$ forms which protects the pipe from corrosion. Consequently, the dissolved iron concentration is lowered and the water quality improved, as shown in Figure 9.3. Therefore dissolved iron concentration is a useful indicator of the formation of protective coatings.

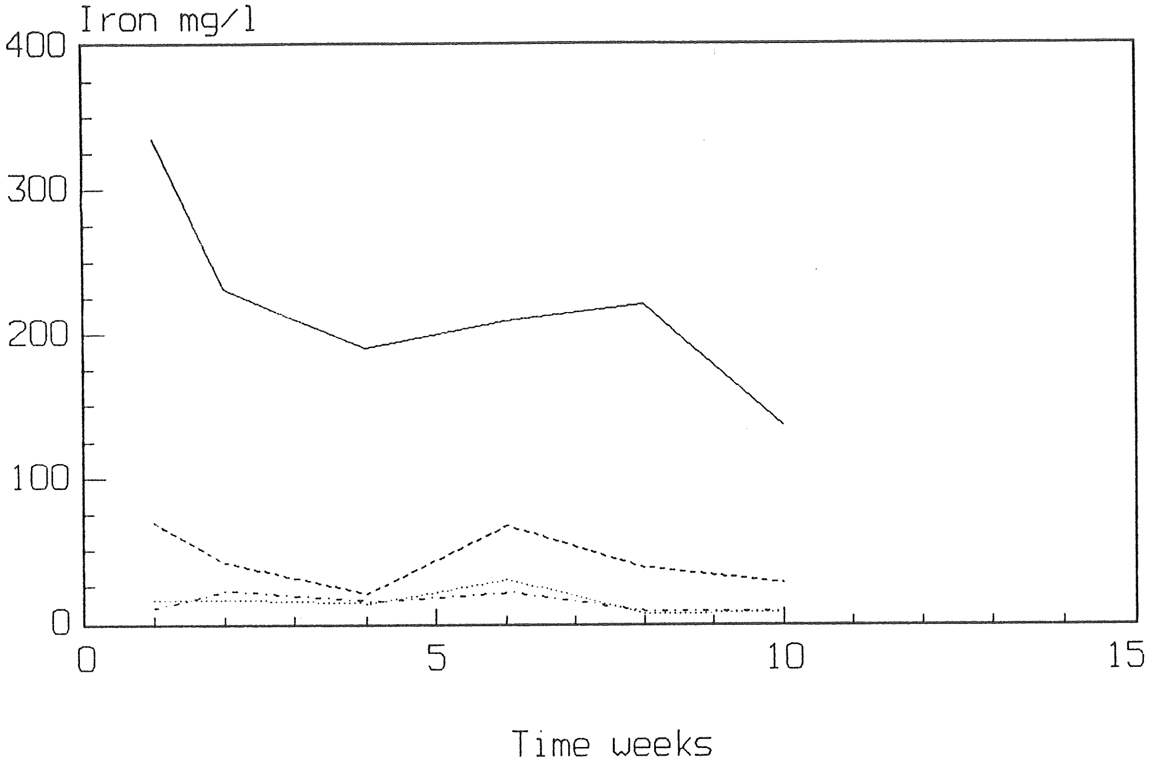

Figure 9.3 Dissolved iron concentration versus time, 15 mg Ca l^{-1}, 100 mg HCO_3^- l^{-1}, (——) pH 5, (----) pH 6, (••••) pH 7, (-••-•-) pH 8.

9.1.4. Calculations of corrosion rate from corrosion measurements

The results for weight loss can be converted to a corrosion rate in two ways. Firstly, the gradient of the weight loss curve can be calculated at a fixed time period. Secondly, the corrosion rate curve, such as in Figure 9.1, can be considered as two curves to provide an initial (up to 30 days) and continuous (> 30 days) corrosion rate.

The first alternative has been generally adopted for the corrosion rate calculations in this study as pipe corrosion is most interesting over a longer time scale than 30 days.

The initial corrosion rate is usually very high and is completed most rapidly in the presence of carbonic species due to the formation of an $FeCO_3$ protective coating (Figure 9.1 and Table 9.2). The continuous corrosion rate is also lower in the presence of carbonic species.

Table 9.2 Duration of initial corrosion in days for waters with different pH and total content of carbonic species in mg HCO_3^- l^{-1}.

	HCO_3^- mg l^{-1}	
pH	10	100
7.5	70	30
8.5	40	35
9.5	50	50

Table 9.3 Initial corrosion rate and continuous corrosion rate in mg $dm^{-2}d^{-1}$ at different pH and total content of carbonic species in mg HCO_3^- l^{-1}.

	Initial corrosion rate mg $dm^{-2}d^{-1}$		Continuous corrosion rate mg dm^{-2} d^{-1}	
	HCO_3^- mg l^{-1}		HCO_3^- mg l^{-1}	
pH	10	100	10	100
7.5	103	108	11	3.5
8.5	101	152	49	21
9.5	144	106	24	7

In order to minimise corrosion, the corrosion rate has to be reduced quickly after the initial state. This process should function independently of physical parameters such as water temperature and flow velocity.

9.2 Importance of pH and content of total carbonic species on corrosion rate and protective layer formation

The pH of the tested waters varied between 5 and 9.5. The importance of pH on the corrosion of iron was studied by weight loss measurements and by dissolved iron concentration measurements both in the laboratory with specified waters and at the water works. The total content of carbonic species was varied at different pH values as in the laboratory tests. The content of HCO_3^- was maintained at 10, 15, 60 and 100 mg l^{-1}. In field tests the variation was between 6 and 137 mg HCO_3^- l^{-1}. The content of carbonic species are important for buffer capacity and $FeCO_3$ precipitation. The pH of the water either at or near the metal surface, influences the amount of CO_2, HCO_3^- or CO_3^{2-} at the metal surface.

The calculated corrosion rate as a function of pH and content of total carbonic species is shown in Figures 9.4 and 9.5. Figure 9.4 shows the corrosion rate converted from iron uptake in iron

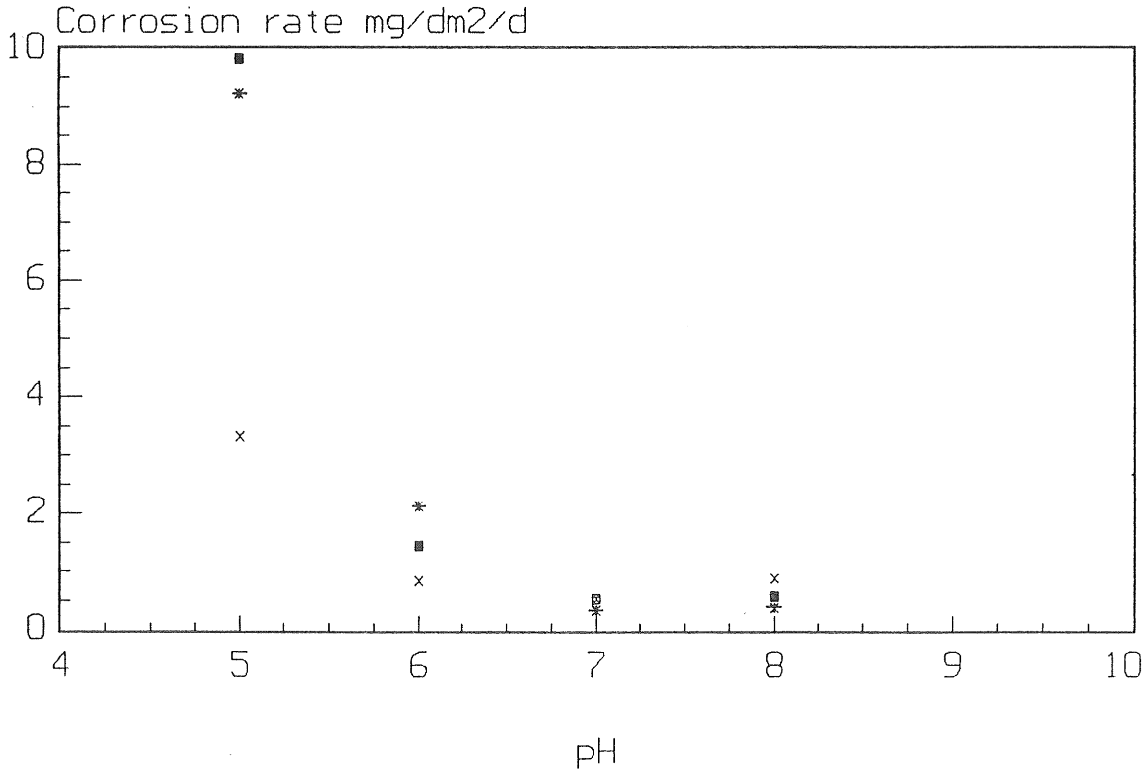

Figure 9.4 Corrosion rate versus pH, at 5 mg Ca^{2+}/l and 20 mg SO_4^{2-}/l at (x) 10, (■) 60 and (*) 100 mg $HCO_3^- l^{-1}$.

pipes at pH between 5 and 8 at 10, 60 and 100 mg HCO_3^- l^{-1}. The tendency for corrosion to increase with decreasing pH is immediately apparent, for example a decrease of pH from 7 to 5 increased the corrosion by a factor of six (Figure 9.4).

Figure 9.5 shows the corrosion rate converted from weight loss in coupon rigs at pH values that correspond to normal values in drinking water (7.5, 8.5 and 9.5) at 10 and 100 mg HCO_3^- l^{-1}.

The corrosion rate increased at pH 8.5 (Figure 9.5). The corrosion rate was lowest at a pH around 7 and 7.5 (Figures 9.4 and 9.5) especially when carbonic species were present.

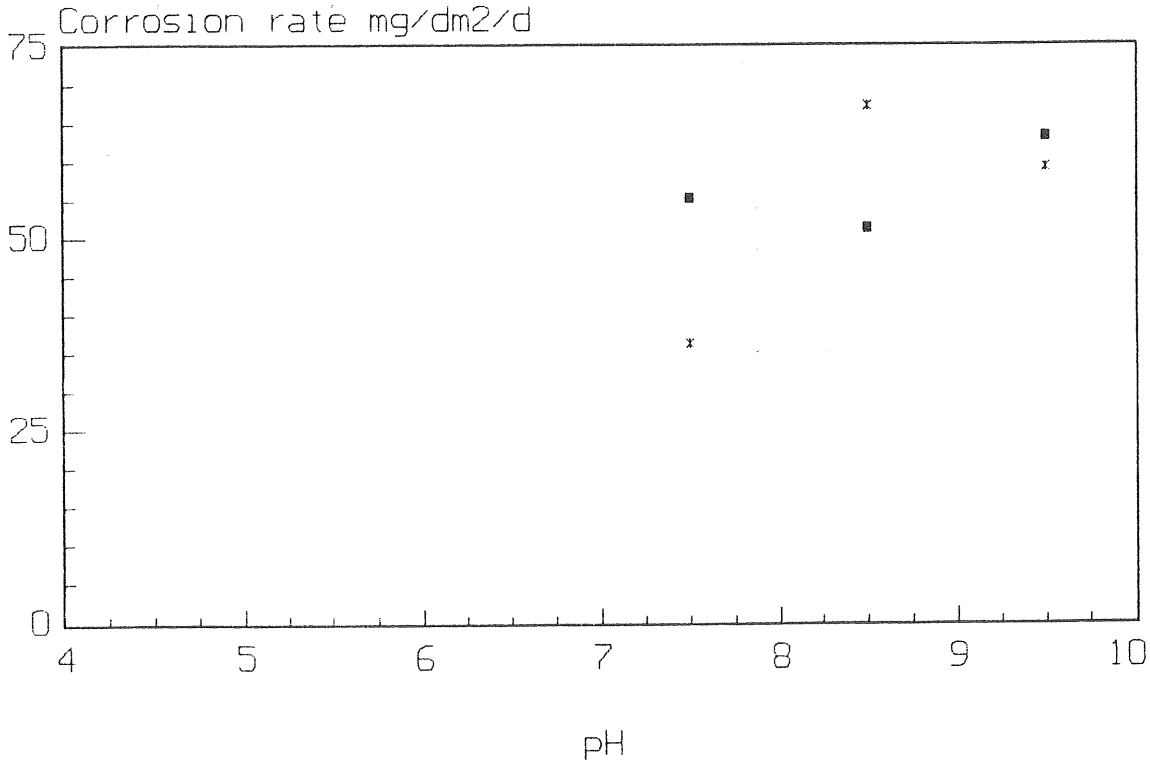

Figure 9.5 Corrosion rate versus pH, at 2.5 mg Ca^{2+} l^{-1} and (*) 10 and (■) 100 mg HCO_3^- l^{-1}.

At a pH value around 8.4 the buffer capacity is low and at 8.5 to 9 the buffer capacity increases (Figure 7.10), where a low carbonic species concentration is present the buffer capacity is low. Corrosion rate increases with increasing pH due to increased oxidation of iron(II) to iron(III) and as a consequence no effective protective layer is formed. In water with a high total carbonic species concentration the buffer capacity has a minimum at pH 8.4 (Figure 7.10) which allows a more rapid corrosion rate. When the buffer capacity is high, at pH < 8.4, the corrosion rate is slow. When the pH is > 9 the corrosion rate will increase because of the oxidation of iron.

In the field tests, where waters from various water works were used correlations between the corrosion rate and buffer capacity were made and these are shown in Figure 9.6.

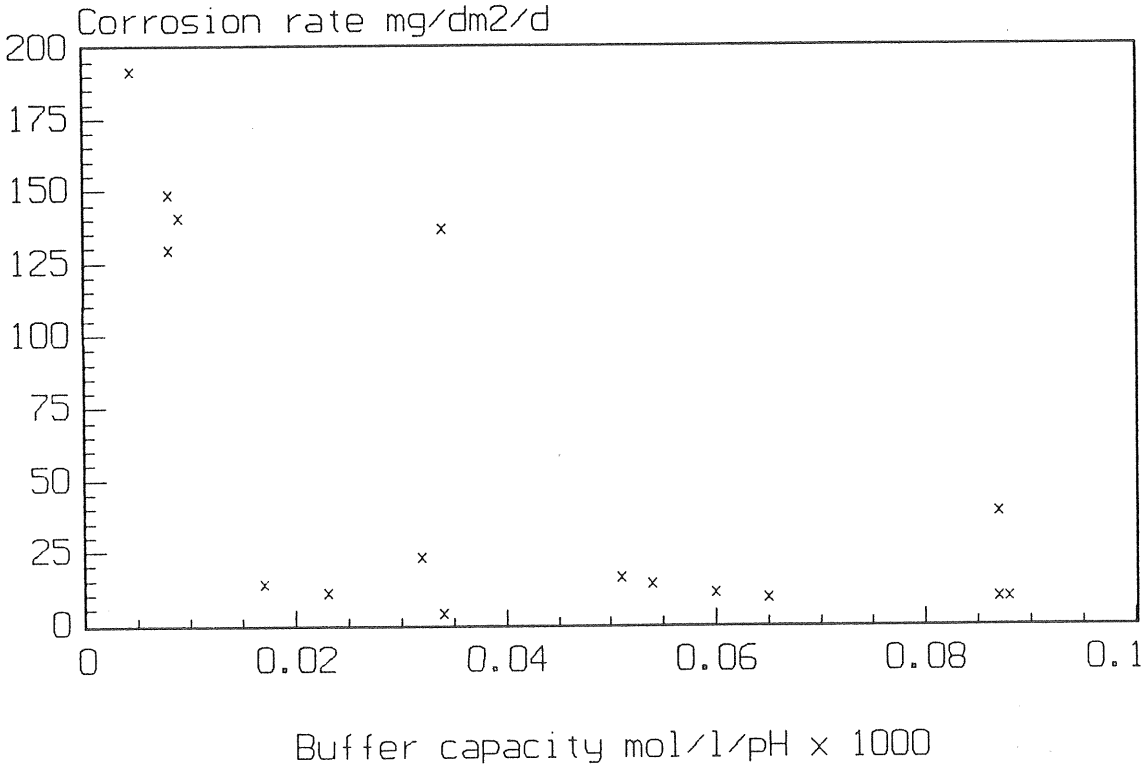

Figure 9.6 Corrosion rate versus buffer capacity from field tests.

Waters with a low buffer capacity have the highest corrosion rate, which means waters with a low content of total carbonic species and a pH of around 8.5.

The oxidation of Fe(II) to Fe(III) depends on the buffer capacity (Jobin and Gosh 1972), the salt content (Sung and Morgan 1980) and the concentration of different inorganic species (Legrand and Leroy (1984) as shown in equations (9.1), (9.2) and (9.3) the same as (7.17), (7.25) and (7.26) from Chapter 7.

$$\frac{d[\mathrm{Fe(II)}]}{dt} = -K[\mathrm{Fe(II)}]\,[\mathrm{OH^-}]^2\, p_{O_2}\, \beta^{\frac{1}{2}} \tag{9.1}$$

$$\frac{d[\mathrm{Fe(II)}]}{dt} = -K[\mathrm{Fe(II)}]\,[\mathrm{OH^-}]^2\, p_{O_2}\sqrt{I} \tag{9.2}$$

$$-\frac{d[\mathrm{Fe(II)}]}{dt} = \frac{k_1[\mathrm{Fe(II)}][O_2][\mathrm{OH^-}]^2}{1 + \frac{[\mathrm{HCO_3^-}]}{K_1} + \frac{[\mathrm{SO_4^{2-}}]}{K_2} + \frac{[\mathrm{Cl^-}]}{K_3} + \frac{[\mathrm{NO_3^-}]}{K_4}}\left(1 + \frac{3}{1 + \frac{[\mathrm{Ca^{2+}}]}{K_7} \quad \frac{[\mathrm{Mg^{2+}}]}{K_8}}\right) \tag{9.3}$$

As a conclusion in waters with a low content of calcium the corrosion rate is high when the pH is under 6 or over 9. At pH < 6 corrosion increases in the presence of carbonic species. When the pH values lie between 6 and 9 the corrosion rate decreases in the presence of carbonic species as compared to in their absence. At a pH value of around 8.5, when the buffer capacity is low, the corrosion rate is high.

Figure 9.7 shows the corrosion rate versus pH from the coupon rigs at different water works for $HCO_3^- < 40$ mg l^{-1} and $HCO_3^- >$ 40 mg l^{-1}. The corrosion rates were lower when the total carbonic species content was > 40 mg l^{-1} than when it was > 40 mg l^{-1}.

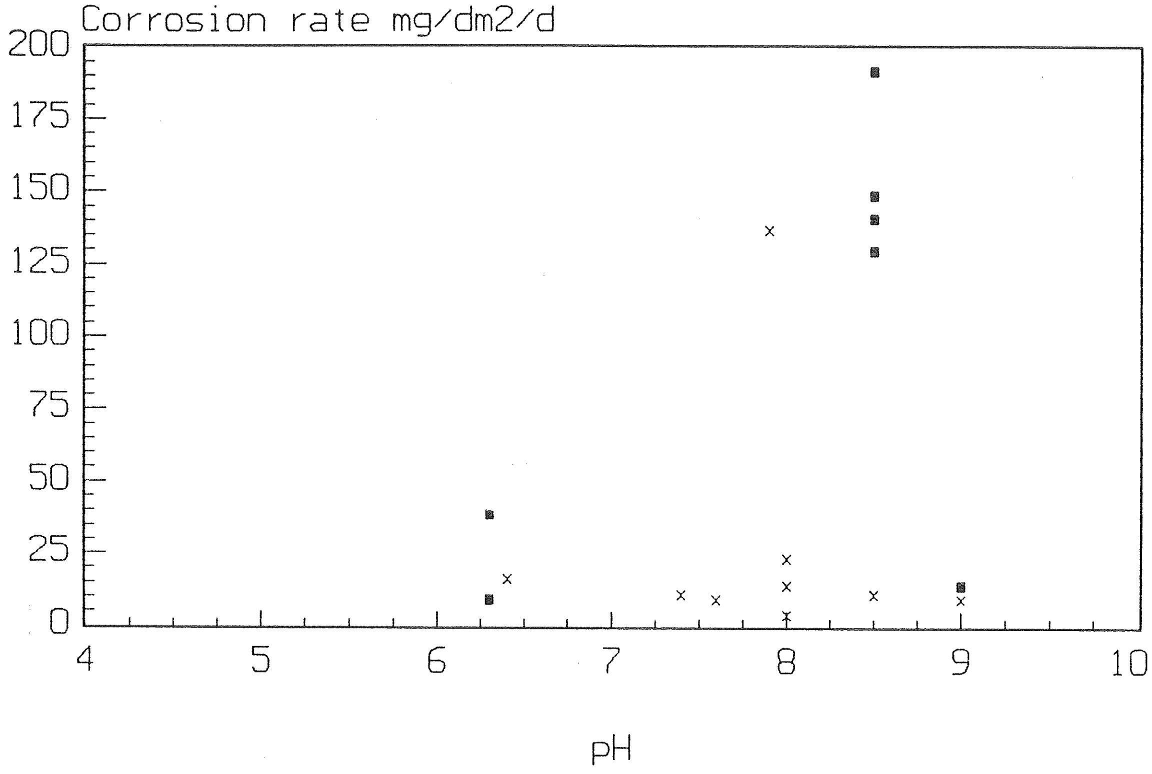

Figure 9.7 Corrosion rate versus pH for tested water at different content of total carbonic acid.
(■) $HCO_3^- < 40$ mg l^{-1}, (x) $HCO_3^- > 40$ mg l^{-1}.

9.3 Importance of calcium on corrosion rate and protective layer formation

The study was also carried out in waters with calcium in laboratory tests. The calcium in the laboratory tests was 2.5, 15, 30 and 35 mg l^{-1} and in field tests the content was between 2 and 39 mg Ca^{2+} l^{-1}.

When the water contains calcium it affects both the weight loss and the corrosion rate. Figure 9.8 shows that the weight loss changes with time in the presence of calcium. The initial corrosion was 81 mg $dm^{-2}d^{-1}$ for the first 25 days and the continuous corrosion was 4.9 mg $dm^{-2}d^{-1}$. The protective layer was formed rapidly and corrosion was significantly reduced in the water containing more calcium.

Compared to the results in a water without calcium the initial corrosion was 50% and the continuous corrosion was 25% for the same time period during initial corrosion (Tables 9.2 and 9.3). The formation of protective layers is dependent on there being a high enough content of carbonic species and calcium in the water at a given pH. The oxidation of Fe(II) to Fe(III) also depends on the calcium concentration according to equation (7.26).

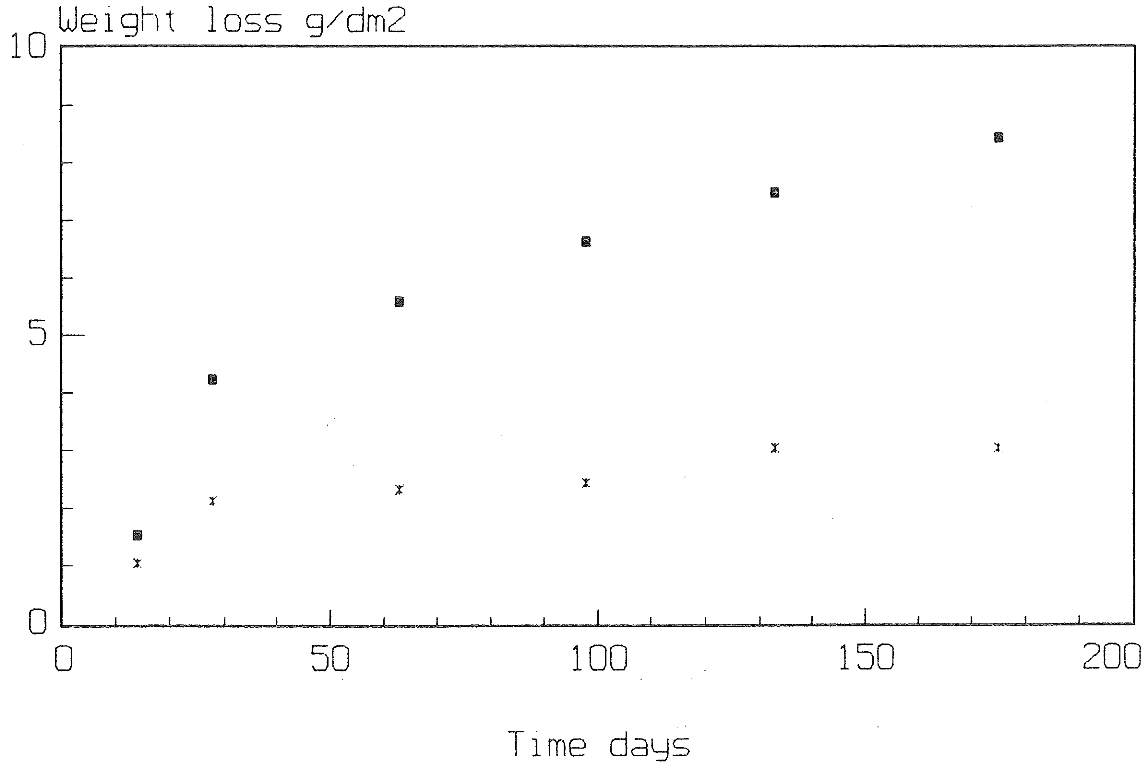

Figure 9.8 Weight loss of coupons versus time at pH 8.5 at 100 mg HCO_3^- l^{-1} and (■) 5 and (*) 35 mg Ca^{2+} l^{-1}.

Calcium distribution throughout the deposits was analysed by Scanning Electron Microscopy with elemental energy dispersive analysis and the micrograph obtained is shown in Figure 9.9. The white dots reveal calcium in the deposits. The photograph shows that the largest amount of calcium has been precipitated on the surface of the deposits and calcium is almost absent in the deposits near the metal surface.

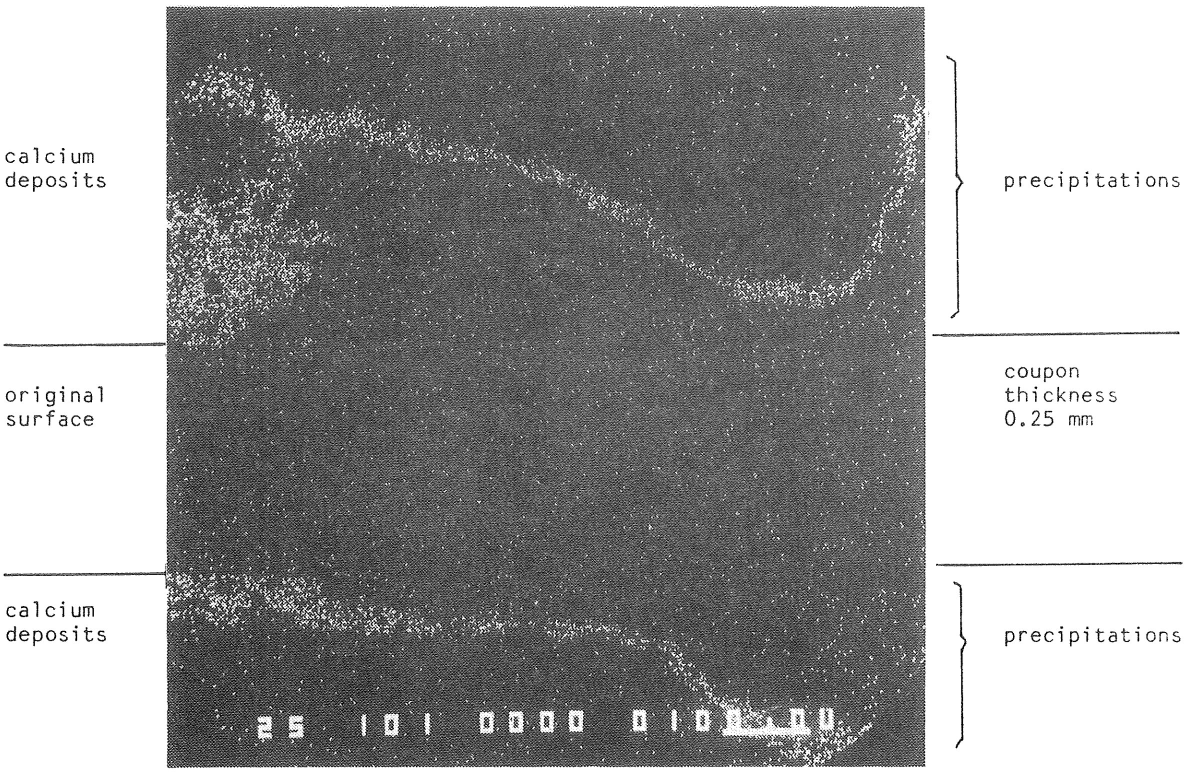

Figure 9.9 The distribution of calcium (white dots) through the deposits on a coupon after 175 days exposure time in water. pH 8.5, Ca^{2+} 35 mg l^{-1} and 100 mg HCO_3^- l^{-1}.

The amount of calcium which accumulates on the surface of the deposit varies with the water composition. The results for water without calcium are presented in Table 9.4 compared to a water containing 35 mg Ca^{2+} l^{-1} and 100 mg HCO_3^- l^{-1} at pH 8.5. The content of calcium is 15.4% of the iron content. It can be clearly seen that the calcium content in the deposits increases with an increase in pH.

Table 9.4 The percentage of calcium in relation to iron in the deposits, at 5 mg Ca^{2+} l^{-1}.

	HCO_3^- mg l^{-1}	
pH	10	100
7.5	0.3	0.4
8.5	0.7	0.9
9.5	1.5	2.0

The analysis of deposits in 56 iron pipes from different waters showed that the Ca^{2+} and Fe(II) content in relation to the total iron content of the deposit, was interdependent. Figures 9.10, 9.11 and 9.12 show the Ca/Fe_{tot} ratio versus pH, the Fe^{2+}/Fe_{tot} ratio versus pH and the Fe^{2+}/Fe_{tot} ratio versus calcium in the deposit, respectively.

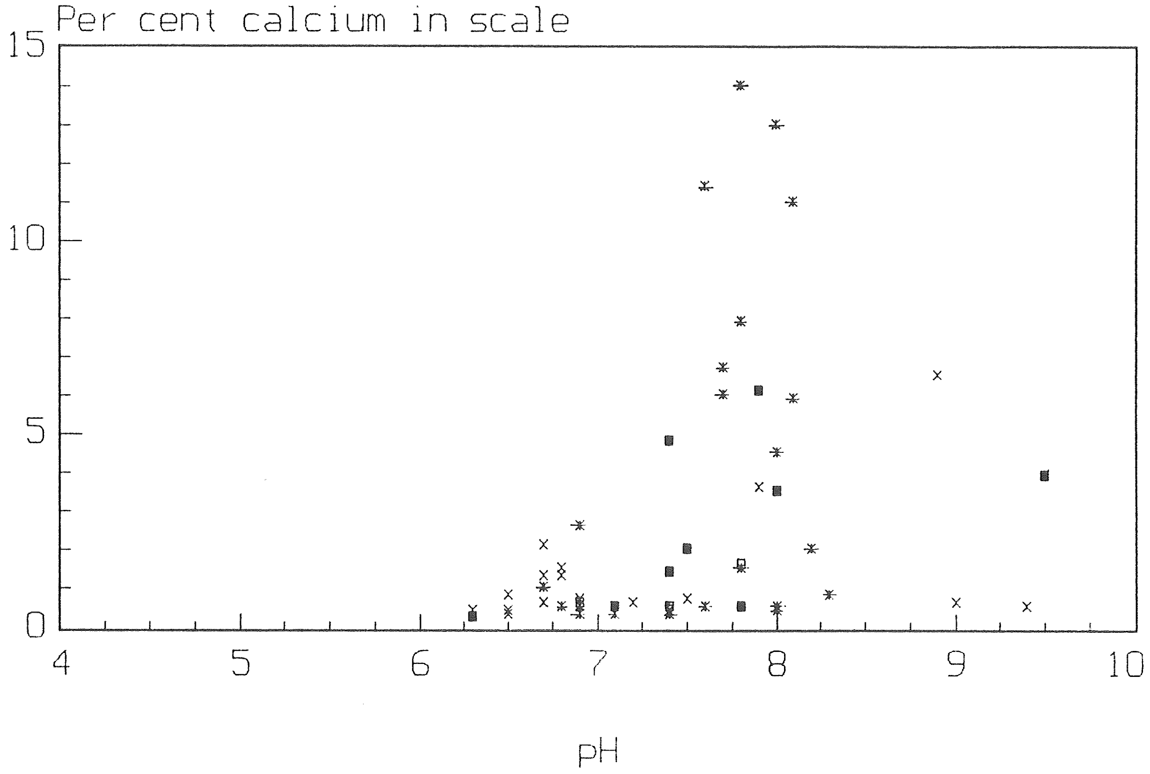

Figure 9.10 Percentage of calcium in the deposits versus pH in the water from iron pipes with flowing water at
x $HCO_3^- < 40$ mg l^{-1}, $Ca^{2+} < 20$ mg l^{-1}
■ $HCO_3^- > 40$ mg l^{-1}, $Ca^{2+} < 20$ mg l^{-1}
* $HCO_3^- > 40$ mg l^{-1}, $Ca^{2+} > 20$ mg l^{-1}

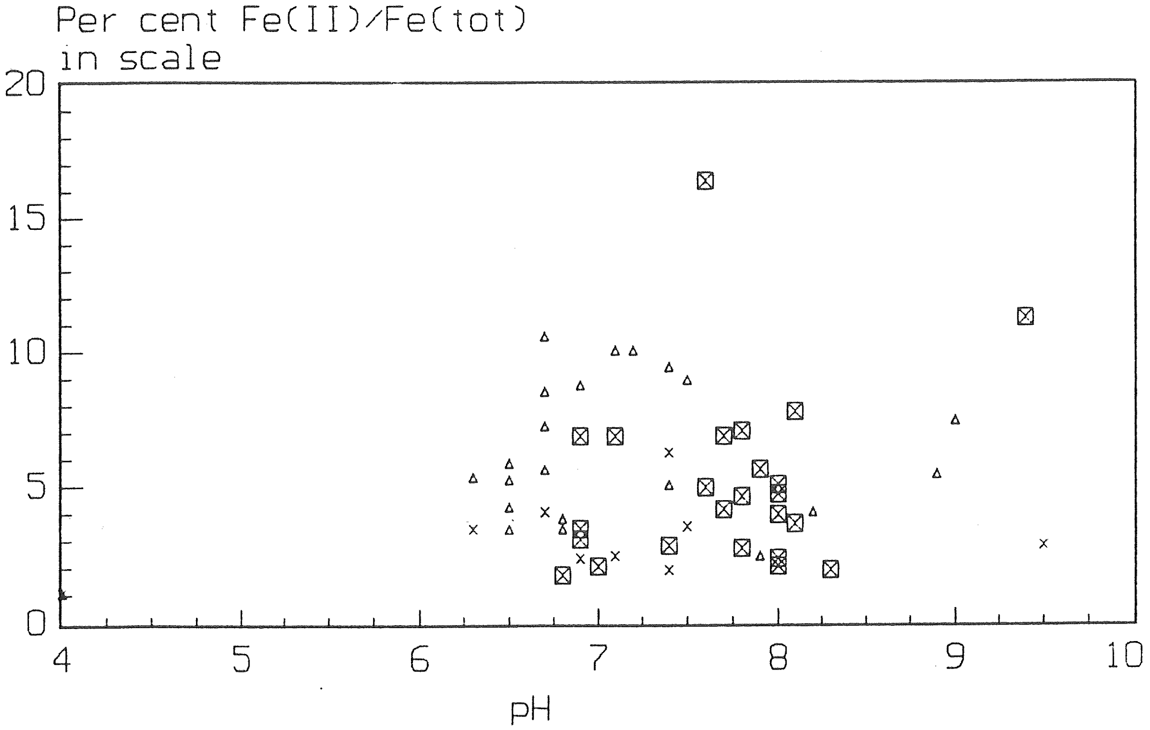

Figure 9.11 Fe^{2+}/Fe_{tot} in the deposits versus pH in the water from iron pipes with flowing water at

x $HCO_3^- < 40$ mg l^{-1}, $Ca^{2+} < 20$ mg l^{-1}

△ $HCO_3^- > 40$ mg l^{-1}, $Ca^{2+} < 20$ mg l^{-1}

☒ $HCO_3^- > 40$ mg l^{-1}, $Ca^{2+} > 20$ mg l^{-1}

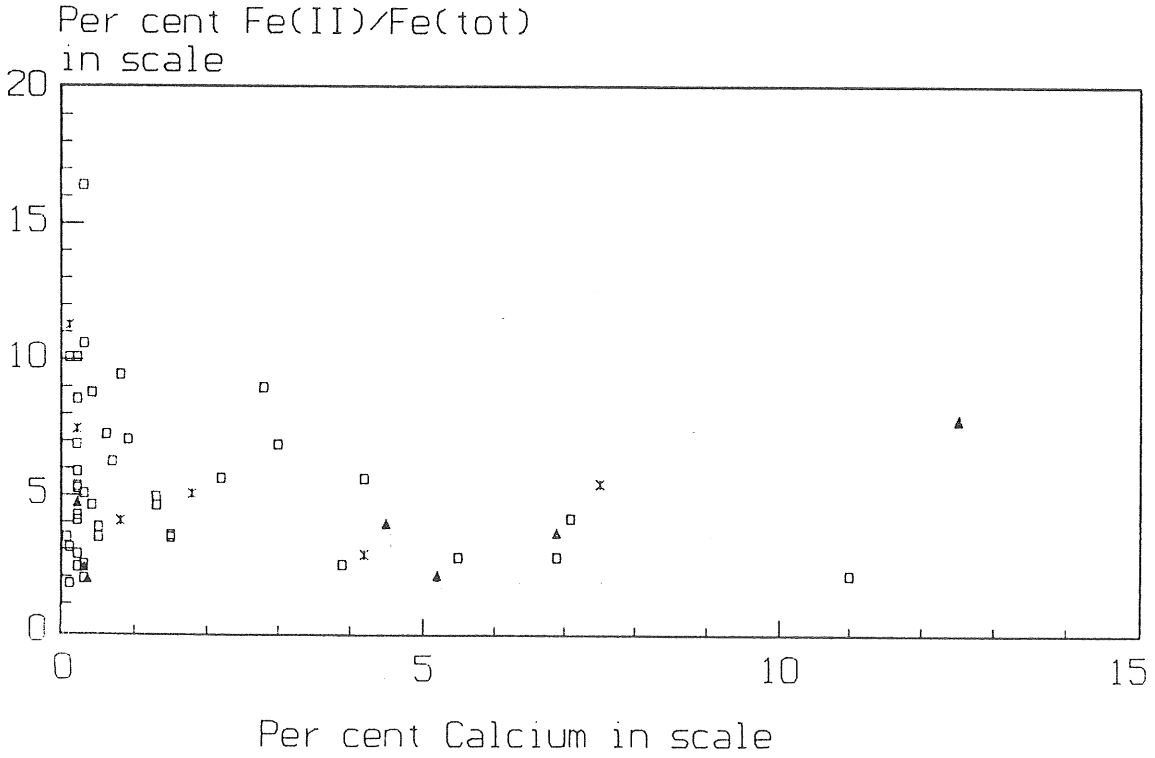

Figure 9.12 Fe^{2+}/Fe_{tot} versus calcium in the deposits from iron pipes with flowing water at

* pH < 8.0, $HCO_3^- < 40$ mg l^{-1}

□ pH > 8.0, $HCO_3^- < 40$ mg l^{-1}

△ pH > 8.0, $HCO_3^- > 40$ mg l^{-1}

More research is required to provide a complete picture and that is why no statistical estimation had been done. It should be mentioned though that the calcium content in the deposit increased with pH in those waters where $CaCO_3$-precipitation was possible; both Ca^{2+} and HCO_3^- were present in sufficient concentrations. In Figure 9.13 the amount of calcium in the deposit is plotted against the dissolved calcium content. No correlation was found. However, calcium concentrations below 6 mg Ca^{2+} l^{-1} and HCO_3^- concentrations below 20 mg l^{-1} do not give calcium in the precipitations (Figure 9.14). The Fe(II) content decreases with increasing pH and increasing Ca^{2+} content in the deposit.

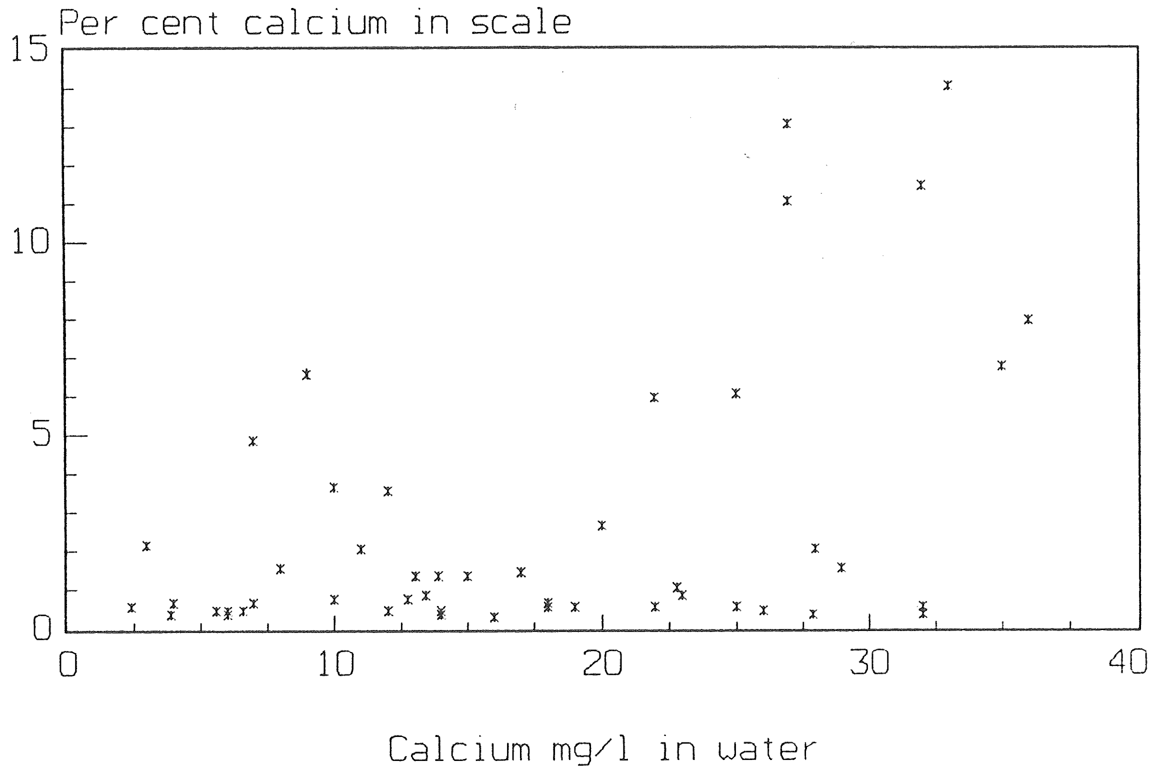

Figure 9.13 Calcium in deposits versus calcium in water from iron pipes with flowing water.

In the cases when $CaCO_3$ was detected in the deposits (pH 8.5, HCO_3^- 100 mg l^{-1} and Ca^{2+} 35 mg l^{-1}), the continuing corrosion rate was higher than for the case where pH was 7.5 and the total carbonic species concentration was 100 mg HCO_3^- l^{-1} with 5 mg Ca^{2+} l^{-1}. Iron(II) was the dominant iron product in the deposits.

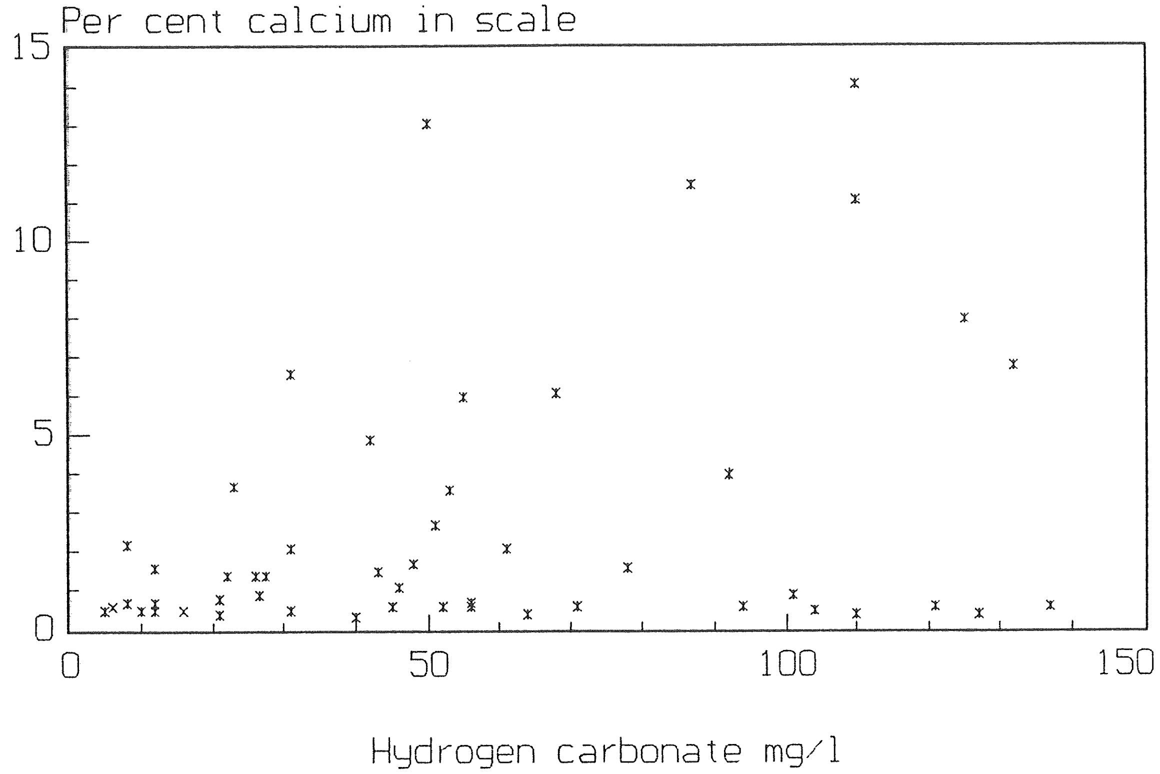

Figure 9.14 Calcium in deposits versus total content of carbonic species as hydrogen carbonate from iron pipes with flowing water.

It can be concluded that a high proportion of iron(II) was found in the deposits in waters containing a high total content of carbonic species at a pH where hydrogen carbonate predominates. At high pH and low total carbonic species concentration the amount of iron(III) is high in the deposits. When the total carbonic species concentration and calcium concentration of the water were so high that the solubility product of $CaCO_3$ was exceeded or when the water was slightly oversaturated with $CaCO_3$, calcium was found atop the deposits but not in them. When the content of total carbonic acid and the content of calcium were high in the water, but at a low pH, no calcium was detected on the deposits although there was a high proportion of iron(II). An increase in pH increases the presence of calcium in the deposits and a further increase in pH favours iron(III) in the deposits. A low content of calcium in combination with a high content of total carbonic acid at low pH results in the absence of calcium in the deposits. An increase in pH increases the calcium in the deposits, and a further increase in pH results in a further increase in calcium due to the high precipitation rate resulting in a low calcium content. Iron(III) is also found in the deposits.

9.4 Importance of chloride and sulphate on iron corrosion

The corrosion rate changed with increasing salt content, i.e. chloride and sulphate. No specific initial corrosion period was found because the tendency for any decrease in corrosion rate did not occur during exposure to waters containing chloride or sulphate. In cases where $CaCO_3$ might precipitate on the coupons the corrosion rate decreased.

Figure 9.15 shows the effect on the corrosion rate at different concentrations of chloride and sulphate at pH 8.5 and with a varying content of total carbonic species and calcium. The corrosion rate decreased when total carbonic species concentration or calcium content increased.

Because of the tendency for pitting corrosion with low oxygen consumption the values are not comparable and therefore the oxygen consumption technique cannot be used for waters containing high salt concentrations. It is only general corrosion that consumes oxygen, during localised corrosion the cathodic conversion of H^+ to H_2 dominates.

The formation of effective protective layers, in waters containing chloride and sulphate, only takes place when calcium is present in the water. The amount of calcium found on the surface of deposits is presented in Table 9.5.

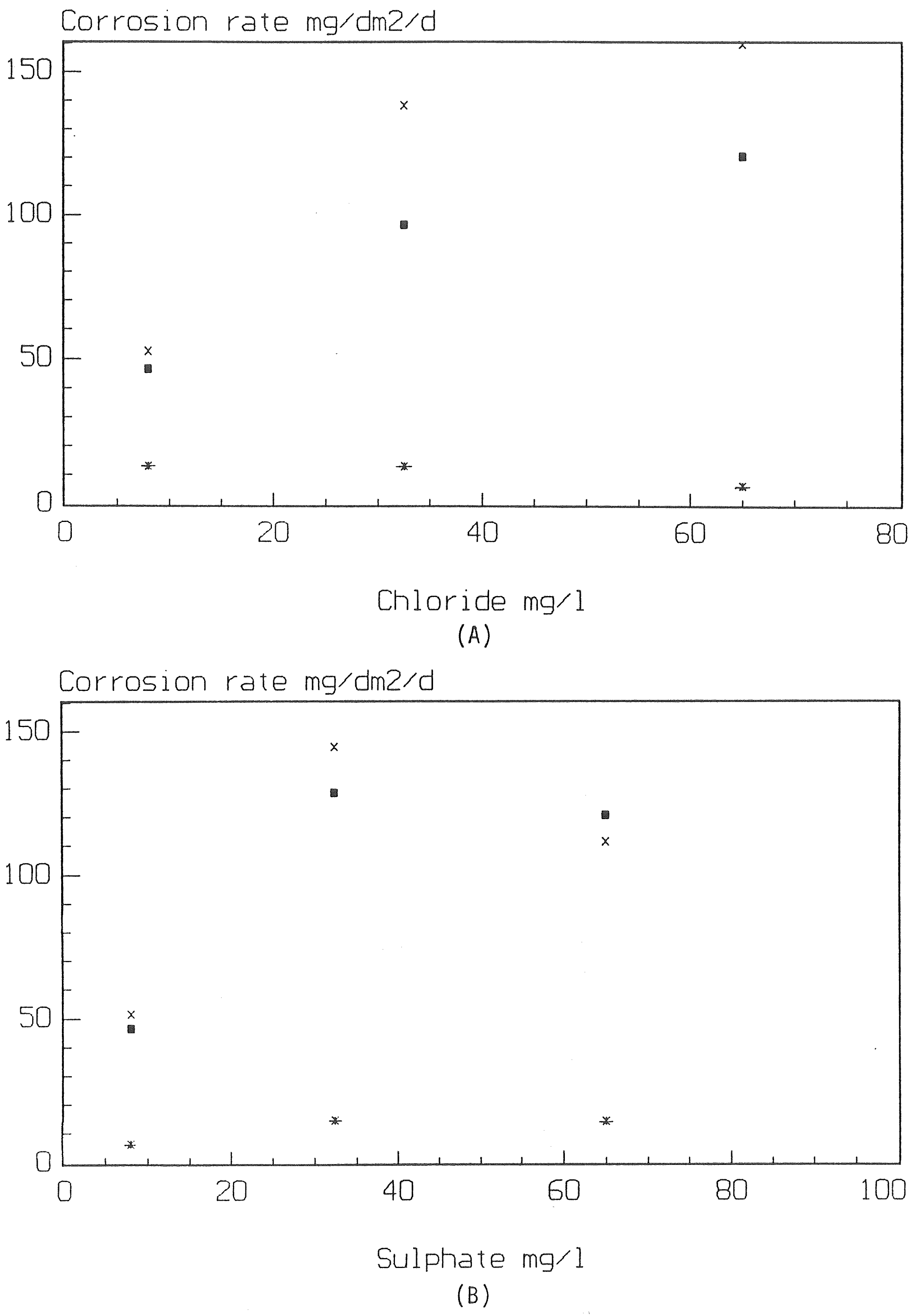

Figure 9.15 Corrosion rate calculated from weight loss versus chloride (A) and sulphate (B) after 60 days exposure at pH 8.5, at various total carbonic species and calcium concentration.

x 10 mg HCO_3^- l^{-1}, 5 mg Ca^{2+} l^{-1}

■ 100 mg HCO_3^- l^{-1}, 5 mg Ca^{2+} l^{-1}

* 100 mg HCO_3^- l^{-1}, 35 mg Ca^{2+} l^{-1}

Table 9.5 The percentage of calcium in relation to iron on the surface of deposits on coupons in waters containing chloride and sulphate at pH 8.5, 100 mg HCO_3^- l^{-1} and 35 mg Ca^{2+} l^{-1}.

	Cl^- mg l^{-1}		SO_4^{2-} mg l^{-1}	
	5	32	5	42.5
% Calcium	15.4	37.5	15.4	29.4

Precipitation of $CaCO_3$ is slower at high salt content which results in an increase of calcium on the deposits. When the chloride and sulphate concentrations are increased, the type of corrosion changes from uniform to localised corrosion. Chloride causes a more pronounced localised attack than sulphate (Figure 9.16).

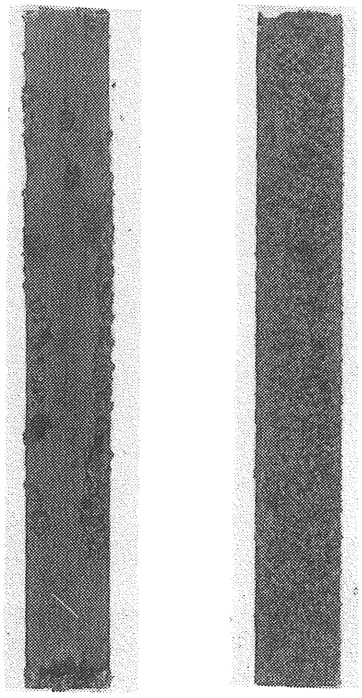

(A) (B)

Figure 9.16 Photograph of corrosion attacks on iron coupons in water containing (A) chloride and (B) sulphate.

Table 9.6 Percentage of corroded metal surface from the original coupons and percentage of depth in the metal body for a water with varying chloride content at pH 8.5, 100 mg HCO_3^- l^{-1} and 35 mg Ca^{2+} l^{-1}.

Chloride in mg l^{-1}	Uniform corrosion (%)	Pitting depth (%)
5	18	55
32	36	73
65	18	73

A cross section measurement of the thickness of the remaining coupons, in relation to the original thickness, was done after 18 weeks exposure time. The presence and depth of localised attack was also studied. Table 9.6 and Figure 9.17 show the change on the surface. It can be seen that both the uniform and the localised corrosion increase with increased chloride concentration. In a comparison between high and low chloride concentration, uniform corrosion remains constant but the localised attacks increase.

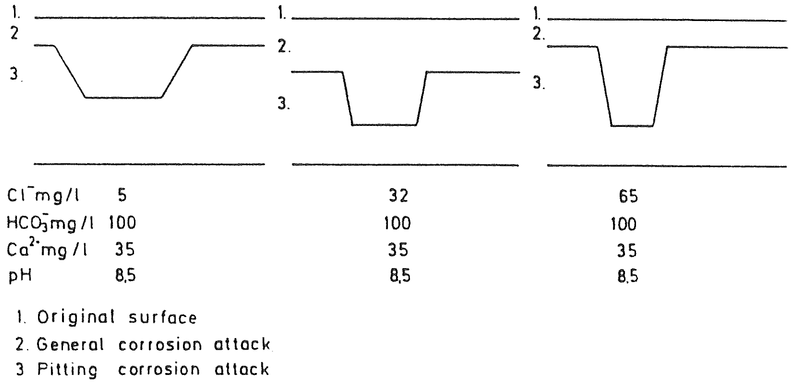

Figure 9.17 A schematic outline of corrosion attack in a water containing chloride, drawn from direct observations on coupons.

Figure 9.18 shows $CaCO_3$ crystals and deposits formed in a water containing 85 mg SO_4^{2-} l^{-1}, 35 mg Ca^{2+} l^{-1} and 100 mg HCO_3^- l^{-1}. The localised corrosion results in no change in pH near the metal surface which allows slow $CaCO_3$ precipitation with a high degree of crystallinity.

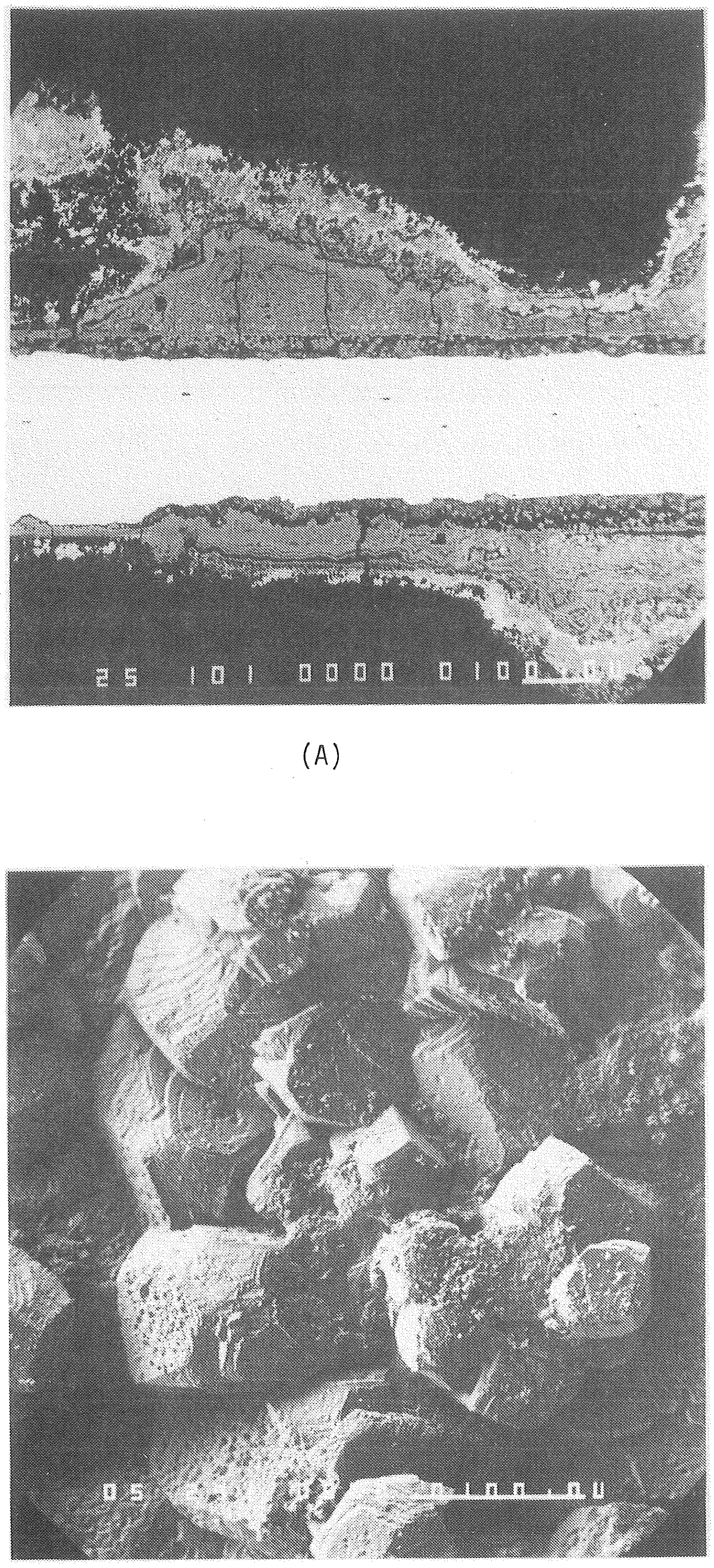

(A)

(B)

Figure 9.18 Scanning electron micrograph of a coupon with $CaCO_3$ on the top of the deposits (A) and crystals of $CaCO_3$ (B).

As a conclusion it can be stated that $CaCO_3$ should provide a reasonable protective layer in pipes when the water contains chloride or sulphate. The $CaCO_3$ deposits contain a high ratio of calcium to iron. A high content of chloride and sulphate in the water increases the localised corrosion and decreases the uniform iron dissolution from the metal, but the damage increases.

9.5 Importance of water velocity on iron corrosion

The water velocity in the iron coupon corrosion rig was maintained at 0.01 ms^{-1} and 0.7 ms^{-1}. Generally the corrosion rate was low at low water velocity. In some cases the corrosion rate decreased immediately to a low level at high water velocity, but in other cases the corrosion rate was higher than for the low water velocity. The appearance of corrosion products on the surface of the coupons varied with the water velocity as shown in Figure 9.19.

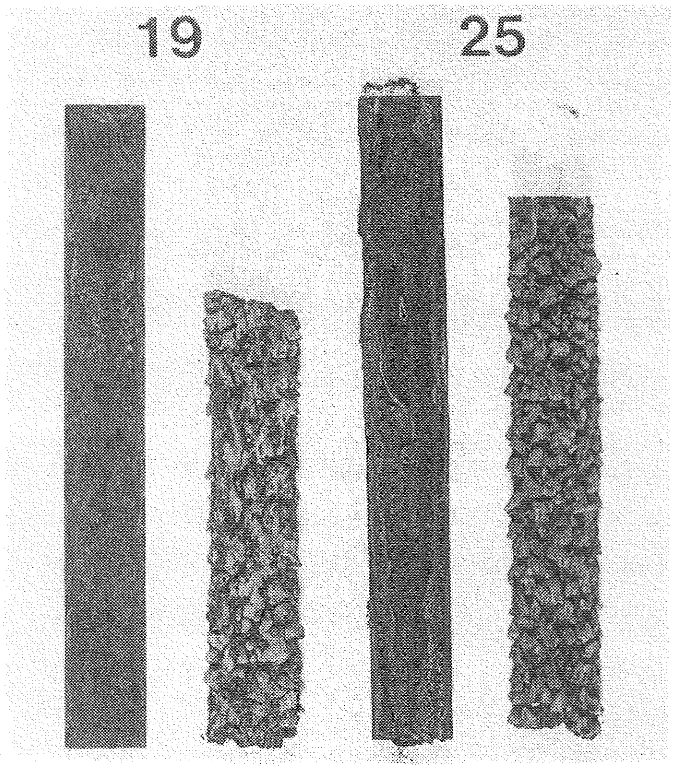

Figure 9.19 Photograph of the surface of the coupons after 19 and 25 weeks exposure. In both cases (weeks 19 and 25) low water velocity is to the left and high water velocity to the right.

Deposits with a wave like appearance were formed on coupons which were exposed to high water velocity. The deposits which gave protection against corrosion were closely attached to the coupon. However, in some cases the corrosion rate can be low even at high water velocity (Appendix C). In Appendix C high or low corrosion is listed at different water velocity versus water composition for test and field waters.

A high water velocity results in high corrosion rate when the water has a low total carbonic species concentration. The most satisfactory explanation is that oxygen can be readily transported through the porous FeOOH precipitation and this results in increased corrosion. An increase in pH occurs at the iron surface during corrosion due to the formation of OH^- and this allows the rapid oxidation of iron(II) to iron(III) and even more FeOOH precipitation.

In a water which contains either chloride or sulphate a high water velocity accelerates the corrosion rate as the high water velocity transports chloride and sulphate through deposits. At low water velocity the corrosion rate is independent of the content of chloride or sulphate in the water.

Protective layers are formed to a lesser extent at low water velocity independent of the water composition. At high water velocity precipitation takes place. This is especially true for calcium carbonate precipitations (Figure 9.20).

Figure 9.20 shows that the corrosion rate at high water velocity decreased after a certain period of time. However, at low water velocity the corrosion rate increased through the whole test period without any initial corrosion period.

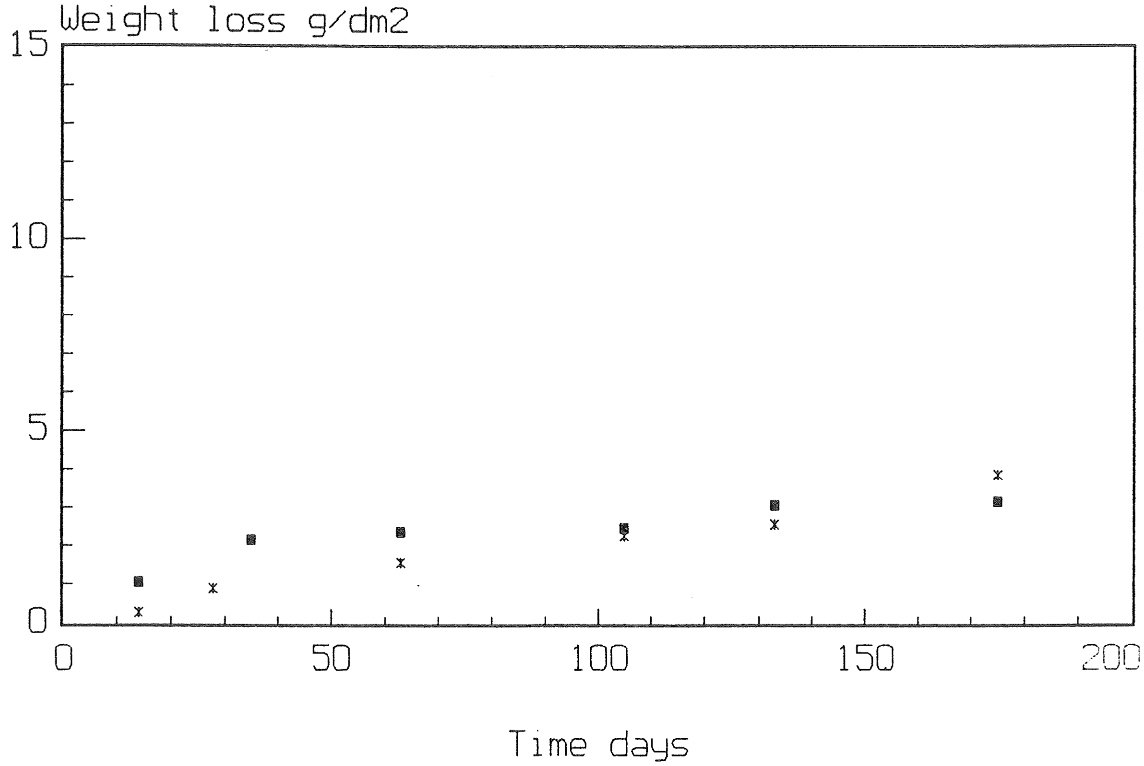

Figure 9.20 Weight loss as a function of time at a water velocity of (x) 0.01 and (■) 0.7 m/s at pH 8.5, HCO_3^- 100 mg l^{-1} and Ca^{2+} 35 mg l^{-1}.

In the water containing 35 mg Ca^{2+} l^{-1} (100 mg HCO_3^- l^{-1} at pH 8.5) 2.5% of the deposits contain calcium on the surface when the water velocity is low, compared to 15.4% at high water velocity. In Table 9.7 the ratio of calcium to iron is shown in the presence of 5 mg Ca^{2+} l^{-1}. Table 9.7 should be compared to Table 9.4 where the calcium content in the deposits is presented for water with a high velocity. $CaCO_3$ only precipitates at high water velocity.

Table 9.7 The percentage of calcium in relation to iron in the deposits, a water velocity of 0.01 m s^{-1}

	HCO_3^- mg l^{-1}	
pH	10	100
7.5	0.6	0.02
8.5	0.4	0.02
9.5	n.d.*	n.d.*

*) n.d. = not detectable.

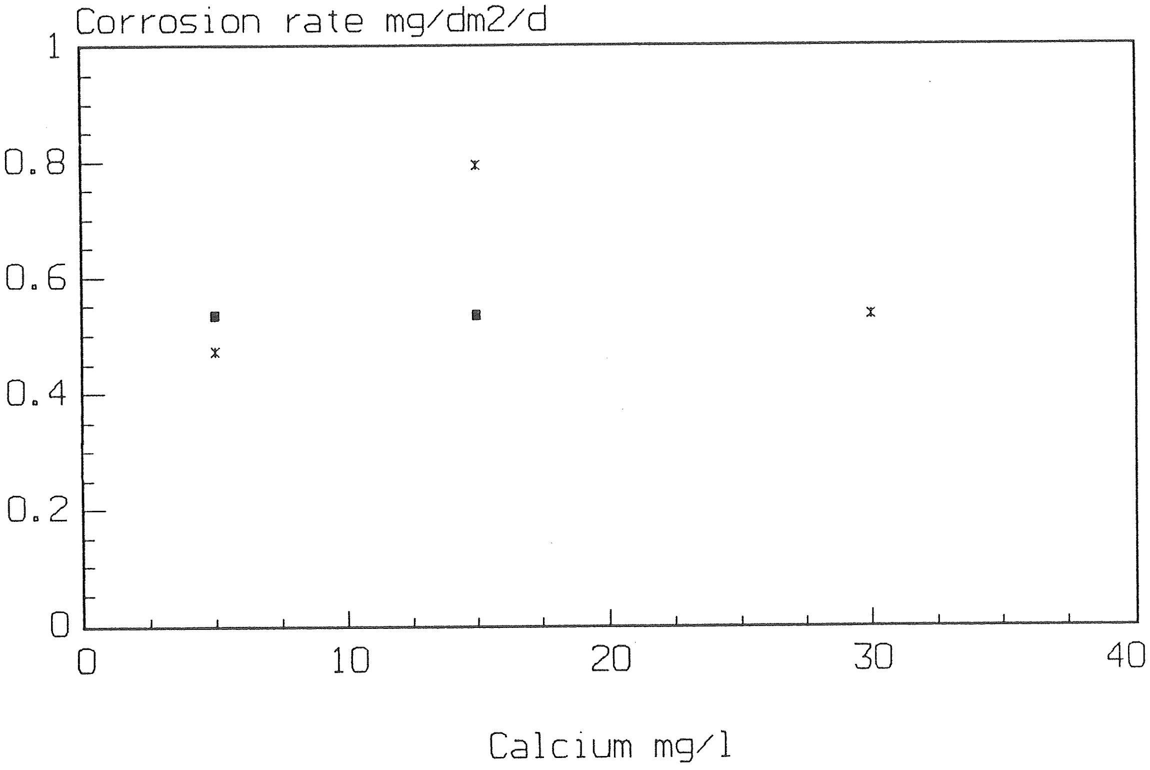

Figure 9.21 Corrosion rate on iron pipes with stagnant water versus calcium at 100 mg SO_4^{2-} l^{-1} and pH 8 at different content of total carbonic species

□ 10 mg HCO_3^- l^{-1}

▲ 60 mg HCO_3^- l^{-1}

* 100 mg HCO_3^- l^{-1}

In the iron pipe study with stagnant water, no noticeable change in iron uptake could be seen in the presence of calcium and a high total carbonic species concentration, even if the solubility product of $CaCO_3$ was theoretically exceeded. This can be explained by the stagnant water having no velocity where no crystallisation takes place (Figure 9.21). The formation of crystal nuclei require energy and a water in motion. Collisions between microcrystals must take place in order to form crystals that can protect the corroded surface.

The importance of water composition at different water velocities is clearly shown in the test from Munkfors water works. Three tests were made on waters treated in different ways.

Treatment:

I Addition of carbon dioxide and pH-adjustment with sodium hydroxide

II Treatment I + addition of phosphates

III Addition of calcium carbonate and pH adjustment with (crushed) lime

Figure 9.22 shows the weight loss versus time at both high and low water velocity. Photographs of the deposits formed on the coupons after various time periods of exposure in water I and III, are shown in Figure 9.23.

There was no difference in weight loss for the coupons when the water velocity was low but at high water velocity the weight loss decreased when corrosion control methods II and III were used.

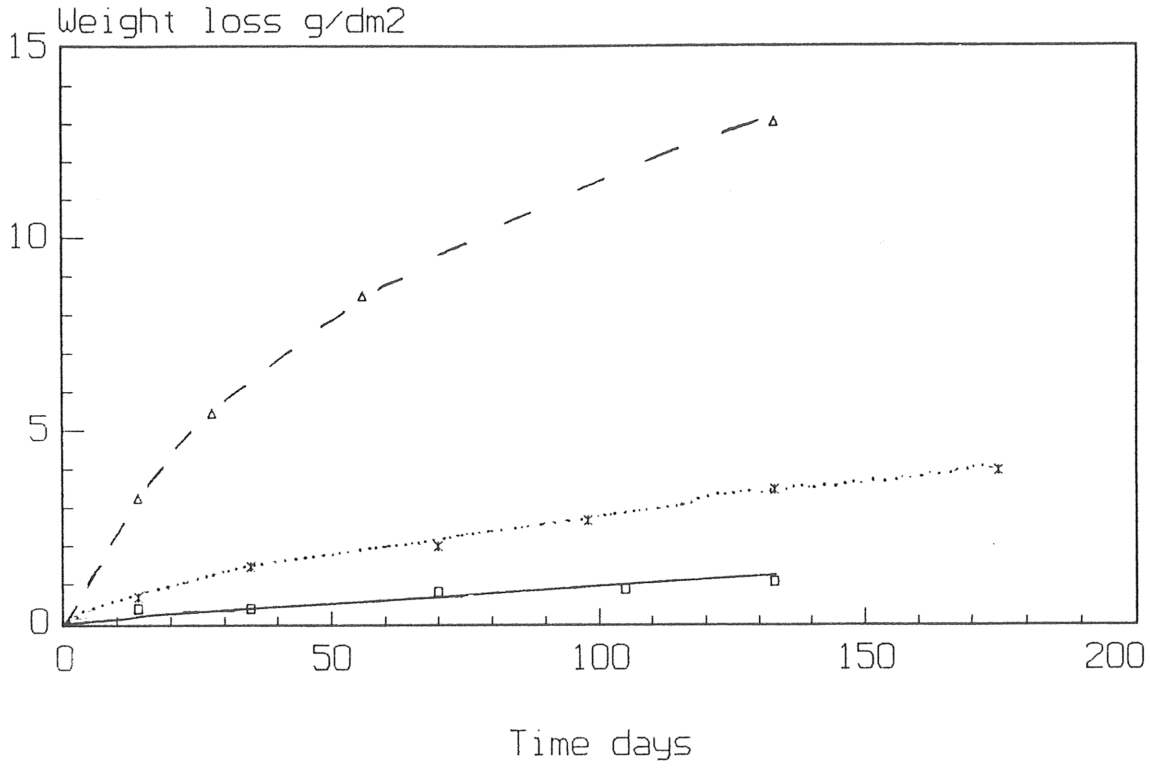

(A)

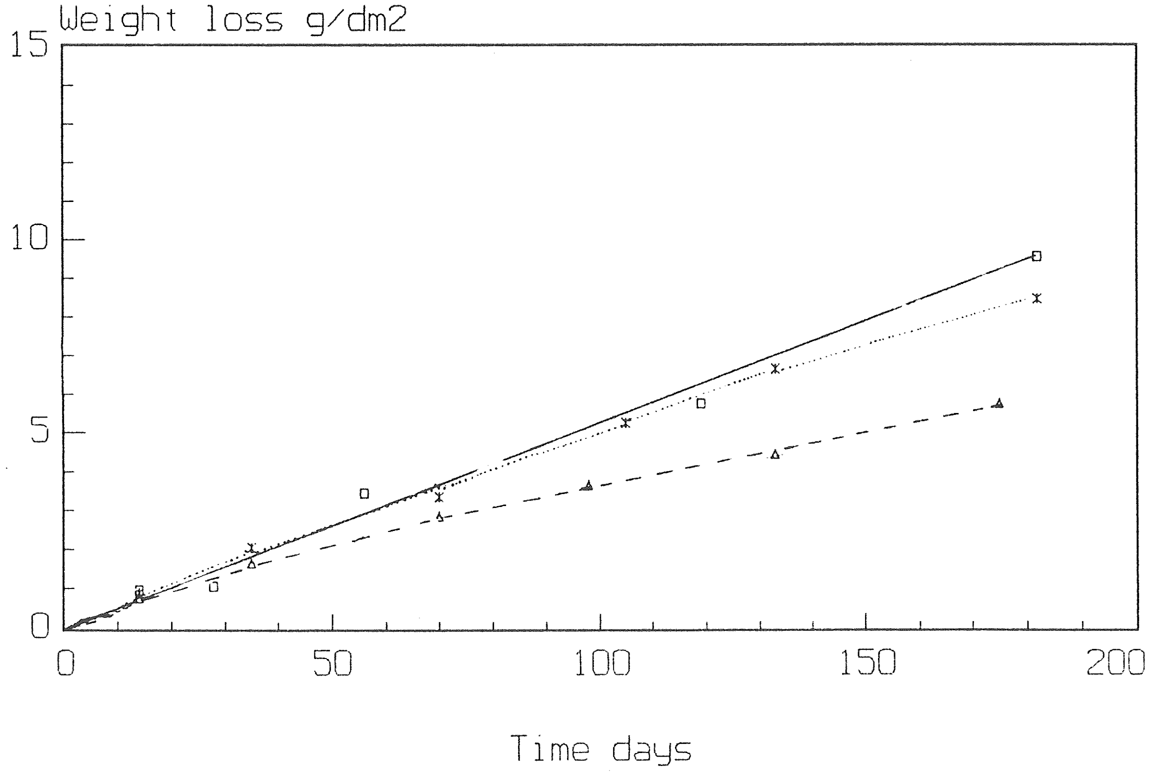

(B)

Figure 9.22 The influence of water velocity on corrosion rate for coupons exposed to water treated by different corrosion control methods at Munkfors water works. (A) Weight loss at high water velocity (0.7 ms^{-1}) (B) Weight loss at low water velocity (0.01 ms^{-1}). Treatment method I (– – –), II (———), II (••••)

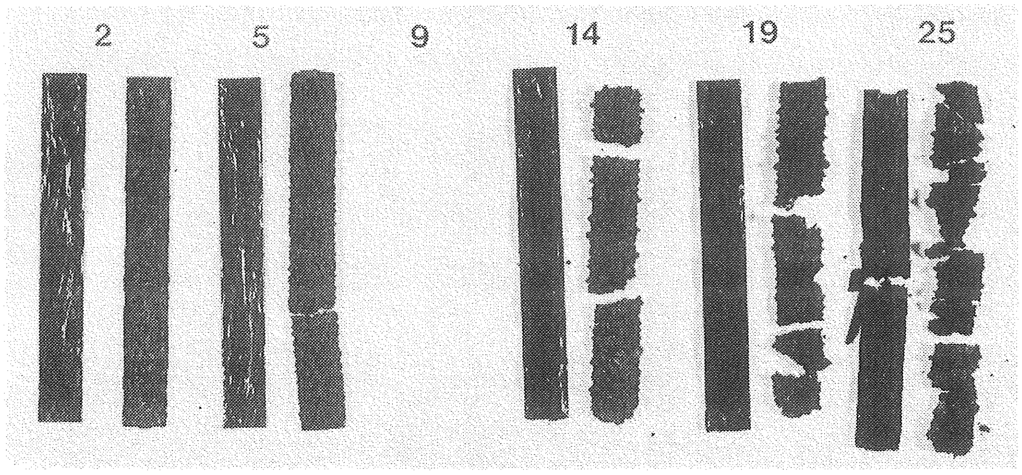

(I)

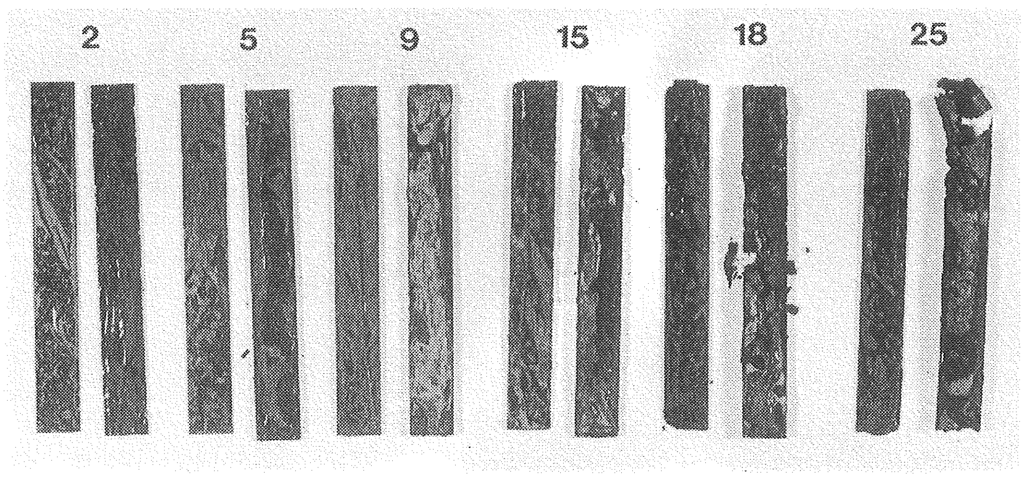

(III)

Figure 9.23 Photographs of deposits on coupons after exposure to water treated by different corrosion control methods (I) and (III) at Munkfors water works. Coupons exposed to high water velocity are placed to the right and those exposed to low water velocity are placed to the left.

Precipitation of phosphates and $CaCO_3$, is dependent on water velocity, and even when the proper chemical composition exists there will be little precipitation at low water velocity.

Another example which illustrates the importance of water velocity for precipitation was obtained at the Lackarebäck Waterworks in Göteborg. No decrease in corrosion rate was found in a water with 100 mg HCO_3^- l^{-1} compared to the same water with 15 mg HCO_3^- l^{-1} at low water velocity (Figure 9.24). In Figure 9.25 the same water condition is illustrated but at a high water velocity. The change in corrosion rate is very drastic at high water velocity.

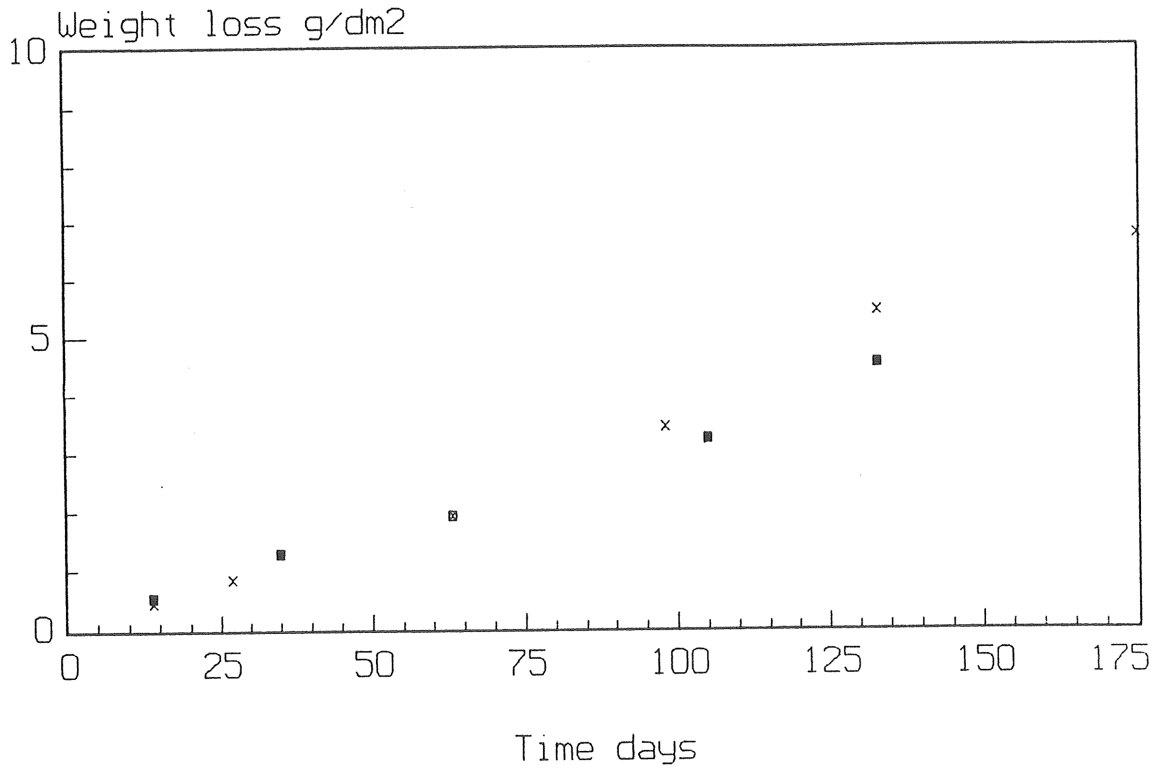

Figure 9.24 Weight loss as a function of time at (x) 15 mg HCO_3^- l^{-1} and (■) 100 mg HCO_3^- l^{-1}, water velocity 0.01 m s^{-1}.

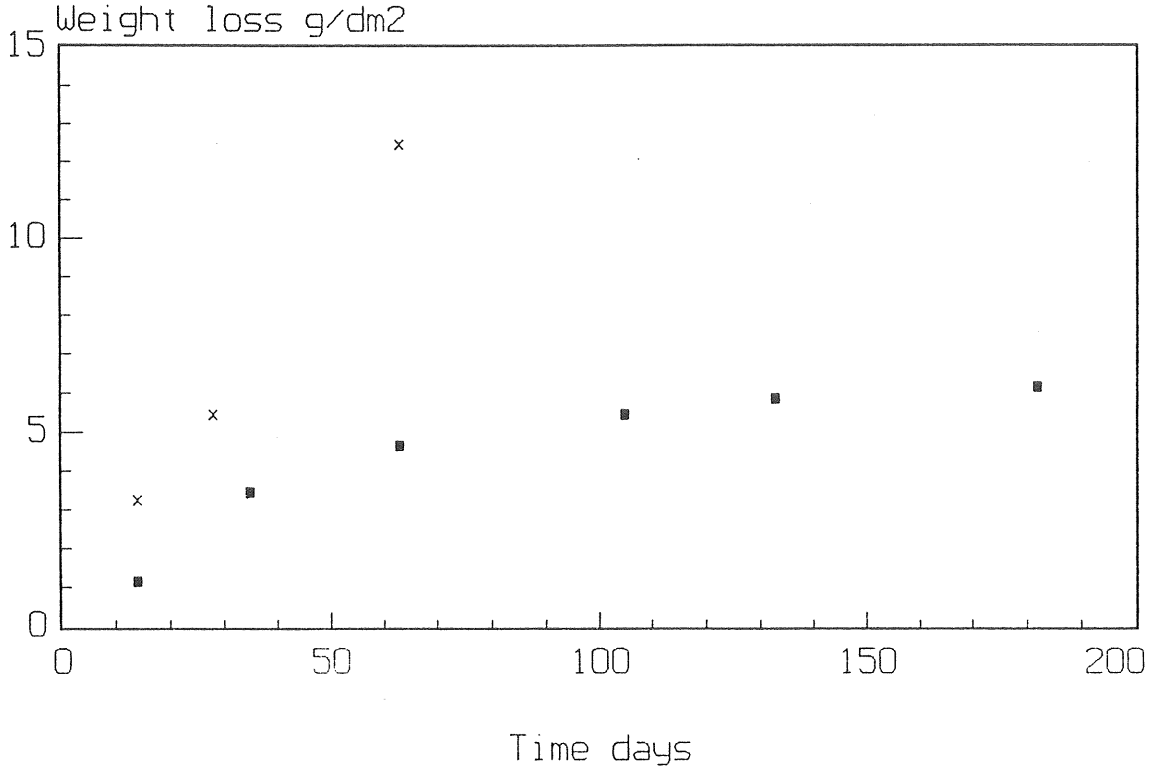

Figure 9.25 Weight loss as a function of time at (x) 15 mg HCO_3^- l^{-1} and (■) 100 mg HCO_3^- l^{-1}, water velocity 0.7 m s^{-1}.

Precipitation of $FeCO_3$ as well as $CaCO_3$ and phosphate compounds were found to be dependent on the water velocity.

9.6 Influence of organic matter on iron corrosion

In order to study the importance of the molecular weight of organic matter for complex formation and corrosion, tests were done on waters in which the organic matter and molecular weight distribution was varied. The variations were made in raw water from a waterworks by different treatment of the same type of raw water or by further treatment of an already treated water. The molecular weight distribution of the organic matter was characterised by gel filtration (Appendix A).

Two types of gel were used, Sephadex G-25 which fractionates the molecular weight range at 1000-5000 and Sephadex G-50 which fractionates 1000-30 000. The eluted water from the gel filtration column was also divided into fractions. Each fraction was analysed by ultra violet spectrophotometry at 254 nm. The iron content of the fractions was also analysed.

The molecular weight distribution carried out by gel filtration is shown in Figures 9.26 - 9.29. The dissolved iron was not always found in the fractions containing the greatest amount of organic matter. Iron formed complexes with rather large molecules and was eluted before the largest peak of the distribution of organic matter.

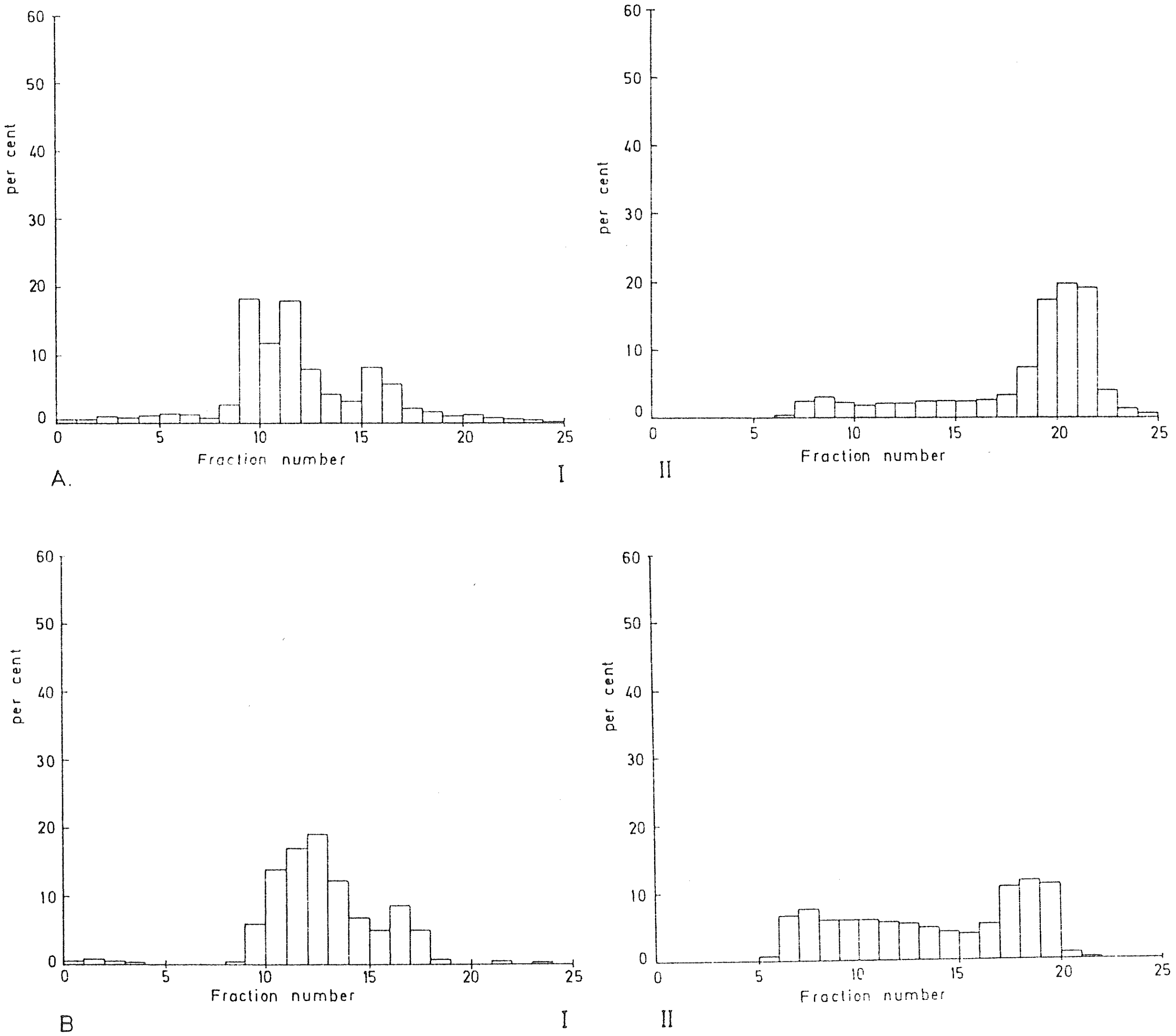

Figure 9.26 Distribution of A) organic matter analysis as UV and B) Fe concentration in different molecular weight fractions after gel filtration of rapid sandfiltered water. I) G-25, II) G-50.

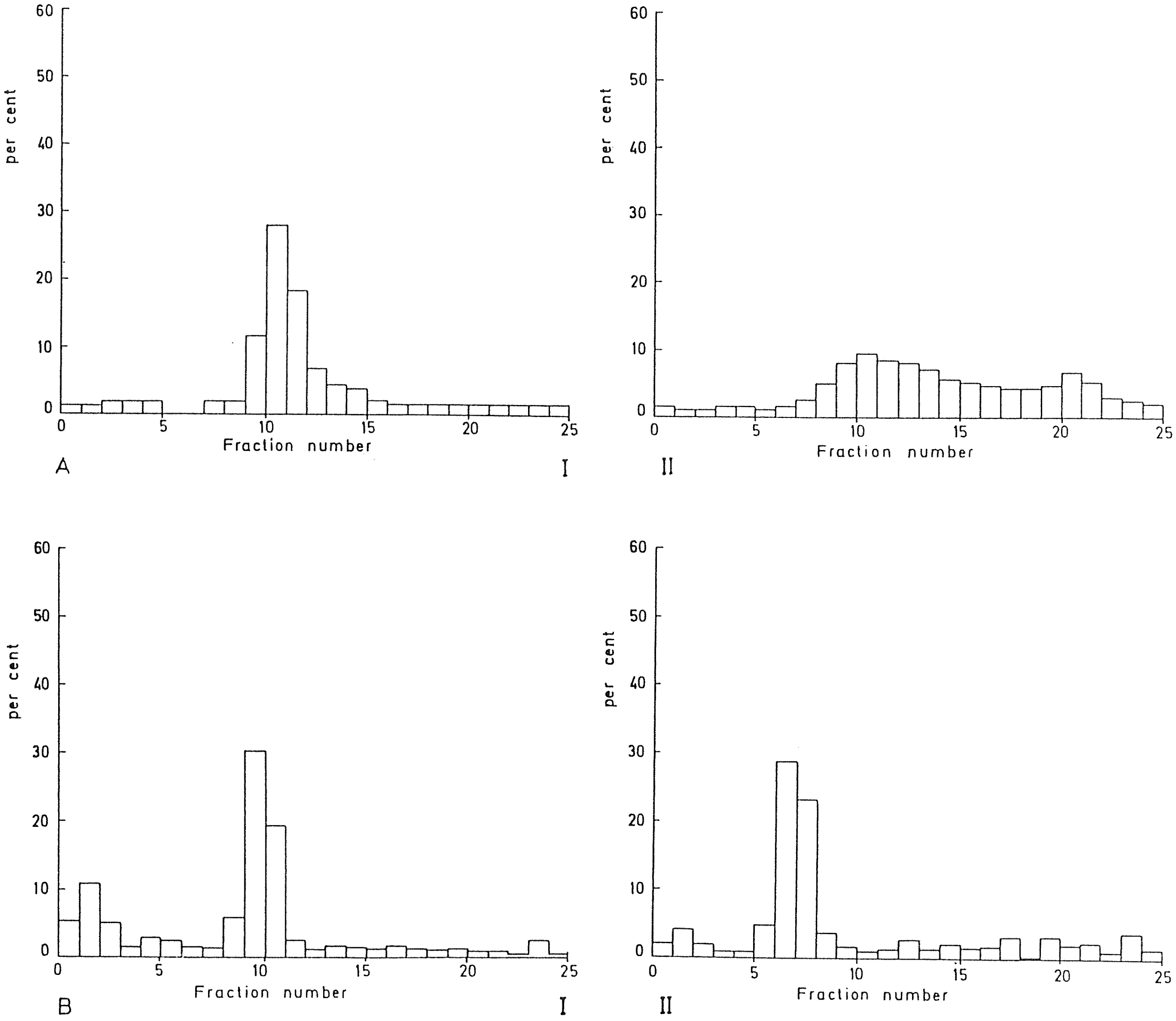

Figure 9.27 Distribution of A) organic matter analysis as UV and B) Fe concentration in different molecular weight fractions after gel filtration of slow sandfiltered water. I) G-25, II) G-50.

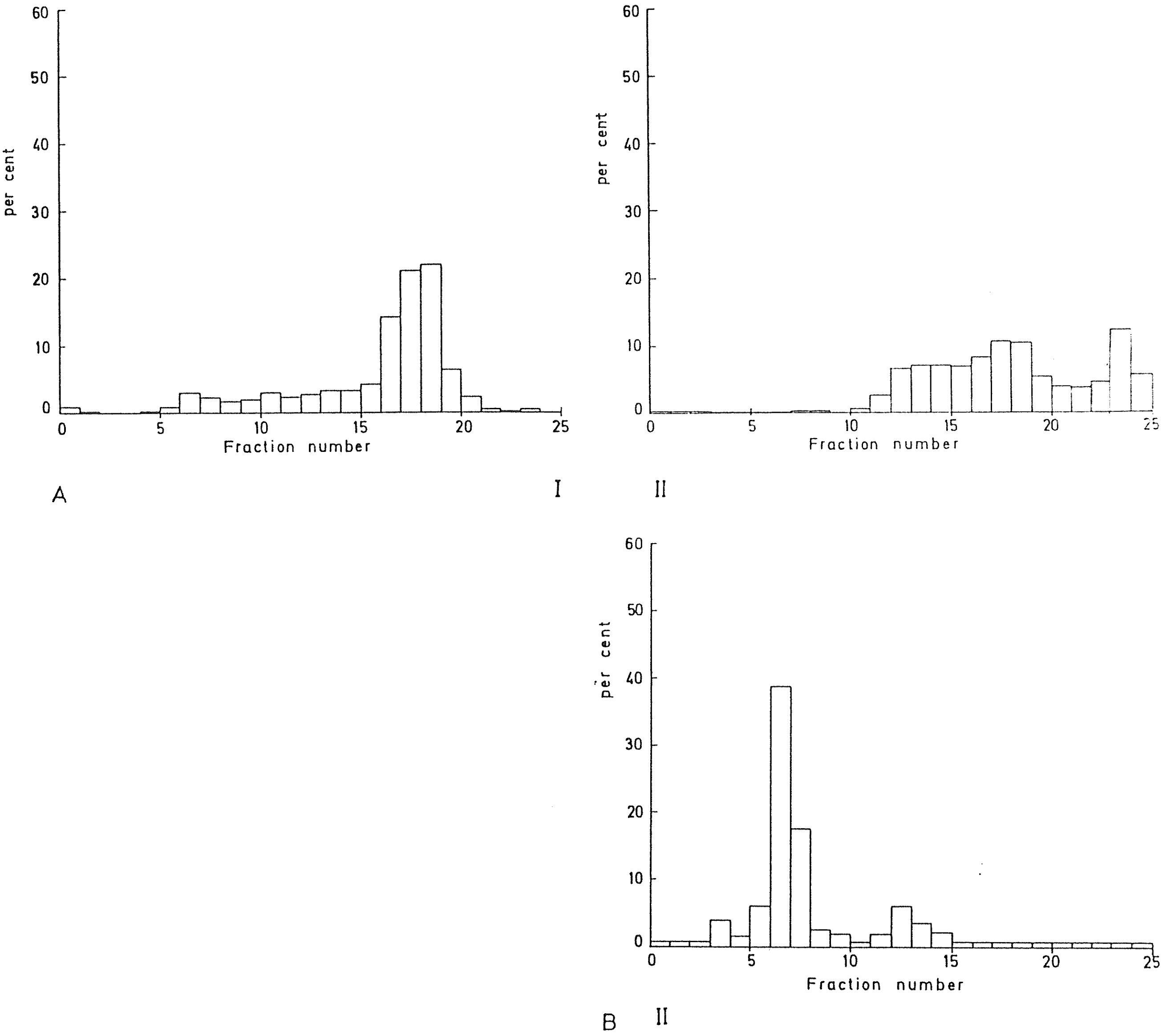

A I II

B II

Figure 9.28 Distribution of A) organic matter analysis as UV and B) Fe concentration in different molecular weight fractions after gel filtration of chemically precipitated water. I) G-25, II) G-50.

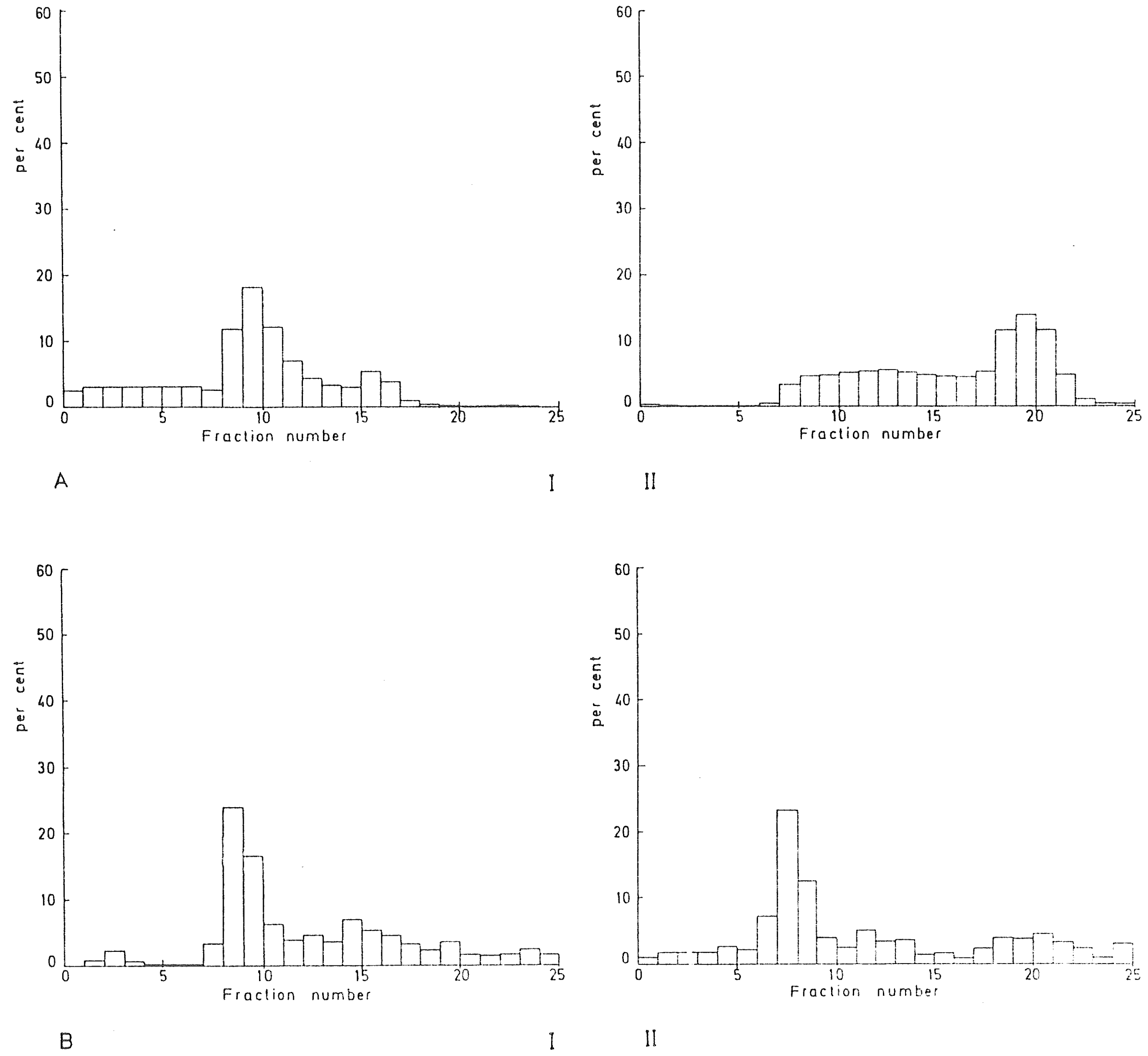

Figure 9.29 Distribution of A) organic matter analysis as UV and B) Fe concentration in different molecular weight fractions after gel filtration of ozone treated water. I) G-25, II) G-50.

The weight loss of coupons after 60 days for waters treated in different ways is shown in Figure 9.30. Figure 9.30 indicates a low corrosion rate for the water that was sand filtered rapidly.

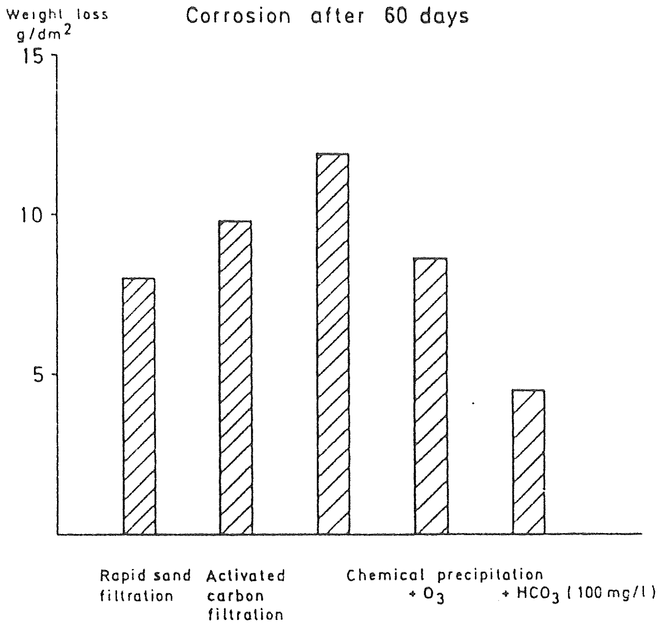

Figure 9.30 The influence of water treatment processes on iron corrosion.

Figure 9.31 is another example where the weight loss was also lowest for the rapid sand filtered water.

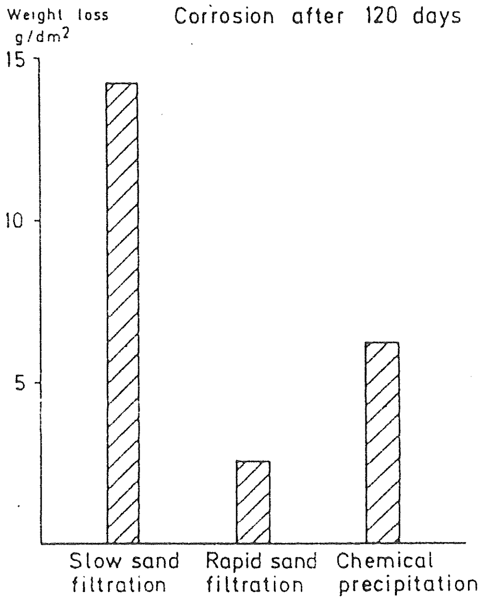

Figure 9.31 The influence of three treatment methods on iron corrosion.

Chemical precipitation, ozone treatment, activated carbon and slow sand filtration, all either change the molecular-size distribution towards smaller molecules or result in a complete removal of organic matter. Iron complex formation is more likely when there are large molecules, the consequence will then be a reduction in iron(II) complexes. After a rapid sand filtration of water it still contains all the original organic matter, which makes it possible for a high degree of complex formation.

The corrosion rigs and iron test pipes, placed in several different water works, were all supplied with waters containing various organic compounds in varying concentrations. The significance of this cannot be explicitly stated, since other species were also present in different concentrations.

During the tests it was found that an increased degree of water purification does not necessarily lead to a decrease in the corrosion rate.

As a conclusion it can be stated that organic matter has an indirect influence on corrosion, by complex formation with free iron. This complex formation changes the precipitation rate and the structure of precipitations in the protective layer. Complex formation retains the iron as iron(II) and forms Fe(II)-organic complexes instead. The iron(II) may precipitate as $FeCO_3$ if carbonic acid species are present and if the complexes are broken up. If calcium is also present in the water then $CaCO_3$ can precipitate without competition from $FeCO_3$ precipitation and without any FeOOH precipitation in the deposits. The precipitation rate decreases and the degree of crystallinity increases when organic matter is present in the water, which results in a layer of $CaCO_3$ with protective properties.

10. DISCUSSION OF IRON CORROSION

10.1 Comparison between proposed model and results

In this section the study results are interpreted using the proposed corrosion prevention model.

The results of the tests with waters containing a low content of total carbonic acid species at different pH confirms the assumptions in Case I. In this case the precipitation of FeOOH was predicted without any formation of protective layers on the metal surface. The result was a high corrosion rate.

In Case II the influence of a high content of total carbonic species was tested at various pH values. When the pH was under six and the water thus had a high content of carbonic acid the corrosion rate was high. This observation was not mentioned in the model. However, in accordance with the model Fe_3O_4 was found on the surface of the coupons and pipes. At pH 7.5 and 100 mg HCO_3^- l^{-1}, $FeCO_3$ was precipitated and formed a protective layer which resulted in a rapid decrease in the corrosion rate.

At pH > 9 the model predicts the formation of FeOOH which provides less protection due to the increased oxidation of Fe(II). But in the experiments the corrosion rate was lower at pH 9.5 and 100 mg HCO_3^- l^{-1} than at pH 8.5 with the same content of total carbonic acid. This is because at pH 8.5 and 100 mg HCO_3^- l^{-1}, the buffer capacity will be at a minimum which results in a high corrosion rate.

Case III corresponds to a water which contains calcium and hydrogen carbonate in various concentrations at different pH. In the tests, and as predicted by the model, $CaCO_3$ was precipitated under saturated conditions (pH 8.5, 35 mg Ca^{2+} l^{-1} and 100 mg HCO_3^- l^{-1}). In the experiments the corrosion rate was low. Precipitation of $CaCO_3$ was found only in tests with a high water velocity (0.7 m s^{-1}) and only on the top of deposits. These observations agree with the model. Another result of interest was that $CaCO_3$ precipitation provides an effective protection in waters containing chloride or sulphate.

The effect of different water velocities can be summarised as follows:

- High water velocity (0.7 m s^{-1}) leads to a high corrosion rate when the chemical conditions for effective protective precipitations are lacking.

- A low corrosion rate is found under high velocity conditions when $FeCO_3$, $CaCO_3$ or phosphate compounds can be formed.

- Low water velocity (0.01 m s^{-1}) causes a low corrosion rate without any specific initial corrosion period.

- In stagnant water $FeCO_3$ may precipitate. Precipitation of $CaCO_3$ or phosphates does not normally occur.

Based on the model as well as experiments the following conclusions can be reached:

- An effective protective layer which prevents corrosion consists of $FeCO_3$ or $CaCO_3$ (precipitated at saturation point) which is formed in waters with a pH less than 8 rather than above 8.

- A relatively high content of total carbonic acid, between pH > 6.5 and < 8, leads to iron carbonate precipitation with a high iron(II) content. This results in a very low corrosion rate.

- Increased pH close to the metal surface due to OH^- production causes oxidation of iron(II) to iron(III) which results in a high degree of iron(III) in the deposits and a high corrosion rate.

The corrosion process can be minimised by the precipitation of compounds which form effective protective layers. The morphology and structure of the protective layers should have properties which prevent species in the water from passing through the precipitation and causing an attack on the metal surface.

Corrosion usually proceeds in one of three ways:

(a) Corrosion which increases with time.

(b) Corrosion which decreases after a certain period of time.

(c) Corrosion which slows and stops after a period of time.

The corrosion type that will predominate depends on both water composition and water velocity. If any parameter should change, then the initial corrosion time or the corrosion rate will change. In a water with a high water velocity under such circumstances that $CaCO_3$ or $FeCO_3$ precipitates, corrosion (c) is found, but if the water velocity decreases the corrosion will follow (b). Corrosion (b) also occurs when the pH is increased due to the formation of more porous $CaCO_3$ precipitations or of other precipitations such as FeOOH.

The water velocity controls the transport of species to and from the metal surface. In a thin layer close to the metal surface there is no movement of water due to the effect of the laminar zone. In the laminar zone the transfer of species takes place by diffusion only. Corrosion is limited by oxygen diffusion through the water and through deposits to the metal surface. Diffusion is possible only when the deposits are porous. The correct water velocity and chemical conditions must be obtained to avoid corrosion and form effective protective layers.

11. CONCLUSIONS AND PRACTICAL ASPECTS

This study has concentrated on the uniform corrosion of copper and iron in drinking water pipes, although other materials such as cement, zinc, polyethylene and PVC may also be present in a distribution network.

11.1 Conclusions

(a) Copper

- pH probably has the greatest effect on Cu corrosion in a drinking water system. Cu corrosion is minimal above pH 8.5 and increases dramatically below pH 7.0.
- Carbonic species induce corrosion at neutral pH, but have no effect at high pH. However, as neutral pH values are usual for untreated drinking water in Sweden, carbonic species concentration may in many cases be critical for copper corrosion.
- Ca, Cl and SO_4 were shown to have a minimal effect on Cu corrosion.
- The presence of organic material may reduce Cu corrosion on a fresh Cu surface due to the formation of a protective organic film. On the other hand, small organic molecules, formed during ozonation, may increase corrosion.
- The best protective layers consist of Cu_2O and CuO, and these are formed at neutral and high pH. A less stable protective layer of $CuOH(CO_3)_{0.5}$ is formed at a high total carbonic species concentration and at a neutral pH. In hard water a $CaCO_3$ precipitation may form which is not thought to provide protective properties.

(b) Iron

- Fe corrosion increases both at high and low pH values and therefore a relatively neutral pH is required to minimise corrosion.

- The presence of carbonic species result in a decrease in Fe corrosion. The slowest corrosion rate found in this study was at pH 7.5 and 100 mg l^{-1} HCO_3.
- The presence of calcium aids in the formation of protective $CaCO_3$ layers in carbonate rich water. This was evidenced in Scanning Electron Micrographs.
- Chloride and sulphate initiate pitting corrosion which results in pipe damage rather than water quality problems. It is therefore important to induce the formation of protective layers by the addition of calcium and carbonic species.
- A high water velocity is required for satisfactory protective layer formation.
- As opposed to copper, iron forms colloidal organic complexes. Therefore treatment processes which reduce the molecular weight distribution also effectively reduce Fe corrosion.

11.2 Guidelines

The following tables provide guidelines for a preferred water composition in drinking water to be fed through mains consisting entirely of either copper (Table 11.1) or iron (Table 11.2).

Table 11.1 Preferable water composition for copper pipes to prevent uniform corrosion.

Parameter	Recommendation
pH	8.5-9.0
Total content of carbonic species	< 20 mg HCO_3^- l^{-1}
Calcium	< 10 mg Ca^{2+} l^{-1}
Chloride	as low as possible
Sulphate	as low as possible
Organic matter	more research required
Inhibitors	not effective

Table 11.2 Preferable water composition for iron pipes.

Parameter	Recommendation
pH	$6.5 < pH < 8$
Total content of carbonic species	> 60 mg HCO_3^- l^{-1}
Calcium	20-40 mg Ca^{2+} l^{-1}
Chloride	as low as possible
Sulphate	as low as possible
Organic matter	more research required
Inhibitors	not in stagnant water

In a practical situation one may be obliged to make a decision and provide recommendations for a water composition which minimises corrosion in combined copper and iron pipe systems. It should be stressed that pH is always important, a soft unbuffered water is detrimental to both Cu and Fe pipe systems and therefore it is always desirable to add carbonic species as a pH control. Table 11.3 is a compromise based on theoretical considerations and the findings of this study indicate that this water composition retards corrosion for a complete distribution system. This recommendation has been implemented at local municipal waterworks and a certain degree of reduction in corrosion-related water quality problems has been found.

Table 11.3 Water composition preferable for a combined copper and iron pipe system.

Parameter	Recommendation
pH	8.0-8.5
Total content of carbonic species	> 60 mg HCO_3^- l^{-1}
Calcium	15-30 mg Ca^{2+} l^{-1}

11.3 Recommendations for future research

- PVC and polyethylene pipes are becoming increasingly popular in the drinking water system. Although they have no direct effect on corrosion, associated biofilms may affect Cu and Fe pipes in the same network.
- Concrete pipes greatly increase pH and have been shown to cause corrosion in subsequent Fe pipes. Further research could focus on measures to reduce this pH change such as carbonic species control or pipe lining.
- It is important to control the formation of $CaCO_3$ protective layers in Fe pipes and therefore further studies could optimise this process.
- It is unknown whether the recommended corrosion prevention measures have an effect on the final disinfection process.
- This study has only touched the surface of the effect of organic material on the corrosion process. A long term study would consider organic biofilms in pipe networks. The effect of Fe and Cu complexation by humic substances in the pipe network could be analysed using established methods from speciation studies. It is also unknown how different treatment processes affect organic substance induced corrosion in the pipe network. The effect of inorganic substances is certainly better understood at this time.
- Although disinfection effectively reduces bacterial populations, micororganisms are present in the pipe network and may have a significant effect on corrosion.

LIST OF SYMBOLS

A, B, C, n	constants	(eq. 7.47 and 7.48)
AI	Aggressiveness Index	(eq. 7.43)
β	buffer capacity	(eq. 7.12 and 9.1)
C	concentration in water	(eq. 7.47)
C*	saturation concentration	(eq. 7.47)
CCPP	Calcium Carbonate Precipitation Potential	(eq. 7.46)
DFI	Driving Force Index	(eq. 7.44)
d	hydraulic diameter	(eq. 7.11)
δ	thickness of laminar layer	(eq. 7.12)
δ	standard deviation	(App. B)
f	friction factor	(eq. 7.12)
f_I	correction factor dependent on ionic strength	(eq. 7.36)
G-25, G-50	gel filtration media	
I	ionic strength	(eq. 7.25 and 9.2)
K or K_n	rate constant	
K_s	solubility product	
LI	Langlier's Index	(eq. 7.40)
ME	Momentary Excess Index	(eq. 7.45)
O	$CaCO_3$ surface area	(eq. 7.36)
p_{O_2}	partial pressure, oxygen	(Fig. 7.23)
Re	Reynold's number	(eq. 7.11)
RI	Ryznar Index	(eq. 7.42)
S	surface area	(eq. 7.47)
V or V_F	water velocity	(eq. 7.11, 7.12 and Fig. 7.26)
ν	viscosity	(eq. 7.11 and 7.12)
$\bar{x}$	mean value	(App. B)
Y	value for corrosion attack or not	(eq. 7.48)

REFERENCES

Ailor, W.H. (1971): Handbook on Corrosion Testing and Evaluation, John Wiley & Son Inc., New York.

Ainsworth, R.G., Calcutt, T., Elvidge, A.F., Evins, C., Johnson, D., Lack, T.J., Parkinson, R.W. and Ridgway, J.W. (1981): A Guide to Solving Water Quality Problems in Distribution Systems, Technical Report TR 167, WRC, England.

Andersson, R. and Berry, D. (1981): Regulating Corrosive Water, Wat. Res. Rec. 17(6), 1571-1577.

ASTM (1973): Standard Recommended Practice for Preparing, Cleaning, and Evaluating Corrosion Test Specimens, G1-72, American National Standard G80 1.

Axt, G. (1961): Die Kohlensäure - Gleichgewichte in Theorie und Praxis, Vom Wasser 28, 208-226.

Baylis, J.R. (1926): Factors other than Dissolved Oxygen Influencing the Corrosion of Iron Pipes, Ind. Eng. Chem. 18, 370-380.

Baylis, J.R. (1953): Cast-Iron Pipe Coatings and Corrosion, J. AWWA 45, 807-900.

Bendixen, S. and Hydén, H. (1981): Underhålls- och förnyelseplanering för kommunala vattenledningsnät (Maintenance and renewal plans for municipal water distribution network), Swedish Council for Building Research (BFR), Research project 810817-9, Stockholm, Sweden.

BFR (1981): Förebygg vattenskador från ledningssystem (Prevent damages caused by water from the distribution network), Swedish Council for Building Research (BFR), Publication G14:1981, Stockholm, Sweden.

Bigham, J.H. and Tuovinen, O.H. (1985): Mineralogical, Morphological and Microbiological Characteristics of Tubercles in Cast Iron Water Mains as Related to their Chemical Activity, Planetary Ecology (D.E. Caldwell, J.A. Brierley and C.L. Brierly, ed.), van Nostrand, Reinhold Company, New York.

Caldwell, D.H. and Lawrence, W.B. (1953): Water Softening and Conditioning Problems, Ind. Eng. Chem. 45, 535-548.

Campbell, H.S. (1954): A Natural Inhibitor of Pitting Corrosion of Copper in Tap-Waters, J. Appl. Chem. 4 (1954), 633-647.

Campbell, H.S. and Turner, M.E.D. (1980): The Influence of Trace Organics on Scale Formation and Corrosion, BNF Metals Technology Centre, MP 596, Oxfordshire, England.

Campbell, H.S. (1971): Corrosion, Water Composition and Water Treatment, Wat. Tret. and Exam. 20, 11-34.

Cornwell, F.J., Wildsmith, G. and Gilbert, P.T. (1973): Pitting Corrosion in Copper Tubes in Cold Water Service, Br. Corros. J. 8, 202-209.

Costello, J.A. (1969): The Corrosion of Metals by Microorganisms, A Literature Survey, Int. Biotechn. Bull. 5, 101-118.

Cox, S.A. and Dillon, B.I. (1980): Cuprosolvency in Adelaide Water, Silver Jubilee Conference, Australian Corrosion Association, Adelaide, Australia.

CRC Handbook of Chemistry and Physics, 69th Ed. (1988). Weast R C et al. Editor, Boca Raton, Florida, USA.

Cruse, H., von Franquê, O. and Pomeroy, R.D. (1985): Corrosion of Copper in Potable Water Systems, Chapter 5, from Internal Corrosion of Water Distribution Systems, Cooperative Research Report, AWWA Research Foundation, USA, and DVGW - Forschungsstelle am Engler-Bunte-Institut der Universität Karlsruhe, Germany.

DeMartini, F.E. (1938): Corrosion and the Langlier Calcium Carbonate Saturation Indexes, J. AWWA 30, 85-111.

Dye, J.F. (1952): Calculations of the Effect of Temperature on pH, Free Carbon Dioxide and the Three Forms of Alkalinity, J. AWWA 44, 356-372.

Eistrat, K. and Thorên, A. (1980): Mikrobiell korrosion - en litteraturöversikt (Microbiological corrosion - a literature survey), KI Rapport 1980:9, Korrosionsinstitutet, Sweden (Swedish Corrosion Institute).

Eliassen, R., Pereda, C., Romeo, A.J. and Skrinde, R.T. (1956): Effects of pH and Velocity on Corrosion of Steel Water Pipes, J. AWWA 48, 1005-1018.

Elzenga, C.H.J. and Boorsma, H.J. (1974): Corrosion of Copper Pipes in Various Types of Drinking Water, International Committee on Corrosion and Protection of Underground Pipelines, Brighton, England.

Elzenga, C.H.J. (1986): Corrosion by Mixing Waters of Different Qualities, 16th IWSA Congress, Rome, Italy.

Elzenga, C.H.J. and von Franquê, O. (1986): Praxiserfahrungen beim Einsatz vom Kupferrohren bei der Trinkwasserinstallation, Gwf-Wasser/Abwasser 127, 5, 209-215.

Feigenbaum, C., Gal-Or, L. and Yahalom, J. (1978a): Microstructure and Chemical Composition of Natural Scale Layers, Corrosion 34, 65-70.

Feigenbaum, C., Gal-Or, L. and Yahalom, J. (1978b): Scale Protection Criteria in Natural Waters, Corrosion 34, 133-137.

von Franqué, O. (1968): Uber Bedeutung, Umfang und Stand der Untersuchungen des Lochfrasses bei Korrosion (On signification, scope and situation of examined pittings caused by corrosion), Werkst. und Korr. 19, 5, 377-384.

von Franqué, O., Gerth, D. and Winkler, B. (1972): Einzelergebnisse aus laufenden Untersuchungen zum Verhalten von Kupferrohren in Trink- und Brauchwässern und Darstellung des neusten Standes der Gesamtschadensentwicklung von Kupferrohren (Some results in the progressed examination around conditions for copper pipes in drinking water compared to the new aspects around the development of complete damage of copper pipes), Werkst. und Korr. 23, 4, 241-246.

von Franqué, O., Gerth, O. and Winkler, B. (1975): Ergebnisse von Untersuchungen an Deckschickten in Kupferrohren (Results from the investigation of protective layers on copper pipes), Werkst. und Korr. 26, 4, 255-258.

Gilbert, P.T. (1966): Dissolution by Fresh Waters of Copper from Copper Pipes, Wat. Tret. and Exam. 15, 165-186.

Haase, L.W. (1935): Korrosion und Schutzschichtbildung bei Kaltwasserleitungen aus Gusseisen (Corrosion and protective layer formation in cold water system of cast iron), vom Wasser 10, 186-196.

Haase, L.W. (1952). Deckschichten- und Schutzschichtenbildung (Formation of deposits and protective layers), Werkst. und Korr., 198-205.

Hall, E.S. and Smith, I.G. (1974): Rusty Water Cured by Oxygen Injection, Wat. Serv. 78, 232-234.

Haupt, H. (1939/40): Natürlicher Korrosionsschutz in Leitungsrohren (Natural corrosion protection in distribution pipes), vom Wasser 14, 255-270.

Hedberg, T. (1982): Water Quality in the Distribution Network, 14th IWSA Congress, Zürich, Switzerland.

Hedberg, T. and Johansson, E. (1986a): Alkaline Filters for Private Wells, Wat. Qual. Bull. 11, 206-211.

Hedberg, T. and Johansson, E. (1986b): Protection of Pipes Against Corrosion, 16th IWSA Congress, Rome, Italy.

Hilburn, R.D. (1983): Modeling Copper Corrosion in Water with Low Conductivity by using Electrochemical Techniques, J. AWWA 75, 149-154.

Hoffmann, M.R. (1981): Thermodynamic, Kinetic, and Extra-Thermodynamic Considerations in the Development of Equilibrium Models for Aquatic Systems, Env. Scien. & Techn. 15, 345-353

Hoover, C.P. (1938): Practical Application of the Langlier Method, J. AWWA 30, 1802-1807.

Ives, D.J. and Rawson, A.E. (1962): Copper Corrosion, 1. Thermodynamic Aspects, J. Electrochem. Soc. 109, 6, 447-451.

Jobin, R. and Gosh, H.M. (1972): Effect of Buffer Intensity and Organic Matter on the Oxygenation of Ferrous Iron, J. AWWA 64, 590-595.

Johansson, E. and Hedberg, T. (1988): Om korrosion på järn, koppar och zink i sura vatten (On corrosion of iron, copper and zink in acid waters), Chalmers Univ. of Technology, Dept. of Sanitary Engineering, Publication 2:88, Göteborg, Sweden.

Kegel, J. (1942): Schutzschichtbildung bei sehr weichen Wässern (Protective layers formation in very soft waters), GWF Wasser Abwasser 45/46, 518-522.

Kelley, K.U. and Andersson, C.T. (1935): Contributions to the Data on Theoretical Metallurgy, IV. Metal Carbonates - Correlations and Applications of Thermodynamic Properties, Bur. Mines Bull. 384, 1-67.

Kirby, P.C. (1978): Internal Corrosion and Loss of Strength of Iron Pipes, WRC Conference Water Distribution Systems, Oxford, England.

van der Kooij, D. and Zoeteman, B.L.J. (1979): Stability Requirements for Drinking Waters, Aqua 4, 31-32.

Kooijmans, J. (1938): Korrosion und Schutzschichtbildung durch Leitungswasser (Corrosion and protective layers formation in drinking water), DGW 81, 611-633.

Kristiansen, H. (1977): Corrosion of Copper by Water of Various Temperatures and Carbon Dioxide Contents, Werkst. und Korr. 28, 11, 743-748.

Kristiansen, H. (1981): Korrosjon og korrosjonsbekjempelse i sanitaeranlegg (Corrosion and corrosion prevention in distribution system), Norsk institutt for vannforskning, Temahefte 5.

Kristiansen, H. (1982): Corrosion of Copper by Soft Water with Different Content of Humic Substances and Various Temperatures, Vatten 38, 2, 181-188.

Kuch, A. (1988): Investigations of the Reduction and Re-oxidation Kinetics of Iron(III) Oxide Scales formed in Waters, Corr. Science 28(3), 221-231.

Kuch, A. and Sontheimer, H. (1986): Instationäre Korrosion - Eine Ursache der Rostwasserbildung in Wasserteilungsnetzen (Instationary corrosion - one cause to rusty water in distribution systems), Gwf-Wasser/Abwasser 127, 621-629.

Kölle, W. (1977): Corrosion in Drinking Water System, 6th Eurocorr. Congr. on Metallic Corrosion, London, England.

Kölle, W. and Sontheimer, H. (1977): Untersuchungen zur Schutzschichtbildung in Gussrohren (Investigation of protective layers formation in cast iron pipes), vom Wasser 49, 277-294.

Kölle, W. and Rösch, H. (1978): Korrosionsvorgänge in Gussrohren (Corrosion process in cast iron pipes), vom Wasser 51, 161-168.

Langlier, W.F. (1936): The Analytical Control of Anti-Corrosion Water Treatment, J. AWWA 28, 1500-1521.

Larson, T.E. (1960): Loss in Pipeline Carrying Capacity Due to Corrosion and Tuberculation, J. AWWA 52, 1263-1270.

Larson, T.E. (1966): Chemical Control of Corrosion, J. AWWA 58, 354-362.

Larson, T.E. and Buswell, A.M. (1942): Calcium Carbonate Saturation Index and Alkalinity Interpretations, J. AWWA 34, 1667-1678.

Larson, T.E. and King, R.M. (1954): Corrosion by Water at Low Flow Velocity, J. AWWA 46, 1-9.

Larson, T.E., Skold, R.V. and Savinelli, E. (1956): Tuberculation of Tar-Coated Cast Iron in Great Lakes Water, J. AWWA 48, 1274-1278.

Larson, T.E. and Skold, R.V. (1957): Corrosion and Tuberculation of Cast Iron, J. AWWA 49, 1294-1302.

Larson, T.E. and Skold, R.V. (1958): Current Research on Corrosion and Tuberculation of Cast Iron, J. AWWA 50, 1429-1432.

Lee, S.H., O'Connor, J.T. and Banerji, S.K. (1980): Biologically Mediated Corrosion and its Effects on Water Quality in Distribution Systems, J. AWWA 72, 636-645.

Legrand, L. and Leroy, P. (1984): Influence des elements majeurs et de certains elements mineurs sur la corrosite des eaux vis-a-vis de metaux ferreux (Influence of important parameters and parameters with less importance for corrosity of waters opposite the iron metal), 15th Congress IWSA, Tunis, Tunisia.

Liao, M.Y. and Randtke, S.J. (1985): Removing Fulvic Acid by Lime Softening, J. AWWA 77, 78-88.

Lihl, F. and Klamet, H. (1969): Zur Frage des Lockfrasses bei Kupferrohren in Trinkwasserleitungen (Regarding the pitting corrosion on copper pipes in drinking water distribution system), Werkst. und Korr. 20, 2, 108-118.

Linder, M. (1979): Punktfrätning av Typ III i kopparrör - en förstudie (Type III Pitting corrosion of copper pipes - an introductory study), Swedish Council for Building Research (BFR), Research project 780028-7, Stockholm, Sweden.

Linder, M. and Lindman, E.K. (1982): Undersökning av punktfrätning Typ III i kopparrör (Examination of Type III pitting corrosion of copper pipes), Swedish Council for Building Research (BFR), Research project 791011-3, Stockholm, Sweden.

Ljunggren, O. (1989): Gothenburg water and sewage works. Personal communication.

Lucey, V.F. (1967): Mechanism of Pitting Corrosion of Copper in Supply Waters, Br. Corros. J. 2, 175-185.

Lucey, V.F. (1972): Developments Leading to the Present Understanding of the Mechanism of Pitting Corrosion of Copper, Br. Corros. J. 7, 36-41.

Lucey, V.F. (1974): Pitting Corrosion of Copper in Supply Water, Summary Report, BNF Metals Technology Centre, Oxfordshire, England.

Lucey, V.F. (1975): Lochkorrosion von Kupfer in Trinkwasser (Pitting corrosion on copper in drinking water), Werkst. und Korr. 26, 3, 185-192.

Mattsson, E. (1980): Corrosion of Copper and Brass: Practical Experience in Relation to Basic Data, Br. Corros. J. 15, 6-13.

Mattsson, E. (1988): Counteraction of Pitting in Copper Water Pipes by Bicarbonate Dosing, Werkstoffe under Korrosion 39, 499-503.

Mattsson, E. and Fredriksson, A.-M. (1968): Pitting Corrosion in Copper Tubes - Cause of Corrosion and Counter-Measures, Br. Corros. J. 3, 246-257.

McCauley, R.F. (1960): Controlled Deposition of Protective Calcite Coatings in Water Mains, J. AWWA 52, 1386-1396.

McClanahan, M.A. and Mancy, K.H. (1974): Effect of pH on Quality of Calcium Carbonate Film Deposited from Moderately Hard and Hard Water, J. AWWA 66, 49-53.

Merill, D.T. and Sanks, R.L. (1977a), (1977b) and (1978): Corrosion Control by Deposition of $CaCO_3$ Films; Part 1 - A Practical Approach for Plant Operators, Part 2 - A Practical Approach for Operators, Part 3 - A Practical Approach for Plant Operators, J. AWWA 69 (1977), 592-599, 634-640, J. AWWA 70 (1978), 12-18.

Meyer, E. (1981): Gesetzmässigheiten des Eintrags von Schwermetallen in das Trinkwasser durch Rohrwerkstofte bei underschiedlicher Wasserbeschaftenheit (The legality to insert heavy metals in drinking water from material in distribution system influenced by different water composition), Schr.-Reihe Verien WaBoLu 52, 9-30.

Milette, J.R., Hammonds, A.F., Pansing, M.F., Hansen, E.L. and Clark, P.J (1980): Aggressive Water: Assessing the Extent of the Problem, J. AWWA 72, 262-266.

Millero, F.J. (1985): The Effect of Ionic Interactions on the Oxidation of Metals in Natural Waters, Geochem. Cosmo Chim. Acta 49, 547-553.

Nielsen, K. (1980): Dissolution of materials from service pipes and house installations and its sanitary aspects, 13th IWSA Congress, Paris.

Obrecht, M.F. and Pourbaix, M. (1967): Corrosion of Metals in Potable Water Systems, J. AWWA 59, 8, 977-992.

Olson, L.K. and Twardowski, C.J. (1975): $FeCO_3$ VS $Fe(OH)_3$, Precipitation in Water-Treatment Plants, J. AWWA 67, 150-153.

Pankow, J.F. and Morgan, J.J. (1981): Kinetics for the Aquatic Environment, Env. Sci. Tech. 15, 1155-1164.

Pisigan, R.A. and Singley, J.E. (1985): Calculating the pH of Calcium Carbonate Saturation, J. AWWA 77, 83-91.

Pisigan, R.A. and Singley, J.E. (1987): Influence of Buffer Capacity, Chlorine Residual, and Flow Rate on Corrosion of Mild Steel and Copper, J. AWWA 79, 62-70.

Pliefke, E. (1979): Struktur und Wirkungsweise von Inhibitoren der Korrosion des Kupfers in Gegenwart von Sauerstoft (Structure and action of inhibitors on copper corrosion in presence of oxygen), Diss. Univ. Mainz, Germany.

Pourbaix, M. (1969): Recent Applications of Electrode Potential Measurements in the Thermodynamics and Kinetics of Corrosion of Metals, Corrosion 25, 267-281.

Pourbaix, M. (1972): Theoretical and Experimental Considerations in Corrosion Testing, Corr. Scien. 12, 161-190.

Rossum, J.R. and Merill, D.T. (1983): An Evaluation of the Calcium Carbonate Saturation Indexes, J. AWWA 75, 95-100.

Rudek, R. (1979): Untersuchungen zum Einfluss von Natürlichen organischen Wasserinhaltsstoften auf die Vorgänge bei der Korrosion in Trinkwasserinstallationen (Investigation of water with natural organic matter and their influence of corrosion on drinking water systems), Dissertation Univ. Karlsruhe.

Rudek, B., Blankenhorn, R. and Sontheimer, H. (1979): Verzögerung der Eisenoxidation durch natürliche organische Wasserinhaltsstofte und deren Auswirkung auf die Korrosion von schwarzen Stahlrohren (Experiments of iron oxidation in water with natural organic matter and their influence of corrosion on black iron pipes), vom Wasser 53, 133-146.

Rudek, R. and Sontheimer, H. (1976): Einfluss natürlicher Wasserinhaltsstofte auf die Ausfallgeschwindigheit von $CaCO_3$ (Importance of natural organic matter on precipitation rate of $CaCO_3$), vom Wasser 47, 421-431.

Ryder, R.A. (1978): Methods of evaluating corrosion. Prol. AWWA W QTC VI.

Ryder, R.A. and Wagner, I. (1985): Corrosion Inhibitors, Chapter 7, from Internal Corrosion of Water Distribution Systems, Cooperative Research Report, AWWA Research Foundation, USA and DVGW - Forschungsstelle am Engler-Bunte Institut der Universität, Karlsruhe, Germany.

Ryznar, J.W. (1944): A New Index for Determining Amount of Calcium Carbonate Scale Formed by a Water, J. AWWA 36, 472-486.

Sanks, R.L. (1980): Water Treatment Plant Design, For the Practicing Engineer, Ann Arbor Science Publ. Inc., 230 Collingwood, P.O. Box 1425, Michigan, USA.

von Schikorr, G. (1930): Uber das beim Rostvorgang auftretende Eisen(III) hydroxyd (On rust formation especially iron(III) hydroxide), Zeit. An All. Chem. 191, 322-332.

Schock, M.R. (1984): Temperature and Ionic Strength Corrections to the Langelier Index - Revisited, J. AWWA 76, 72-76.

Singley, J.E. (1981): The search for a Corrosion Index, J. AWWA 73, 579-582.

Singley, J.E. and Ahmadi, A. (1985): Pitting and Tuberculation, Chapter 2 from International Corrosion of Water Distribution Systems, Cooperative Research Report, AWWA Research Foundation, USA and DVGW - Forschungsstelle am Engler-Bunte-Institut der Univ. Karlsruhe, Germany.

Singley, J.E. and Lee, T.Y. (1984a): Pipe Loop System Arrangements Corrosion Studies, J. AWWA 76, 77-82.

Singley, J.E. and Lee, T.Y. (1984b): Determining Internal Corrosion Potential in Water Supply Systems, J. AWWA 76, 83-88.

Singer, P.C. and Stumm, W. (1970): The Solubility of Ferrous Iron in Carbonate-bearing Waters, J. AWWA 62, 198-202.

Sjölander, B., Hanaeus, J. and Hedberg, T. (1982): Kartläggning av vattenkvalitetsförändringar i distributionsnät Malmö 1980 (Survey of Water Quality Deterioration in the Distribution Network in the City of Malmö), Chalmers Univ. of Technology, Dept. of Sanitary Engineering, Publication 4:82, Göteborg, Sweden.

Snoeyink, V.L. and Jenkins, D. (1980): Water Chemistry, Ed. by Johan Wiley & Sons, New York, USA.

Sontheimer, H., Kölle, W. and Rudek, R. (1979): Aufgaben und Methoden der Wasserchemie - dargestellt an der Entwicklung der Erkenntnisse zur Bildung von Korrosionsschutzschichten auf Metallen (Determination and analysis methods of water chemistry - from the development and understanding of corrosion protection layer formation on metals), vom Wasser 53, 1-18.

Sontheimer, H., Kölle, W. and Snoeyink, V.L. (1981): The Siderite Model for the Formation of Corrosion-Resistant Scales, J. AWWA 73, 572-579.

Sotkovski, P. (1980): Metallurgisk undersökning av gjutjärnsrör (Metallurgical investigation of cast iron pipes), K110/80 and K98/80, Göteborgs vatten- och avloppsverk, Sweden.

Standard Methods (1987): Standard Methods for the Examination of Water and Wastewater, 17th edition, APHA, AWWA and WPCF, Printed in USA.

Stone, A., Spyridakis, D., Benjamin, M., Ferguson, J., Reiber, S. and Osterhus, S. (1987): The Effects of Short-Term Changes in Water Quality on Copper and Zinc Corrosion Rates, J. AWWA 79, 75-82.

Strohecker, R. (1937): Uber die Bestimmung der Angriftslust von Wässern (On determination of aggresivity of water), vom Wasser 12, 128-134.

Stumm, W. (1956): Calcium Carbonate Deposition at Iron Surfaces, J. AWWA 48, 300-310.

Stumm, W. and Lee, G.F. (1961): Oxygenation of Ferrous Iron, Ind. Eng. Chem. 53, 143-146.

Stumm, W. and Morgan, J.J. (1981): Aquatic chemistry, 2nd Ed. by John Wiley & Sons, New York, USA.

Sunda, W.G. and Hanson, P.J. (1979): Chemical Speciation of Copper in River Water, Chapter 8. Effect of Total Copper, pH, Carbonate and Dissolved Organic Matter, Chemical Modeling in Aqueous System, ACS Symposium Series, American Chemical Society, Washington, D.C., USA.

Sung, W. and Morgan J.J. (1980): Kinetics and Product of Ferrous Iron Oxygenation in Aqueous Systems, Env. Scienc. & Techn. 14, 561-568.

Svensk Byggnorm (SBN 1980), Swedish Building Code, Statens planverks förvaltningssamling, The National Swedish Board of Physical Planning and Building, PFS 1983:2, utgåva 2, Ed. Liber Förlag.

Svensk standard (1987): Abonnemangsklass 3210 Vatten (Swedish Standard Methods (Water)), SS 028112-SS028191.

Svensson, G., ed. (1984): Byggande, drift och förnyelse av kommunala VA-ledningar. (Construction, maintenance and rehabilitation of water and sewage pipes), Report nr 73, Urban Geohydrology Research Group, Chalmers Univ. of Technology, Göteborg, Sweden.

Säfwenberg, U. (1984): Bakgrund - Behov - Medel - Mål (Background - Necessity - Resources - Purpose), från Va-ledningsnät, underhåll och förnyelse (from water and sewage network, maintenance and renewal), Swedish Water and Waste Water Works Association, VAV M46, Stockholm, Sweden.

Theis, T.L. and Singer, P.C. (1974): Complexation of Iron(II) by Organic Matter and Its Effect on Iron(II), Oxygenation, Env. Sci. Tech. 8, 569-595.

Tillmans, J., Hirsch, P. and Weintraud, W. (1927): Die Korrosion von Eisen under Wasserleitungswasser (The corrosion on iron in drinking water), DGW 70, 919-925.

Tronstad, L. and Veimo, R. (1940): J. Preliminary Researchers on the Action of Water on Copper Pipes, J. Inst. Metals 66 (1940), 17-33.

Tuovinen, O.H., Button, K.S., Vuorinen, A., Carlson, L., Mair, D.M. and Yut, L.A. (1980): Bacterial, Chemical and Mineralogical Characteristics of Tubercles in Distribution Pipe Lines, J. AWWA 72, 626-635.

Uusitalo, E. and Heinanen, J. (1962): Corrosion of Steel in Soft Waters, Corr. Sci. 2, 281-291.

Wagner, I. (1977): Influence of Water Quality and Water Treatment on Corrosion and Coatings in Steel and Galvanized Steel Tubes, 6th Eurocor. Congr. on Metallic Corrosion, London, England (1977).

Wagner, I. (1980): Korrosionsschutz und Steinverhütung (Corrosion prevention and mineralization), DVGW-Schiftenreihe Wasser 206.

VAV (1979): Allmänna vattenledningsnät, anvisningar för utformning och beräkning. (General water network, Instruction for calculation and design), Swedish Water and Waste Water Works Association, VAV P38, Stockholm, Sweden.

Werner, G. (1976): Untersuchungen zum Korrosionsverhalten feuerverzinkter Installationsrohe in kalten Trinkwässern (Investigation of conditions, corrosion on galvanized pipes in system with cold drinking water), Diss. Engler-Bunte-Institut der Univ. Karlsruhe.

Westlund, L. (1984): Försäkringar - vattenskador och orsaker (Insurance - damages in water pipes and causes), Bygg & Teknik, Vol. 6, 27-30.

Whitman, G.W., Russell, R.P. and Altieri, V.J. (1924): Effect of Hydrogen - Ion Concentration on the Submerged Corrosion of Steel, Ind. Eng. Chem. 16, 665-670.

Vik Arctander, E. and Bjerkelund, E. (1985): Alkalisering av drikkevann, korrosjonskontroll (Adjust of alkalinity and content of calcium in drinking water, corrosion control), NTNF:s utvalg for drikkevannsforskning, Drikkevannsrapport (Drinking Water Report) 12, Oslo, Norway.

Williams, S.M., Ainsworth, R.G. and Elridge, A.F. (1984): A Method of Assessing the Corrosity of Water Towards Iron, WRC, England.

Wranglén, G. (1974): Pitting and Sulfide Inclusions in Steel, Corrosion Science 14.331-349.

Vuorinen, A. Carlson, L. and Tuovinen, O.H. (1985): Surface Characteristics of Tubercle Mass and Graphitic Residue in Cast Iron Water Pipelines, Materials Chem. and Phys. 12, 275-285.

APPENDIX A. MATERIALS AND METHODS

A.1 Laboratory Test Water

A.1.1 Water production

The laboratory test water used in this study was a water containing low concentrations of organic and inorganic species to which different chemicals were added. When the water was produced in this way it was easy to observe the influence on metals from each of the chemicals added and each water composition.

The water was produced as a mixture of deionised drinking water and rapidly filtered water after chemical precipitation at the Lackarebäck waterworks, Göteborg. The concentration of inorganic species in the drinking water was reduced by ion-exchange and the concentration of organic matter was reduced by activated carbon filtration. The treated drinking water was then blended with the rapidly filtered water in a 2:1 ratio. This mixing reduced the frequency of regeneration of the ion-exchangers.

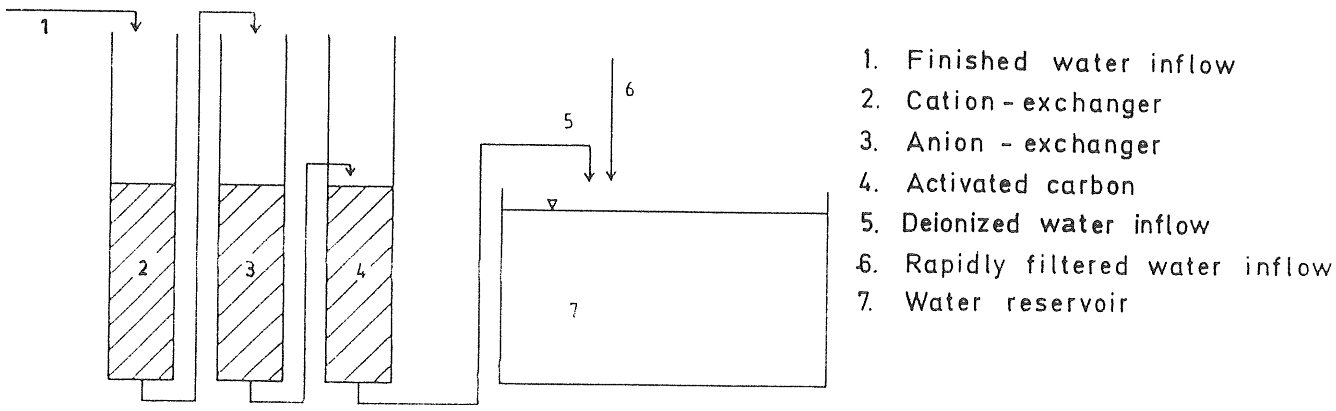

Specifications

Strongly-acid cation-exchanger, 200 l, Duolite C20

Weakly-basic anion-exchanger, 150 l, Duolite A378

Figure A.1 The system for water production.

The amount of water produced was regulated by the water level in the reservoir (Figure A.1). When the level in the reservoir (7) was low, a flow of 260 l min^{-1} (1) was passed through the cation-exchanger (2), then through the anion-exchanger (3) and finally through the activated carbon filter (4) via a mixing chamber into the reservoir. Simultaneously, 85 l min^{-1} of rapidly filtered water (6) flowed into the mixing chamber. When the reservoir was full, an electrical conductor activated magnetic valves and the flow of deionised water and rapidly filtered water stopped.

The water temperature was kept at 15^{0}C by water heating equipment. The water production equipment operated approximately 15 hours per day and four days per week.

After 250 hours of operation the ion-exchangers were regenerated. Regeneration started with back-washing of the beds. The cation-exchanger was regenerated by passing 370 l of 4% hydrochloric acid through the resin bed at 9 m h^{-1}. Afterwards the resin was rinsed with the same volume of water. The anion-exchanger was regenerated by passing 500 l of 4% sodium hydroxide solution through the bed at 6 m h^{-1}. Finally the resin was rinsed with water.

The test waters were produced by adding chemicals directly to the reservoir water. A total of 59 different water qualities were produced in this way. Each test water was stored in a supply tank, and from the tanks the water was fed to the corrosion test systems via membrane hose pumps or by gravity flow.

A.1.2 Water composition

Various amounts of hydrochloric acid or sodium hydroxide were added to the test waters as pH adjusting chemicals. Carbon dioxide, hydrogen carbonate, calcium, chloride and sulphate (in various combinations) were also added. In Tables A.1 and A.2 the water compositions are listed for the laboratory corrosion test systems.

Table A.1 List of water compositions used in laboratory corrosion rigs.

		1	2	3	4	5	6	7	8	9	10	11	12	13	14	15	16	17	18	19	20	21	Base water
pH		7.5	7.5	8.5	8.5	8.5	9.5	9.5	8.5	8.5	8.5	8.5	8.5	8.5	8.5	8.5	8.5	8.5	8.5	8.5	8.5	8.5	6.8
Calcium	mg Ca^{2+}/l	2.5	2.5	2.5	2.5	35	2.5	2.5	2.5	2.5	2.5	2.5	35	35	35	2.5	2.5	2.5	2.5	17	35	35	2.5
Iron	µg Fe/l	15	15	15	15	15	15	15	15	15	15	15	15	15	15	15	15	15	15	15	15	15	15
Sodium	mg Na^{+}/l	3	40	3	40	3	3	40	40	75	40	75	3	40	40	40	75	40	75	3	40	40	3
Silica	mg Si/l	1.0	1.0	1.0	1.0	1.0	1.0	1.0	1.0	1.0	1.0	1.0	1.0	1.0	1.0	1.0	1.0	1.0	1.0	1.0	1.0	1.0	1.0
Hydrogen carbonate	mg HCO_3^-/l	10	100	10	100	100	10	100	10	100	10	100	10	100	100	10	100	10	100	10	100	100	10
Chloride	mg Cl^-/l	5	5	5	5	5	5	5	65	65	5	5	65	65	5	32	32	5	5	32	32	5	5
Sulphate	mg SO_4^{2-}/l	5	5	5	5	5	5	5	5	5	85	85	5	5	85	5	5	42	42	5	5	42	5
Total nitrogen	µg N/l	165	165	165	165	165	165	165	165	165	165	165	165	165	165	165	165	165	165	165	165	165	165
Total phosphate	µg P/l	75	75	75	75	75	75	75	75	75	75	75	75	75	75	75	75	75	75	75	75	75	75
Copper	µg Cu/l	5	5	5	5	5	5	5	5	5	5	5	5	5	5	5	5	5	5	5	5	5	5
TOC	mg/l	0.7	0.7	0.7	0.7	0.7	0.7	0.7	0.7	0.7	0.7	0.7	0.7	0.7	0.7	0.7	0.7	0.7	0.7	0.7	0.7	0.7	0.7
UV (256nm)	cm^{-1}	0.7	0.7	0.7	0.7	0.7	0.7	0.7	0.7	0.7	0.7	0.7	0.7	0.7	0.7	0.7	0.7	0.7	0.7	0.7	0.7	0.7	0.7

Table A.2 List of water compositions used in the laboratory test pipes.

pH	HCO_3^- mg l^{-1}	Ca^{2+} mg l^{-1}	SO_4^{2-} mg l^{-1}	Cl^- mg l^{-1}
5,6,7,8	10	5	20	25
5,6,7,8	10	5	100	25
5,6,7,8	10	15	100	25
5,6,7,8	60	5	20	25
5,6,7,8	60	5	100	25
5,6,7,8	60	15	100	25
5,6,7,8	100	5	20	25
5,6,7,8	100	5	100	25
5,6,7,8	100	15	100	25
8,6,7,8	100	30	20	25

A.2 Field Test Water

A.2.1 Water production

Surface waters as well as ground waters were treated in different waterworks in Sweden and were then used in the field tests. The waterworks, the treatment methods and corrosion control methods where field tests were carried out are listed below.

Alingsås (surface water)

Treatment method	Chemical precipitation
Corrosion control	Addition of sodium hydroxide Addition of calcium carbonate

Floda (groundwater)

Treatment method	-
Corrosion control	-

Kallebäck (groundwater)

Treatment method	-
Corrosion control	-

Lackarebäck (surface water)

Treatment method	Chemical precipitation Chemical precipitation and ozonation Rapid sand filtration Rapid sand filtration and activated carbon filtration
Corrosion control	Addition of sodium hydroxide Addition of hydrogen carbonate

Lerum (surface water)

Treatment method	Rapid sand filtration
Corrosion control	Addition of sodium hydroxide Addition of carbon dioxide Calcium carbonate filtration

Ljungskile (surface water)

Treatment method	Ozonation
Corrosion control	Addition of sodium hydroxide Addition of carbon dioxide Calcium carbonate filtration

Mark (groundwater, surface water)

Treatment method	Chemical precipitation Rapid sand filtration
Corrosion control	Addition of sodium hydroxide Calcium carbonate filtration Dolomite filtration Aeration

Marstrand (surface water)

Treatment method	Chemical precipitation
Corrosion control	Addition of sodium hydroxide

Mellerud

Treatment method	
Corrosion control	Addition of sodium hydroxide

Munkfors (surface water)

Treatment method	Chemical precipitation
Corrosion control	Addition of sodium hydroxide Addition of carbon dioxide Addition of phosphate Addition of calcium carbonate

Mölndal (surface water)

Treatment method	Chemical precipitation
Corrosion control	Addition of carbon dioxide Addition of calcium hydroxide

Mölnlycke (surface water)

Treatment method	Slow sand filtration
Corrosion control	Addition of sodium hydroxide Addition of carbon dioxide Addition of calcium carbonate

Orust (surface water)

Treatment method	Chemical precipitation
Corrosion control	Addition of sodium hydroxide

Stenungsund (surface water)

Treatment method	Chemical precipitation Rapid sand filtration Slow sand filtration
Corrosion control	Addition of sodium hydroxide Addition of phosphate

Varberg (groundwater)

Treatment method	-
Corrosion control	Addition of sodium hydroxide

Örebro (surface water, groundwater)

Treatment method	Artificial infiltration Slow sand filtration Rapid sand filtration
Corrosion control	Addition of sodium hydroxide Addition of calcium carbonate

A.2.2 Water composition

The composition of the waters depends on the treatment and the addition of chemicals at the waterworks. In Table A.3 the water composition was listed for water supplied to the corrosion test rigs. In Table A.4 the water composition for water supplied to iron pipes placed in the waterworks is shown.

Table A.3 Water composition for water supplied to the corrosion test rigs.

	pH	HCO_3^- mg l^{-1}	Ca^{2+} mg l^{-1}	SO_4^{2-} mg l^{-1}	Cl^- mg l^{-1}	TOC mg l^{-1}
Munkfors I	7.9	55	2	10-30	3-20	2-3
II	8.0	60	3	10-30	3-20	2-3
III	8.2	63	23	10-30	3-20	2-3
Lackarebäck						
finished water I	8.5	15	14	30	14	2.4
II	9.0	100	15	30	15	2.5
III	8.5	15	14	30	15	2.4
raw water (IV)	8.5	15	8	14	14	3.5
(V)	8.5	15	8	14	14	1.0
Kallebäck	6.4	60	33	49	120	2.6
Mölndal	8.0	50-70	20-25	24	22	3.0
Mölnlycke	8.5	65	26	10	22	3.3
Lerum	8.0	75	20	10	13	3.4
Ljungskile	7.4	78	17	15	22	4.0-6.0
Stenungsund I	9.3	13	6	25-30	18-21	1.6-2.4
II	6.4	9	3-6	9-46	12-21	2.0-3.0
III	6.4	9	3	8	12	3.0-4.0

Table A.4 Range of analysis parameters from 56 waters used in tests with iron pipes.

pH	HCO_3^- mg l^{-1}	Ca^{2+} mg l^{-1}	SO_4^{2-} mg l^{-1}	Cl^- mg l^{-1}	TOC mg l^{-1}
6.3-9.5	6-137	6-39	7-72	3-155	0.5-15

A.3 Description of Corrosion Test Systems

A.3.1 Copper corrosion rigs

The construction of copper test rigs can be seen in Figure A.2.

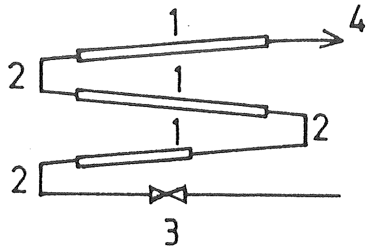

1. Copper pipes
2. pVC tube
3. Magnetic valve to control the inflow
4. Water to analysis

Specifications

Type of copper	SMS-0026-02	Copper composition % in pipes			
Internal diameter	9 mm	Cu	99.94	As	0.002
Copper area	8.8 dm^2	Zn	0.012	Si	0.001
Volume	225 ml	Pb	0.003	Cr	<0.001
Residence time	0.5 min	Sn	0.004	S	<0.001
Velocity of water	0.1 $m\ s^{-1}$	Al	<0.001	Se	<0.001
Flow	250 ml min^{-1}	Fe	0.001	Bi	<0.001
Flow cycle	Stop 20 h, flow 4 h	Ni	0.002	Sb	0.002
		Mn	<0.001	Te	0.001
		P	0.021	B	<0.001
		Cd	0.001	Carbon No.	1-2
		Ag	0.007		

Figure A.2 Copper corrosion rig

The copper pipe consisted of soft-dioxidised phosphorus copper.

The copper rigs were intermittently supplied with water in order to simulate the conditions in a household. The cycle started with a flow of 250 ml min^{-1} for four hours followed by a stagnant period of twenty hours and a new four hour flow period, and so on. The duration of the tests was 18-25 weeks.

When the flow started, the first 220 ml of rig effluent was collected in an Erlenmeyer flask. The water was analysed for pH, alkalinity and copper content.

These rigs were used in laboratory tests and in field tests.

A.3.2 Copper pipes

Copper pipes were used in an investigation to simulate the cuprosolvency of copper pipes in a household. The study considered the influence of acid water on corrosion and only laboratory tests were made. The water composition is presented in Table A.2 (Johansson and Hedberg 1988).

The water was stagnant for 24 hours in the pipes and was changed daily for ten weeks. For each type of water two pipes were used. The copper dissolved from the pipe surface was analysed six times during a ten week period.

Specifications

Length of copper pipe	50 cm
Internal diameter	20 mm
Copper area	3.1 dm^2
Volume	144 ml

A.3.3 Iron coupon rigs

The construction and specifications of the coupon rigs are illustrated in Figure A.3.

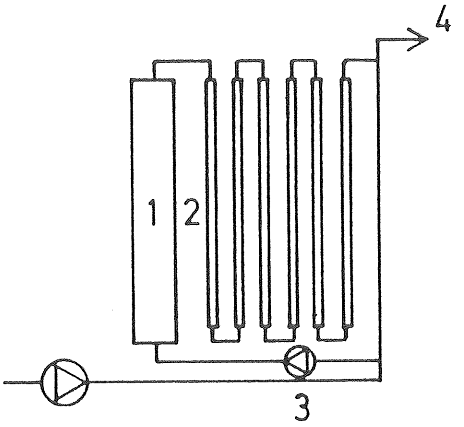

1. Large plexi - glas pipe
2. Small plexi - glas pipe
3. Circulation pump
4. Water to analysis

Specifications

Volume	18 l	Coupon composition %	
Rate of flow	100 ml min^{-1}	Fe	98.115
Normal residence time	2.5 h	C	1.0
Circulation flow	10 l min^{-1}	Mn	0.40
Large plexi-glas pipe		Si	0.30
internal diameter	140 mm	Cr	0.15
length	1000 mm	P	0.020
water velocity	0.01 m s^{-1}	S	0.015
No. of coupon holders	6		
No. of coupons per holder	6		
total iron area	0.09 m^2		
Small plexi-glass pipe			
internal diameter	21 mm		
length	800 mm		
water velocity	0.7 m s^{-1}		
No. of coupon holders	6		
No. of coupons per holder	6		
total iron area	0.09 m^2		
Coupons: thickness	0.25 mm		
length	100 mm		
width	12.2 mm		

Figure A.3 Iron coupon rig

The coupons were cut from band steel (100 x 12.2 x 0.25 mm). The surface of the coupons was much smoother than pipe surfaces. Thus the coupons were tumbled with sand for 13 hours in a rotating drum. The surface structure of the coupons was then similar to that of the internal surface of an iron pipe.

After cutting and tumbling, the coupons were contaminated with grease and particles and therefore needed to be cleaned. The coupons were cleaned with carbon tetrachloride and placed in an ultrasonic vessel for a few seconds. Finally, they were rinsed with ethanol, dried in a stream of hot air and weighed.

Test water (Table A.1 and Table A.3) was continuously fed into the rig. The flow was 0.1 l min^{-1}. Two different water velocities were maintained in the corrosion rig by a circulation pump. This design made it possible to simulate two different residence times in a distribution network. Each coupon was thus exposed to the same water velocity water at all times. The rigs were used both in laboratory and field tests. The effluent was analysed weekly for pH, alkalinity, iron content, colour and turbidity.

In each rig one coupon holder was removed from each pipe after 2, 4-5, 8-9, 14-15, 18-19 and 23-25 weeks. The coupons were analysed for corrosion rate by weight loss. Weight loss determination was made on four of the six coupons in each coupon holder. The other two coupons were saved for scanning electron microscopy and energy dispersive analysis (SEM/EDA) and conventional photography. The corrosion attack and the development of deposits or protective layers were determined.

A.3.4 Oxygen consumption rigs

These rigs consist of iron pipes formed as a loop. A rig is shown with specifications in Figure A.4.

The oxygen consumption rig for determination of the corrosion rate was introduced and used by Werner (1976).

Test water was continuously circulated (10 l min^{-1}) in the rigs. The circulating water was continuously exchanged. Inflows and outflows were between 200 and 400 ml min^{-1}. The influent and effluent from each rig was continuously monitored for oxygen concentration, temperature and pH.

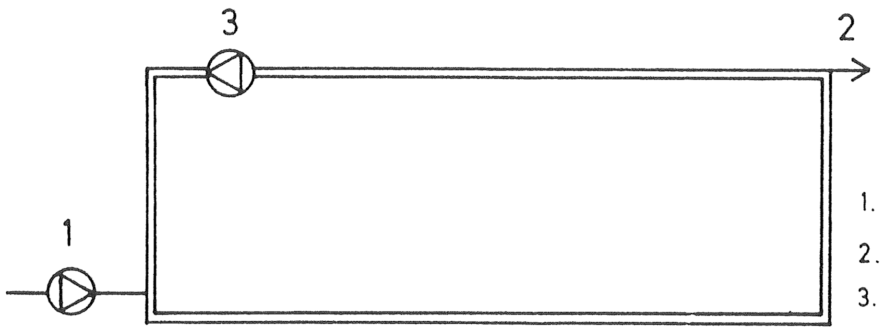

1. Inflow, control of oxygen
2. Outflow, control of oxygen
3. Circulation pump

Specifications

Volume	4.5 l
Flow	200-400 ml min^{-1}
Circulation flow	10 l min^{-1}
Nominal residence time	22.5 min
Water velocity	0.45 m s^{-1}
Dimension of iron pipe	21 mm
Total length	12 m
Iron area	0.82 m^2

Iron composition %

Fe	99.441
C	0.08-0.12
Mn	0.36-0.43
Si	0.01-0.02
P	0.01-0.02
S	0.021-0.027

Figure A.4 Oxygen consumption rig.

In addition to the continuous registration, the effluent was analysed weekly for Fe, HCO_3, colour and turbidity.

Waters numbered 1, 2, 8, 9, 15 and 16 in Table A.1 were supplied to the oxygen consumption rigs.

A.3.5 Iron pipes

Iron pipes were used in two different corrosion studies. In one study laboratory test water (Table A.2) was used. The water was stagnant in the pipes for 24 hours and was then changed. In the other study iron pipes were located at the water works listed in Section A.2.1. The water flowed continuously through these pipes for one year. Water composition is shown in Table A.4.

Specifications

Length	50 cm
Internal diameter	21 mm
Iron area	3.3 dm^2
Volume	163 ml
Flow	2 l min^{-1}

Analysis for iron content was done on the waters from the pipes with stagnant water. This was done for each water 6 times during a 10 week test period for each water. Two pipes were used for each water.

The iron pipes, installed at the water works, were exposed to the water for one year, and were then removed for examination. The pipes were, after a preliminary visual inspection of the deposits, analysed chemically for Fe(II), Fe(III) and Ca.

A.4 Analytical Methods

A.4.1 Analysis of the water

A.4.1.1 Chemical analysis of water flowing into corrosion test systems

The laboratory test waters were analysed during production and after the addition of chemicals. The pH and conductivity of the water in the reservoir, after ion-exchange and carbon filtration, were measured continuously. After each water production period the water was analysed for chloride, calcium and hydrogen carbonate. Once a month a complete physical and chemical analysis was done. The mean values for the water composition can be seen in Table A.1. After the addition of chemicals to the water, the water composition again had to be measured. The analyses of the water were for pH, hydrogen carbonate, calcium, chloride and sulphate.

The field test water composition was determined by chemical analyses for pH, hydrogen carbonate, calcium, sodium, chloride and sulphate.

A.4.1.2 Chemical analysis of water from corrosion test systems

The effluent water was analysed for iron or copper, pH, alkalinity, calcium concentration and the effluent from iron rigs were also analysed for oxygen, colour and turbidity.

All analyses followed Swedish Standards. Most of these methods are similar to Standard Methods (1987). The concentration of metal in the water was analysed using atomic absorption spectrophotometry (AAS).

A.4.1.3 Analysis of organic matter

The total concentration of organic matter was analysed by a TOC analyser for total organic carbon.

Characterisation of the organic matter in the water by molecular weight distribution was done using gel filtration chromatography with two different gels, Sephadex G-25 and G-50. According to the manufacturer, the Sephadex G-25 and G-50 separate molecules in the molecular weight range of 1000-5000 and 1000-30000 respectively. The gel filtration columns have a diameter of 16 mm and a height of 70 mm and were filled with Sephadex G-25 or Sephadex G-50. The height of the Sephadex bed was 60 mm. Before the water was analysed by gel filtration, the organic matter was concentrated 10 times in a rotary evaporator at 50°C. Approximately 10 ml of the concentrate was placed in the gel column. The column was then eluted with distilled water at a flow rate of 1.2 ml min^{-1} for G-25 and 0.6 ml min^{-1} for G-50. Using a fraction collector, 25 fractions of 6 ml each were collected. The fractions were analysed for TOC, UV-absorption at 254 nm or iron content.

A.4.2 Analysis of the corroded metals and deposits

A.4.2.1 Weight loss determination of iron coupons

The weight loss method used in this study is a standard method taken from ASTM (1973) and is a useful method to measure corrosion of coupons. The weight loss is expressed as loss in weight per unit area or loss in weight per unit area and time.

After the tests, loose corrosion products were brushed from the coupons. The coupons were than placed in a chemical treatment bath for dissolution of the remaining corrosion products. The cleaning solution was prepared from one litre of concentrated hydrochloric acid with an addition of 31 g antimony chloride and

50 g stannous chloride. The dissolution was allowed to proceed at room temperature until the coupons were completely free from corrosion products, usually about 5-30 min. The coupons were subsequently treated in an ultrasonic vessel, rinsed in ethanol, dried in hot air and weighed.

A.4.2.2 Chemical analysis of deposits

The deposits on the iron pipes that had been exposed to water for a year were examined for content of iron(II), iron(III), calcium and total iron content.

The deposits were removed from the pipes by the following treatment sequence (Sontheimer et al. 1981).

- The middle 20 mm of the 50 cm pipe was cut out.
- The surface deposits were brushed clean.
- The pipe piece was then dipped in 100 ml HCl for 30 s.
- 25-30 mg of the brushed deposits were dissolved in HCl solution at 70-80 °C.
- The solution was analysed chemically using AAS for calcium and total iron.
- A part of the solution was analysed using the phenanthroline method according to Sung and Morgan (1980).

A.4.2.3 SEM/EDA analysis

Surface characteristics of deposits and corrosion attack can be detected by Scanning Electron Microscopy (SEM). The chemical composition of the layers was detected by SEM/EDA (Energy Dispersion Analysis).

A.4.2.4 Photographic documentation of coupons

One of the two coupons, that had been saved at each removal during the test period for the iron corrosion rigs, was collected for photographic documentation. The photographs show the development of deposits or protective layers on the metal surface. The contrast in appearance between deposits from the pipes with low and high water velocity were documented in this way.

The EDA analysis of the content of deposits and the SEM illustration of the cross section and surface structure are also photographed. The morphology of deposits were detected by a visual analyzer in the SEM instrument which appears on micrographs.

APPENDIX B. IRON CORROSION CALCULATIONS

B.1 Statistical estimation of weight loss measurements

The coupons were weighed before installation in the rigs. After a determined time (2, 4-5, 8-9, 14-15, 18-19, 24-25 weeks) four of them, exposed to two water velocities (0.01 m s^{-1} and 0.7 m s^{-1}), were taken out and reweighed. The weight loss was compared and a mean value was calculated and used in the estimation.

Table B:1 shows statistical data for the tests. Most of the standard deviation values are around 0.02-0.05. A general observation is that when the corrosion rate is high, the standard deviation is also high and vice versa.

Table B.1 Mean value of weight losses, standard deviation for the weight losses, maximum weight loss and minimum weight loss over a test period. A) Test with the lowest standard deviation, B) Test with the greatest standard deviation.

A

Weeks	2	5	8	13	19	25
$\bar{x}$	0.1306	0.1767	0.2089	0.2618	0.3280	0.4802
δ	0.0012	0.0099	0.0108	0.0070	0.0174	0.0129
max	0.1323	0.1846	0.2221	0.2696	0.3680	0.4932
min	0.1296	0.1622	0.2095	0.2544	0.3288	0.4623

B

Weeks	2	5	9
$\bar{x}$	0.4886	1.3223	2.0008
δ	0.1072	0.0650	0.1944
max	0.5822	1.3761	2.1718
min	0.3500	1.2292	1.8079

$\bar{x}$ = mean

δ = standard deviation

B.2 Corrosion rate calculated from weight loss measurements

The weight loss values are related to the coupons with a specific area and after a certain exposure time. The area of the coupons are 0.246 dm^2 and time represents the time of exposure.

Corrosion rate = weight loss/area x time ($mg\ dm^{-2}\ d^{-1}$ = $mg\ dm^{-2}$ x days).

The corrosion rates were calculated after 50, 60, 70 or 120 days dependent on the shape of the weight loss curve. When the weight loss curve did not decrease the corrosion rates were calculated for shorter time periods. When the weight loss decreased or decreased slightly the calculations were done for a longer test period.

B.3 Corrosion rate calculated from iron uptake

Iron dissolved from pipes containing stagnant water was analysed after a 24 hour residence time.

The pipe length was 4.7 dm and the diameter was 0.21 dm which results in an area of 3.10 dm^2 and a volume of 0.163 dm^3. The corrosion rate can be calculated from this.

Corrosion rate = iron uptake x volume/area x time ($mg\ dm^{-2}\ d^{-1}$ = $mg\ l^{-1}$ x $dm^3\ dm^{-2}$ x days.

B.4 Corrosion rate calculated from oxygen consumption

Oxygen is consumed when iron dissolves to iron(II) and during the oxidation of iron(II) to iron(III). To measure the corrosion rate only 2/3 of the oxygen is used in the corrosion process (equations B.1-B.4).

$$\mathrm{Fe} \rightarrow \mathrm{Fe}^{2+} + 2e^- \qquad (B.1)$$

$$2\mathrm{Fe} + \mathrm{O}_2 + 2\mathrm{H}_2\mathrm{O} \rightarrow 2\mathrm{Fe}^{2+} + 4\mathrm{OH}^- \qquad (B.2)$$

$$\tfrac{1}{2}\mathrm{O}_2 + \mathrm{H}_2\mathrm{O} + 2e^- \rightarrow 2\mathrm{OH}^- \qquad (B.3)$$

$$2\mathrm{Fe}^{2+} + \tfrac{1}{2}\mathrm{O}_2 + 4 \rightarrow 2\mathrm{FeOO} + (s) + \mathrm{H}_2\mathrm{O} \qquad (B.4)$$

and hence:

Corrosion rate = 2/3 oxygen consumption x water flow x M_{Fe}/M_O /area x time (mg dm^{-2} d^{-1} = mg l^{-1} x l s^{-1} x $M_{Fe}/M_O/dm^2$ x days)

But if protective layers such as $FeCO_3$ are formed then only iron dissolution will occur, and the right way to handle the calculations is according to the following equation:

Corrosion rate = oxygen consumption x water flow x M_{Fe}/M_O/area x time (mg dm^{-2} d^{-1} = mg l^{-1} x l s^{-1} x $M_{Fe}/M_O/dm^2$ x days)

B.5 Estimation of initial corrosion and continuing corrosion rate

Three types of corrosion rate can be identified:

1. Corrosion which does not decrease with time. No protective layer formation.

2. Corrosion which decreases after a certain period of time t.

3. Corrosion which slows and stops completely after a certain period of time t.

When the weight loss is plotted against time (Figure B.1) the corrosion rate is the tangent of the curve both for initial corrosion (a) and continuing corrosion (b). Figure B.1A refers to Corrosion rate type 1, B.1B refers to type 2 and B.1C to type 3. In Figure B.1A, curve I showed high corrosion rate and curve II low corrosion rate from the start.

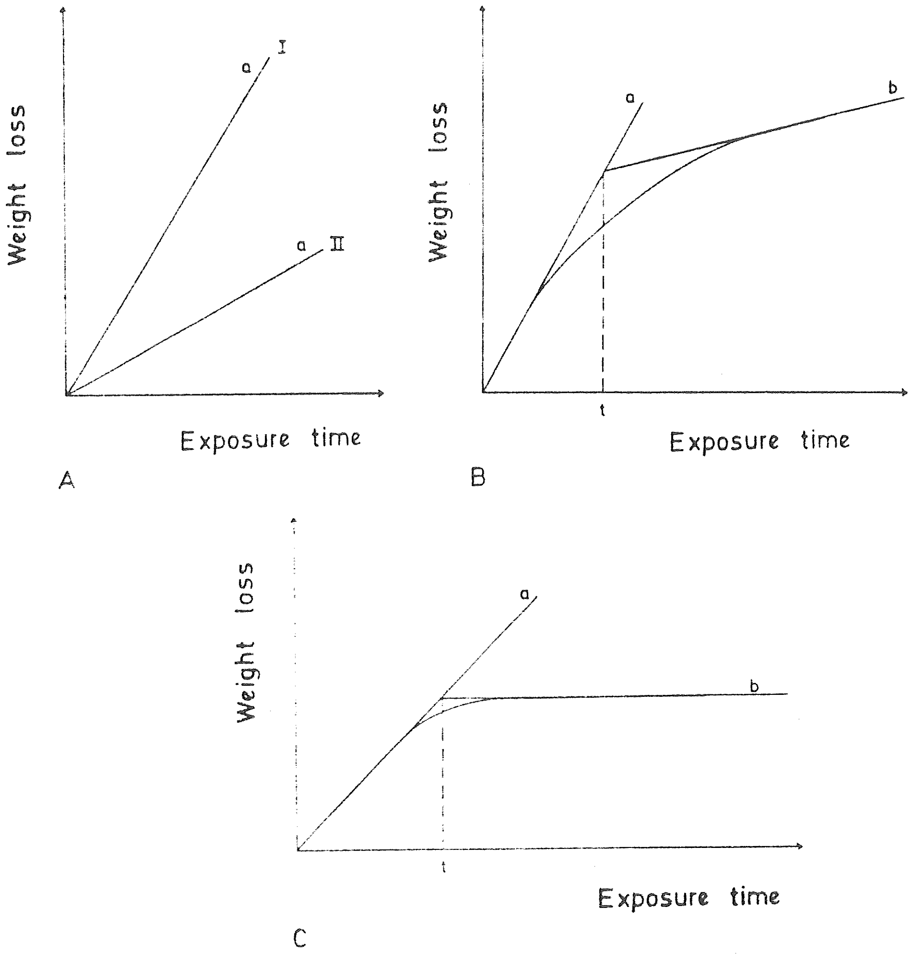

Figure B.1 Weight loss as a function of time when corrosion rate decreases in different ways, A, B and C. The tangents a and b show different corrosion rates for initial and continuing corrosion after a certain period of time t.

The three types of corrosion rate are in accordance with the test results as below:

1. Waters with chloride or sulphate (Figure II.1AI), or water at low velocity 0.01 m s^{-1} more or less independent of the water composition (Figure B.1AII).

2. Water with various pH and content of total carbonic acid at high water velocity (0.7 m s^{-1}), Figure B.1B.

3. Water with low pH (7.5) and high content of total carbonic acid (100 mg HCO_3^- l^{-1}) and waters under saturation conditions for $CaCO_3$ (pH 8.5, 35 mg Ca^{2+} l^{-1} and 100 mg HCO_3^- l^{-1}), Figure B.1C.

APPENDIX C. IMPORTANCE OF WATER VELOCITY ON CORROSION RATE

In tables are listed corrosion rate as a function of water velocity and water composition for test water in the laboratory and in field water at different waterworks.

Table C.1 Water with low corrosion rate at a water velocity of 0.7 ms^{-1}

		Test water			
pH	HCO_3	Ca^{2+}	Cl^-	SO_4^{2-}	(mg l^{-1})
8.5	100	35	5	5	
7.5	100	2.5	5	5	
8.5	100	35	65	5	
8.5	100	35	5	85	
8.5	100	35	32	5	
8.5	100	35	5	42	

		Field water			
pH	HCO_3	Ca^{2+}	Cl^-	SO_4^{2-}	(mg l^{-1})
7.9	53	2	11	20	Chemical precipitation, phosphate addition
7.5	42	12	13	10	
8.3	60	20	13	30	Chemical precipitation Calcium carbonate addition
9.0	13	6	19	27	Chemical precipitation

Table C.2 Water with low corrosion rate at a water velocity of 0.01 ms^{-1}.

		Field water			
pH	HCO_3	Ca^{2+}	Cl^-	SO_4^{2-}	(mg l^{-1})
8.0	60	28	22	24	
8.4	14	13	13	30	Chemical precipitation
8.0	15	125	12	26	Chemical precipitation, ozonization
8.5	15	13	13	14	Rapid sand filtered
8.5	15	13	13	14	Rapid sand and activated carbon filtered

Table C.3 Water with high corrosion rate at a water velocity of 0.7 ms^{-1}.

		Test water			
pH	HCO_3	Ca^{2+}	Cl^-	SO_4^{2-}	(mg l^{-1})
8.5	10	2.5	5	5	
8.5	10	2.5	32	5	
8.5	100	2.5	32	5	
8.5	10	2.5	65	5	
8.5	100	2.5	65	5	
8.5	10	2.5	5	42	
8.5	100	2.5	5	42	
8.5	10	2.5	5	85	
8.5	100	2.5	5	85	
9.5	10	2.5	5	5	

		Field water			
pH	HCO_3	Ca^{2+}	Cl^-	SO_4^{2-}	(mg l^{-1})
6.25	8.5	6	20	9	Slow sand filtered
8.0	6.0	28	22	24	
8.4	14	13	13	30	Chemical precipitation
8.0	15	13	13	14	Chemical precipitation, ozonization
8.5	15	13	13	14	Rapid sand filtered
8.5	15	13	13	14	Rapid sand filtered Activated carbon filtered

Table 9.12 Water with high corrosion rate at a water velocity of 0.01 ms^{-1}.

		Test water			
pH	HCO_3	Ca^{2+}	Cl^-	SO_4^{2-}	(mg l^{-1})
7.5	100	2.5	5	5	

		Field water			
pH	HCO_3	Ca^{2+}	Cl^-	SO_4^{2-}	(mg l^{-1})
6.25	8.5	6	20	9	Slow sand filtered
7.9	53	2	11	20	Chemical precipitation
7.9	53	2	11	20	Chemical precipitation Phosphate addition

VASASTADENS BOKBINDERI AB
1989